

ABSTRACT

Title of Dissertation: PURPLE PEPPER PLANTS,
AN ANTHOCYANIN POWERHOUSE:
EXTRACTION, SEPARATION AND
CHARACTERIZATION

Cassandra Lynn Taylor
Doctor of Philosophy, 2014

Dissertation directed by: Professor Alice C. Mignerey
Department of Chemistry and Biochemistry

Most plants have multiple anthocyanins present that produce their color. In contrast, the foliage of the purple pepper plant (*Capsicum annuum L.*) contains high concentrations of a single anthocyanin delphinidin-3-*p*-coumaroylrutinoside-5-glucoside (Dp-3-*p*-coumrut-5-glc) in the foliage, making it very unique. This provides an excellent platform to extract the single anthocyanin at high concentrations.

A food-grade extraction method was developed using 1% hydrochloric acid and 200 proof ethanol (1% HCl/EtOH) in order to remove the intact anthocyanin. A separation method using High Performance Liquid Chromatography (HPLC) was developed to identify Dp-3-*p*-coumrut-5-glc. The retention time was compared with the Blue Ribbon Iris, a known source of Dp-3-*p*-coumrut-5-glc. The HPLC results confirmed the presence of Dp-3-*p*-coumrut-5-glc in the pepper extract, but the chromatograms also demonstrated the presence of additional highly colored compounds. The extract was injected onto the HPLC and the major anthocyanin peak (Dp-3-*p*-coumrut-5-glc) was collected over the course of multiple injections. The collected fractions were dried down and re-solubilized in 1% HCl/methanol for analysis by mass spectrometry.

A HPLC coupled to a photodiode array detector and an electrospray ionization tandem mass spectrometer (LC-PDA-ESI-MS/MS) was utilized to characterize Dp-3-*p*-coumrut-5-glc. The precursor compound was confirmed at m/z 919 with product ions at m/z 757, 465 and 303 by comparing against plant extracts of freeze-dried purple pepper foliage, Chinese eggplant and Chinese celery. The extract's structure was elucidated by Nuclear Magnetic Resonance (NMR) by analyzing both proton (^1H) and carbon (^{13}C) spectra. The ^1H and ^{13}C data matched very well with previous NMR data of Dp-3-*p*-coumrut-5-glc elucidated in eggplant peels. The major difference was that the *trans* isomer of Dp-3-*p*-coumrut-5-glc greatly dominated over the *cis* in the purple pepper extract.

PURPLE PEPPER PLANTS, AN ANTHOCYANIN POWERHOUSE:
EXTRACTION, SEPARATION AND CHARACTERIZATION

by

Cassandra Lynn Taylor

Dissertation submitted to the Faculty of the Graduate School of the
University of Maryland, College Park in partial fulfillment
of the requirements for the degree of
Doctor of Philosophy
2014

Advisory Committee:

Professor Alice C. Mignerey, Chair
Dr. John R. Stommel
Professor Frederick Khachik
Professor Catherine Fenselau
Professor Philip DeShong
Professor Thomas W. Castonguay

© Copyright by
Cassandra Lynn Taylor
2014

Thesis Overview

When you wake up in the morning do you take a daily supplement as part of your routine? Something to help you get those extra vitamins and minerals that you just can't find time to eat during the day? I know I do. It's very common in today's busy society for people of all ages to supplement their diets. We are on the go all day long and often times cannot consume the daily recommended values suggested by the U.S. Department of Agriculture (USDA). This is particularly true of fruits and vegetables. The USDA recommends at every meal to fill half of your plate with fruits and vegetables. This can be exceptionally difficult for children or anyone who does not enjoy the tastes and flavors of fruits and vegetables. It is essential for everyone to make healthy food choices and obtain the majority of their nutrients from fresh foods instead of highly processed or fast food. But we often need some help to get these nutrients in our bodies and that is where supplements play a role in our healthy diet plan.

At the USDA, a group of scientists cultivated an ornamental purple pepper plant with beautiful dark purple foliage and brilliant red peppers that are no bigger than a quarter. This plant is not a culinary pepper, so it cannot be consumed. The amazing thing about this pepper plant is that the dark purple foliage is attributed to a very high concentration of a class of compounds known to be a member of the anthocyanins. Anthocyanins (ACNs) are the compounds that are largely responsible for the dark colors seen in fruits, vegetables, and flowers in nature. Biologically they are part of the large plant group called flavonoids. The flavonoids are compounds found in almost every part of the plant and they usually are colorless. Anthocyanins are special because they range in color from red to blue. The color changes based on multiple factors, but how the ACNs

are arranged and chemically linked will affect the color we see with the naked eye in nature.

ACNs have been shown to have multiple health-promoting benefits when consumed, thus making them a great choice for healthy diets and a promising candidate for possible supplementation sources. We can naturally ingest ACNs by consuming fruits and vegetables like blueberries, strawberries, and blackberries, eggplants, red cabbage, and red radishes, as well as many more. All of these sources contain many different ACNs and scientists are unsure which ACN or what combination of ACNs provides the health benefits. The purple pepper is very unique because it has a very high concentration of a single ACN known as delphinidin-3-*p*-coumaroylrutinoside-5-glucoside (Dp-3-*p*-coumrut-5-glc). If this ACN could be safely removed from the foliage it could potentially be used in a supplement for people who don't consume enough fruits and vegetables. This idea was the basis of my research project.

The project originally had four main objectives:

1. Grow the purple pepper foliage in a $^{13}\text{CO}_2$ labeled environment with a large enough yield to utilize the foliage in an anthocyanin extraction method;
2. Develop an extraction method to remove Dp-3-*p*-coumrut-5-glc from the purple pepper foliage so it was safe for human consumption (i.e. food-grade);
3. Identify the specific anthocyanin in the foliage using analytical techniques like HPLC, MS and NMR;
4. Utilize the ^{13}C labeled extract in a human feeding study.

The purple pepper plants were grown in the greenhouse until mature enough to be defoliated (i.e. removal of leaves) and placed in the $^{13}\text{CO}_2$ growth chamber environment.

The idea was to have the plants uptake the $^{13}\text{CO}_2$ as they grew new leaves, then utilize these leaves in a food-grade extraction and have the result be a ^{13}C -labeled ACN extract. Since the purple pepper's leaves and fruit (i.e. the pepper) are not edible a food-grade extraction method was created to remove the intact anthocyanin from the foliage. It was important for the extraction method to use chemicals that would produce an extract that was safe for human consumption, therefore all of the chemicals utilized were Generally Recognized As Safe (GRAS) by the U.S. Food and Drug Administration (FDA).

In this thesis, the specifics of the food-grade extraction method and the analytical identification techniques used will be discussed at length. Unfortunately, the funding for the $^{13}\text{CO}_2$ labeling environment and the feeding study were lost after the creation of the food-grade anthocyanin extract, therefore the first objective was only partially achieved and fourth objective never came to fruition. Overall, the food-grade extraction method was proven to be successful. The success was determined by the analytical data collected from the various techniques, which confirmed the identity of *Dp-3-p-coumru-5-glc* in the purple pepper extract. All of the analytical data is presented in this thesis, along with background information regarding anthocyanins, as well as the discussion of what the data means in terms of a successful extraction of the anthocyanin from the purple pepper foliage and then followed by the conclusions for this research project.

Dedication

To my family,

for always loving me unconditionally, standing by my side and never giving up on me even during the most difficult times. Thank you for keeping me laughing and smiling along my journey. Your love kept me grounded when I needed it most. And for your constant encouragement to finish my Ph.D., despite how long it took me to complete, you always believed I could do it. Thank you for always being there. You are my rock.

Especially to Mom and Dad,

you both are forever my greatest supporters in life and have helped me become the woman I am today. When I was born you named me Cassandra because you thought it sounded like a good doctor name. You always encouraged me to utilize my gifts and talents, to set goals and to follow my heart. Your capacity to love is amazing. Thank you for your patience and for pushing me when I needed it. I am humbled and honored that I could achieve the dream you had for me at birth. Thank you for believing in my greatness, especially on the days when I could not see it myself.

This dissertation is for you both.

Acknowledgements

This section was my most favorite to write because it is the space where I can be myself and finally thank everyone who has helped me on this wonderful journey. It is not scientific it is straight from my heart and it is lengthy because anyone who knows me is aware that I love to talk. When I started the dissertation writing process I mentally made a list of the people I wanted to thank in this section for helping me along the way. That was almost four years ago. Since that time there have been so many outstanding people who have given me support and encouragement to help me achieve this goal. Throughout my nine years in graduate school countless people have touched my life and assisted me in my journey to academic success that I could write an entire dissertation on those experiences alone. But to spare everyone from that novel, I will do my best to mention them all here. Please know that I will never be able to repay all of you for your kindness, support, encouragement and guidance, patience, scientific knowledge and expertise. There is a famous quote by an Unknown author that describes this situation perfectly. It says,

“You have never really lived until you have done
something for someone who can never repay you.”

To every single person who helped me, thank you for daring to really live.

I am eternally grateful to you.

I promise to really live and help others, just as you did for me.

I am very blessed to have had excellent mentors during my time in graduate school. My biggest thanks go to Dr. Alice Mignerey, my advisor at the University of Maryland, College Park. You accepted me into the group despite me not wanting to

participate in a nuclear chemistry project. You provided me an opportunity to work on a nuclear forensics project at the Naval Research Laboratory, where I realized that I needed to do a more hands-on project and my true passion was in food chemistry. We then went and interviewed multiple research groups at the U.S. Department of Agriculture in Beltsville, MD so that I could find a project that I wanted to work on. We found a group and project that was perfect for me. I don't know any other graduate students who had the opportunity to pick their own group to work with at a government agency. I'm so grateful you stood by me in my decision to switch projects. Alice, thank you for supporting me and allowing me to participate in an unconventional project where I was able to discover my true passion for food and grow as a scientist. Thank you for caring about my personal growth, happiness and providing encouragement throughout my many years here. I appreciate your sincere heart and how you treated me like family. You have always been there to lend a helping hand in my time of need. Your constant encouragement for me to complete this process, even after I left, was outstanding. Your superior guidance throughout my rocky road of graduate student was something I sincerely appreciate. I am exceptionally grateful for your support and excitement when I decided to quit my job and return to school to finish my degree. You believed in me. You knew how hard I had worked and how important it was for me to finish and graduate. Thank you for all the assistance you have provided me during my time here. I will never forget your selflessness, guidance and our mutual passion for nutrition and food. If ever there were an award for "Greatest Advisor in the Universe" you would win it, no contest.

My second biggest thanks go to Dr. John Stommel, my mentor at the U.S. Department of Agriculture, Beltsville Agricultural Research Center. John, you took me

under your wing on this pepper project and taught me more about plants than I ever could have dreamed. Your expertise and experience were invaluable to me. I learned so much from you that I could never thank you for everything. You allowed me to be involved in every aspect of the project and to make my own decisions as to what to do next. You encouraged me to try new things, and when I failed, you were right there to guide me, get me back on track and to push me forward. Thank you for all of your wisdom and your willingness to teach me. I am so grateful for the freedom you gave me to make mistakes so that I could truly learn and grow as a scientist. You always fought for the project when budget time came around and you did everything you could to support me. Thank you for your endless amounts of patience during this project. I will never forget your kindness and willingness to help me achieve my goals. Thank you for being so supportive.

There are many people at BARC that I want to thank for their assistance and help during my time there. I'd like to thank Dr. Robert Griesbach for teaching me all about anthocyanin chemistry and sharing his years of knowledge with me so that I could develop my own extraction method. To Dr. James Harnly for allowing me to utilize his MS facilities and to Dr. Long-ze Lin for his patience at teaching me mass spectrometry and for sharing his extensive polyphenol collection with me so that I was able to have plant standards for this project. I would like to thank everyone who worked in the greenhouse for teaching me how to grow, care for and fertilize plants properly. As well as everyone at the Beltsville Human Nutrition and Research Center who participated in the early stages of this project to help me determine safe chemicals to use to produce a food-grade extract. Especially, to Dr. Steven Britz and Roman Mirecki who spent over a year helping to optimize the growing conditions for our plants so that we could eventually

conduct a labeling experiment. Lastly, everyone in the Genetic Improvement of Fruits and Vegetables Laboratory who supported and encouraged me everyday to finish my research so that I could graduate.

There are many people at the University of Maryland that I need to thank. I want to start with Dr. Frederick Khachik, who always offered me his endless amounts of chemistry knowledge and expertise from the beginning of this project, as well as his laboratory space when I needed it. The NMR expertise of Dr. Yiu-Fai Lam and Dr. Yinde Wang was exceptional. Without your guidance I would not have been able to obtain my NMR results. Thank you for spending so much time to optimize the instrument with me. The assistance my fellow graduate student, Frederick Nytko, III, provided was outstanding. Fred, thank you so much for taking the time to help me analyze my data and for explaining NMR principles to me over and over, and also for answering every question I ever asked you. You are a great teacher and you have the patience of a saint. I sincerely appreciate your time and help.

I also want to give a special thank you to my friends Dr. Kathy Goodson and Dr. Lynne Heighton, who have helped me immensely since I met them nearly 10 years ago on the first day of graduate school. You both have always supported me and helped me to finish my degree. I could not have asked for better friends to journey through graduate school with. We jumped through all the hoops together and all eventually came to the finish line. As always, I'm last to arrive, but you both know how I like to make an entrance. I could not have done it with out your friendship. Thank you so much for being there for me and always understanding.

I would not be finishing this thesis without every single member of the Mignerey group from the past, present and future. Thank you all very much for being my school family and for caring about me. In particular, I want to thank my incredibly amazing friends, Dr. Mara Dougherty and Dr. Lenny Demoranville. I would not have survived the first few years of graduate school without the two of you. Thank you for continuing to encourage me today and for being outstanding friends. You both will always have a special place in my heart. There is no doubt in my mind that you have helped me achieve this goal. I especially want to thank the current members of the Mignerey Group who accepted and welcomed me with open arms when I returned to the group. I am so grateful to have met all of you and I am appreciative of the warmth, support, encouragement and especially the laughs and happiness that you provided me during the most intense months of my life as I was writing. Thank you so much for giving me high fives when I would show you figures I spent hours making the night before and for getting excited every single time I finished a chapter. You will never know how much I appreciate you and how much your positivity helped me to get through this very demanding process. I thank each of you from the bottom of my heart.

I feel extremely fortunate to have attended Saint Francis University in Loretto, PA for my undergraduate degree. The professors who taught me chemistry are outstanding people and have continuously encouraged me to finish my graduate degree. The friends that I made in Loretto are the most amazing friends anyone could ask for. I am lucky that many of my close friends live here in the Maryland, DC and Virginia area so they were right here to support me when I returned. To all of them I have to express my extreme gratitude for your support, encouragement and kindness during my years in graduate

school, especially these last few months of writing. It was so motivating to read and hear all of your words of encouragement as I wrote my thesis. But the best was when everyone expressed how proud they were of me on graduation day. I appreciate your years of friendship and for being there to help support me. Thank you all so much for loving and caring about me. At Saint Francis our motto is “Reach Higher. Go Far”. I am proud to say that I continue to live by that motto with the completion of my Ph.D.

I also must thank all of my friends, teammates and professors outside of the University of Maryland for supporting me during my tenure in graduate school. I would not have survived without the stress relief of playing on my soccer teams, attending my boot camp classes, having listening ears and shoulders to lean on. I want to thank my friends and colleagues at my job who encouraged me to return to school because they knew how important it was for me to complete my degree. Thank you for being selfless, wanting what was best for me and for continuing to support me through this process. Friends, thank you all very much for being there for me and for the years of encouragement you provided me. I can’t express how much I appreciate all of you.

When it comes to encouragement, my family is exceptional. I want to thank Scotty and Nick for being the best brothers I could ever ask for. You both supported me through this entire process and never gave up on me. I cannot thank you enough for all the words you have given to me over the years. You both make me a better person and I can’t imagine my life without you. Thank you both for loving me and supporting me. To the rest of my extended family, I love each and every one of you. Your words of encouragement were what helped to keep me going and more importantly you all

believed that I could finish. That helped fuel me through the toughest days and I am forever grateful for all your love and support.

Scotty, you have been an immense source of positive energy for me since you were born. You and I are two peas in a pod. You were my number one supporter when I decided to quit my job and move back to Maryland to finish my dissertation. Words cannot express how much your support means to me. Your jokes, funny sayings and support have helped me during the toughest times. Thank you so much for listening to me on my worst days, offering words of support and never complaining for the number of times I would call or text you. Thank you for being my balance when I got frustrated and overwhelmed. I'm so glad you got that trait from Mom so that you could share it with me when I need it. I am eternally grateful that you understand me so well and always know what to say to me to make me laugh. No one understands our connection except us and I wouldn't have it any other way. Thank you for being the most awesome little brother in the universe.

Nick, you have always been a wonderful teacher and guider. You helped me to stay grounded when things became very difficult and I could not see the light at the end of the tunnel. You helped me to make plans, organize and take steps to move forward in my life. Thank you for sharing your planning skills with me so that I could be successful and get unstuck. You always give great advice and you are the best at thinking of every possible pathway to take, but always allow me to make my own decisions. Thank you for being gentle and providing me options so that I could figure out the best path to take. Thank you so much for teaching me to persevere and to not give up. I sincerely

appreciate all the wisdom you continue to share with me. Thank you for being the best older brother in the world.

Last, and certainly not least, I want to thank you, Mom and Dad. I never would have finished this without all of the love, support and encouragement you both provide me everyday. Thank you for your endless amounts of patience with me over the years. I know I'm a lot to handle and it was not easy for you guys. Especially when I would call you everyday on my breaks to talk with you about this paper. I'm absolutely certain it got very boring at times and I appreciate you pretending to sound interested and excited on those days. I know you were both scared when I quit my job to come back to school, but I told you to trust me because I had a goal that I had to complete and I'm grateful that you trusted me. Thank you for pushing me to finish my dissertation, particularly when I was exhausted with life. Thank your for instilling in me the values of persistence, goal setting, determination and discipline. You did not raise a quitter and I promised you I would never quit on this degree. But there was a time when I thought I could not finish this degree, and you both assured me repeatedly that I could do it. Thank you for believing in me. Thank you for being there to pick me up on the days when I needed it most and for loving me more then I ever thought was possible. I would not have accomplished this without the both of you. Mom and Dad, with all of my heart, I thank you.

Table of Contents

Thesis Overview.....	ii
Dedication.....	v
Acknowledgements.....	vi
List of Tables.....	xvii
List of Figures.....	xviii
List of Abbreviations.....	xxiii
Chapter 1: Background.....	1
Overview.....	1
1.1: Objectives.....	1
1.2: Purple Peppers and Anthocyanins.....	3
1.2.1: The Uniqueness of the Major Anthocyanin from Purple Peppers.....	5
1.2.2: Current Research on delphinidin-3- <i>p</i> -coumaroylrutinoside-5-glucoside.....	7
1.3: Factors that Affect the Bioavailability of Anthocyanins.....	8
1.3.1: Anthocyanin Bioavailability Trends.....	10
1.4: Food-Grade Extraction.....	15
1.4.1: Techniques Used to Confirm the ACN Structure.....	16
1.5: Loss of Funding for Feeding Study.....	16
Chapter 2: Anthocyanins.....	18
Overview.....	18
2.1: Anthocyanin Structure.....	18
2.2: Anthocyanin Color.....	25
2.3: Copigmentation.....	28
2.3.1: Intramolecular and Intermolecular Copigmentation.....	28
2.3.2: Metal Copigmentation.....	31
2.4: Anthocyanin Stability.....	32
2.5: Possible Health Benefits.....	33
2.6: Nomenclature.....	36
2.7: Anthocyanin Standards.....	37
Chapter 3: Food-Grade Extraction Method.....	40
Overview.....	40
3.1: New Methodologies.....	40
3.2: Extraction Method.....	42
3.2.1: Sample Preparation.....	44
3.2.2: Experimental.....	45
3.2.3: Color Check and Sample Homogenization.....	48
3.2.4: Filtration.....	51

3.2.5: Initial Drying Process.....	54
3.3: Cleaning and Drying the Sample.....	57
3.3.1: Removal of Chlorophyll and other Polyphenols	58
3.3.2: Final Drying of Extract	60
3.4: Confirmation of Food-Grade Extraction Technique	61
Chapter 4: High Performance Liquid Chromatography	63
Overview.....	63
4.1: High Performance Liquid Chromatography (HPLC)	63
4.2: HPLC Separation Method.....	66
4.2.1: Fraction Collection.....	68
4.3: Drying Fractions and Resolubilizing Concentrated Extract	77
4.4: Analysis of Concentrated Extract.....	78
4.5: Comparison of Concentrated Pepper Extract to Blue Ribbon Iris Standard.....	83
4.6: Confirmation of HPLC Separation Technique.....	86
Chapter 5: Mass Spectrometry.....	88
Overview.....	88
5.1: Characterization Technique	88
5.2: Electrospray Ionization Tandem Mass Spectrometry (ESI-MS/MS)	89
5.3: Preparation of Standard Plant Material for MS/MS	92
5.3.1: Preparation of Plant Extracts.....	93
5.3.2: Preparation of Concentrated Purple Pepper ACN Extract.....	93
5.4: Instrumentation Conditions.....	94
5.4.1: LC-PDA-ESI-MS/MS Conditions	94
5.5 Characterization Data.....	96
5.5.1: LC-PDA-ESI-MS/MS Characterization Data	96
5.6: Confirmation of the Major Anthocyanin by MS/MS	111
Chapter 6: Nuclear Magnetic Resonance	112
Overview.....	112
6.1: Elucidation Technique	112
6.2: Preparation of Dry ACN Material for NMR Analysis.....	113
6.3: Instrument Conditions.....	114
6.3.1: Instrument Parameters and Sequences.....	115
6.4: Reconcentration of ACN sample for NMR analysis	116
6.5: Elucidation Data	117
6.5.1: ¹ H Analysis Data.....	117
6.5.2: ¹³ C Analysis Data.....	127
6.6: NMR Conclusions	135
Chapter 7: Summary of Results and Conclusion	137
Overview.....	137
7.1: Summary of Results.....	137
7.1.1: Food-Grade Extraction Method.....	140
7.1.2: HPLC Separation and Fraction Collection.....	140

7.1.3: Mass Spectrometry Characterization with LC-PDA-ESI-MS/MS	142
7.1.4: NMR Elucidation.....	143
7.2: Conclusions	147
7.3: Future Work	148
Appendix A: HPLC Data.....	151
Appendix B: Mass Spectrometry Data	155
Appendix C: NMR	160
C.1: Pulse Sequences	161
Appendix D: CO ₂ Plant Chambers.....	167
D.1: Background	167
D.2: Study Objectives.....	167
D.3: Carbon Dioxide (CO ₂) Chamber	169
D.4: Growing Conditions for Pepper Plants	175
D.5: Conclusions	177
References.....	179

List of Tables

Table 2.1: List of the seventeen naturally occurring aglycones (also referred to as anthocyanidins), their substitution patterns and their color. Figure from Kong, <i>et al.</i> (82).....	21
Table 3.1: Investigated combinations of solvents, temperature and time for the sample preparation method. Combination utilized to obtain pepper extract is highlighted in purple. Abbreviations: EtOH = 200 proof ethanol, HCl = hydrochloric acid, HAc = acetic acid and Fridge = Refrigerator.	47
Table 3.2: Criteria used to accept/reject the extraction combinations listed in Table 3.1.48	
Table 4.1: Values from original ACN pepper extract: (a) 340 nm and (b) 540 nm. The major ACN values are highlighted in yellow.....	71
Table 4.2: Summary of major ACN values for the concentrated extract at 340 & 540 nm.	80
Table 4.3: Chromatographic data from the concentrated pepper extract at 340 nm. The major ACN is highlighted in yellow, combined % Peak Area is 94.40 for peaks 7 and 8.....	81
Table 4.4: Chromatographic data from the concentrated pepper extract at 540 nm. The major ACN peak is highlighted in yellow with a % Peak Area of 98.10.	82
Table 4.5: Comparison of values from the original pepper extract and the concentrated pepper extract at 340 and 540 nm. The total # identified peaks and the % Peak Areas for the major ACN are reported here.....	83
Table 5.1: Identification of peaks in the freeze-dried purple pepper foliage plant extract.	100
Table 6.1: Instrument parameters for the pulse sequence “zg30”. All acronyms are defined in Appendix C.....	115
Table 6.2: Instrument parameters for the pulse sequence “zgdc”. All acronyms are defined in Appendix C.....	116
Table 6.3: Comparison of proton NMR data. On the left in blue, eggplant peel data from Ichiyangi <i>et al.</i> (9). On the right, purple pepper data from this investigation. ^b	126
Table 6.4: Comparison of ¹³ C NMR data. ^a	134
Table A.1: NMR Fraction Collection Data. These fractions were dried down then prepared for NMR analysis.	151
Table A.2: Counterpart to Table 4.2. Comparison table for duplicate analysis of concentrated pepper extract at 340 and 540 nm.	152
Table A.3: Counterpart to Table 4.3. Chromatographic data from the duplicate analysis of the concentrated pepper extract at 340 nm. The major ACN is highlighted in yellow with a % Peak Area of 94.24.....	153
Table A.4: Counterpart to Table 4.4. Chromatographic data from the duplicate analysis of the concentrated pepper extract at 540 nm. The major ACN is highlighted in yellow with a % Peak Area of 95.67.....	154
Table C.1: Defined NMR acronyms.....	160
Table D.1: Collected CO ₂ data from Plexiglas chamber during growth optimization experiment for purple peppers.....	174

List of Figures

Figure 1.1: Backbone structure of all anthocyanins is the aglycone (i.e. anthocyanidin) and it must have a sugar (i.e. glycosyl) and usually an acylation group (i.e. <i>p</i> -coumaric acid) attached to the sugar in order to form an anthocyanin.....	3
Figure 1.2: Illustrations of delphinidin-3- <i>p</i> -coumaroylrutinoside-5-glucoside (a) <i>cis</i> isomer, and (b) <i>trans</i> isomer.	6
Figure 1.3: Common acylation groups found attached to the sugars, which are attached to the aglycones, that form anthocyanins. (a) <i>p</i> -coumaric acid, (b) caffeic acid, (c) ferulic acid, (d) sinapic acid, (e) malonic acid and (f) <i>p</i> -hydroxybenzoic acid.....	12
Figure 1.4: Structures of the six most common aglycones (i.e. anthocyanidins) in nature.	13
Figure 1.5: Structures of common sugar moieties attached to the aglycone.	14
Figure 2.1: (a) The flavylium cation. R values: –H = hydrogen; –OH = hydroxide;..... –OCH ₃ = methoxyl group; (b) A glycosyl group.....	19
Figure 2.2: Structures of the six most common aglycones found in nature.	21
Figure 2.3: The chemical structures of the six most common aglycones (also called anthocyanidins) occurring in nature, with R ₁ and R ₂ as the possible substituents. Below are the common sugars that attach to the aglycones at the 3– position.	22
Figure 2.4: Common acylation groups found attached to sugars on the flavylium cation, (a) <i>p</i> -coumaric acid, (b) caffeic acid, (c) ferulic acid, (d) sinapic acid, (e) malonic acid and (f) <i>p</i> -hydroxybenzoic acid.	24
Figure 2.5: Structural transformations of ACN pigments with change in pH. Pyrylium ring is designated by red oval in flavylium cation. Figure adapted from Wrolstad, 2004 (74).	26
Figure 2.6: The generalized effect of pH value on ACN equilibria. Figure from Clifford, 2000 (87).	27
Figure 2.7: Illustrations of delphinidin-3- <i>p</i> -coumaroylrutinoside-5-glucoside (a) <i>cis</i> isomer, and (b) <i>trans</i> isomer.	37
Figure 2.8: (a) Picture of a Blue Ribbon Iris (141). (b) Picture of the purple pepper plant (Copyright: Dr. John Stommel).	39
Figure 3.1: Picture of purple pepper foliage (<i>Capsicum annuum</i> L.) in the field. (Copy: Cassandra L. Taylor).	41
Figure 3.2: Schematic drawing of developed extraction protocol.	43
Figure 3.3: Diagram of food-grade extraction of the ACN from the purple pepper foliage.	44
Figure 3.4: Comparison of leaf color after adding differing ratios of 1% HCl to EtOH and storing in freezer for minimum of 48 h. (a) 5:1 ratio demonstrates correct leaf and solution color to maintain flavylium cation; (b) significantly < 5:1 ratio reveals incorrect leaf and solution color to demonstrate flavylium cation is not maintained.	46
Figure 3.5: After 48 h in freezer, (a) leaves stored in 1% HCl/EtOH; (b) leaves stored in 200 proof EtOH.	50
Figure 3.6: (a) Filtration setup. (b) Filter paper once ready to remove.	52
Figure 3.7: Final filtrate color from the purple pepper foliage extract.	53

Figure 3.8: These pictures represent what the product should look like when it is (a) dry, and (b) almost dry.....	56
Figure 3.9: This sample requires twenty 10 mL acetone aliquot rinses to achieve a successfully rinsed sample. Demonstrates: (a) side view of all 20 rinses; (b) top view of all 20 rinses; (c) side view of last rinse and first 5 rinses to show dramatic color differences; (d) top view of last rinse and first 5 rinses.....	59
Figure 3.10: Comparison of (a) original dry sample and (b) acetone rinsed sample.....	60
Figure 3.11: Comparison of (a) original dry sample and (b) acetone dried sample.....	61
Figure 4.1: Diagram from Anouar <i>et al.</i> (202) of experimental versus calculated λ_{\max} values for various polyphenols that include: dihydroflavonols/flavanones, flavones/flavonols and anthocyanidins.	67
Figure 4.2: Chromatograms of original ACN pepper extract at (a) 340 nm (b) 540 nm. The retention times of the major ACN peak at 340 nm is 32.149 min and at 540 nm is 32.859 min.	70
Figure 4.3: Example of a contaminated/impure pepper extract that cannot be used for fraction collection due to co-elution of components. The retention times for these co-eluting peaks are at 34 minutes.	72
Figure 4.4: Bright pink colored run off solution collected as a fraction from the HPLC.	73
Figure 4.5: Sample chromatogram of fraction collection above 2.00 AU (red line); collection time corresponds to $t_R = 35.82$ min to 36.55 min (0.73 min or 43.8 sec).	74
Figure 4.6: Chromatogram of concentrated purple pepper extract at 340 nm. The retention times are 34.328 and 34.974 minutes for the major ACN peaks.....	81
Figure 4.7: Chromatogram of the concentrated purple pepper extract at 540 nm. The retention time is 34.260 minutes for the major ACN peak.	82
Figure 4.8: Gradient curve shape graph provided with the HPLC by the manufacturer, Waters Corporation (206).	85
Figure 4.9: HPLC chromatograms of (a) concentrated purple pepper extract at 540 nm; (b) Blue Ribbon Iris standard at 540 nm and (c) eggplant peels at 520 nm by Ichiyanagi <i>et al.</i> (10).....	86
Figure 5.1: Illustration of the application ranges of different mass spectrometric and chromatographic coupling methods (207).	90
Figure 5.2: Image of electrospray ionization source (208).....	91
Figure 5.3: Chromatograms from LC-PDA-ESI-MS/MS. Abbreviations, PP = purple pepper (freeze-dried), CC = Chinese celery, CE = Chinese eggplant. (a) PP at 350 nm; (b) PP & CC at 350 nm; (c) CC at 350 nm; (d) PP at 520 nm; (e) CE & PP at 520 nm; (f) CE at 520 nm. Peak identifications are listed in Table 5.1.....	98
Figure 5.4: Chromatograms from LC-PDA-ESI-MS/MS for the freeze-dried purple pepper at (a) 350 nm and (b) 520 nm. Peak identifications are listed in Table 5.1...	99
Figure 5.5: The UV spectra of peaks in the freeze-dried purple pepper foliage identified as peaks (a) 1, (b) 3, (c) 4, (d) 5, (e) 9, (f) 10, and (g) 11 in Figures 5.3 and 5.4...	100
Figure 5.6: MS/MS spectrum of Dp-3- <i>p</i> -coumru-5-glc, m/z 919 (precursor compound). Loss of the glucose minus water is highlighted in green at m/z 757, loss of the <i>p</i> -coumaroyl and rutinose minus water is highlighted in red at m/z 465 and the remaining aglycone (delphinidin) is highlighted in purple at m/z 303. On the far right is a table of the six common anthocyanidins. Note the molecular weight of delphinidin is 303 g/mol.	104

Figure 5.7: MS/MS spectra of (a) Dp-3- <i>p</i> -coumrut-5-glc; (c) Dp-3-caffrut-5-glc; (b) HPLC chromatogram of purple pepper foliage identifying peaks 3 and 4 in Table 5.1. The UV spectra of each compound is found in the inset.	105
Figure 5.8: HPLC chromatograms for the mass range <i>m/z</i> 918 to 920 of (a) Chinese Eggplant; (b) Purple Peppers. The retention times are circled in blue and nearly identical at 18.85 and 18.71 minutes. The full ion count from the ESI-MS/MS (c) Chinese Eggplant; (d) Purple Peppers. Precursor ion at <i>m/z</i> 919 is circled in green. Product ions at <i>m/z</i> 757, 465 and 303 are circled in red.	108
Figure 5.9: (a) Total Ion Count (TIC) MS spectrum of purple pepper foliage; (b) Total PDA scan; (c) MS/MS spectrum from 18.28 – 19.67 minutes highlighted in blue; (d) MS/MS spectrum from 33.90 – 34.43 minutes highlighted in red.	110
Figure 6. 1: Full scale spectrum of the ¹ H analysis utilizing “zg30” pulse sequence. Abbreviations: MeOD = deuterated methanol and TMS = tetramethylsilane.	118
Figure 6.2: Drawing of the <i>trans</i> isomer of delphinidin-3- <i>p</i> -coumaroylrutinoside-5-glucoside. The molecule is labeled in accordance with the previous NMR data reported by Ichiyanagi <i>et al.</i> (9). This drawing will be used as a key to identifying all of the peaks labeled in the ¹ H spectra. Colors of text correspond to the section of the molecule and are used throughout the zoomed in spectra. Abbreviations: Delphinidin = Dp.	120
Figure 6.3: (a) Spectrum from 9.25 – 7.25 ppm; (b) spectrum from 7.25 – 6.00; (c) spectrum from 5.75 – 4.25. Abbreviations: Dp = delphinidin, <i>p</i> -coum = <i>p</i> -coumaroyl, glyc = glycoside, rham = rhamnosyl, * = possible degradation product or <i>cis/trans</i> isomer and # = unknown impurity. Text color and molecule identification key is in Figure 6.2. Full list of ¹ H shifts can be found in Table 6.3.	122
Figure 6.4: Some zoomed in ¹ H spectra (a) Dp-6 & Dp-8 (<i>cis</i> & <i>trans</i>); (b) 3- <i>O</i> -glyc (<i>cis</i> & <i>trans</i>); (c) rham-4 (<i>trans</i>); (d) <i>p</i> -coum-Cβ (<i>trans</i>). Abbreviations: Dp = delphinidin, glyc =glycoside, rham = rhamnosyl, coum = coumaroyl and * = possible degradation product or <i>cis/trans</i> isomer. Full list of ¹ H shifts in Table 6.3.	125
Figure 6.5: Full scale spectrum of ¹³ C analysis utilizing “zgdc” pulse sequence with CPD sequence “WALTZ-16”. Abbreviations: MeOD = deuterated methanol and TMS = tetramethylsilane.	127
Figure 6.6: Drawing of the <i>trans</i> isomer of delphinidin-3- <i>p</i> -coumaroylrutinoside-5-glucoside. The molecule is labeled in accordance with the previous NMR data reported by Ichiyanagi <i>et al.</i> (9). This drawing will be used as a key to identifying all of the peaks labeled in the ¹³ C spectra. Colors of text correspond to the section of the molecule and are used throughout the zoomed in spectra. Abbreviations: Delphinidin = Dp.	129
Figure 6.7: (a) ¹³ C spectrum from 170 – 145 ppm; (b) spectrum from 135 – 110 ppm. Abbreviations: Dp = delphinidin, <i>p</i> -coum = <i>p</i> -coumaroyl, * = possible degradation product or <i>cis/trans</i> isomer and # = unknown impurity. Full list of ¹³ C shifts can be found in Table 6.4.	130
Figure 6.8: (a) ¹³ C spectrum from 110 – 90 ppm; (b) spectrum from 455 – 0 ppm. Abbreviations: Dp = delphinidin, glyc = glycoside, rham = rhamnosyl, # = unknown impurity and TMS = tetramethylsilane. Full list of ¹³ C shifts can be found in Table 6.4.	131

Figure 6.9: ^{13}C spectrum from 80 – 62 ppm. Abbreviations: glyc = glycoside, rham = rhamnosyl, * = possible degradation product or <i>cis/trans</i> isomer and # = unknown impurity. Full list of ^{13}C shifts can be found in Table 6.4.	132
Figure A.1: Counterpart to Figure 4.6. Chromatogram of duplicate analysis of the concentrated purple pepper extract at 340 nm.	153
Figure A.2: Counterpart to Figure 4.7. Chromatogram of duplicate analysis of the concentrated purple pepper extract at 540 nm.	154
Figure B.1: Spectra from concentrated purple pepper: (a) Total Ion Count MS, (b) UV-PDA, and (c) full ESI MS, circled in blue are the $m/z = 919$ (precursor ion), product ions at $m/z = 757$ and 303.	155
Figure B.2: Spectra of the freeze-dried purple pepper: (a) Total Ion Count MS, (b) PDA, and ESI Full MS, circled in blue are the $m/z = 919$ (precursor ion), product ions at $m/z = 757$, 465 and 303.	156
Figure B.3: Spectra of the Chinese eggplant plant extract: (a) Total Ion Count MS, (b) PDA, and ESI Full MS, circled in blue are the $m/z = 919$ (precursor ion), product ions at $m/z = 757$ and 303.	157
Figure B.4: Spectra from concentrated purple pepper: (a) Total Ion Count MS, (b) UV-PDA, and (c) full ESI MS, circled in blue are the $m/z = 919$ (precursor ion), product ions at $m/z = 757$ and 303.	158
Figure B.5: Spectra from concentrated purple pepper: (a) Total Ion Count MS, (b) UV-PDA, and (c) full ESI MS, circled in blue are the $m/z = 919$ (precursor ion), product ions at $m/z = 757$ and 303.	159
Figure C.1: Graphical representation of pulse sequence “zg30”. D1 = relaxation delay, DE = Pre-scan delay, AQ = Acquisition Time, P1 = pulse length.	161
Figure C.2: Graphical representation of pulse sequence “zgdc”; D1 = relaxation delay, DE = Pre-scan delay, AQ = Acquisition Time, P1 = pulse length, PL12 = power level for CPD/BB decoupling.	162
Figure C.3: Waltz-16, the composite pulse decoupling (CPD) sequence utilized in the ^{13}C measurement with ^1H decoupling for the concentrated ACN sample (241).	162
Figure C.4: (a) ^1H spectrum from 4.25 – 3.23; (b) ^1H spectrum from 1.73 – -0.5; Abbreviations: MeOD = deuterated methanol, rham = rhamnosyl and * = possible degradation product or <i>cis/trans</i> isomer. Full list of ^1H shifts in Table 6.3.	164
Figure C.5: Some zoomed in ^1H spectra (a) Dp-4 (<i>cis</i> & <i>trans</i>); (b) Dp-2' (<i>cis</i> & <i>trans</i>); (c) rham-1 (<i>trans</i>); (d) rham-6 (<i>trans</i>). Abbreviations: Dp = delphinidin, rham = rhamnosyl, * = possible degradation product or <i>cis/trans</i> isomer and # = unknown impurity. Full list of ^1H shifts in Table 6.3.	165
Figure C.6: Some zoomed in ^1H spectra (a) 5- <i>O</i> -glyc (<i>trans</i>); (b) <i>p</i> -coum-2 (<i>cis</i> & <i>trans</i>); (c) <i>p</i> -coum-3 (<i>trans</i>); (d) <i>p</i> -coum-C α (<i>trans</i>). Abbreviations: glyc = glycoside, coum = coumaroyl and * = possible degradation product or <i>cis/trans</i> isomer and # = unknown impurity. Full list of ^1H shifts in Table 6.3.	166
Figure D.1: Mature pepper plants that have been stripped of their leaves and placed in the carbon dioxide (CO_2) Plexiglas chamber inside of a larger growth chamber. See Section D.3 for definitions of PID controller, IRGA, Solenoid Valve and sub-irrigation opening.	168

Figure D.2: Photograph outside of the growth chamber, on the back wall of the growth chamber (adjacent to muffin fan, which is inside Plexiglas box, inside growth chamber). The micrologger, PID controller, IRGA and solenoid valve setup (linked directly to CO ₂ tank). Water bath setup is shown in Fig. D.3.....	171
Figure D.3: Outside of the growth chamber, on back wall of the growth chamber. The water bath that controls the coldfinger inside of the Plexiglas box that is inside the growth chamber. This helps to control the humidity inside the Plexiglas box. See a picture of the coldfinger in Fig D.4.	172
Figure D.4: Picture of inside the Plexiglas box, inside of the growth chamber. The coldfinger, which is controlled by the water bath (outside the growth chamber) is seen along the side of the Plexiglas chamber and helps to maintain the humidity levels inside the Plexiglas chamber.	173
Figure D.5: Graphical representation of the data in Table D.1 depicting the volume of CO ₂ consumed (i.e. entered the Plexiglas chamber) each day that data was collected.	174
Figure D.6: Growth chamber in Building 010A that is temperature and humidity controlled. Testing optimal growing conditions for purple peppers.	178

List of Abbreviations

ACN – Anthocyanin

ACNs – Anthocyanins

ARS – Agricultural Research Service

AU – Absorbance Units

BARC – Beltsville Agricultural Research Center

BBO – Broadband Observe

brs – Broad singlet

caff – Caffeoyle

coum – Coumaroyl

CPD – Composite Pulse Decoupling

Cy – Cyanidin

d – Doublet

δ – Multiplicity

Dp – Delphinidin

Dp-3-*p*-coumru-5-glc – Delphinidin-3-*p*-coumaroylrutinoside-5-glucoside

ESI – Electrospray Ionization

EtOH – 200 proof Ethanol

FDA – U.S. Food and Drug Administration

FW – Fresh weight

GIFVL – Genetic Improvement of Fruits and Vegetables Laboratory

glc/gluc – Glucoside

glyc – Glycoside

GRAS – Generally Recognized As Safe

HAc – Acetic Acid

HCOOH – Formic Acid

HPLC – High Performance Liquid Chromatography

IRGA – Infrared Gas Analyzer

J – Indirect coupling, spin-spin splitting, in Hertz

LC-PDA-ESI-MS/MS – Liquid Chromatography with Photodiode Array detection coupled with Electrospray Ionization Tandem Mass Spectrometry

m/z – Mass to Charge ratio

MeOD – Deuterated Methanol

MS – Mass Spectrometry

MS/MS – Tandem Mass Spectrometry

Mv – Malvidin

MW – Molecular Weight

NMR – Nuclear Magnetic Resonance

NOE – nuclear Overhauser effect

p – Para substitution

PDA – Photodiode Array

Pg – Pelargonidin

PID – Proportional-Integral-Derivative

Pn – Peonidin

PSI – Plant Sciences Institute

Pt – Petunidin

RB – Round bottom (flask)

rham – rhamnosyl

rotovap – Rotary Evaporator

rut – Rutinoside

s – Singlet

t – Triplet

TFA – Trifluoroacetic Acid

TIC – Total Ion Count

TLC – Thin Layer Chromatography

TMS – Tetramethylsilane

t_R – Retention Time

USDA – U.S. Department of Agriculture

USP – U.S. Pharmacopeial Convention

z_0 – Start position of NMR pulse on z-axis at 0°

Chapter 1: Background

Overview

Chapter 1 outlines the objectives and goals of this study in Section 1.1. A brief description of purple peppers, anthocyanins and the uniqueness of the major anthocyanin known as delphinidin-3-*para*-coumaroylrutinoside-5-glucoside (Dp-3-*p*-coumrut-5-glc) found in the purple pepper foliage is given in Section 1.2. Section 1.3 is a discussion on the factors affecting the bioavailability of anthocyanins in both human and animals. A concise description of the developed food-grade extraction protocol to remove the intact major anthocyanin from the purple pepper foliage is presented in Section 1.4. The analytical techniques utilized to confirm the presence and structure of Dp-3-*p*-coumrut-5-glc are listed in Section 1.4.1. Finally, Section 1.5 is a discussion on the loss of funding for the human feeding study to investigate the bioavailability of the anthocyanin extract that was produced from the food-grade extraction protocol.

1.1: Objectives

Today many people have begun to take a closer look at their eating habits and are trying to live a healthier lifestyle. This includes eating a well balanced diet, regular exercise and taking supplements such as flavonoids, specifically anthocyanins (ACNs) to promote overall health. As science seeks to promote healthy lifestyles, data must be collected to inform the public about what to eat, what supplements to consume and in what quantities. Anthocyanins (ACNs) are part of the larger plant group known as the flavonoids (1). Anthocyanins give color to fruits, vegetables and flowers (2). Research

suggests that they have health-promoting properties, such as antioxidative activity (3). Anthocyanins (ACNs) will be discussed at length in Chapter 2. The healthy-living movement and the economic impact (4) of the 30 billion dollar supplemental nutrition industry prompted scientists at the U.S. Department of Agriculture (USDA), Agricultural Research Service (ARS) in Beltsville, Maryland, to investigate plant material as potential supplement sources of ACN. Previous research suggests the major component present in the foliage of *Capsicum annuum* L. (Family: Solanaceae), a purple pepper cultivar, is an ACN. The ACN associated with purple peppers is robust and well suited for extraction making it an excellent candidate for nutritional studies. (5).

The objectives of this study were to:

1. Grow purple pepper foliage in a controlled $^{13}\text{CO}_2$ environment (Appendix D) to be harvested and utilized in a food-grade extraction of the major anthocyanin.
2. Develop an efficient food-grade extraction and isolation method (Chapter 3) for the major anthocyanin found in purple peppers.
3. Apply analytical techniques that would confirm the anthocyanin structure including high performance liquid chromatography (HPLC) analysis (Chapter 4), mass spectral (MS) analysis (Chapter 5) and nuclear magnetic resonance (NMR) (Chapter 6).
4. Use isolated and structurally confirmed ACN in a human feeding study in order to determine which form of ACN, acylated or non-acylated, was more bioavailable.

1.2: Purple Peppers and Anthocyanins

Researchers worldwide have studied anthocyanins for the last century. They are found ubiquitously in nature coloring the fruits, vegetables, and flowers. Anthocyanins are composed of an aglycone (i.e. anthocyanidin), a sugar and usually an acylation group, as shown in Figure 1.1.

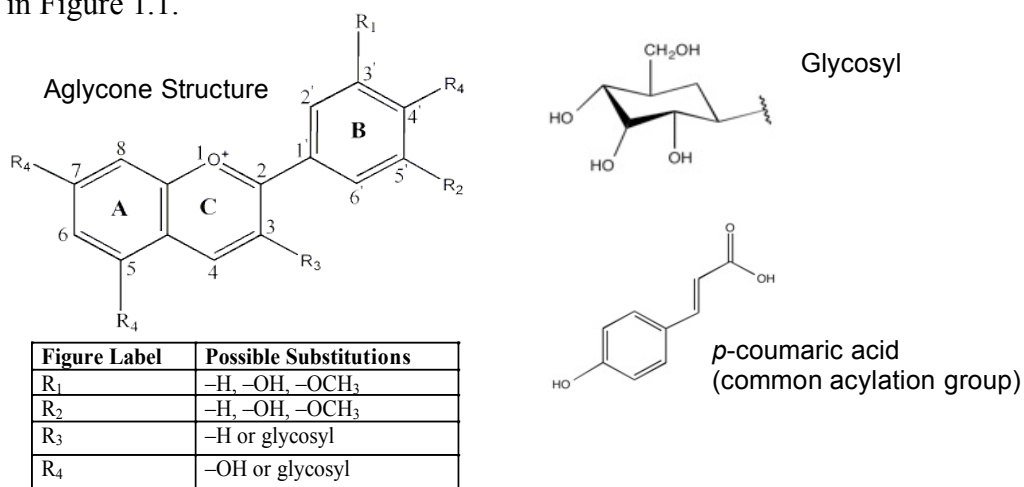


Figure 1.1: Backbone structure of all anthocyanins is the aglycone (i.e. anthocyanidin) and it must have a sugar (i.e. glycosyl) and usually an acylation group (i.e. *p*-coumaric acid) attached to the sugar in order to form an anthocyanin.

All anthocyanins are created from the aglycone backbone structure, which is also known as an anthocyanidin (discussed in Section 2.1), and every natural aglycone is created using the four substituents of -H, -OH, -OCH₃ and -glycosyl at the sites labeled R₁, R₂, R₃ and R₄ in Fig. 1.1. Anthocyanins must have a sugar attached to the aglycone and usually one or more acylation groups attached to the sugar. Many colored fruits and vegetables with blues, purples and reds hues contain anthocyanins. Foods containing anthocyanins are almost always found with a combination of multiple anthocyanins. More than 600 structurally different anthocyanins have been isolated from fruits and vegetables in combinations that can range from 2 anthocyanins all the way up to > 20

anthocyanins (6,7). As examples, blueberries contain 15 structurally different ACNs and grapes have been found to contain 21 ACNs (6,7). Due to these complex combinations of ACNs it is difficult to identify the most bioavailable ACN structural form. A contributing factor is that nutritional studies are usually conducted by feeding humans (or animals) whole fruits and vegetables. Although this type of study actively maintains the natural ACN structure, it introduces many variables when determining bioavailability because there is no way to distinguish what ACN or combination of ACNs is producing the suggested health-promoting effects. These health effects are discussed at length in Chapter 2, Section 2.5. The unique attribute about this investigation is the purple pepper is known to have a high concentration of a single anthocyanin, known as delphinidin-3-*p*-coumaroylrutinoside-5-glucoside (5,8); shorthand name in this document will be Dp-3-*p*-coumrut-5-glc. This allows the researcher to more easily extract and concentrate the major ACN so that it can be utilized in a feeding study, thus reducing the variables dramatically (i.e. only analyzing urine and blood for presence of a single ACN instead of many ACNs) and more accurately determine the most bioavailable ACN form. An extensive discussion of anthocyanin structure, chemistry, and research are found in Chapter 2.

The purple pepper plant used in this investigation is not a culinary pepper, but instead an ornamental plant. As an ornamental pepper it is not used for consumption of the fruit produced, but instead to beautify gardens and flowerbeds with its dark purple leaves and bright red, mature peppers. The scientists responsible for the development of this pepper plant are from the Beltsville Agricultural Research Center (BARC) Plant Sciences Institute (PSI), specifically the Genetic Improvement of Fruits and Vegetables

Laboratory (GIFVL) and specialize in plant genetics, as well as anthocyanin chemistry at the USDA-ARS in Beltsville Maryland.

1.2.1: The Uniqueness of the Major Anthocyanin from Purple Peppers

Lightbourn *et al.* (5) and Sadilova *et al.* (8) identified the anthocyanin in *Capsicum annuum* fruit (i.e. violet and black peppers) and black/purple leaves to be delphinidin-3-*p*-coumaroylrutinoside-5-glucoside (Dp-3-*p*-coumru-5-glc). Lightbourn *et al.* (5) reported a very high concentration of Dp-3-*p*-coumru-5-glc in the black foliage, at 152.5 mg/100 g fresh weight (FW). Sadilova *et al.* (8) identified both the *cis* and *trans* isomers of Dp-3-*p*-coumru-5-glc in violet pepper fruit and reported much lower concentrations at 1.47 mg/100 g FW for the *cis* isomer and 28.62 mg/ 100g FW for the *trans* isomer. This data was obtained through the use of HPLC and MS analyses. These studies correlate well with the research and findings of Ichianagi *et al.* (9,10) who also identified the *cis* and *trans* isomers of Dp-3-*p*-coumru-5-glc in eggplant peels, as shown in Figure 1.2, but also reported low recoveries of the two isomers at 0.125 mg/100g FW for the *cis* isomer and 0.57 mg/100 g FW. Interestingly, these plant sources are both in the family Solanaceae. Based on previous data, the purple pepper foliage has a much higher ACN concentration in terms of mg/100g FW when compared to the ACN values reported for violet pepper fruit and eggplant peels.

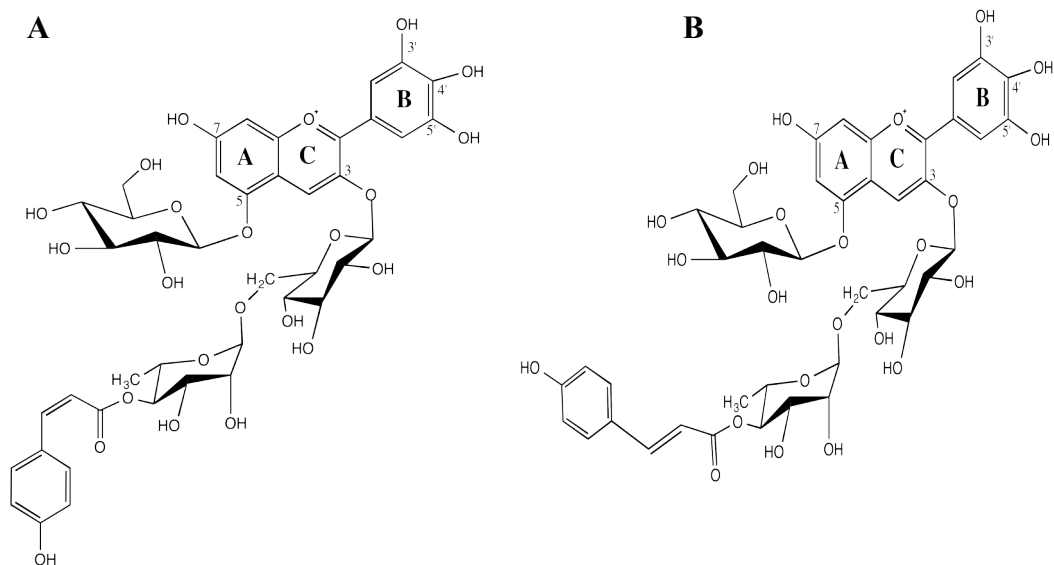


Figure 1.2: Illustrations of delphinidin-3-*p*-coumaroylrutinoside-5-glucoside (a) *cis* isomer, and (b) *trans* isomer.

The high concentration of ACN in the purple pepper foliage, both the *cis* and *trans* isomers of Dp-3-*p*-coumrut-5-glc, was a driving force to form the collaborative study at BARC and for the scientists to seek out a chemist (i.e. the researcher of this investigation) to create an effective extraction method so this single anthocyanin could be subjected to bioavailability studies. Bioavailability studies usually consist of a human or animal consuming a sample containing a known concentration of an analyte. In this project, the analyte would be Dp-3-*p*-coumrut-5-glc from the pepper foliage. Then analyzing the blood (including plasma), urine or stool for the presence of the intact analyte through the use of HPLC separation and UV-Vis or photodiode array (PDA) detection (11). The pharmacological definition of bioavailability (12) is the fraction of the dose of an analyte that remains unchanged after ingestion and excretion. It states the analyte is considered more bioavailable if a large concentration of the intact analyte is able to pass through the body unaltered or un-metabolized versus an analyte that is less

bioavailable that would only detect a small concentration of the intact analyte (11). At first glance this definition seems counterintuitive for a natural product where you expect it to be metabolized by the body. Natural products chemists are more interested in what reacts with the body, especially when health benefits have been claimed, so what is being metabolized by the body and altered has significance. As discussed in Section 1.3.2, many bioavailability studies use whole foods, but extracts and powders are also acceptable. It goes without saying that very few people would volunteer to eat bitter leaves as part of an anthocyanin bioavailability study, thus the great importance of developing a food-grade extraction method so that the scientists could feed the volunteers a more palatable extract. Additionally, this ACN is naturally acylated and more research is still needed to determine the absorption of acylated ACNs in order to clarify the most bioavailable form of ACNs.

1.2.2: Current Research on delphinidin-3-*p*-coumaroylrutinoside-5-glucoside

The compound of interest, delphinidin-3-*p*-coumaroylrutinoside-5-glucoside (Fig. 1.2), was identified in the foliage of purple peppers by both Lightbourn *et al.* (5) and Sadilova *et al.* (8) and initiated further investigations on Dp-3-*p*-coumrut-5-glc in the purple pepper, and ultimately this research project was the result. This delphinidin derivative is not only found in purple pepper foliage but also in eggplant peels. The most in-depth identification of this compound was conducted by Ichianagi *et al.* (9,10) and utilized HPLC, MS and NMR to determine both the *cis* and *trans* isomers. Specifically, the HPLC, MS and NMR data from Ichianagi *et al.* were utilized as a guide for this research investigation, and were extremely helpful for comparison purposes of the major

ACN found in purple pepper foliage (Chapters 3-6). Other researchers also studied this compound in eggplant peels but with a focus on different areas such as: the antioxidant capacity by Noda *et al.* (13), antioxidant activity by Azuma *et al.* (14), and early identification using thin layer chromatography (TLC) by Tanchev *et al.* (15). Another investigation by Tatsuzawa *et al.* (16) found the ACN of interest, as well as other ACNs, in the flower *Petunia reitzii* through the use of MS and NMR analyses.

1.3: Factors that Affect the Bioavailability of Anthocyanins

For the purpose of this investigation it was vital to learn what forms of anthocyanins had already been subjected to absorption or bioavailability studies. It is well known that anthocyanins are water-soluble molecules and are found abundantly in nature in many flowers, fruits and vegetables (1), with over 600 naturally occurring ACNs. There has been an abundance of research utilizing animal models, such as rats, pigs and rabbits (17–38), as well as human models (39–55), to study anthocyanin bioavailability. The animal studies traditionally use very large doses on the order of several hundred milligrams per kilogram body weight (11). Food sources used in these studies are very anthocyanin-rich foods like elderberry, bilberry, black currant and purple corn, purple rice, chokeberry and raspberry. In nearly all of these studies, the ACN glycosides were the only ACNs being observed (no aglycones were observed) in the plasma and urine from these animals. According to Novotny (11), all these studies demonstrated three major trends that include: (a) peak plasma response after the dose is very quick, usually ≤ 2 hours, (b) low peak plasma concentrations, usually ≤ 1 micromolar, and (c) $\leq 1\%$ recovery of ACNs in urine. Overall, these researchers concluded that for, the most part,

ingested ACNs are absorbed intact and reach their peak plasma concentrations very quickly (11).

When it comes to human studies, the research supports the conclusions of the animal studies despite the fact that it is unclear how important ACN degradation products are in understanding bioavailability and how scientists can detect these effectively. The human studies tend to also use large doses of ACNs in the forms of extracts, powders or whole foods like blueberry, blackberry, elderberry, boysenberry, and chokeberry. These ACN doses are more realistic in nature and could actually be achieved by consumption of a large serving of an anthocyanin-rich food, such as blueberries or strawberries. The dosage is traditionally around several hundred milligrams, but some studies have used doses ≥ 1 gram, which is extremely high (11). Again, the results have similar trends to those seen in the animal studies, with short peak plasma concentration times, usually ≤ 2 hours. This is interesting because other polyphenols that are consumed by humans absorb at a much slower rate than what is observed in the ACN studies (56). The ACNs are detected in the urine anywhere between 2 and 4 hours after consumption, which is also very fast. Observed low peak plasma concentrations (> 100 ng/mL) and a fraction of a percent for urinary recovery do not match data for other polyphenols, which tend to have high peak plasma concentrations in most studies (56). Again, these studies conclude that ACNs are absorbed as intact molecules, but many of the researchers suggest that metabolites and degradation products are truly the key to deciphering the real bioavailability of ACNs (11).

1.3.1: Anthocyanin Bioavailability Trends

Many research studies on the bioavailability of anthocyanins have been performed using grape juice and/or red wine due to the high number of anthocyanins (6) found in grapes (21 ACNs) and the abundant consumption of both grape juice and red wine by humans. A majority of the ACNs found in grapes are mono or diglucosides and only a small percentage of these glucosides are acylated (6); anthocyanin structures are discussed in Chapter 2, Section 2.1. In the grape ACN absorption investigations (17–19,39–43,47,49,57–59) most research has shown that red grape anthocyanins are only absorbed in small amounts and then excreted from the body as intact glucosides, meaning the body is able to absorb a percentage of the ACNs without having them breakdown. Since the majority of these grape ACNs are non-acylated the data suggests non-acylated ACNs are more bioavailable in comparison to acylated ACNs.

In terms of acylated ACNs, there is a lot of research correlating to increased stability (13–15,35–39,43,45,53–55), specifically the increased stability of pigments (2,6,60–78). Anthocyanin structure and coloring are discussed in Chapter 2, Sections 2.1 – 2.2, copigmentation in Section 2.3 and stability in Section 2.4. When it comes to bioavailability, acylation is certainly a factor but there is not a definitive trend toward acylated or non-acylated ACNs being more bioavailable. One trend leans more toward reducing the bioavailability of an ACN when there is an acyl moiety, as shown in Figure 1.3, such as *p*-coumaric, caffeic, ferulic, and sinapic acid attached to the sugar of the ACN (6). Some research has shown acylated ACNs are not recovered in urine and plasma as effectively as their non-acylated counterparts (11,24,50,52,55,79). This suggests acylated ACNs are less bioavailable in comparison to non-acylated ACNs due to the low

reported recoveries from multiple research investigations by various scientific teams. On the other hand, research by Ichiyanagi *et al.* (10) prepared a Dp-3-*p*-coumru-5-glc mixture (*cis/trans*) using semi-preparative HPLC and demonstrated recovery of intact Dp-3-*p*-coumru-5-glc, by HPLC, in rat plasma at levels of 0.29 μM for the *trans* and 0.04 μM for the *cis* isomers when 94.7 μmol of *trans* and 14.2 μmol of *cis* per kilogram were administered. The rats were starved for 24 h and the Dp-3-*p*-coumru-5-glc mixture (*cis/trans*) was added to the polyethylene tube that had been inserted in the neck vein of the rats, while under anesthesia (10). These levels were compared to Dp-3-glucose, normalized to the orally administered dose (micromoles per kg) and were found comparable (*trans* = 0.2809, *cis* = 0.2655, and Dp-3-glc = 0.2553). This suggests in this case that acylation increases the bioavailability of ACNs, thus making this research investigation so interesting since it could help to solve the mystery of acylation's role in bioavailability. But it is important to note that other factors also play a role in bioavailability.

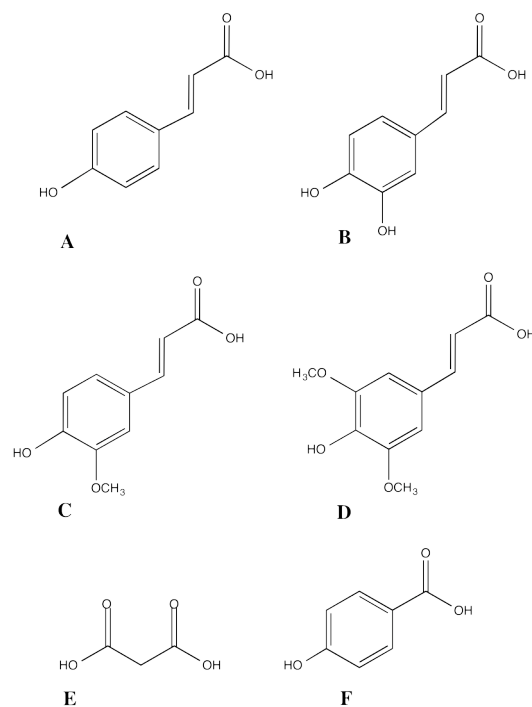


Figure 1.3: Common acylation groups found attached to the sugars, which are attached to the aglycones, that form anthocyanins. (a) *p*-coumaric acid, (b) caffeic acid, (c) ferulic acid, (d) sinapic acid, (e) malonic acid and (f) *p*-hydroxybenzoic acid.

Research on acylated ACNs demonstrates varied effects on bioavailability when acylation groups are attached to the sugars on the aglycone. It has been shown that the aglycone structure (or anthocyanidin) significantly affects how well the ACN is absorbed by the body (11). Specifically, pelargonidin anthocyanin derivatives (the major ACN in strawberries) have been observed to be the most easily absorbed ACN in comparison to the other 5 major aglycones (cyanidin, malvidin, peonidin, delphinidin, petunidin), as seen in Figure 1.4, found in nature because they have shown to have high recoveries of intact ACNs around 2% versus a fraction of a percent recoveries for other ACNs (11,19,20,25,41–49,52–55). Some research has found that cyanidin and malvidin derivatives are absorbed more efficiently in comparison to delphinidin derivatives (25,44). In a separate study, Ichiyanagi *et al.* (80) demonstrated delphinidin and cyanidin

glycosides absorbed more effectively than mono- or di-*O*-methyl glycosides of peonidin and malvidin. At best, the data does not give a consistent trend, but it is clear the aglycone plays a role in effectiveness of uptake.

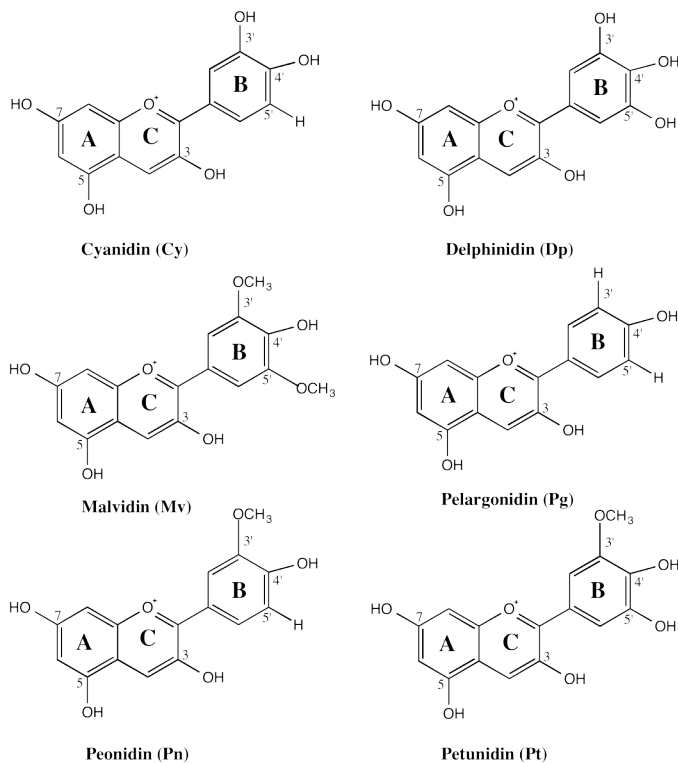


Figure 1.4: Structures of the six most common aglycones (i.e. anthocyanidins) in nature.

Aside from the aglycone affecting how bioavailable an ACN is another major contributor is the sugar moiety, as shown in Figure 1.5, attached to the ACN structure. In the exact same aglycone (e.g. cyanidin) researchers have seen higher rutinose (Fig. 1.5) recovery in urine when compared to glucoside recovery (21). The same phenomenon was observed with sambubioside when it was attached to cyanidin. The recovery for cyanidin monglycosides was lower in comparison to cyanidin-3-sambubioside and cyanidin-3-sambubioside-5-glucoside (21). The research suggests some sugars, possibly disaccharides, are more bioavailable than others. Also, the more sugar moieties that are

attached to the ACN the higher the recovery in urine, therefore increasing the bioavailability (11).

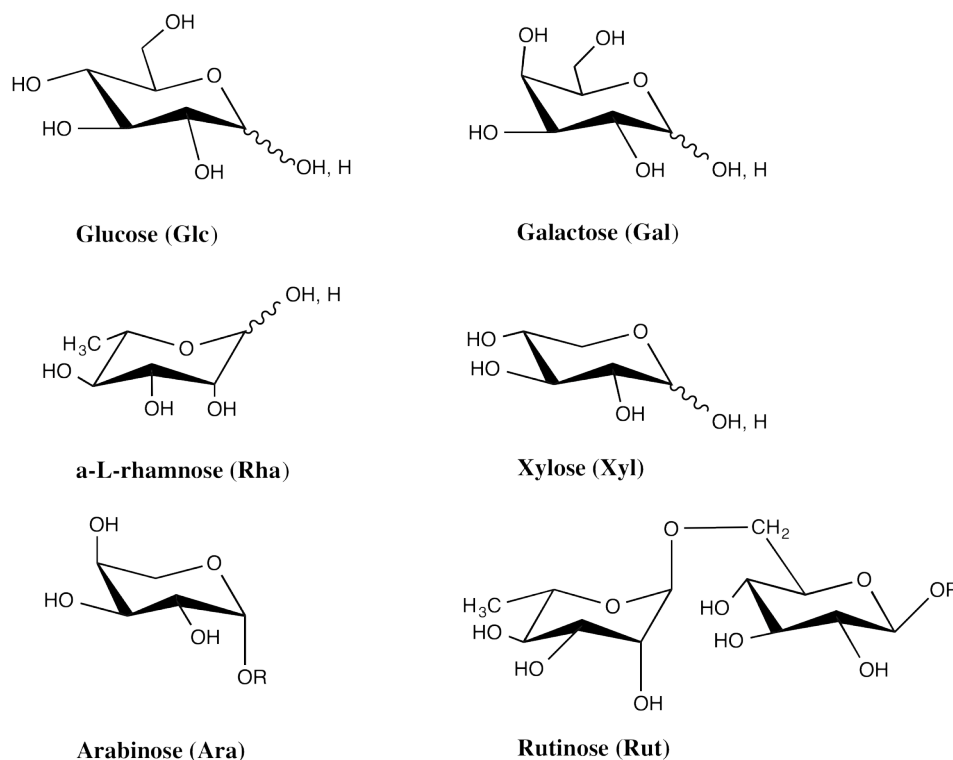


Figure 1.5: Structures of common sugar moieties attached to the aglycone.

Despite all of this research on the sugars and acyl moieties attached to the aglycones there is still not a clear picture of why certain ACNs are more bioavailable than others (i.e. acylated versus non-acylated). Scientists still do not know the exact pathways for ACN absorption and concurrently are unaware of all the possible metabolites or degradation products that are produced when ACNs are absorbed into the body. There is some research demonstrating the formations of different metabolites, such as: protocatechuic acid by Tsuda *et al.* (18), methylation of ACNs by Miyazawa *et al.* (17), and glucuronidation of ACNs by Wu *et al.* (49). Most of this research utilizes photodiode array detection (PDA), i.e. absorption of color, when determining the

presence of intact ACNs in blood, plasma or urine. The major issue with this form of detection is that the body's pH is close to neutral (i.e. pH 7) and ACNs only maintain their original color and structure in acidic conditions around pH 1-2 (See Chapter 2, Section 2.2 for discussion of ACN color). Once the pH rises to 4.5 the ACN changes conformation to the colorless carbional pseudo-base (hemiketal form) and then will irreversibly open to the colorless chalcone (See Fig. 2.3). This would make it nearly impossible to detect ACNs with a PDA if they have been degraded or metabolized since they would no longer be colored.

To date, researchers still need to improve their methods of detection so it is possible to effectively measure ACN metabolites and degradation products. The lack of detection of these compounds could be a large reason why the recoveries of ACNs tend to be so low and, subsequently, why ACNs are currently labeled as compounds with inefficient bioavailability.

1.4: Food-Grade Extraction

The purple pepper extract containing the delphinidin derivative was intended for use in a human feeding study. The human feeding study would facilitate quantification of bioavailability, or how well the body can uptake (i.e. absorb) the compound before it is excreted from the body. Therefore, the extraction method must be food-grade and only use chemicals that are approved by the U.S. Food and Drug Administration (FDA) and considered Generally Recognized As Safe (GRAS) chemicals.

1.4.1: Techniques Used to Confirm the ACN Structure

First, a food-grade extraction protocol was developed to remove the intact ACN from the purple pepper foliage. The extraction method is outlined in Chapter 3, Sections 3.2 thru 3.3. The ACN structure was separated and concentrated through the use of High Performance Liquid Chromatography (HPLC) and is outlined in Chapter 3 and Section 4.2.1 – 4.2.3. Once the ACN was concentrated the purity was evaluated by re-injecting the concentrated sample back onto the HPLC and determining the percent peak area of the Dp-3-*p*-coumru-5-glc peak since there was no commercially available standard of a known concentration available to determine purity. The first characterization technique employed was tandem mass spectrometry (MS/MS). This mass spectrometry technique includes the use of liquid chromatography (LC) with photodiode array detection (PDA) coupled with electrospray ionization (ESI) tandem mass spectrometry (LC-PDA-ESI-MS/MS) and is outlined in Chapter 5. This mass spectrometry technique will validate the molecular mass of the ACN. The MS/MS method of analysis assists in compound identification by determining the total ion mass (i.e. precursor ion) and its ion fragment masses (i.e. product ions), but alone it will not completely identify the structure. Structural elucidation can only be achieved using Nuclear Magnetic Resonance (NMR), and this analysis is outlined in Chapter 6. NMR analyses will confirm exact connectivity of the substituents and provide the structure's name.

1.5: Loss of Funding for Feeding Study

Unfortunately, after the extraction method had produced enough extract for a human feeding study, the funding for this particular feeding study was not renewed at the

Beltsville Human Nutrition Research Center (BHNRC) at BARC. Therefore, the feeding study was never able to take place despite the immense interest from all the scientists in the collaboration. But it must be noted that all of the decisions for chemical choices were based on the goal of this investigation, which was to produce a food-grade extract safe for human consumption, and these chemicals had to be GRAS. If funding were to be reinstated in the future the scientists could produce additional extract using the food-grade extraction method described in this investigation (Chapter 3, Section 3.2 to 3.3) and continue with a human feeding study. If the study required a more concentrated ACN product, the scientists could follow the protocol to concentrate the extract that is described in Section 4.2.1 to 4.2.3. It would be extremely interesting to conduct this study in the future so as to shed some light on the topic of ACN absorption and bioavailability, particularly the role of acylation on the anthocyanin's ability to absorb. This data would enhance the scientific community's knowledge of ACN bioavailability and would allow the USDA to continue to educate the public on ways to live a healthier lifestyle.

Chapter 2: Anthocyanins

Overview

The background information on anthocyanins (ACNs) and how they occur in nature will be articulated here in Chapter 2. Their basic structures are described in Section 2.1 and how the anthocyanins produce a range of colors from reds to blues is discussed in Section 2.2. Copigmentation plays a major role in the color of an anthocyanin and this phenomena is described in Section 2.3. The stability of ACNs is important when dealing with a food-grade extraction protocol and will be covered in Section 2.4. The possible health benefits that ACNs offer are described in Section 2.5, followed by the nomenclature for the major anthocyanin found in the foliage of the purple pepper in Section 2.6. Lastly, a description of the anthocyanin standard utilized in this investigation is discussed in Section 2.7.

2.1: Anthocyanin Structure

Anthocyanins (ACNs) are a class of compounds largely responsible for the colors of many fruits, vegetables, flowers and other plant tissues because of their ability to strongly absorb visible light (*1*). These water-soluble pigments are part of a much larger plant group known as the flavonoids (*1*). Flavonoids are polyphenolic compounds found in virtually all parts of the plant (*1*) and are usually colorless. They are categorized according to their chemical structure into seven categories: flavonols, flavones, flavanones, isoflavones, catechins, anthocyanidins and chalcones (*62*). ACN colors range from red to blue in plants (*81*) and their name comes from the Greek, *anthos* meaning

flower and *kyanos* meaning blue. Multiple factors such as, copigmentation, pH and acyl moieties affect the anthocyanin colors observed in fruits and vegetables today.

The flavylium cation presented in Figure 2.1 a is the basic structure of all ACNs. It consists of an aglycone (also referred to as an anthocyaninidin, Fig. 2.1 a), a sugar(s) (Figure 2.1 b) and usually one or more acyl groups in Figure 2.2 (82). In nature, ACNs are found in a dissolved state at a pH range from 3.5 – 5.5 (63) in the cell sap inside the vacuole of plant cells (81) and may accumulate in the epidermal cells (64). Sequestered in the vacuole, ACNs are relatively stable and hydrophilic, but once extracted through acid hydrolysis they become hydrophobic and unstable, especially to light, temperature and pH (2). These limitations make them slightly more difficult to work with in comparison to other flavonoids, therefore proper handling and storage is necessary to maintain ACN structure and color.

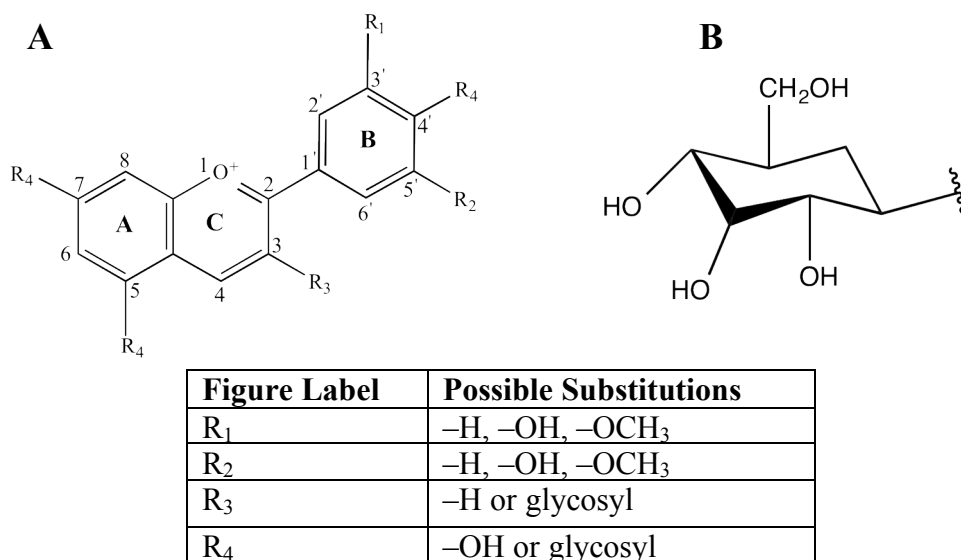


Figure 2.1: (a) The flavylium cation. R values: -H = hydrogen; -OH = hydroxide; -OCH₃ = methoxyl group; (b) A glycosyl group.

All ACNs have the flavylum cation as their skeleton, but variations occur based on the substitutions at the available sites in rings A, B and C. The cyclical structures are in a C6–C3–C6 pattern known as a phenyl-2-benzopyrilium (83) or flavylum cation. Anthocyanins are simply glycosides of flavylum salts (1,6,84,85) and each ACN differs from another by its substituents. These distinguishing factors are: the number of hydroxyl groups attached to the molecule; the degree of methylation of the hydroxyl groups; the nature, number and location of attached sugars (i.e. glycosylation); and the number and location of aliphatic or aromatic acids (i.e. acylation groups) attached to these sugars (6). The commonly attached sugar structures are shown in Figure 2.3. The common acylation groups that attach to the sugars are shown in Figure 2.4. Glycosylated ACNs are found to be more stable and water soluble due to the slow hydrolysis of the 3-O-sugar unit in acidic conditions (1,6). These variables allow for numerous combinations to occur in nature, with the current estimation at greater than 600 ACNs (86). There are a total of seventeen aglycones known to naturally occur and are listed in Table 2.1. The six most common aglycones are: cyanidin (Cy), delphinidin (Dp), malvidin (Mv), pelargonidin (Pg), peonidin (Pn), and petunidin (Pt) (82). The structures of the six common aglycones are shown in Figure 2.2.

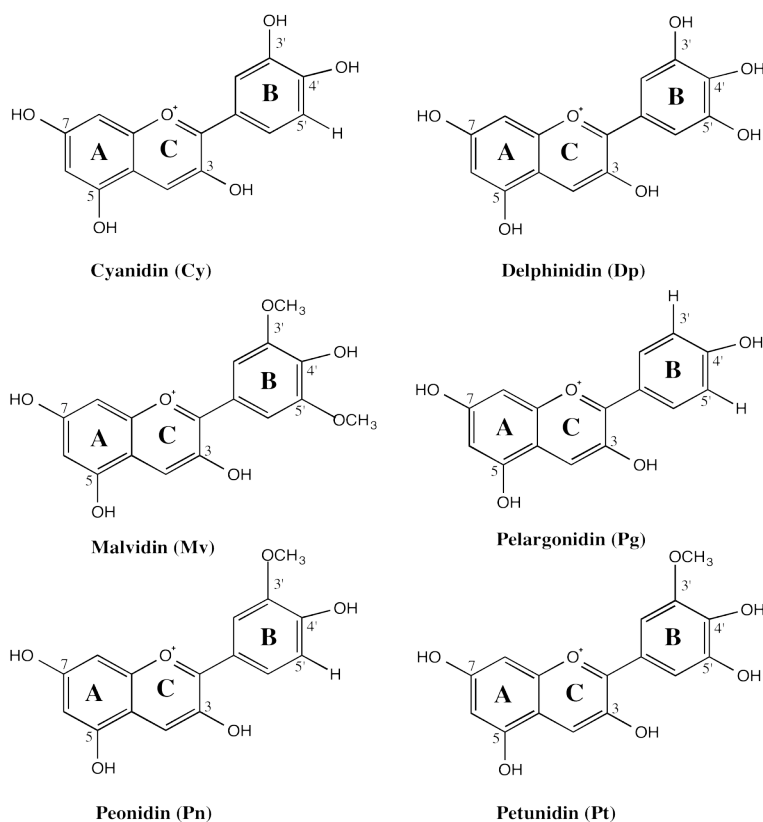


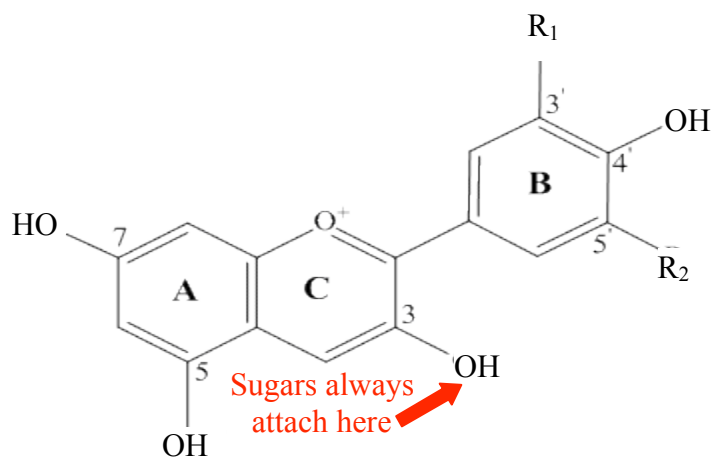
Figure 2.2: Structures of the six most common aglycones found in nature.

Table 2.1: List of the seventeen naturally occurring aglycones (also referred to as anthocyanidins), their substitution patterns and their color. Figure from Kong, *et al.* (82).

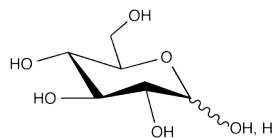
Naturally occurring anthocyanidins

Name	Abbreviation	Substitution pattern							Color
		3	5	6	7	3'	4'	5'	
Apigeninidin	Ap	H	OH	H	OH	H	OH	H	Orange
Aurantininidin	Au	OH	OH	OH	OH	H	OH	H	Orange
Capensininidin	Cp	OH	OMe	H	OH	OMe	OH	OMe	Bluish-red
Cyanidin	Cy	OH	OH	H	OH	OH	OH	H	Orange-red
Delphinidin	Dp	OH	OH	H	OH	OH	OH	OH	Bluish-red
Europinidin	Eu	OH	OMe	H	OH	OMe	OH	OH	Bluish-red
Hirsutidin	Hs	OH	OH	H	OMe	OMe	OH	OMe	Bluish-red
6-Hydroxycyanidin	6OHCy	OH	OH	OH	OH	OH	OH	H	Red
Luteolinidin	Lt	H	OH	H	OH	OH	OH	H	Orange
Malvidin	Mv	OH	OH	H	OH	OMe	OH	OMe	Bluish-red
5-Methylcyanidin	5-MCy	OH	OMe	H	OH	OH	OH	H	Orange-red
Pelargonidin	Pg	OH	OH	H	OH	H	OH	H	Orange
Peonidin	Pn	OH	OH	H	OH	OMe	OH	H	Orange-red
Petunidin	Pt	OH	OH	H	OH	OMe	OH	OH	Bluish-red
Pulchellidin	Pl	OH	OMe	H	OH	OH	OH	OH	Bluish-red
Rosininidin	Rs	OH	OH	H	OMe	OMe	OH	H	Red
Tricetinidin	Tr	H	OH	H	OH	OH	OH	OH	Red

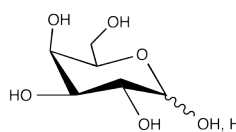
All ACNs are formed from one of the 17 naturally occurring aglycones and will have one or more of the sugars shown in Figure 2.3 attached at the 3 – position.



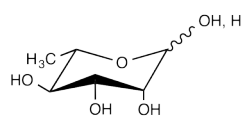
Aglycone	R ₁	R ₂
Cyanidin (Cy)	-OH	-H
Delphinidin (Dp)	-OH	-OH
Malvidin (Mv)	-OCH ₃	-OCH ₃
Pelargonidin (Pg)	-H	-H
Peonidin (Pn)	-OCH ₃	-H
Petunidin (Pt)	-OCH ₃	-OH



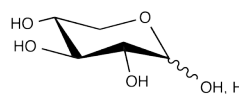
Glucose (Glc)



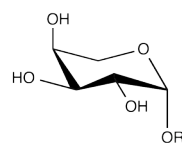
Galactose (Gal)



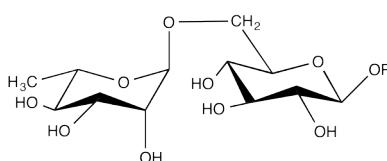
α -L-rhamnose (Rha)



Xylose (Xyl)



Arabinose (Ara)



Rutinose (Rut)

Figure 2.3: The chemical structures of the six most common aglycones (also called anthocyanidins) occurring in nature, with R₁ and R₂ as the possible substituents. Below are the common sugars that attach to the aglycones at the 3– position.

Aglycones are customarily glycosylated and/or acylated by various sugars and acids to form the various anthocyanins found in nature. Sugars are always attached at the 3- position (indicated by the red arrow in Fig. 2.3) but can also be connected to the 5-, 7-, 3'-, 4'-, and 5'- hydroxyl groups (63), and these positions are clearly marked in Figure 2.3. Glycosylated aglycones occur most frequently as: 3-monosides, 3-biosides, and 3, 5-diglycosides, but more rarely occur as 3, 7-diglycosides (82). Glycosylation of the 3'-, 4'-, and 5'- hydroxyl groups have also been found (6). It is less common to have methoxylation, but it does sometimes occur (6). The common sugars (structures are shown in Fig. 2.3) that attach to the aglycones to create ACNs are glucose, galactose, rhamnose, arabinose, and xylose (84); additionally formations of di- and tri-saccharides from these sugars are possible and can glycosylate some aglycones (6). These sugars are usually acylated by the aromatic acyl groups (most common acylation group structures are shown in Fig. 2.4) containing *p*-coumaric, caffeic, ferulic, sinapic, and *p*-hydroxybenzoic acid but acylation by malonic, oxalic, malic, succinic or acetic acid has also been reported (6).

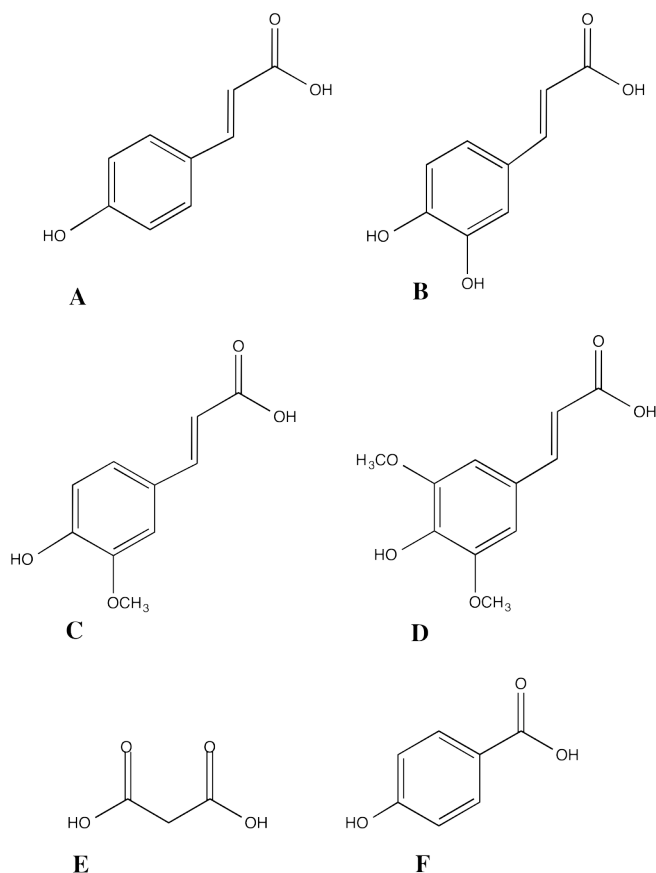


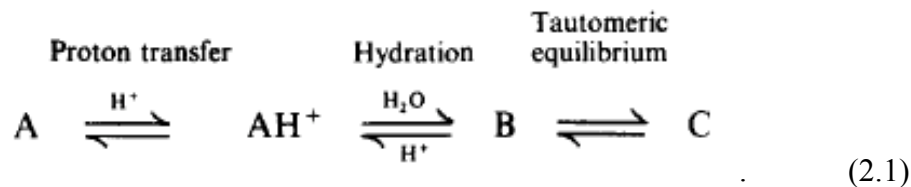
Figure 2.4: Common acylation groups found attached to sugars on the flavylum cation, (a) *p*-coumaric acid, (b) caffeic acid, (c) ferulic acid, (d) sinapic acid, (e) malonic acid and (f) *p*-hydroxybenzoic acid.

In terms of structure, the 3-, 5- and 7- positions are the most substituted positions of the aglycone and define all the different ACN variations illustrated in Table 2.1. The 3-position of the aglycone is essential to ACNs for two reasons. First, this is where acylated sugars always attach and secondly, every ACN contains a sugar in this position even if it is not acylated (63). If acylated, the acyl moiety is most often linked to the 6-position of the sugar substituent, but can occur at the 2-, 3- and 4- positions as well (60). There are no known ACNs that have all three hydroxyl groups substituted at the 5-, 7- and 4'- positions simultaneously. It is imperative to have a free hydroxyl group in one of

these three positions in order to form the colored quinonoidal structure, which gives flowers and fruit their colors. According to (82) Kong *et al.*, the glycosides of the most prevalent non-methylated aglycones, Dp, Cy and Pg, can be found in 80% of pigmented leaves, 69% of fruits and 50% of flowers. This fact demonstrates why extracting and isolating the major ACN in purple pepper foliage is so advantageous because the amount of Dp-3-*p*-coumru-5-glc is at such a high concentration (152.5 mg/100 g FW) (5) and will be an excellent plant source.

2.2: Anthocyanin Color

Inside the plant cell vacuole, ACNs occur in equilibrium as four molecular species known as: the quinonoidal base (A), flavylium cation (AH⁺), carbinol pseudobase (B) and colorless chalcone (C) and this equilibrium is best represented in Figure 2.4 (63). There is an interconversion between these four structures and it is based on the kinetics studies of Brouillard & Dubois, 1977, and Brouillard & Delaporte, 1977 & 1978 (65–67). This interconversion is best illustrated by Equation 2.1 from Timberlake, 1980 (63):



The flavylium cation and quinonoidal base are the only two species that absorb visible light and the degree of their color absorption depends on their concentration at a certain pH (68). According to Timberlake (63), the red flavylium cation forms (AH⁺) when the blue quinoidal base (A) of a 3-glucoside ACN is protonated. AH⁺ can then be

hydrated to form a carbinol pseudobase (B), which is colorless. B can also exist in tautomeric equilibrium with its colorless chalcone (C) that is formed by the opening of the heterocyclic (i.e. pyrylium) ring (63). The simplest way to explain the formation at equilibrium of each of the four species based on pH changes is in the distribution graph seen in Figure 2.6.

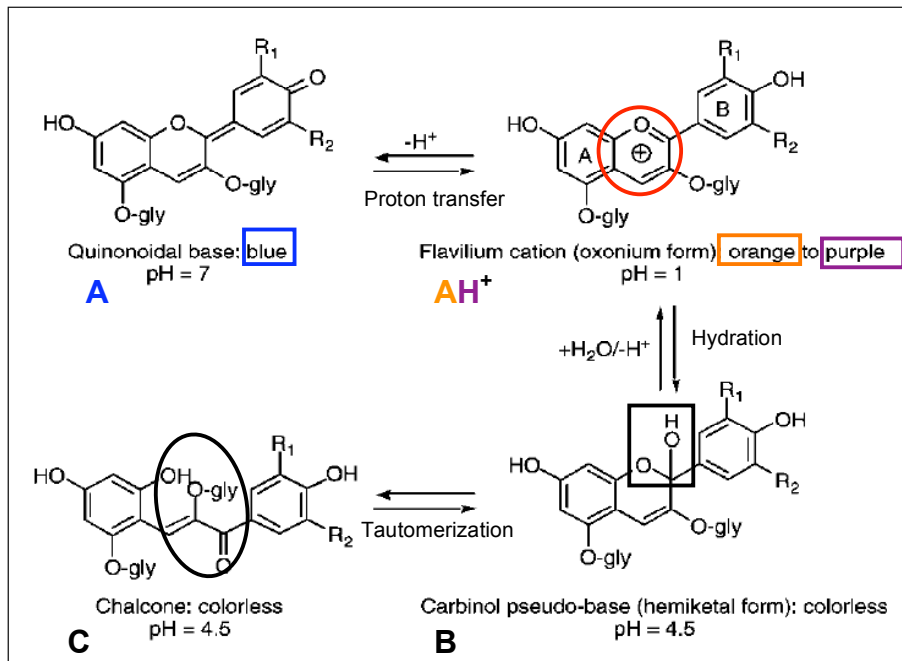


Figure 2.5: Structural transformations of ACN pigments with change in pH. Pyrylium ring is designated by red oval in flavilium cation. Figure adapted from Wrolstad, 2004 (74).

These four equilibrium species are a large contributor to the ACN colors observed in nature. If the hydration reaction can be inhibited or deterred during the food-grade extraction then the flavilium cation will be maintained, thus the deep purple color of Dp-3-*p*-coumru-5-glc from the foliage will not change once it has been extracted from the foliage.

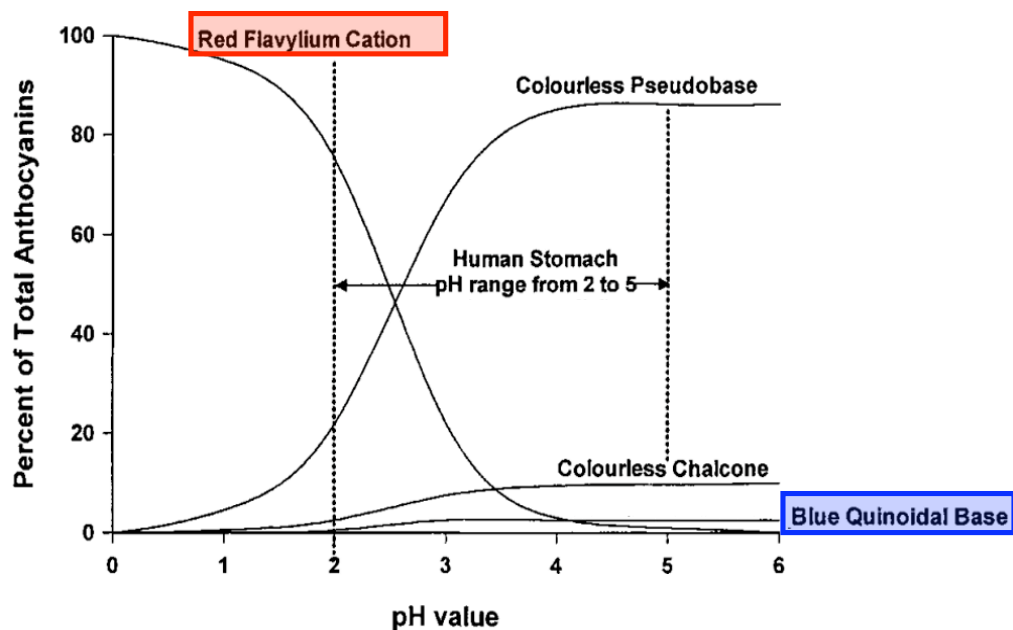


Figure 2.6: The generalized effect of pH value on ACN equilibria. Figure from Clifford, 2000 (87).

The four molecular species in equilibrium depicted in Figures 2.5 and 2.6 are extremely important to the development of the food-grade extraction method because if the colored flavylium cation is not maintained at a $\text{pH} \leq 2.5$ then the percent of total ACN will significantly drop to $< 50\%$. If the $\text{pH} > 4.5$, there is nearly no flavylium cation and the colorless pseudobase and colorless chalcone will form with a very small concentration of the blue quinoidal base. It is essential to understand the kinetics of molecular species in order to maintain a high percent of total ACN in the extract from the purple pepper foliage.

2.3: Copigmentation

In nature, ACNs form complexes with other flavonoids called copigments in order to produce the colors seen in plants. Copigmentation was defined as early as 1931, by Robison & Robison (69) as a bluing effect on ACNs by flavones and other related compounds. Osawa (70) defines copigmentation as, "...the phenomenon which makes the color of anthocyanins bluer, brighter, and stabler due to interactions between organic substances and anthocyanins, even at the pH of living tissues." The role of the copigment is to protect the pyrylium ring (red circle in Fig. 2.5) from the nucleophilic attack of water (71). It is known that the most common copigments are tannins, but flavones, flavonol glycosides and anthocyanins themselves can in fact be copigments (72). Copigmentation is affected by nine major factors: type of ACN, ACN concentration, and type of copigment, copigment concentration, pH, and temperature, metals, heredity, and multifactorial effects on copigmentation (64, 70, 72). Every ACN reacts differently to these copigments based on the nine major factors and the molar ratio of copigment to anthocyanin is important since Asen *et al.* (72, 73) determined the ACN concentration was the limiting factor in copigmentation.

2.3.1: Intramolecular and Intermolecular Copigmentation

The two types of copigmentation that occur in ACNs are known as intramolecular and intermolecular copigmentation. According to Brouillard (64), intramolecular copigmentation involves a copigment that is a part of the ACN molecule, while intermolecular copigmentation involves a copigment that is not covalently bound to the ACN molecule itself. In general, copigments themselves are colorless, but when

concentrations are high enough they have the ability to enhance the color and stability of the ACN significantly. Studies have shown that intramolecular copigmentation is more favorable and efficient than intermolecular copigmentation (64).

When an ACN has one or more acyl groups, they deter the hydrolysis of the red flavylum cation, thus inhibiting the formation of the colorless pseudobase and instead forming the more favorable blue quinonoidal base (Figs. 2.5 and 2.6). This is known as intramolecular copigmentation and usually yields more bluish colored ACNs at pH values < 7 (60).

Intramolecular copigmentation occurs in ACNs with two or more aromatic acyl groups. It involves the stacking of the aromatic residue of acyl groups with the pyrylium ring of the flavylum cation. This stacking decreases hydration at the C-2 and C-4 positions (Fig. 2.1 a) of the flavylum cation, thus forming a more stable complex with a more intense color (6,63,64,71). The most accepted reasoning for these highly stable colors is water's inability to attach to the molecule at the C-2 and C-4 positions when a complex forms. The stacking does not affect the proton transfer between rings nor the hydrophilic $-OH$ groups or the sugar(s), therefore the stacking does not affect overall structure (71).

Once the structures stack the electrons are able to interact between the rings. How this interaction occurs is still unknown, but it has been shown that the distance between these rings determines the color of the ACN (64). The interactions are stronger the closer the rings are to one another and in turn the ACN shows a bluer color. Weaker interactions occur as the rings move further apart and the ACN appears redder in color. The pH of the system affects the distance between the rings by redistributing the charge

on the flavylium cation (64). Therefore, each ACN can be a different color depending on its copigment interactions in addition to the pH of the system (72). Figure 2.6 from Clifford's research (87) best illustrates these phenomena. The observed colors of our fruits, vegetables and flowers are mostly due to the ACNs transformations with changes in pH (74).

The less favorable intermolecular copigmentation is proposed to occur between the flavylium cation or the neutral quinonoidal base of the ACN and other flavonoids, which are unbound to the anthocyanin. It is not necessary to have a hydroxyl group or glycosyl residue present in order for intermolecular copigmentation to occur (72,75). Spectrophotometry shows intermolecular copigmentation causes a bathochromic shift (i.e. shift to longer wavelength) toward higher wavelengths in the maximum absorption of the visible spectra (λ_{max}), thus making the ACN appear bluer, but there is also an increase in absorptivity and a hyperchromic shift (i.e. shift to greater absorbance) toward increased color intensity (2,63,64,68–70,72). The assumption is that the reaction to form the ACN – copigment complex competes with the hydration reaction, but in the case of intermolecular copigmentation the hydration reaction does not occur (64). Association of the ACN – copigment complex has been suggested to occur because of hydrogen bonding (64), but due to water's excellent ability to both donate and accept hydrogen bonds it is highly unlikely this is the only process. Especially since an end-to-end complex would not prevent nucleophilic attack (of water) on the pyrylium ring. Goto *et al.*(76), suggests it is more likely to occur because of a stacking process associated with hydrophobic forces, which would protect the pyrylium ring from water nucleophilic attack and the ensuing color loss. There is currently no data for rates of formation of these ACN –

copigment complexes, but this reaction most likely falls into the fast reaction category (64).

Brouillard gives a reasonable thermodynamic explanation for why intramolecular copigmentation is more efficient than intermolecular copigmentation in nature (64). In terms of entropy, intramolecular copigmentation is more favorable because its copigment is bound to the ACN, and conversely, intermolecular copigmentation must first assemble the molecules dissociated in solution (i.e. copigments) and then form the ACN-copigment complex. Usually, when intramolecular copigmentation occurs, little or almost no intermolecular copigmentation exists in the same molecule.

2.3.2: Metal Copigmentation

It is important to note ACNs also stabilize their colors by chelating with metal ions. Metal chelation of ACNs occurs with ions such as Al^{3+} and Fe^{3+} to form deeply colored coordination complexes (68). This can only occur when the ACN has an *ortho*-dihydroxy group in its B-ring (Fig. 2.3), like delphinidin (68,72). Generally speaking, copigmentation can still occur without the presence of metals, but since metals are one of the nine factors affecting copigmentation, they can restrict or promote copigmentation in certain ACNs (73,77).

The copigment's role is well-known, therefore it is plausible for hydrophobic interactions to occur between the pyrylium ring and the acyl moieties in order to produce vibrant and stable colors (71). At this time researchers still do not fully understand how the color of ACNs is produced in nature, but copigmentation is essential for colors to appear while inside the cell sap where the pH ranges from 3.5 to 5.5 (63). Research has

shown that the *p*-coumaroyl moiety increases stability of the ACN-copigment complex (64). In the vacuoles of colored cells found in higher plant organs there is a large population of colorless flavonoids and other polyphenols, which associate with the ACNs that are present (62). This demonstrates how nature commonly utilizes copigmentation to help stabilize the colors of fruits and vegetables, as well as the products made from them, such as wine and fruit juices (78).

2.4: Anthocyanin Stability

It is well-known that most anthocyanins are less stable when exposed to certain chemical and physical parameters such as: high temperatures, oxygen, light and varying pH values (60). The most recognized trend is that the stability of ACNs decreases as pH values increase. These restrictions have led to research on the stability of ACNs and it has shown that both stability and water solubility are increased when a sugar is attached to the ACN (60). Acylated anthocyanins are more stable than non-acylated ACNs because the non-acylated ACNs usually degrade more quickly when exposed to these chemical and physical parameters (9). The stability of acylated ACNs is attributed to intramolecular stacking. Once the sugar is attached, the ACN becomes more stable because it prevents the ring structure from being broken and therefore water is unable to attach to the molecule (6).

With studies showing that acylation improves the stability of the anthocyanin complex, it is logical to explore techniques to remove these more stable ACNs from their natural state for further investigation and possible applications. In fact, the major anthocyanin in the foliage of the purple pepper is an acylated delphinidin derivative. In

theory it is more stable than its non-acylated counterparts and has the potential for applications such as: a food coloring, food additive, or supplement in the food industry. This anthocyanin's known stability makes it easier to analyze *in vitro* as long as precautions are taken to control the pH, temperature and light requirements in order to maintain its natural structure, consequently preserving its color. Thus, creating an efficient food-grade extraction method for this ACN is very advantageous. The food-grade extraction method that was developed for the foliage of the purple pepper will be discussed in detail in Chapter 3.

2.5: Possible Health Benefits

For years researchers have investigated the potential health benefits of ACNs and have found them to be very favorable. ACNs have exhibited a variety of health benefits and a central focus has been on their ability to act as strong antioxidants. The levels of antioxidant activity vary with the source of the ACN because the degree of glycosylation of the aglycone may affect the antioxidant capacity of the ACN, based on the aglycone present (4,21-27). It is well-known different sugars have different effects on the antioxidant activity of an ACN, as well as its bioavailability (3,24,25,27,45,49,93). An antioxidant's radical scavenging ability depends on its own ability to form a stable radical (94,95). By varying the sugars that are attached to the aglycones (Fig. 2.3) different molecular structures are made. These sugars in turn either amplify or weaken the stability of the antioxidant as well as affecting the antioxidant potency. In 2003, Zheng and Wang (96) reported some possible explanations for the above results: (a) an increase in $-OH$ groups might increase antioxidant activity (97); (b) *ortho*-dihydroxy group in the B-ring

of the ACN stabilizes the radical form and participates in electron delocalization, therefore the dihydroxylation of the 3', 4' positions of the B-ring affects the antioxidant activity (98); and (c) it is required for the 3-, 5-OH groups with 4-oxo function in the A and C-rings to be present for maximum radical scavenging potential (98).

Research results on plant phenolics has demonstrated antioxidative activity to be the predominant characteristic and ACNs have followed this same trend (57). Some of the prominent health benefits reported are: antioxidant activity (of fruits and vegetables in particular), effects on vision (25,99–102) and anticancer activities (103–111). Other benefits reported in the last 30 years revolve around multiple health factors such as: the treatment of diabetic or hypertensive vascular retinopathy (112–114); memory enhancement (91); protection from cardiovascular disease (115); maintaining normal vascular permeability (116,117); radiation-protective agents (118,119); hepatoprotective agents (114,120–122); chemoprotective agents against platinum toxicity in anticancer therapy (123); anti-influenza properties (124–126); and vasoprotective and anti-inflammatory agents (127,128).

Among all these health benefits there are two ACNs that have shown more promise in the inhibition of cell growth. Meiers *et al.*, demonstrated the aglycones of both cyanidin (Cy) and delphinidin (Dp), which are the most abundant ACNs found in food, have shown the ability to inhibit the growth of human tumor cells in vitro in the micromolar range (129). Their research project also revealed both Cy and Dp inhibited the epidermal growth-factor receptor, therefore stopping downstream signaling cascades.

Sarma *et al.* (130), describes that by metal chelation ACNs have the ability to stop the oxidation of ascorbic acid caused by metal ions. This is achieved by forming the

complex of anthocyanin-metal-copigment (82). The copigment here is the ascorbic acid and it is proposed that metal chelation can stabilize the coordinate complex, thus this copigmentation could be why ascorbic acid is protected from oxidation. Eddy *et al.*, used cress seedlings as examples to demonstrate the factors affecting ACN synthesis (131). The results showed those seedlings with the most ascorbic acid also had the highest ACN content, suggesting the concentration of ascorbic acid is proportional to ACN content in plant cells (130,131). This study, along with others, led to investigations of the major anthocyanin in the foliage of the purple pepper for potential health benefits.

The specific major anthocyanin found in the foliage of the pepper plant, delphinidin-3-*p*-coumaroylrutinoside-5-glucoside or the shorthand Dp-3-*p*-coum-5-glc, is the same major ACN identified in eggplant skins by Kuroda and Wada (132,133), Sadilova *et al.* (8) and Ichiyanagi *et al.* (9,10). Noda *et al.*, conducted two experiments on eggplant (13,134) in which they described how Dp-3-*p*-coum-5-glc, which they refer to as 'nasunin', has the ability to directly scavenge superoxide anion radicals ($\bullet\text{O}_2^-$) and inhibit the production of hydroxyl radicals ($\bullet\text{OH}$). The studies utilized an electron spin resonance spectrometer and a 5,5-dimethyl-1-pyrroline-*N*-oxide (DMPO) spin trapping method. Both $\bullet\text{OH}$ and $\bullet\text{O}_2^-$ were generated by a Fenton reaction and the results displayed that nasunin directly scavenged the $\bullet\text{O}_2^-$, which was produced by the hypoxanthine-xanthine oxidase system. The results also showed how nasunin inhibited $\bullet\text{OH}$ from being generated versus direct scavenging of $\bullet\text{OH}$ (13,134). Similar to Sarma *et al.*, Noda *et al.* (13) suggests metal chelation was a key in protecting ascorbic acid from oxidation. They spectrophotometrically determined nasunin formed an iron complex with

a molar ratio of 2:1 (nasunin: Fe³⁺) to inhibit •OH. This shows nasunin does not directly scavenge •OH, but instead the chelating iron (Fe³⁺) inhibits the •OH generation (13).

In 2000, Noda *et al.*, also provided data for nasunin's ability to protect against H₂O₂- induced lipid peroxidation in rat brain homogenate (13). When hydrogen peroxide (H₂O₂) is added the levels of both malonaldehyde and 4-hydroxyalkenals increases, therefore the protection was measured by nasunin's ability to reduce these levels. After 60 minutes of co-incubation nasunin did reduce H₂O₂-induced lipid peroxidation in a dose-dependent manner (13). These studies have shown how Dp-3-*p*-coumru-5-glc has the ability to provide health benefits and thus providing another meaningful reason to study the major ACN found in the foliage of the purple pepper.

2.6: Nomenclature

The major anthocyanin in the foliage of the purple pepper is delphinidin-3-*p*-coumaroylrutinoside-5-glucoside. When reviewing the literature multiple names for this compound were found. The most common name is nasunin and is referenced in multiple literature sources (9,10,13,134–138). Another common name referenced in the literature is delphanin (72,73,77,139). There are also the specific names when discussing *cis* and *trans* isomerization, as well as in identifying specific attachments of glucosides and acyl moieties. An example of this naming is found in Ichiyanagi *et al.*, delphinidin 3-[4-(*cis-p*-coumaroyl)-L-rhamnosyl(1→6)glucopyranoside]-5-glucopyranoside (9). Organic chemistry defines a glucopyranoside as any glycoside of glucopyranose, where glucopyranose is the pyranose form of glucose, and pyranose is defined as any cyclic hemiacetal form of a monosaccharide having a six-membered ring. While rhamnosyl is

defined as a radical derived from rhamnose, and rhamnose is methyl-pentose. Lastly, rutinose is the combination of rhamnose and glucose. For simplicity, this work will refer to delphinidin-3-*p*-coumaroylrutinoside-5-glucoside as Dp-3-*p*-coumrut-5-glc or the ACN of interest. The *cis* and *trans* forms of the compound identified by Ichiyanagi *et al.* (9) are shown in Figure 2.7.

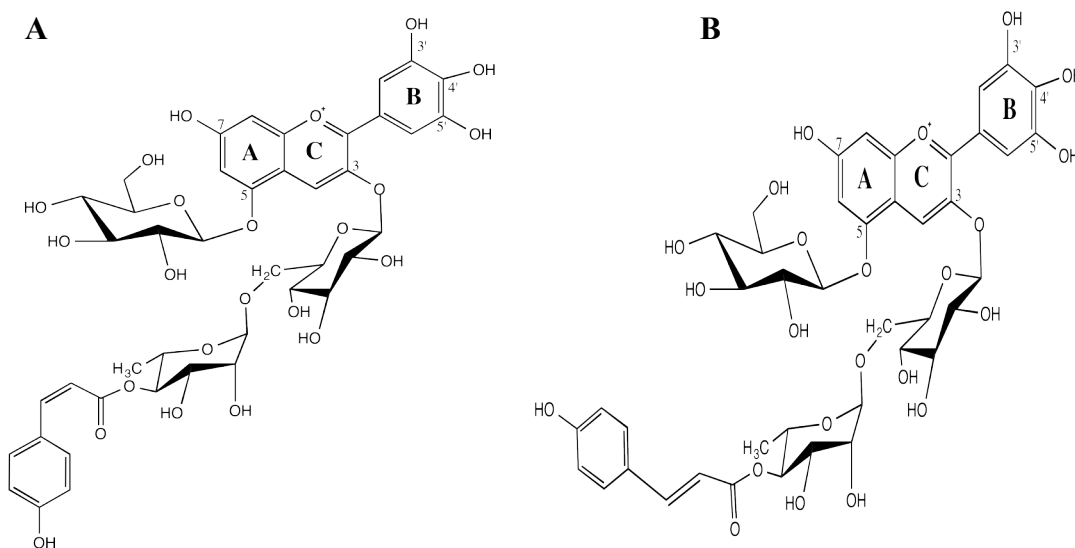


Figure 2.7: Illustrations of delphinidin-3-*p*-coumaroylrutinoside-5-glucoside (a) *cis* isomer, and (b) *trans* isomer.

2.7: Anthocyanin Standards

A majority of the 600+ anthocyanins created in nature do not have commercially available standards. In order to produce high quality standards an immense amount of time and money would need to be invested and most companies cannot possibly commit their services to these in-depth research projects and still make a profit in the industry. Fairly pure phytochemical standards are available through reliable companies, such as ChromaDex™, but usually only the anthocyanidin or an anthocyanin with one glucoside

attached is the best available for purchase. Therefore, it is impossible to purchase a complex anthocyanin standard such as Dp-3-*p*-coumrut-5-glc.

Fortunately, Dr. Sam Asen and his colleagues (72,73,77,139,140), which included Dr. Robert Griesbach, conducted extensive work on anthocyanins in blue flowers. His work was carried out at the USDA-BARC facility and Dr. Griesbach was a collaborator on this research project, which therefore had access to an extensive collection of stable anthocyanins that had been extracted from various plant materials. The anthocyanin collection dates all the way back to the mid 1960s and includes hand drawn graphs, as well as UV spectra. All the anthocyanins in this collection were stored in one of two ways. First, the anthocyanins were dried and stored in an airtight container in the dark in a temperature-controlled room; most of the standards collected prior to 1990 were stored in this manner. Second, the anthocyanins were stored in a dark freezer in acidified methanol. This collection is currently maintained and housed at the Food Composition and Methods Development Laboratory at USDA-BARC.

In early 1970, Asen *et al.* (77) detected delphinidin-3-*p*-coumaroylrutinoside-5-glucoside in Prof. Blaauw Iris, which is a hybrid of *Iris tingitana* Boiss. & Reut., but is commonly known as the Blue Ribbon Iris and shown in Figure 2.8 a. It was found to be stable and a non-metallic, anhydro-base of Dp-3-*p*-coumrut-5-glc that is associated with pectin and complexed with the copigment *C*-glycosylflavones. The flower's color is a more bright blue color (Fig. 2.8 a) in comparison to the darker foliage of the purple pepper (seen in Fig. 2.8 b), which has undertones of black. The Blue Ribbon Iris also has other flavonoids present in various concentrations, so the coloring will not be exactly the same as the foliage of the purple pepper.



Figure 2.8: (a) Picture of a Blue Ribbon Iris (*Iris*). (b) Picture of the purple pepper plant (Copyright: Dr. John Stommel).

The most important factor is that Dr. Asen and his colleagues extracted what they identified as Dp-3-*p*-coumrut-5-glc from the Blue Ribbon Iris. This allowed it to be used as a visual standard for HPLC trials in order to compare retention times from the Blue Ribbon Iris and the ACN extract from the purple pepper. Unfortunately, there was a very limited quantity and it could not be utilized in the MS or NMR trials for additional identification and characterization. Ideally, it would have been best practice to utilize this standard for comparison purposes in all of the analytical techniques where the ACN of interest was separated, characterized and elucidated.

Chapter 3: Food-Grade Extraction Method

Overview

This chapter will discuss the development of the food-grade extraction method for Dp-3-p-coumru-5-glc from the foliage of purple pepper. Section 3.1 will briefly discuss the varying methods that were utilized in this research project. The extraction method will be described in detail in Section 3.2. Descriptions of how the purple pepper samples were prepared is described in Section 3.2.1, color check and sample homogenization described in Section 3.2.2, and filtration of the sample in Section 3.2.3. The initial drying process of the sample is described in Section 3.2.4, how the chlorophyll and other polyphenols were removed is covered in Section 3.2.5, the final drying of the ACN extract is in Section 3.2.6, and the resolubilizing of the original extract is discussed in Section 3.2.7. Lastly, the success of the food-grade extraction technique is briefly described in Section 3.3.

3.1: New Methodologies

This work first required an extraction protocol to be developed followed by an efficient separation method. The goal of this project was to produce a food-grade anthocyanin extraction product from purple pepper foliage, shown in Figure 3.1, with the intent of using it for nutritional studies on bioavailability in humans. The methods were developed with this goal in mind and the solvents were chosen based on this premise. There are restrictions when creating food-grade products and specific FDA guidelines must be followed (Section 3.2). This collaborative study included scientists from the

USDA, Beltsville Human Nutrition Research Center (BHNRC) who are well versed on these guidelines and provided the necessary information so the resulting protocol was in accordance with these regulations. If the project had not required a food-grade product then the methodologies, as well as solvents would have differed.

An effective extraction method for the anthocyanins in the purple pepper foliage was developed by referencing many published ACN extraction methodologies for other plant material, as well as a multitude of separation techniques to form an effective separation method (5,6,8–10,16,77,82,83,86,132–134,137,139,140,142–172). These references led to the development of the basic extraction and separation methods. Many versions of these two methods were cultivated throughout the research project in order to arrive at the final extraction and separations methods, which are presented here. Once separated and concentrated by HPLC (Chapter 4), the ACN extract was analyzed for composition and structural elucidation. These characterization and elucidation techniques will be discussed in Chapters 5 (MS) and in Chapter 6 (NMR).



Figure 3.1: Picture of purple pepper foliage (*Capsicum annuum* L.) in the field. (Copyright: Cassandra L. Taylor)

3.2: Extraction Method

It was essential to construct an efficient extraction method to obtain the greatest amount of anthocyanin from the pepper foliage. The schematic shown in Figure 3.2 offers a visual representation of the food-grade extraction process. This process was optimized over time from its original version, which was derived from previously researched extraction methods (6,24,25,27,49,61,63,72–74,77,78,85,86,100,139,140,145,146,149,151–153,157,159,161,173–196). The chemicals available for use according to the U.S. Food and Drug Administration (FDA) are those certified by the U.S. Pharmacopeial Convention (USP) and those classified as Generally Recognized as Safe (GRAS) substances, which are listed at the U.S. FDA website (197). USP certified chemicals are clearly labeled by chemical producers as “USP”, meaning these chemicals meet or surpass the specifications of the USP. Unfortunately, after the development of the extraction protocol and the isolation of the ACN extraction product from the pepper foliage, the nutritional portion of the study that included a human feeding study and toxicological work were unable to be completed due to a lack of funding.

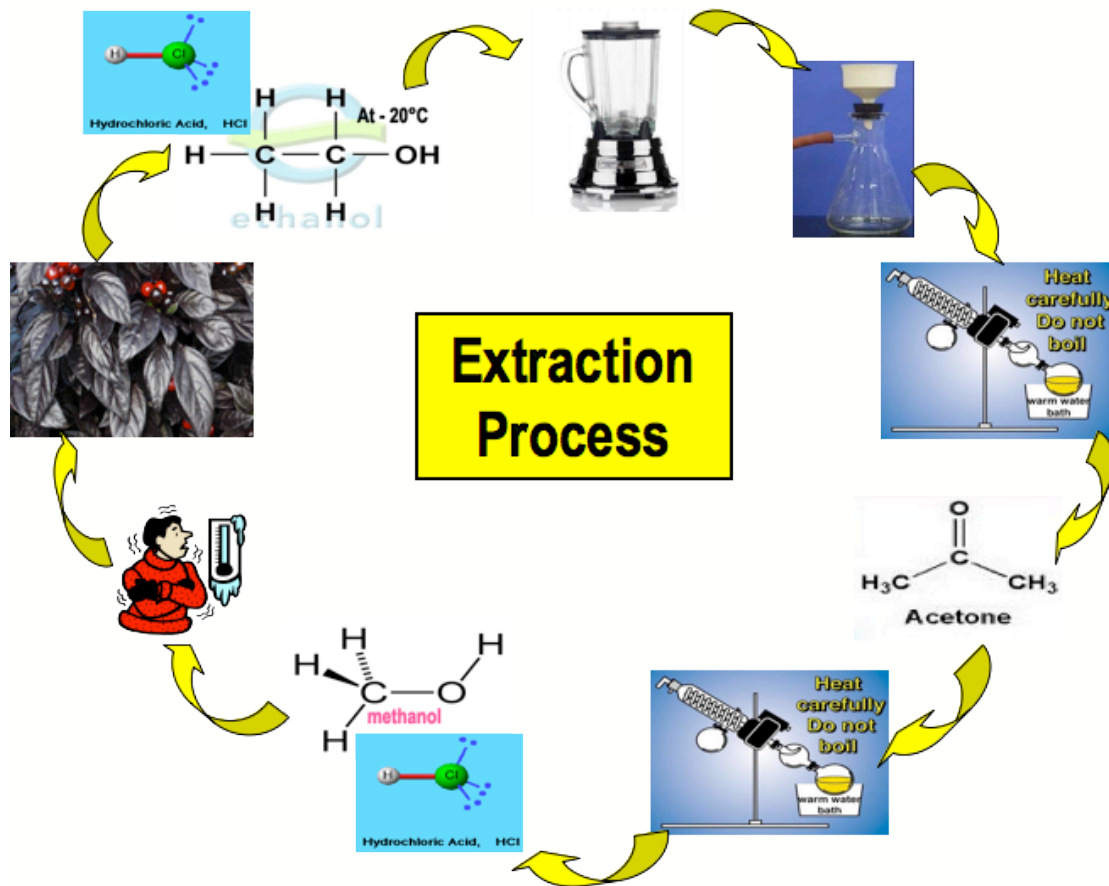


Figure 3.2: Schematic drawing of developed extraction protocol.

The schematic above visually demonstrates the process utilized during the food-grade extraction process, followed by resolubilization of the ACN extract for further analysis by HPLC in 1% hydrochloric acid in methanol. The extract that was resolubilized does not follow GRAS regulations because it is only used to confirm the presence of Dp-3-*p*-coumru-5-glc and will never be utilized in a feeding study. An extraction diagram, shown in Figure 3.3, briefly describes the food-grade extraction protocol steps to produce a food-grade ACN extract from the foliage of the purple pepper plant.

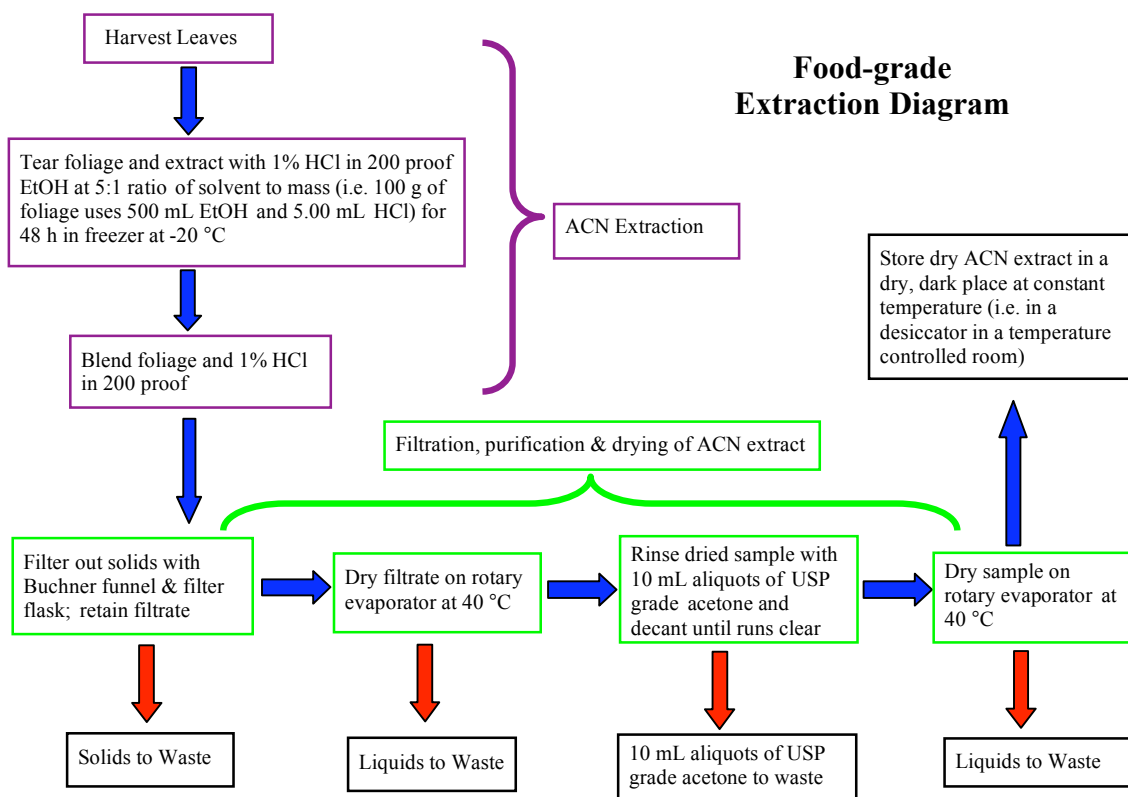


Figure 3.3: Diagram of food-grade extraction of the ACN from the purple pepper foliage.

3.2.1: Sample Preparation

First, collect the darkest leaves of the purple pepper plants (*Capsicum annuum* L.) from the field or greenhouse (Fig. 3.1) to compose the sample. In this study, those leaves with dark purple underside as well as tops are preferred, but leaves with slightly green undersides are acceptable. Figure 3.1 is an excellent example of optimal leaf coloring to collect for the sample. Not all leaves are equal in terms of color darkness due to shading from other leaves on the plant. Leaves that are not mostly purple should be discarded from the sample. Next, while wearing surgical gloves, tear the leaves and accompanying stems into small pieces.

3.2.2: Experimental

First, tare a non-corrosive, freezer safe plastic or glass container with the lid removed. Add the torn leaves to the container to reach the desired mass. In this study, the typical total leaf mass range is 35 to 100 grams, depending on the size of the pepper plant and how many purple leaves are available for harvest at time of collection. Add the solvents of hydrochloric acid (HCl) and 200 proof ethanol (EtOH) to the container as 1% HCl/EtOH (v/v). Specific solvent volume ratios were determined based off the volume of EtOH needed to cover the mass of leaves in the container. For this study a 5:1 ratio of solvent volume to leaf mass is used (i.e. 100.0g of leaves uses 500mL EtOH and 5.00mL HCl). The color of the solvent in the container should be bright purple at this stage, as seen in Figure 3.4 a. If color is more greenish/brown, as shown in Fig. 3.4 b, then there is not enough HCl to maintain the colored flavylum cation structure of the ACN. Therefore, add more HCl in order to reduce the pH so the values fall between 1-3, thus protecting the flavylum cation from converting to the colorless carbinol pseudo-base at pH~ 4.5 (Fig. 2.5). If leaves are stored in non-acidified 200 proof EtOH the color will turn green along with the EtOH, as shown in Figure 3.5 b, and the purple ACN color cannot be recovered. It is imperative to fully submerge all leaves in the solvent in order to obtain the best extraction. Release the trapped air bubbles in between leaves by running a clean glass stirring rod down the sides of the container as well as down the middle to compress the torn leaves. This helps to submerge all the purple pepper leaves in solvent and produce the best extraction of the ACN of interest from the foliage. Screw the top onto the container and place it in a dark -20 °C freezer for a minimum of 48 hours (h).



Figure 3.4: Comparison of leaf color after adding differing ratios of 1% HCl to EtOH and storing in freezer for minimum of 48 h. (a) 5:1 ratio demonstrates correct leaf and solution color to maintain flavylum cation; (b) significantly < 5:1 ratio reveals incorrect leaf and solution color to demonstrate flavylum cation is not maintained.

In order to determine the most efficient sample preparation method for the extraction various solvents, solvent to leaf mass ratios, temperatures and time were investigated. After each sample preparation setup was completed the sample and liquid were blended, dried down on the rotovap and injected on the HPLC at 340 nm and 540 nm to obtain chromatograms of the ACN of interest. The resulting chromatograms were used as a way to determine the success of the preparation, especially the absorbance units (AU) of the peak for Dp-3-p-coumrut-5-glc. The retention time for Dp-3-p-coumrut-5-glc was known to be at 25 minutes because an extract of the same compound previously identified in the Blue Ribbon Iris was injected first. The Blue Ribbon Iris extract was used as a retention time standard. The other most important factor was maintaining the flavylum cation so the purple color of the foliage would be preserved. This was determined by the color of the leaves and liquid after the sample was removed from the refrigerator or freezer, as seen in Figure 3.5 a. Table 3.1 displays all of the

combinations that were tested in this investigation. After many months of investigative work, it was determined that the best sample preparation was to use 1% HCl/EtOH (at a ratio of 5:1 with leaf mass) as the solvent and the foliage should remain for 48 h in a freezer at -20 °C to achieve the most efficient extraction of ACN from the foliage.

Table 3.1: Investigated combinations of solvents, temperature and time for the sample preparation method. Combination utilized to obtain pepper extract is highlighted in purple. Abbreviations: EtOH = 200 proof ethanol, HCl = hydrochloric acid, HAc = acetic acid and Fridge = Refrigerator.

Solvents	Refrigerator or Freezer	Temperature (°C)	Time (h)
100% EtOH	Fridge	3	24
100% EtOH	Freezer	-21	24
1% HCl/EtOH	Fridge	4	24
1% HCl/EtOH	Freezer	-18	24
1% HAc/EtOH	Fridge	5	24
1% HAc/EtOH	Freezer	-18	24
100% Acetone	Fridge	5	24
100% Acetone	Freezer	-18	24
100% EtOH	Fridge	5	48
100% EtOH	Freezer	-15	48
1% HCl/ EtOH	Fridge	4	48
1% HCl/ EtOH	Freezer	-16	48
2% HCl/ EtOH	Fridge	4	48
2% HCl/ EtOH	Freezer	-16	48
2% HCl/ EtOH	Fridge	4	168
2% HCl/ EtOH	Freezer	-15	168
20% HAc/EtOH	Fridge	5	168
20% HAc/EtOH	Freezer	-17	168

A majority of the extraction combinations listed in Table 3.1 were unable to maintain the color of the flavylum cation and were therefore rejected. All of the extraction combinations were evaluated by a set of criteria, which are listed in Table 3.2.

Table 3.2: Criteria used to accept/reject the extraction combinations listed in Table 3.1.

Criteria	Pass	Fail
Maintain flavylum cation after extraction time period ended	Observed dark purple color in leaves and solvent	Observed green, green/brown, brown color in leaves and solvent
HPLC retention time for major ACN peak at 340 & 540 nm	25 +/- 0.5 min	No peak at 25 min or major peak is outside 25 +/- 0.5 min range
Absorbance of major ACN peak	> 0.30 AU	< 0.30 AU

The criteria helped to narrow down the acceptable extraction combinations. All combinations that did not include at least 1% HCl were rejected due to their inability to maintain the flavylum cation. There was no significant difference in the HPLC chromatograms for the extracts utilizing 1% HCl/EtOH and 2% HCl/EtOH, therefore the lesser amount of HCl was utilized. The combinations in the refrigerator usually had observed green spots in the leaves, but when the purple color was maintained the HPLC retention time criteria was either not met or the absorbance values were < 0.30 AU.

3.2.3: Color Check and Sample Homogenization

After 48 h, remove the container and observe the color. As long as the color of solution and leaves are bright purple (Fig. 3.5 a), the sample preparation is a success. If color of leaves and solution are greenish/brown (Fig. 3.5 b) this means the pH of the solution was not low enough to maintain the flavylum cation and it is nearly impossible

to add enough HCl at this point to transform the colorless ACN structure (either a colorless pseudobase or chalcone) into the correct conformation of the flavylum cation, as shown in the ACN equilibrium transformations in Fig. 2.5. If the color change phenomenon from purple to green in solution occurs, it is most likely due to a high pH value (>3) during sample preparation and results in a colorless ACN structure, as shown in Fig. 2.6, when $\text{pH} > 3$. Research has shown that once the C-ring of the ACN skeleton is open to the chalcone form it takes a sufficient amount time (i.e. at $25\text{ }^{\circ}\text{C}$ a 3,5-diglycoside takes 12 h and 3-glycoside takes 6 h) for it to re-equilibrate back to the colored flavylum cation (198), and this process is prolonged as the temperature decreases. Since this extraction protocol is maintained at or around $-20\text{ }^{\circ}\text{C}$ for at least 48 h the best solution to this problem is to begin the sampling process again and be vigilant when adding the volume of HCl to the EtOH, and check the ratio (5:1) of solvent to leaf mass carefully. It is always best to double check the calculation of the solvent ratio before adding the solvents to the leaves.



Figure 3.5: After 48 h in freezer, (a) leaves stored in 1% HCl/EtOH; (b) leaves stored in 200 proof EtOH.

Next, put on surgical gloves and empty all contents of the container into a glass blender, which is used solely for purple pepper extractions so as to avoid the transfer of any materials and solvents not pertaining to this study. The blender is equipped with two settings, HIGH and LOW. This method utilizes the HIGH setting when blending the sample. Cover and blend the contents on HIGH for 5 seconds, then open blender and using a clean glass stirring rod check for large foliage remaining and push toward blades at bottom. Cover and blend again for an additional 5 seconds on HIGH if necessary to ensure all plant material is broken down.

3.2.4: Filtration

Once sample homogenization is complete, setup the vacuum filtration as shown in Figure 3.5 A. Using a large Buchner funnel (128 mm) place Whatman #2 paper (110 mm, Ø) in the filter and connect it to a 1 liter (1 L) glass filter flask (use smaller flask and funnel for smaller samples) via a rubber stopper. Wet the filter paper with a few drops of 200 proof EtOH so it sticks to the funnel, then turn on the vacuum to achieve an airtight seal. Pour small aliquots of the homogenized liquid sample into the funnel so as not to overload the filter paper. The filter holes clog very easily due to the large amount of plant material. Therefore change the filter paper once a thin layer of plant material residue dries on the top of the filter paper, as seen in Figure 3.6 b. The large sample masses in this study require quick work of the filtration process so the ACN structure does not degrade. Thus the residue is not completely dry when the filter paper is removed, but instead a mostly dry residue with some moisture remaining. It is imperative to change the filter paper multiple times in order to filter the entire sample. It is obvious small amounts of ACN are lost in this process since the filter paper never fully dries, but some losses were necessary to maintain the integrity of the ACN compound for this analysis.

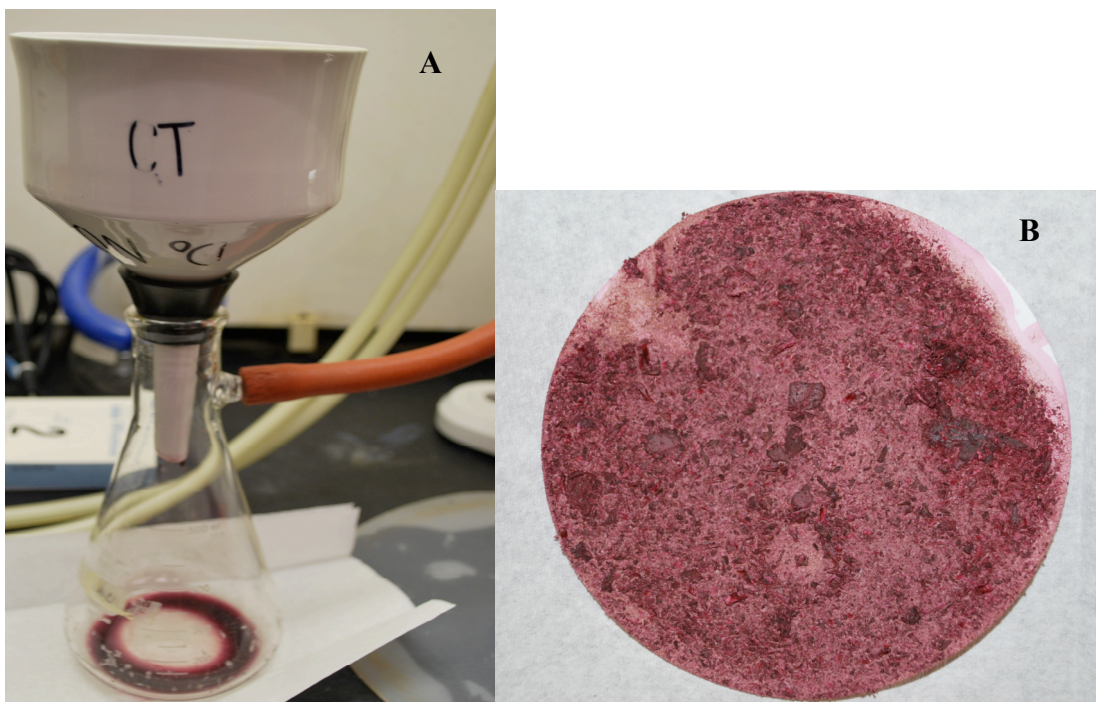


Figure 3.6: (a) Filtration setup. (b) Filter paper once ready to remove.

To change the filter paper, first turn off the vacuum and break the seal from the 1 L filter flask by removing the vacuum hose from the flask. Carefully loosen the Buchner funnel and lift upwards to detach it from the filter flask. Turn the funnel 90° on its side and place it on a clean paper towel. Then use a clean glass stirring rod to pull up the filter paper's edge. The funnel is always held 90° from the counter top to prevent any residual liquid from leaving the funnel. Using a gloved hand for assistance, carefully slide the filter paper with the dry residue onto the paper towel on the counter. Be mindful not to clog the funnel's holes with any of the plant material left on top of paper. Using a dry paper towel wipe out any plant material which may be stuck to the sides of the funnel so the next piece of filter paper does not push the material through the filter and down into the filtrate. Change the filter paper as many times as necessary in order to filter out as much of the liquid from the remaining plant material inside the blender. For a large

mass sample (i.e. 100 grams), this study usually uses 8-10 pieces of filter paper.

Remember to add a few drops of 200 proof EtOH to each new piece of filter paper so it sticks to the funnel.

Reattach the Buchner funnel to the filter flask and then re-establish the vacuum. Be sure the vacuum is steady before pouring more homogenized liquid into the filter. Check the vacuum by lightly pushing down on the funnel with a gloved hand and feeling the “pull” from the vacuum. Be sure not to press too hard, as the suction is strong. Continue the process of filtering and removing the paper as needed and filter until liquid no longer drips from funnel. The resulting liquid (filtrate) in the filter flask should be very dark purple in color, similar in color to cabernet wine, as shown in Figure 3.7.



Figure 3.7: Final filtrate color from the purple pepper foliage extract.

3.2.5: Initial Drying Process

First step is to turn on the hot water bath and set the temperature to 40 °C on the Buchi rotary evaporator (rotovap) equipped with an externally attached cold-water chiller. Turn on the chiller and allow it to adequately cool the coils. Water droplets will appear on the coils of the condenser tube and it will be cold to the touch when ready. Also, turn the water aspirator (attached to the condenser through tubing) all the way on to help create a vacuum source. The vacuum will seal once the system is ready and the stopcock is closed. For this study, turn on the hot water bath, water chiller and faucet for a minimum of 15 minutes (min) prior to any use and allow the system to equilibrate. An external thermometer, held in place by a ring stand, is monitoring the temperature of the hot water bath to ensure the temperature does not exceed 40 °C. This is to protect the delicate flavylum cation structure of the ACN from damage that can be caused by high temperatures.

The next step is to weight an empty, clean and dry round bottom (RB) flask and record the mass value. A change of gloves may be necessary before weighing if these same gloves were used for the extraction and filtration steps. Be sure not to add mass to the weight of the RB flask, since the mass of the recovered ACN is quite small. When selecting a RB flask it is important to choose a size that will allow the sample to have room to rotate and move in case of a bump in pressure. Keep in mind the best approach is to fill the flask no more than halfway with sample filtrate. If there is not enough room inside the flask the liquid sample will boil and shoot into the distillation tube, whereby the sample may be contaminated and even lost. By using a larger RB flask, in the event of a bump in the system there is still enough space inside the RB flask to reduce or

prevent the loss of sample. This study usually utilizes 100 mL, 500 mL or 1000 mL RB flasks to house the liquid filtrate depending on the size of the sample. In future studies, installation of a bump guard would be helpful to reduce any sample contamination or loss.

After weighing the dry RB flask place it securely on a cork flask holder and carefully fill it with the filtrate. Again, note the color of the filtrate and be sure it is still a dark purple color. Check the condenser is cool to the touch and for the appearance of water droplets on the coils. Then check the hot water bath to be sure it is at optimal temperature (40 °C). If bath is above 40 °C, add some cool water and wait 10 min for the temperature to fall ≤ 40 °C. It is acceptable to have the bath temperature ≤ 40 °C, but not above because this can potentially disrupt the delicate ACN structure and degrade it. Record the actual temperature of the bath. This study usually operates with a water bath temperature range from 37 °C – 40 °C.

Now the system is ready to begin drying down the sample. Add the RB flask containing the sample by attaching the flask to the distillation tube and switching the stopcock to the closed position. Be vigilant and check that the vacuum is completely sealed before lowering the RB flask into the hot water bath. Check vacuum by lightly pulling on the RB flask and resistance will demonstrate the vacuum is ready. If there is no resistance and the RB flask moves easily, immediately check all seals for leaks and hold the flask in place with a gloved hand or remove it from the system until the vacuum is ready. For safety, it is best to use a flask clamp so the flask will not fall into the water bath. Utilize a rotation setting between levels 2 and 3 then gently lower the flask into the water bath.

Watch the sample closely for the first 15 minutes, especially for large sample sizes. There are often bumps in the now reduced pressure system of the RB flask that can cause excessive boiling. Resolve this issue by slowly releasing some pressure via the stopcock and allow the vacuum to re-equilibrate. For a sample in this study the drying time varies between 20 – 40 min depending on the sample size. A sample is dry when no liquid is seen in the motionless RB flask. More importantly, turn off the rotation, break the vacuum, carefully remove the flask (with gloved hands) and inspect the dry product. A dry sample has a dark purple-colored product with a noticeable sheen and a very smooth-looking surface, as shown in Figure 3.8 a, almost like the shiny surface of an ice cube. If the product is still a dull, dark purple color with a rough-looking surface or has visible liquid remaining in the RB, as shown in Fig. 3.8 b, then the sample is not completely dry. If this occurs, place the RB flask back on the system and monitor the dryness every 10 – 15 min until the product matches the description and looks like the model in Fig. 3.8 a.

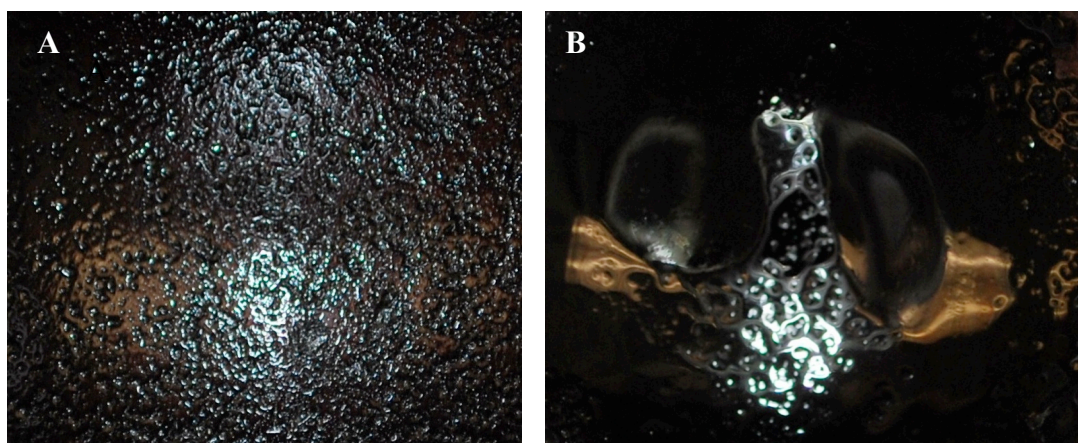


Figure 3.8: These pictures represent what the product should look like when it is (a) dry, and (b) almost dry.

In some instances, the amount of water in the plant material cannot evaporate on its own. This study resolves the issue by adding a small aliquot (1 – 2 mL) of 200 proof EtOH to the mostly dry sample. The sample then returns to the rotovap until dry. Occasionally the sample may not dry completely after one addition of EtOH. In this case, add multiple aliquots of EtOH to help drive off the excess water. As the sample size increases the number of EtOH aliquots needed to dry the sample may also increase due to the extra water inside the pepper's foliage.

Although the sample looks dry there will still be minute amounts of water remaining in the sample since 1% HCl/EtOH is the extracting solvent. It is well known that both HCl and EtOH azeotrope with water (199). This project's solvent choices are restricted by food-grade regulations, also known as GRAS and USP grade chemicals (197), so other acids such as trifluoroacetic acid (TFA) are not a viable option for this protocol. Literature shows (198) the substitution of TFA with food-grade HCl in HPLC mobile phases still provides acceptable resolution.

3.3: Cleaning and Drying the Sample

Once all of the initial solvent (1% HCl/EtOH) is removed from the sample by the rotovap, it is essential to rinse the sample. The removal of additional polyphenols, such as chlorophyll and carotenoids, from the sample needs to occur in order to get a more pure ACN extract (Section 3.3.1).

3.3.1: Removal of Chlorophyll and other Polyphenols

Now that the sample is dry, remove the RB flask with a gloved hand and place it on the cork flask holder. Using USP grade acetone in 10 mL aliquots, slowly pour it down the sides of the flask while gently spinning the flask on the holder with a gloved hand. This helps to distribute the acetone evenly throughout the sample and not overwhelm one section of the dry sample. Chlorophyll, lipids and carotenoids are all acetone soluble (62,68,81), but ACNs are not. Therefore, this rinsing will keep the ACNs intact. Decant the liquid into a clean beaker and note the color. Initially, the acetone phase varies in color from dark bluish/green to brownish/green, as shown in Figure 3.8 (see FIRST), which denotes the presence of chlorophyll, thus its removal from the sample. Discard the acetone into a waste container after examining the color. Continue adding aliquots of USP grade acetone and decanting until the eluate runs clear (see LAST in Fig. 3.9). This study has total volumes of added acetone ranging from 150 – 3000 mL, depending on sample size.

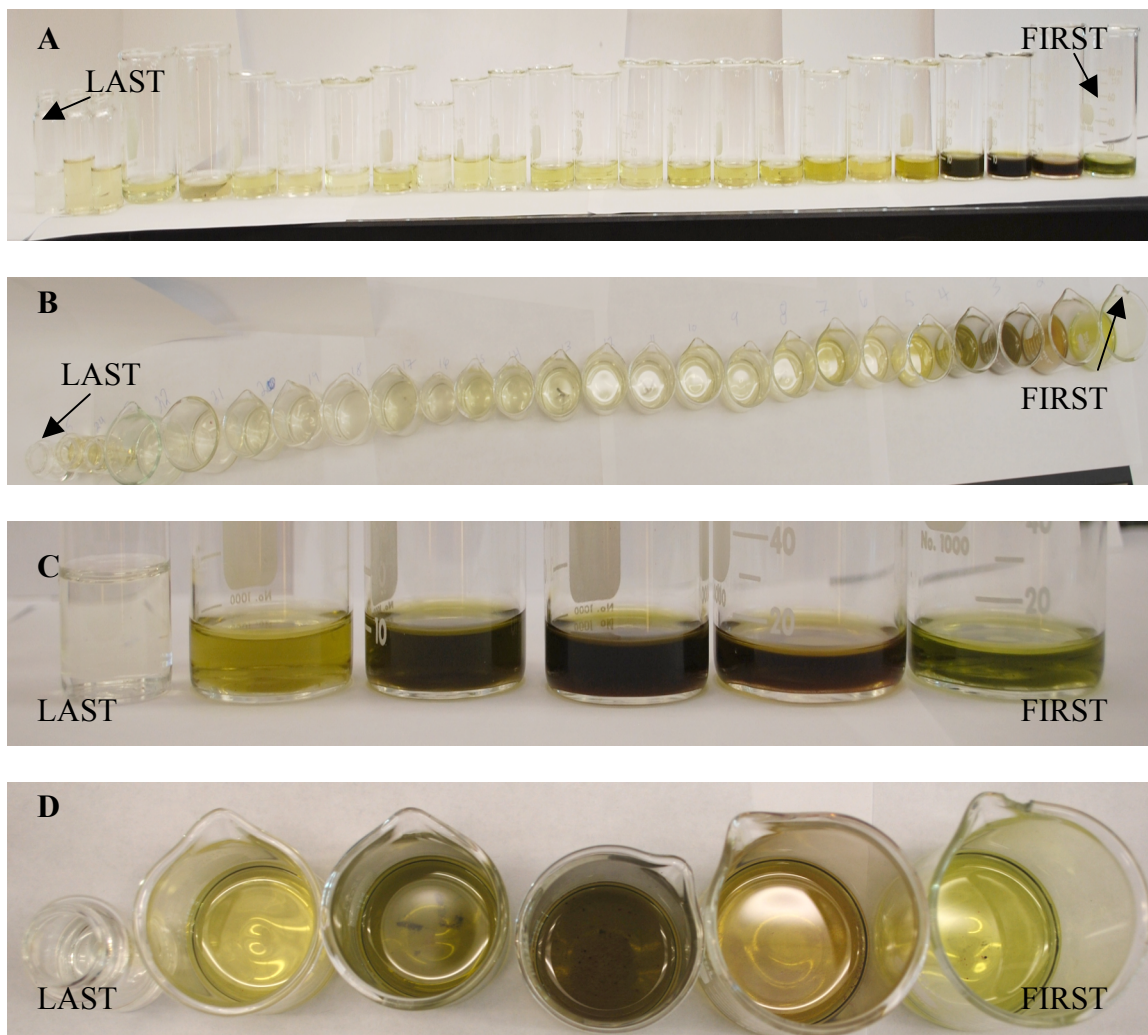


Figure 3.9: This sample requires twenty 10 mL acetone aliquot rinses to achieve a successfully rinsed sample. Demonstrates: (a) side view of all 20 rinses; (b) top view of all 20 rinses; (c) side view of last rinse and first 5 rinses to show dramatic color differences; (d) top view of last rinse and first 5 rinses.

Once the chlorophyll is removed the color of the sample now distinctively changes to a dull, light purple color as shown in Figure 3.10 b. The color is now much closer to fuchsia versus the dark purple color of the original dry sample (Fig. 3.10 a) when it comes off of the rotovap. It is obvious that some solvent is still present in the sample, as seen in Fig. 3.10 b, and needs to be dried.

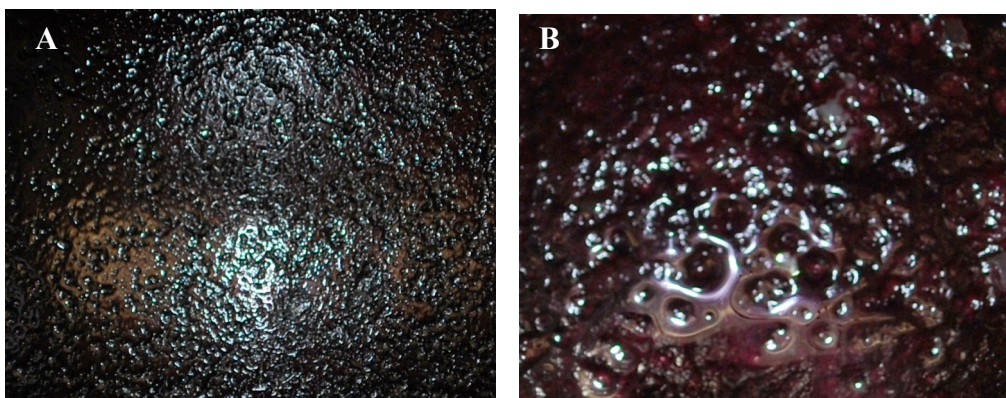


Figure 3.10: Comparison of (a) original dry sample and (b) acetone rinsed sample.

3.3.2: Final Drying of Extract

Place the RB flask back on the rotovap at 40° C until dryness. This process usually takes 5 – 10 min and the color will be getting lighter and more “white” around the edges as the sample dries and the acetone evaporates. The sample will start looking more brittle as if it is forming flakes on its surface, as shown in Figure 3.11 b. This looks very different from the smooth, shiny surface of the original dried sample shown in Figure 3.11 a. Once there are no visible dark purple spots remaining in the sample, remove the RB flask from the rotovap. The sample is now dry and is identified as an extract for the remainder of this investigation. The extract is ready to be prepared for HPLC analysis. To store the extract, cover the entire RB flask with aluminum foil and place in a dark, dry place with a consistent temperature until it is ready to be resolubilized for further HPLC separation. A dark cupboard is an ideal storage location, as anthocyanins are very stable once they are dried. It is not essential to store the extract in the freezer, as the flavylum cation is now very stable.

At this point if the human feeding had continued the dried extract described above would be the ACN product fed to participants in the study. No other chemicals would

have been added to the extract in order to maintain the safety of the participants and to adhere to GRAS regulations.

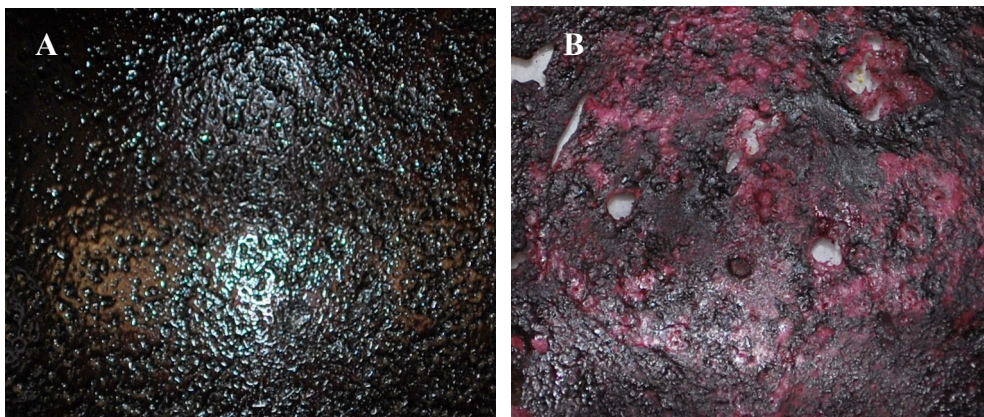


Figure 3.11: Comparison of (a) original dry sample and (b) acetone dried sample.

3.4: Confirmation of Food-Grade Extraction Technique

Upon completion of the food-grade extraction protocol the extract will be analyzed by HPLC. GRAS regulations will no longer be followed from this point forward in the research. The proceeding analytical techniques (i.e. HPLC, MS and NMR) are utilized only for identification and characterization of Dp-3-*p*-coumrut-5-glc in the food-grade ACN extract, but the analyzed sample will not be fed to any animals or humans. This study most often resolubilizes the dry extract immediately after the completion of the final drying step. It is well known that ACNs are both alcohol and water soluble (6,62,68,81,84,159,198) and the common solvent (5,6,8–10,16,77,82,83,86,132–134,137,139,140,142–172) to resolubilize dry ACN samples is acidified methanol (MeOH). These extracts utilize 1% HCl/MeOH because experimentation found it best stabilizes the flavylum cation and preserves the color and structure of the purple pepper's major ACN. Once the extract is fully dry, resolubilize it in the least amount of

solvent possible (range 1 – 16 mL depending on original sample size) in order to keep the extract concentrated. Transfer the extract by clean micropipette to an autoclaved plastic vial and immediately store in a dark freezer at -20° C until the HPLC separation system is ready to begin the analysis.

Liquid chromatography will assist in separating the components in the purple pepper extract and will help to confirm the effectiveness of the extraction technique. This analysis will be discussed at length in Chapter 4, along with the fraction collection procedure utilized to concentrate the purple pepper extract. The ACN of interest in the concentrated pepper extract will be further characterized by MS/MS (Chapter 5) and elucidated by NMR (Chapter 6).

Chapter 4: High Performance Liquid Chromatography

Overview

The use of High Performance Liquid Chromatography (HPLC) to separate the ACN of interest from the purple pepper foliage will be the focus of Chapter 4. A short background about HPLC and gradient methodologies are covered in Section 4.1. The specific method utilized to separate the original ACN extract from the foliage of the purple pepper plant is covered in Section 4.2. Once separated, the major ACN fraction is collected from the HPLC. These fractions are then dried and concentrated *in vacuo* in Section 4.3. The concentrated extract was injected back onto the HPLC for analysis in Section 4.4 to confirm that the fraction collection was successful. Using the Blue Ribbon Iris as a standard of comparison in Section 4.5, the concentrated extract's retention times were compared to those of the Blue Ribbon Iris to visually confirm the presence of Dp-3-*p*-coumru-5-glc in the concentrated pepper extract. The HPLC separation was confirmed as a plausible separation technique in Section 4.6.

4.1: High Performance Liquid Chromatography (HPLC)

The separation technique of choice for this study is reverse phase high performance liquid chromatography (HPLC) using a C₁₈ column. HPLC utilizes a non-polar stationary phase (C₁₈) that keeps non-polar molecules on the column longer in conjunction with a moderately polar aqueous mobile phase that helps the more polar molecules elute faster. In terms of retention time (t_R), the less polar molecules have

longer t_R values in comparison to the more polar molecules that elute from the column first.

When choosing a separation method for ACNs it is important to remember the extractions are originating from live plants that contain many other polyphenols. In order to separate the components effectively a gradient method should be used that features an acidified aqueous solution (polar) and acetonitrile (less polar, i.e. more non-polar). In the past, researchers often utilized isocratic methods that held the solvent ratios constant throughout the entire run and this led to co-eluting peaks, noisy chromatograms, mislabeled components and non-detected polyphenols.

Gradient methods were developed as the instruments and detectors became more sensitive. This was to help resolve the peaks by having the solvent ratios change over time. Conventionally, the gradient method starts with the more polar solvent at a higher percentage than the non-polar solvent and over time decreases the polar to non-polar solvent ratio. This idea is based on the fact that the non-polar column holds more tightly to the non-polar molecules in the sample as the polar solvent moves through the column. A gradient allows the researcher to elute the more polar components early and slowly elute the less polar (or more non-polar) molecules as the solvent ratios change over time. For these reasons a gradient method is suggested when separating polyphenols, and particularly for ACN separation because these compounds are less polar than water.

HPLC operates on the principles of hydrophobic forces. These originate from the partial positive and negative charges present in the dipolar water (H_2O) chemical structure. The interactive forces of these processes can be measured by HPLC. There is proportionality between the binding of the analyte to the stationary phase and the surface

area around the non-polar segment of the analyte molecule once it associates with the ligand in the aqueous eluate. Energy is released during this process and is proportional to the surface tension of the eluate and the analyte's hydrophobic surface. The most popular way to reduce the surface tension of water is to add a less polar solvent such as acetonitrile to the mobile phase. This addition allows for greater separation of the plant polyphenols, most specifically ACNs (200).

A gradient method is implemented in this research because it automatically reduces the polarity and surface tension of the aqueous mobile phase throughout the analyses, therefore leading to greater separation of the extract's components. Thus, compounds elute faster, the peaks are taller and narrower, and the peak height increases giving the peaks a "sharper" look. The principle of increasing the amount of less polar solvent (i.e. acetonitrile) to the mobile phase throughout the run is to reduce the surface tension of the water. Research has shown the attachments to anthocyanins play a role in how they are separated via HPLC. According to Harborne & Grayer (62), when an ACN is injected onto a reverse phase (i.e. C-18) column if it is glycosylated then it will be more mobile and elute more quickly, with 3,5-diglycosides eluting faster in comparison to 3-diglycosides. Hydroxylation has also been shown to increase an anthocyanin's mobility, while *O*-methylation decreases mobility and results in longer retention times. Additionally, when ACNs are acylated with aromatic acids, such as *p*-coumaric acid, or an aliphatic acid like malonic acid, the retention times have been shown to increase (62). The acetone rinsing step of the extraction protocol should have removed a majority of the chlorophyll from the extract, but if some remnants remain, chlorophyll a and b are both

polar compounds (201) and would run off before the ACN using the current gradient method discussed in Section 4.2.

There are multiple advantages to the use of HPLC, such as: shorter analysis times; a high degree of resolution (more complete constituent separation); reusability of columns; highly reproducible results; low detection limits; and both instrumentation and quantitation can be automated. It is advantageous for this study to utilize HPLC because the ACN source is a pigment in the foliage of the purple pepper plant that contains many other phytochemicals and the ACN itself is a polar molecule. This study requires a high number of separation analyses to obtain a concentrated ACN sample and this technique provides higher purity fractions versus other chromatography techniques, such as column chromatography.

4.2: HPLC Separation Method

The ACN separation method takes place on a Waters system (Waters Corp. Milford, MA, USA) equipped with two Waters 515 HPLC pumps (labeled A and B to correspond to solvents), a Waters 2487 Dual λ Absorbance Detector and a Waters 3.9 x 300 mm μ Bondapak C₁₈ analytical column with particle size (dp) 10 μ m, 125Å. This method utilizes a gradient system with two major solvents. Solvent A is 4.5% formic acid (HCOOH), 14.5% acetic acid (HAc) and 81% distilled water (DI H₂O) and Solvent B is HPLC grade acetonitrile. The gradient system is at a constant flow of 1.0 mL/min. It begins at 99%A/1%B (v/v) and increases linearly to 80%A/20%B over 30 min and then is held constant for an additional 30 min. This elution profile is monitored for 60 min at

340 nm to identify the majority of polyphenols present. This wavelength was chosen based on the diagram in Figure 4.1 that demonstrates most flavones and flavonols have a λ_{\max} in the 300 – 400 nm range, while anthocyanidins (i.e. aglycones) have a λ_{\max} in the 500 – 550 nm range. A second run is monitored at 540 nm for 60 min to identify the anthocyanins present. This longer wavelength is chosen because as the number of hydroxyl groups increases on the B-ring of the aglycone structure (Fig. 2.3), the λ_{\max} of the aglycone shifts to longer wavelengths (6) and the colors change from orange to purple. Delphinidin has a known λ_{\max} of 534-545 nm (81), and has a bluish-red color (6). The dry purple pepper ACN extract is resolubilized in 1% HCl/MeOH and stored until further separation on HPLC (Section 3.2.7). The sample injection volume is 15 μ L of ACN extract onto a 20 μ L loop for each wavelength monitored.

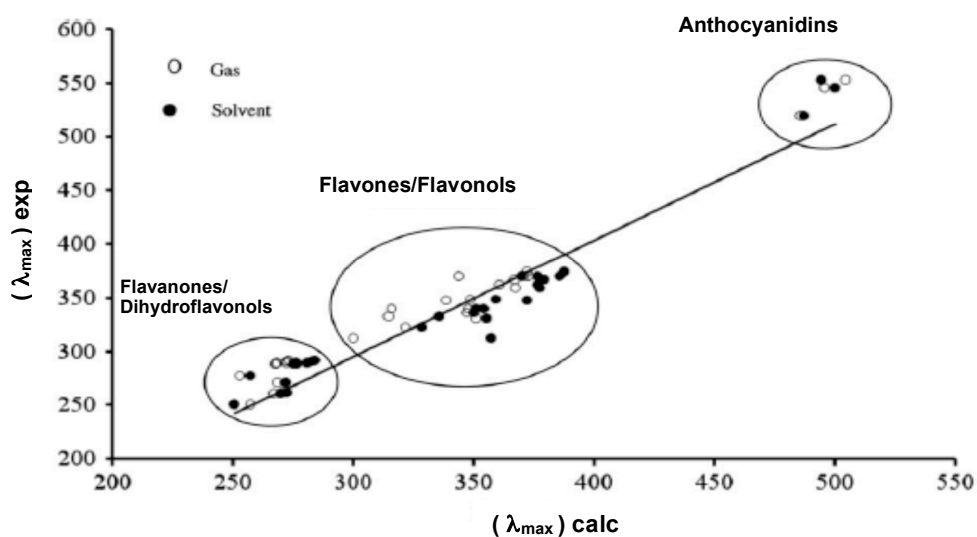


Figure 4.1: Diagram from Anouar *et al.* (202) of experimental versus calculated λ_{\max} values for various polyphenols that include: dihydroflavonols/flavanones, flavones/flavonols and anthocyanidins.

After each run is complete the gradient is at 80%A/20%B. A rinse cycle commences to help remove any particles still on the column or in the system by ramping

the gradient from 80%A/20%B to 50%A/50%B over 5 min and is held for 5 min. The gradient is then set to ramp up to 99%A/1%B over 5 min. Once the rinse is complete the system is ready for another injection. There was no auto sampler available for this investigation therefore each injection was manually performed.

The extract has a shelf life ≥ 12 months when stored in a dark freezer at -20°C as long as the original extraction method was performed well. Due to the stock extract's stability and longevity this allows time to collect as many fractions of the major ACN as necessary from the stock extract. This stock extract is injected onto the column and the major ACN peak is collected from each run. This process is repeated many times until there is a sufficient amount of ACN collected. These fraction collections are then dried down using a rotovap.

4.2.1: Fraction Collection

In order to calculate fraction collection time the first step is to determine the elution time of the major ACN (Dp-3-*p*-coumru-5-glc) and the following criteria are useful to determine elution time. Compare the largest peak, presumably the major ACN, on both chromatograms ($\lambda = 340$ and 540 nm) using the following criteria: t_R , area, % area, peak height and % peak height, peak width and absorbance value. Perform initial injections in triplicate (at minimum) to ensure the precision of the separation method and instrument, as well as the accuracy of the peak elution.

Retention times will vary slightly with each run due to factors such as temperature changes and fresh solvents, but the peak elution order and spacing should be relatively constant. Keeping this in mind, every chromatogram will not demonstrate the exact same

retention time for the major ACN, therefore the peak area and height are used for correct identification. If the major ACN peaks are comparable at 340 nm and 540 nm then fraction collection may proceed. It is important to note the start and end times of the major ACN peak for each run, this allows the calculating of the fraction collection time. An example of comparable chromatograms for the major ACN peak can be seen in Figure 4.2 a and b. The corresponding data tables are found in Table 4.1. These data tables display the similarities between the two wavelengths based off the criteria previously mentioned. If there is no peak agreement then there is the possibility of contamination and/or impurities. Examples of contamination would be the presence of many peaks in or around the major peak of interest, a very broad peak spanning multiple minutes near the peak of interest or peaks overlapping the major peak of interest thus making fraction collection of the major ACN extremely difficult or impossible. A clear example of contamination/impurities is in Figure 4.3, where the chromatogram shows other components co-eluting with the major ACN. It is possible other polyphenols were not removed when the sample was rinsed with acetone in the extraction protocol and therefore are co-eluting. In this case the HPLC column needs to be rinsed thoroughly to avoid further co-elution and the extract is no longer a viable source for fraction collection and a new leaf sample must be obtained and extraction protocol performed, drying the extract and then test the extract by HPLC (as this section describes) before proceeding with the fraction collection. For this investigation any suspicious samples were discarded and not used for fraction collection.

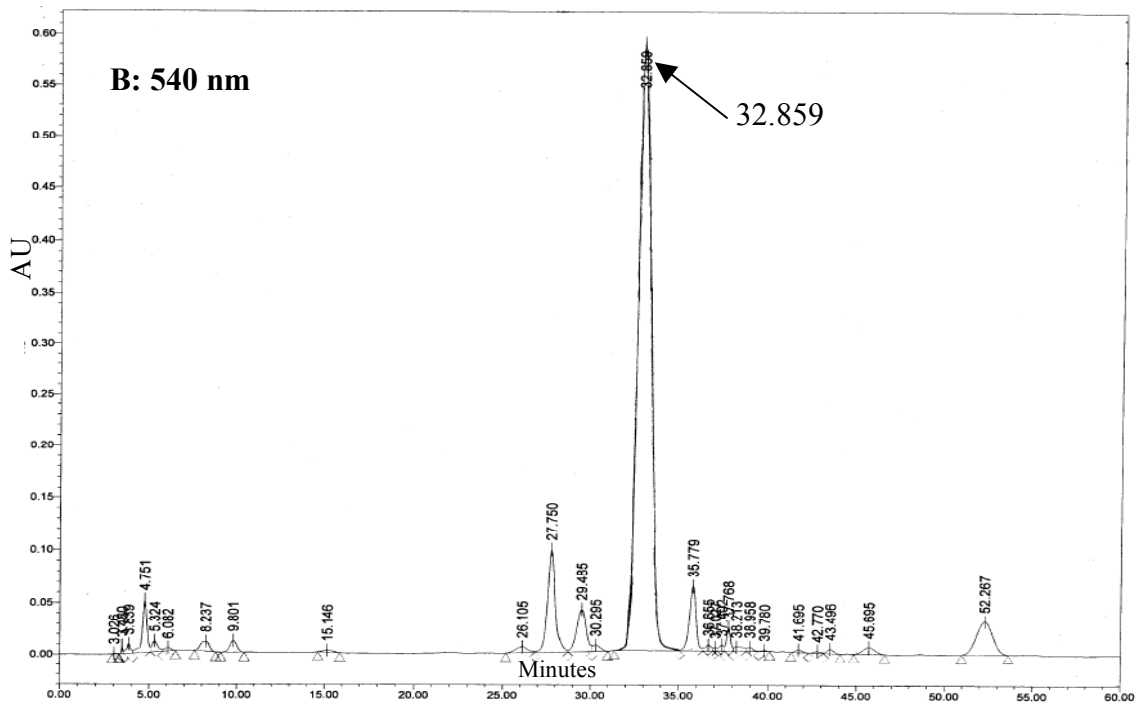
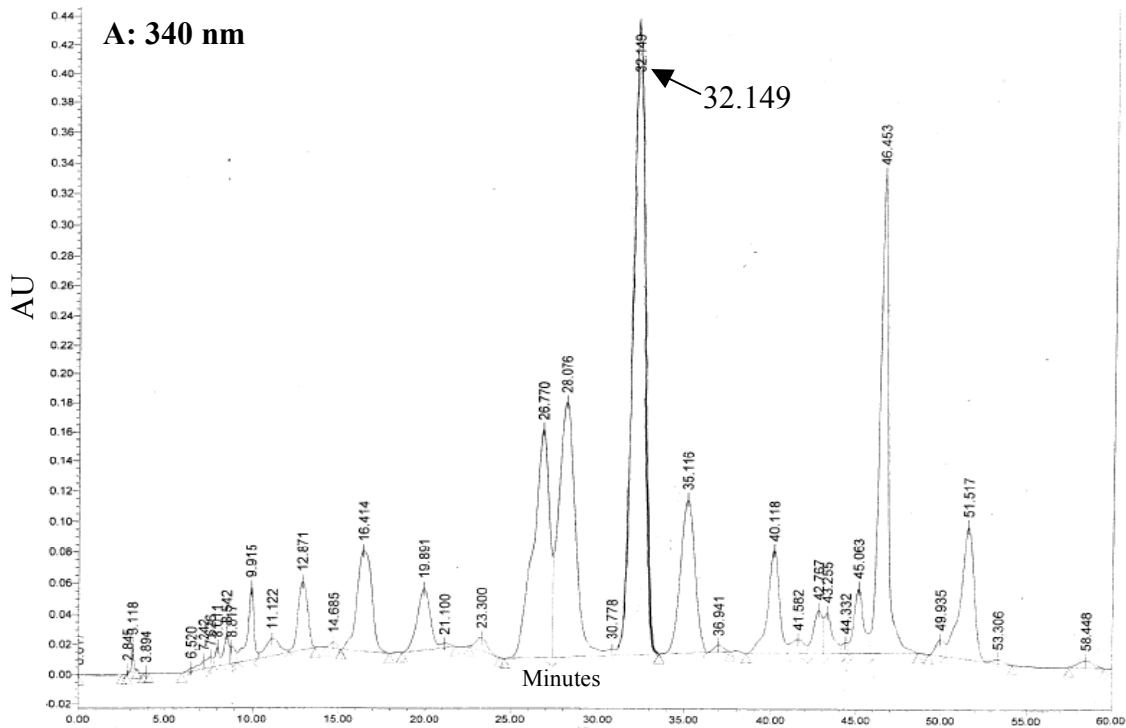


Figure 4.2: Chromatograms of original ACN pepper extract at (a) 340 nm (b) 540 nm. The retention times of the major ACN peak at 340 nm is 32.149 min and at 540 nm is 32.859 min.

Table 4.1: Values from original ACN pepper extract: (a) 340 nm and (b) 540 nm. The major ACN values are highlighted in yellow.

A: Comparison Table for Values Collected for Original ACN Pepper Extract at 340nm							
Peak #	Retention Time (min)	Area (µV *s)	% Area	Height (µV)	%Height	Width (sec)	Absorbance (AU)
1	0.017	61970	0.074	917	0.052	149	0.00012
2	2.845	7828	0.010	2403	0.136	8	0.00294
3	3.118	124130	0.148	18317	1.039	27	0.02119
4	3.894	6419	0.008	807	0.046	22	0.00211
5	6.520	32868	0.039	1984	0.113	37	0.00435
6	7.242	157532	0.188	5470	0.310	45	0.00936
7	7.626	172223	0.205	7384	0.419	28	0.01186
8	8.011	214981	0.256	12904	0.732	24	0.01876
9	8.542	415571	0.495	21029	1.193	33	0.02844
10	8.817	216489	0.258	11226	0.637	23	0.01879
11	9.915	1222690	1.457	47453	2.691	73	0.05680
12	11.122	658970	0.785	11317	0.642	106	0.02394
13	12.871	1740949	2.074	44730	2.537	92	0.06110
14	14.685	99868	0.119	3999	0.227	50	0.02180
15	16.414	4023786	4.794	65399	3.709	170	0.08060
16	19.891	2124956	2.531	40206	2.280	127	0.05620
17	21.100	107939	0.129	2726	0.155	58	0.02050
18	23.300	410837	0.489	8943	0.507	106	0.02580
19	26.770	9635204	11.479	150868	8.556	163	0.16230
20	28.076	11077057	13.196	169052	9.588	174	0.18080
21	30.778	172648	0.206	4326	0.245	46	0.01860
22	32.149	20733978	24.701	421775	23.921	148	0.43800
23	35.116	5816582	6.929	100176	5.681	170	0.11480
24	36.941	169521	0.202	4587	0.260	76	0.02190
25	40.118	3264304	3.889	66910	3.795	147	0.09410
26	41.582	502202	0.598	9227	0.523	68	0.02610
27	42.767	1057531	1.260	28613	1.623	56	0.04410
28	43.255	929909	1.108	26973	1.530	61	0.04270
29	44.332	157495	0.188	6949	0.394	25	0.02330
30	45.063	1747318	2.082	42456	2.408	77	0.05660
31	46.453	11306106	13.469	319450	18.117	172	0.33530
32	49.935	376266	0.448	10875	0.617	61	0.02610
33	51.517	4773484	5.687	86564	4.909	145	0.09820
34	53.306	119384	0.142	2586	0.147	90	0.01196
35	58.448	301983	0.360	4629	0.263	126	0.01052

B: Comparison Table for Values Collected for Original ACN Pepper Extract at 540nm							
Peak #	Retention Time (min)	Area (µV *s)	% Area	Height (µV)	%Height	Width (sec)	Absorbance (AU)
1	3.026	12369	0.029	794	0.0793	23	0.00142
2	3.480	39459	0.092	8153	0.815	14	0.00899
3	3.839	150256	0.351	9469	0.946	30	0.01020
4	4.751	959999	2.243	50854	5.081	61	0.05229
5	5.324	240985	0.563	10638	1.063	42	0.01323
6	6.082	77150	0.180	3269	0.327	43	0.00686
7	8.237	334337	0.781	9612	0.960	73	0.01323
8	9.801	316809	0.740	11268	1.126	81	0.01382
9	15.146	67153	0.157	1533	0.153	75	0.00414
10	26.105	277643	0.649	5699	0.569	98	0.00837
11	27.750	3039327	7.102	98183	9.810	114	0.10114
12	29.485	1549447	3.621	40984	4.095	82	0.04451
13	30.295	179342	0.419	5977	0.597	53	0.00960
14	32.859	30400950	71.037	588055	58.755	221	0.59262
15	35.779	1603337	3.746	61993	6.194	79	0.06584
16	36.655	130344	0.305	5763	0.576	33	0.01044
17	37.027	47193	0.110	3307	0.330	15	0.00800
18	37.402	108886	0.254	5814	0.581	24	0.01044
19	37.768	341909	0.799	22999	2.298	30	0.02770
20	38.213	151780	0.355	3965	0.396	43	0.00883
21	38.958	83687	0.196	3845	0.384	41	0.00853
22	39.780	16537	0.039	889	0.089	37	0.00592
23	41.695	73449	0.172	2617	0.261	60	0.00623
24	42.770	54389	0.127	1921	0.192	49	0.00499
25	43.496	120524	0.282	4410	0.441	58	0.00700
26	45.695	318203	0.743	6539	0.653	105	0.00822
27	52.267	2100549	4.908	32315	3.229	161	0.03370

The chromatograms in Figure 4.2 and the data in Table 4.1 demonstrate how the food-grade extract contains some other polyphenols in addition to the major ACN in the purple pepper foliage. It is possible to have these other compounds co-elute with the major ACN peak, as shown in Figure 4.3, which would contaminate the major ACN peak with other polyphenols.

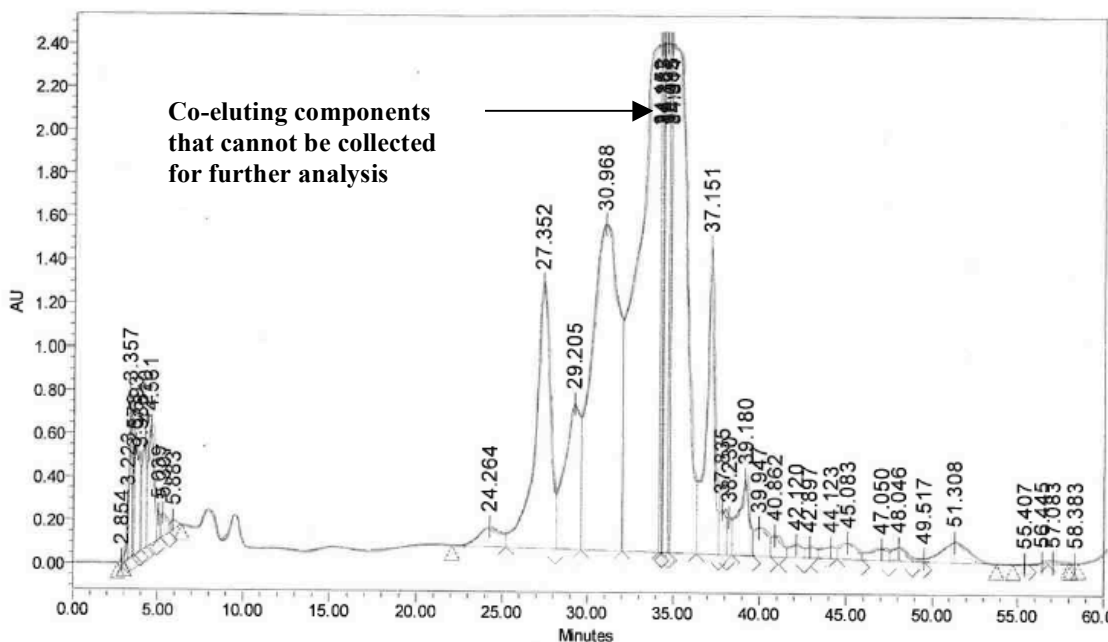


Figure 4.3: Example of a contaminated/impure pepper extract that cannot be used for fraction collection due to co-elution of components. The retention times for these co-eluting peaks are at 34 minutes.

Injecting the extract onto the HPLC and seeing a chromatogram like the one shown in Fig. 4.2, fractions of the major ACN are collected. If the chromatogram resembles Fig. 4.3, fractions should not be collected, and it is best practice to thoroughly rinse the HPLC system and the column before injecting another extract. Many fractions will be collected and used for further characterization and structural analysis. These fractions will later be concentrated (i.e. dried on the rotovap) to increase the success of the MS and NMR analyses because the ACN of interest will be the main component and

not be diluted by the other polyphenols that are present in the original extract. The chromatograms of a clean sample demonstrate the major ACN peak and are free of co-eluting peaks. The clean fractions are analyzed at both 340 and 540 nm. The similarities in peak shape, peak area, retention time and absorbance should be noted, as seen in Table 4.1 and the major ACN values are highlighted in yellow to demonstrate the difference between 340 and 540 nm.

The elution time for the major ACN peak usually begins ~32.00 min and ends ~37.00 min. Due to this long elution time a specific absorbance value of ≥ 2.00 AU is set to determine the collection of the fraction for the major ACN peak. The real-time collection into a clean plastic vial begins as the peak on the chromatogram for the major ACN raises to an absorbance value ≥ 2.00 AU and the column run off solution is a bright pink color, as seen in Figure 4.4.



Figure 4.4: Bright pink colored run off solution collected as a fraction from the HPLC.

Collection ends when the real-time chromatogram demonstrates an absorbance value ≤ 2.00 AU. It does not matter if the color of the column run off is still bright pink, collection stops at ≤ 2.00 AU, as shown by the red line in Figure 4.5. This specific absorbance value is used as a marker because it represents the most concentrated portion of the major ACN peak and it will help to keep the fraction free of contaminants, such as neighboring peaks or shoulders.

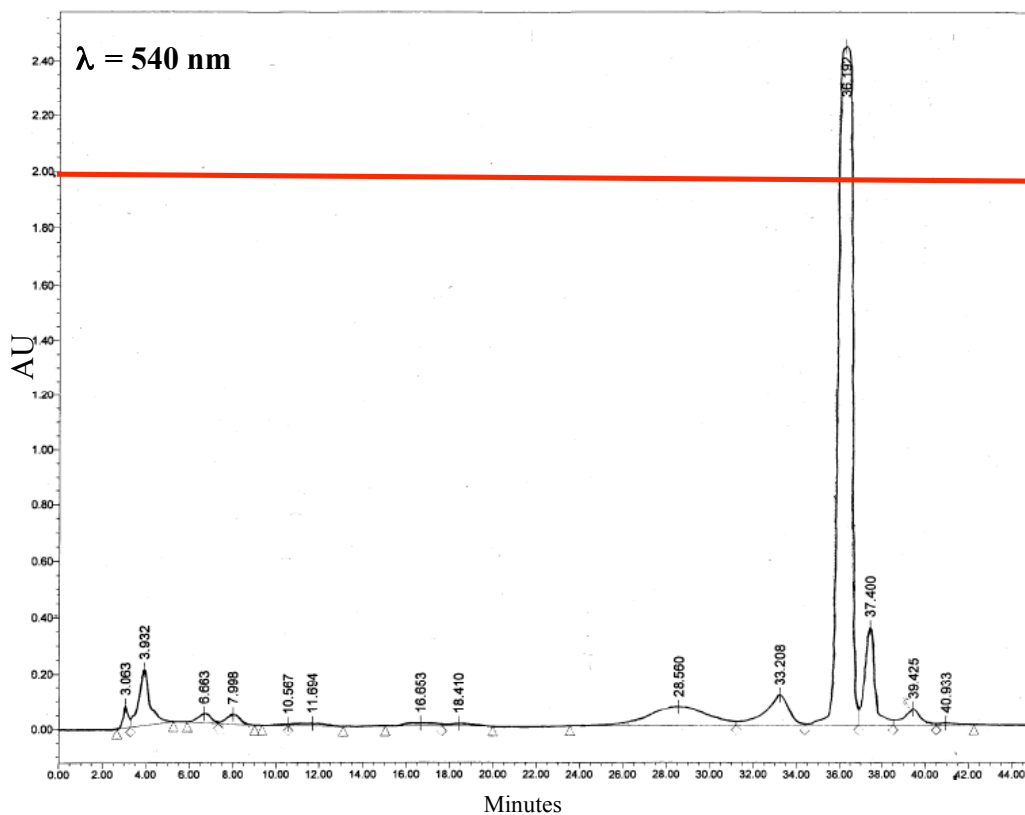


Figure 4.5: Sample chromatogram of fraction collection above 2.00 AU (red line); collection time corresponds to $t_R = 35.82 \text{ min}$ to 36.55 min (0.73 min or 43.8 sec).

For this investigation the extract run time is 45 min, which is a 15 min reduction from the original separation method. This reduction helps to maximize the number of fraction collections per day. To compensate, there is an increase in the rinse cycle time between each run. The final gradient at the end of a sample run is 80%A/20%B and

ramps over 5 min to achieve 50%A/50%B. This ratio holds for 15 mins and then the gradient ramps up to 99%A/1%B over 5 min to complete the rinse cycle.

A volume of 15 μ L of extract is injected onto the column and the chromatogram is monitored until 30.00 min. The fraction collection vial has a dark colored lid and is wrapped in aluminum foil to protect the fractions from exposure to light. In between collections store the vial in a refrigerator at temperature ($T = 4\text{ }^{\circ}\text{C}$) to maintain the integrity of the ACN complex. The fraction collection only includes the very top of the ACN peak off the chromatogram in real-time to avoid collecting any neighboring components. Collection begin when the absorbance value ≥ 2.00 AU and concludes when the absorbance value falls back down to ≤ 2.00 AU. Record the fraction collection time because t_R varies slightly with each injection. The collection times range from 0.70 to 1.44 min for this investigation. See Appendix A for the complete list of collection times for all fractions. This range is due to variations in the temperature of the room, the time of day, different collection day and duration the HPLC system has been running on the collection day.

Repeat the fraction collection process as many times as necessary until there is enough concentrated extract available for further structural analysis. Collect a minimum of 10 fractions to test for purity. Purity testing consists of drying down the fractions, resolubilizing them in 1% HCl/MeOH, and then injecting the concentrated extract onto the HPLC system. There should be a minimum of 3 replicates to ensure reproducibility. In this investigation, a pure extract is defined as: a chromatogram consisting of one peak whose % area is $\geq 94\%$ and any neighboring peaks are $\leq 2\%$ of the total % area. If the purity test fails, new fractions need to be collected and retested for purity. In this

investigation, the purity will never reach 100% due to the constraints of the chemicals used in the extraction method (reference Section 3.2 and 3.3).

In relation to industry purity standards from ChromaDex™ the concentrated extract of Dp-3-*p*-coumru-5-glc from the foliage of purple peppers in this research project would fall under the definition of a secondary standard (203). By ChromaDex™ definition this means the standard was created for “in-house” laboratory use, the purity is determined by HPLC, gas chromatography (GC) or TLC only and the purity depends upon the source from which it was obtained. For comparison purposes, a primary standard of delphinidin chloride at ChromaDex™ has a purity of 94.7% and is confirmed by an adjusted total purity as calculated by HPLC, Karl Fischer (water content), and GC (residual solvent), including mass spectra and NMR profiles.

This investigation has a maximum of 60 fractions. It took approximately three months to collect the 60 fractions. The first 10 fractions were tested for purity and passed. The collection continued until 60 fractions were obtained. For this investigation, a minimum of 2 mg (dry weight) is necessary to further analyze by NMR, so at least 60 fractions (equivalent ~45 mL) were collected to ensure sufficient NMR sample mass once the fractions were dried down. All fractions were collected in foil-covered plastic containers, with multiple containers needed to collect a sufficient amount. After collection, the samples were stored in the refrigerator at T = 4 °C until next the fraction collection. Once collection is complete for the day, store the vial containing the fractions in the refrigerator if the contents cannot be dried on the same day.

For future research, it may be best to dry the aqueous fractions as soon as possible to avoid any possible degradation that may occur from long storage times at T = 4 °C.

After drying, the researcher can store the fractions at room temperature in a dark, dry place or resolubilize the concentrated fractions in 1% HCl/MeOH and store them in the freezer at $T = -20\text{ }^{\circ}\text{C}$ more safely (Section 4.2.2). One major drawback would be the loss of product due to multiple transfers. For this reason, this investigation dries all the fractions at once.

4.3: Drying Fractions and Resolubilizing Concentrated Extract

Using surgical gloves remove the vial containing the fractions from the refrigerator. Obtain an empty 1000 mL RB flask and record its mass before adding all the fractions (~45mL) from the foil-covered plastic containers. Use a large RB flask to avoid loosing any product during an occasional “bump” in pressure. Place the flask on the rotovap in a water bath at $T = 40\text{ }^{\circ}\text{C}$, initiate the vacuum system and set the turning dial to a level of 2 or 3. Keep the RB flask on the rotovap until the sample is dry. This time will vary based on the volume of fractions in the RB flask.

Once dry, remove the RB flask from the rotovap. Inside the hood, allow it to cool to room temperature on a cork flask support ring (~5 to 10 min.). After cooling, weigh the RB flask again in order to calculate the mass of dry ACN extract present. Calculate the mass of dry ACN extract. This investigation has 24 mg of dry ACN extract. The extract will still have trace amounts of water due to the azeotrope issue previously discussed (Section 3.2.4), subsequently minute amounts of other water-soluble components possibly may be present. The majority of the dry extract is ACN due to the component specific extraction method that was developed for the ACN found in purple

pepper leaves. Specifically, the acetone rinse step assisted in removing many of the other polyphenols (Section 3.2.5).

Resolubilize the concentrated extract in the smallest amount of 1% HCl/MeOH possible. Transfer the solvent by pipette to ensure accuracy. This investigation utilizes 2.0 mL of 1% HCl/MeOH. Transfer the concentrated ACN in 1% HCl/MeOH with a new, clean pipette tip into an autoclaved plastic vial and place it in a -20 °C dark freezer until analysis.

4.4: Analysis of Concentrated Extract

For the analysis of the concentrated extract the same HPLC method was used as described in Sec. 3.4. A volume of 15 μ L of concentrated extract was injected onto the column at $\lambda = 540$ nm and $\lambda = 340$ nm, independently. The concentrated extract was analyzed in duplicate. For purposes of demonstration, only one analysis is shown here. Additional data and chromatograms can be found in Appendix A. This investigation shows the t_R for the major ACN of the purple pepper foliage at $\lambda = 540$ nm is 34.260 min. The % peak area for the major peak is 98.104% of the total area of the curve, while the % peak height is 96.601% and the absorbance value is 1.33. The t_R for the major ACN of the purple pepper foliage at $\lambda = 340$ nm is split into two peak at 34.328 min and 34.974 min. The most likely cause of this split peak is the partial separation of the *cis* and *trans* isomers of the major ACN. Previous literature from Ichiyanagi *et al.* (9) describes a similar ACN chromatogram in eggplant peel extract and they resolved the peaks of the *cis* and *trans* isomers at 520 nm. Results for this investigation are given in Table 4.1. At

$\lambda = 340$ nm, the % peak area for the two major peaks are 42.18% and 52.22% (total 94.40%) of the total area of the curve, while the % peak heights are 33.58% and 52.78% (total 86.36%) and absorbance values of 0.448 and 0.703 (total 1.15). The difference in % peak heights is due to the peak at 3.038 min that is most likely a solvent peak.

In the anthocyanin chemistry community it is common to express the total anthocyanin content based on the pH-differential method as delphinidin-3-glucoside (Dp-3-glc) equivalents (204) and is calculated with the formula:

$$c \text{ (mg/L)} = A \cdot M \cdot DF / \epsilon_M \cdot d \quad (4.1)$$

Where c = total anthocyanin content, A = absorption value, M = molecular weight of delphinidin-3-glucoside (465 g/mol), DF = dilution factor, ϵ_M = molar extinction coefficient of delphinidin-3-glucoside at pH 1 (29000 L/mol·cm), and d = path length of the cuvette (1cm) (205). This method of calculating total anthocyanin content does not utilize Dp-3-*p*-coumru-5-glc found in purple pepper plants because the molar extinction coefficient is not known, therefore the best estimate would be to use Dp-3-glc equivalents. Industry practice is to assume that the molar extinction coefficient is approximately the same for the major analyte and any other observed peaks. Once the total anthocyanin content is calculated as Dp-3-glc equivalents with Equation 4.1, the % peak area can then be multiplied by the value obtained to determine the total anthocyanin content. At 340 nm, the two peaks at 34.328 and 34.974 min (in Fig. 4.6) representing the presumed *cis* and *trans* isomers of Dp-3-*p*-coumru-5-glc would be expressed as 3.02 mg/L (for 34.328 min) and 5.89 mg/L (for 34.974 min) of Dp-3-glc equivalents.

Table 4.2: Summary of major ACN values for the concentrated extract at 340 & 540 nm.

Comparison of the Major ACN Peak Values for the Concentrated Pepper Extract				
Wavelength	# of Peaks	Retention Time (min)	% Peak Area	% Peak Height
340	2	34.328, 34.974	42.18, 52.22	33.58, 52.78
			Total: 94.40	Total: 86.36
540	1	34.260	98.10	96.60

Significant absorbance values ($A \geq 1.00$ AU) are observed at both 340 and 540 nm, as presented in Tables 4.3 and 4.4, demonstrating the extract is fairly concentrated due to the amount of light that is being absorbed by the major ACN peak. These values are an indicator of the success of the fraction collection protocol to concentrate the purple pepper extract. Visually, it is easy to see on the chromatograms in Figures 4.6 and 4.7 that the concentrated extract is much cleaner in comparison to the original extract (Fig. 4.2). When the values from the original extract (Table 4.1) are compared to the values from the concentrated extract shown in Tables 4.2 – 4.4, the data corroborates what is shown in the chromatograms. One noticeable difference between the original and concentrated extract chromatograms is the split peak seen in the concentrated extract at 340 nm. The assumption for the cause of the split peak is the *cis* (34.328 min) and *trans* (34.974 min) isomers of the major ACN are trying to separate, thus the combination of their values in Table 4.2 for comparison.

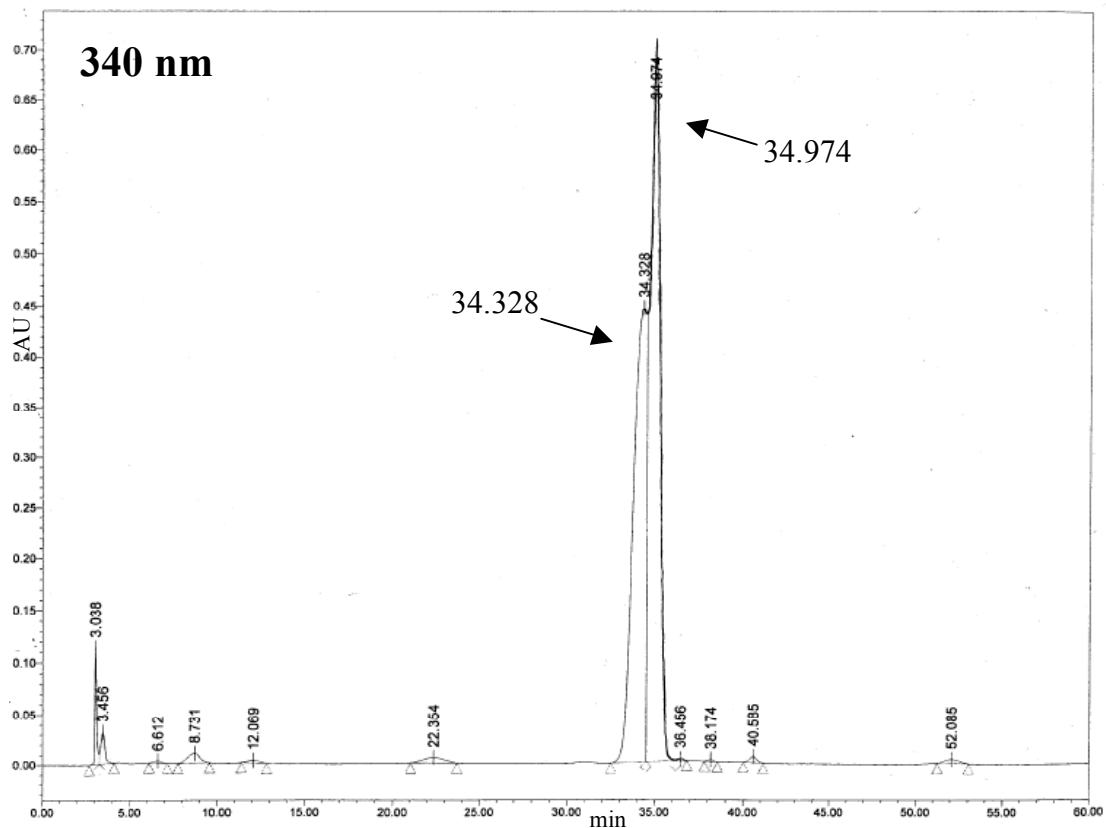


Figure 4.6: Chromatogram of concentrated purple pepper extract at 340 nm. The retention times are 34.328 and 34.974 minutes for the major ACN peaks.

Table 4.3: Chromatographic data from the concentrated pepper extract at 340 nm. The major ACN is highlighted in yellow, combined % Peak Area is 94.40 for peaks 7 and 8.

Chromatographic Data from the Concentrated Extract at 340 nm							
Peak #	Retention Time (min)	Area ($\mu\text{V} \cdot \text{s}$)	% Area	Height (μV)	% Height	Width (sec)	Absorbance (AU)
1	3.038	845960	1.573	114412	8.616	36	0.114
2	3.456	519088	0.965	31933	2.405	50	0.034
3	6.612	68803	0.128	2208	0.166	63	0.005
4	8.731	471044	0.876	9518	0.717	107	0.012
5	12.069	116455	0.217	2459	0.185	87	0.005
6	22.354	471132	0.876	5452	0.411	161	0.008
7	34.328	22682062	42.180	445941	33.584	122	0.449
8	34.974	28080922	52.220	700801	52.778	100	0.703
9	36.456	55780	0.104	2425	0.183	38	0.006
10	38.174	43964	0.082	2197	0.165	43	0.005
11	40.585	179560	0.334	6240	0.470	69	0.008
12	52.085	239426	0.445	4249	0.320	109	0.006
Total	-	53774196	100.000	1327835	100.000	-	-

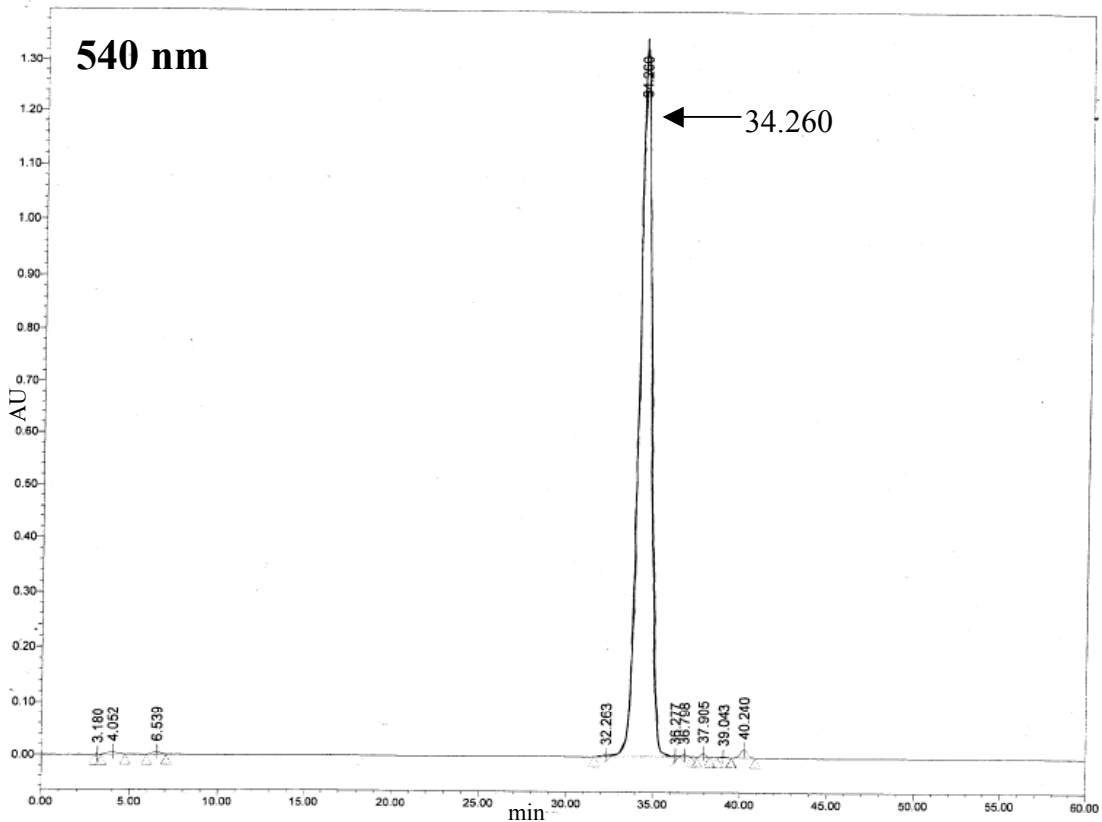


Figure 4. 7: Chromatogram of the concentrated purple pepper extract at 540 nm. The retention time is 34.260 minutes for the major ACN peak.

Table 4.4: Chromatographic data from the concentrated pepper extract at 540 nm. The major ACN peak is highlighted in yellow with a % Peak Area of 98.10.

Chromatographic Data from the Concentrated Extract at 540 nm							
Peak #	Retention Time (min)	Area ($\mu V * s$)	% Area	Height (μV)	% Height	Width (s)	Absorbance (AU)
1	3.180	36295	0.056	2781	0.202	22	0.002
2	4.052	220750	0.338	5661	0.411	84	0.006
3	6.539	150695	0.230	5312	0.385	65	0.006
4	32.263	88296	0.135	2382	0.173	56	0.004
5	34.260	6415456	98.104	1331100	96.601	208	1.333
6	36.277	62732	0.096	2631	0.191	32	0.005
7	36.798	68228	0.104	3205	0.233	41	0.006
8	37.905	119112	0.182	6830	0.496	44	0.009
9	39.043	39518	0.060	1995	0.145	46	0.003
10	40.240	454098	0.694	16034	1.164	84	0.016
Total	-	65395179	100.000	1377930	100.000	-	-

It is obvious that the concentrated extract demonstrates significantly fewer peaks when compared to the original pepper extract. At 340 nm, the original extract identified a

total of 35 peaks and the major ACN peak was only 24.70% of the total peak area. While the concentrated extract identified 12 peaks and the two major ACN peak areas (for the presumed *cis* and *trans* isomers) combined to be 94.40% of the total peak area. At 540 nm, the original extract identified 27 peaks and the major ACN peak was 71.04% of the total area. In comparison, the concentrated extract identified 10 peaks and the major ACN peak was 98.10% of the total area as shown in Table 4.5. These numbers demonstrate the extract was concentrated successfully so as to increase the concentration of the ACN of interest and decrease the other polyphenols that were present in the original extract.

Table 4.5: Comparison of values from the original pepper extract and the concentrated pepper extract at 340 and 540 nm. The total # identified peaks and the % Peak Areas for the major ACN are reported here.

Comparison of the Total # Identified Peaks and % Peak Areas for the Major ACN between the Original Extract and Concentrated Extract at 340 and 540 nm		
	Original Extract	Concentrated Extract
Total # Identified Peaks, 340 nm	35	12
Total # Identified Peaks, 540 nm	27	10
% Peak Area, 340 nm	24.70	94.40 (combined <i>cis</i> & <i>trans</i> peaks)
% Peak Area, 540 nm	71.04	98.10

4.5: Comparison of Concentrated Pepper Extract to Blue Ribbon Iris Standard

The concentrated pepper extract is presumed to have high concentrations of the anthocyanin Dp-3-*p*-coumru-5-glc. Previous work by Dr. Sam Asen and his colleagues (72,73,77,139,140) found the same anthocyanin in Prof. Blaauw Iris, which is a hybrid of *Iris tingitana* Boiss. & Reut., but is commonly known as the Blue Ribbon Iris. As discussed in Section 2.7, anthocyanin standards are very difficult and expensive to

manufacture. Luckily, this work had access to Dr. Asen's extensive anthocyanin collection. It was housed at the Plant Sciences Institute at USDA-BARC, where the HPLC analyses were conducted. A very minute amount of the Dp-3-*p*-coumrut-5-glc extract from the Blue Ribbon Iris was available and could be used as a visual marker standard for comparison of retention times. The Blue Ribbon Iris extract was stored in a dark freezer in 1% HCl/MeOH for > 20 years. When the extract was removed from the freezer all of the solution had evaporated and only dry ACN was present in the vial. The least amount of solvent possible was added to resolubilize the sample (0.8 mL) because on the vial was written "0.4 mg/ 0.8 mL 0.5%HCl/MeOH" as the original concentration. This amount of solvent was sufficient to resolubilize the standard and remove enough to analyze on the HPLC.

The Blue Ribbon Iris standard was then injected onto the HPLC system in a volume of 15 μ L, the same injection volume as the purple pepper foliage. An initial injection showed only one major peak and 2 very small minor peaks in the standard. Therefore, on the second injection the curve shape was set to 10 instead of 6 to alter the rate of the solvent change during the gradient. Figure 4.8 depicts the curve shape graph to demonstrate how the user can set the rate that the solvent is changed to the new proportions throughout the gradient.

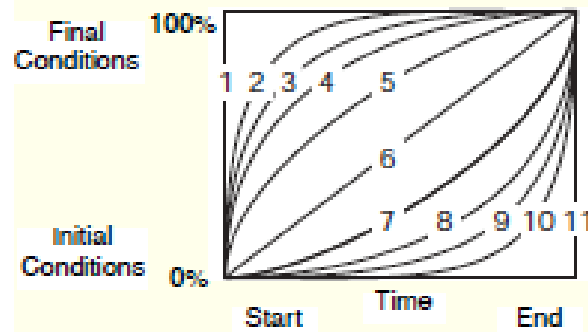


Figure 4.8: Gradient curve shape graph provided with the HPLC by the manufacturer, Waters Corporation (206).

No evidence of late eluting peaks were seen in the second run, only the major peak at 25.120 min, which is highlighted in red in Figure 4.9 b, two very small peaks at 6.567 and 27.205 min and a noticeable peak at 30.064 min that is highlighted in black in Figure 4.9 b. There was also a grouping of peaks around 5 minutes that are most likely a solvent front. The concentrated pepper extract was then injected and the major peak was at 24.946 min (highlighted in red in Fig. 4.9 a). This matched closely the major peak retention time from the Blue Ribbon Iris at 25.120 min (highlighted in red in Fig. 4.9 b). There were three extremely small peaks at 3.148 (in the noise of chromatogram), 18.132 and 33.341 minutes (highlighted in black in Fig. 4.9 a). Overall, the Blue Ribbon Iris standard visually matched the concentrated pepper extract very well by displaying similar retention times. These results correlate with previous research where the two major ACN peaks for the *cis* and *trans* isomer were clearly separated (Fig. 4.9 c) from Ichiyanagi *et al.* (9). The major differences between the studies are that Ichiyanagi *et al.* had a much larger sample size of eggplant skins (10 kg) and they were able to separate both the *cis* and *trans* isomers of Dp-3-*p*-coumru-5-glc with a gradient system that utilized TFA and MeOH as solvents. In contrast, this research investigation had a much smaller sample

size of purple pepper foliage (≤ 100 mg) and was unable to separate both *cis* and *trans* isomers completely.

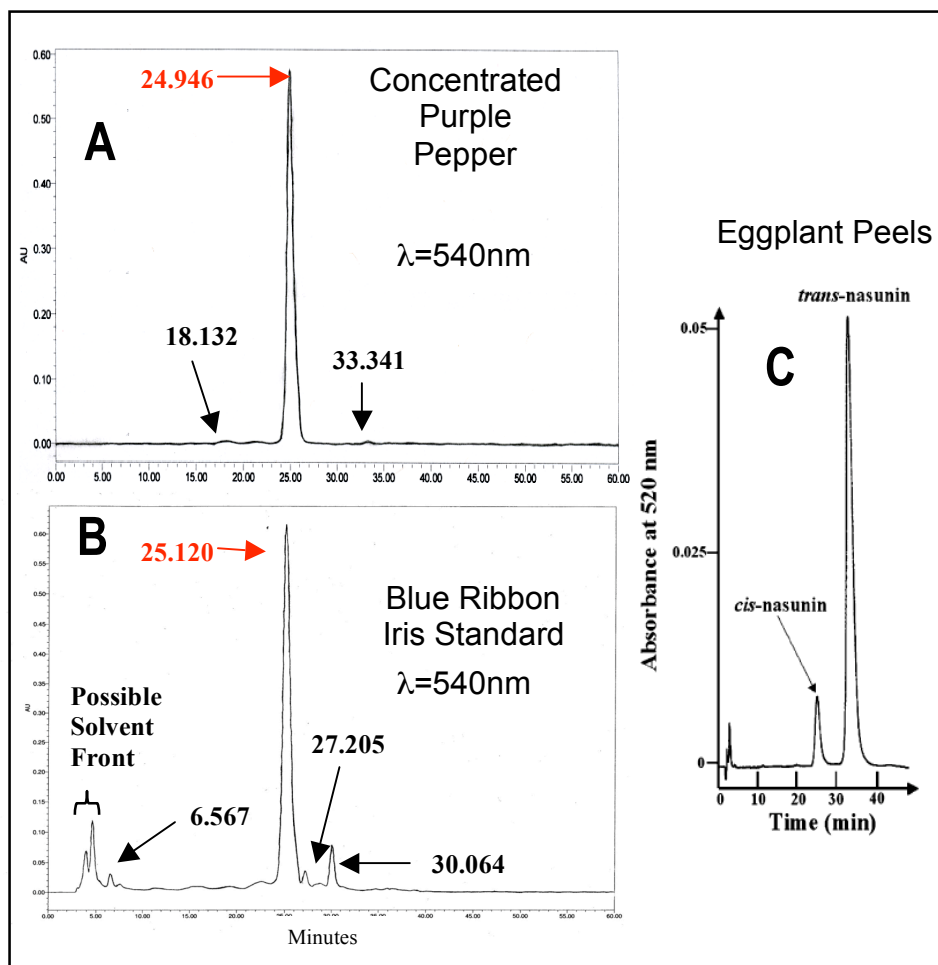


Figure 4.9: HPLC chromatograms of (a) concentrated purple pepper extract at 540 nm; (b) Blue Ribbon Iris standard at 540 nm and (c) eggplant peels at 520 nm by Ichiyanagi *et al.* (10).

4.6: Confirmation of HPLC Separation Technique

Based on these results, the HPLC confirmed by comparison of retention times at 540 nm that the ACN of interest present in the Blue Ribbon Iris standard, identified as Dp-3-*p*-coumru-5-glc by Asen *et al.* (72,73,77,139,140), is also present in the purple

pepper foliage. This separation technique shows the success of the food-grade extraction method, as well as the success of the fraction collection technique used to concentrate the original purple pepper foliage extract (Sections 4.2 – 4.2.4). The concentrated pepper extract is now ready for further analysis by MS and NMR. The MS (Chapter 5) and NMR (Chapter 6) data will assist in the characterization and structural elucidation of the ACN present in the foliage of the purple pepper concentrated extract.

Chapter 5: Mass Spectrometry

Overview

Chapter 5 focuses on a discussion of the characterization technique known as mass spectrometry (MS). In Section 5.1, the use of a specific MS technique in this investigation to characterize the anthocyanin of interest is briefly described. Next, in Section 5.2, is the discussion of why the use of Electrospray Ionization Tandem Mass Spectrometry (ESI-MS/MS) is essential to this investigation. The preparation of the standard plant materials for MS/MS analysis is covered in Section 5.3, followed by the preparations of the plant extracts (Section 5.3.1) and the concentrated purple pepper ACN extract (5.3.2). The instrument conditions are optimized for each individual investigation and these are explained in Section 5.4 for the coupled instrument known as the Liquid Chromatography Photodiode Array Electrospray Ionization Tandem Mass Spectrometer (LC-PDA-ESI-MS/MS), which was utilized to analyze the purple pepper ACN extract. The characterization data obtained from the LC-PDA-ESI-MS/MS are exhibited in Section 5.5. Finally, the confirmation of the major anthocyanin in the foliage of the purple pepper extract by MS/MS is discussed in Section 5.6.

5.1: Characterization Technique

This investigation requires a coupled characterization method in order to elucidate the purple pepper foliage ACN structure. Multiple methodologies, with differing strengths, are used to assist in characterizing the ACN of interest. The three techniques chosen for this portion of the investigation are: liquid chromatography with photodiode array detection coupled with electrospray ionization tandem mass spectrometry

(LC-PDA-ESI-MS/MS). It was essential to use this coupled instrument in order to properly separate the compounds found in the purple pepper foliage by HPLC and then characterize them with PDA and ESI-MS/MS detectors in order to determine the most accurate composition of the ACN of interest.

5.2: Electrospray Ionization Tandem Mass Spectrometry (ESI-MS/MS)

When it comes to choosing a mode of ionization for mass spectrometry, it is important to use a technique that is amenable to the polar anthocyanin compound shown in Figure 5.1 and, particularly, a separation technique that would maintain the integrity of the ACN compound before ionization. Electrospray ionization (ESI) is a good choice because it is appropriate for the compound of interest and has a limit of sensitivity in the femtogram range. Also, by coupling liquid chromatography and photo diode array detection with ESI-MS/MS it provides more accurate data than HPLC with UV-Vis detection alone to assist in describing the structure of the ACN of interest. This setup provides the opportunity to run the pepper extract under similar conditions to the previous LC separation method in Chapter 4, but have added characterization components that offer crucial data to determine the ACN present in the purple pepper concentrated extract.

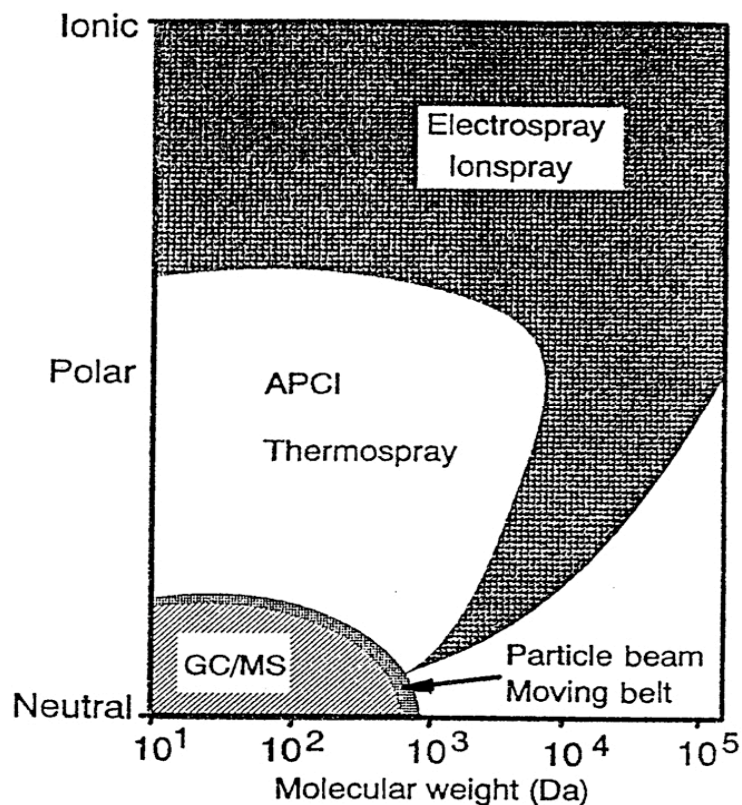


Figure 5.1: Illustration of the application ranges of different mass spectrometric and chromatographic coupling methods (207).

ESI-MS/MS is a form of ionization commonly used for compounds that range from polar to ionic and a mass range of $10^1 - 10^5$ Daltons (Fig. 5.1), which is appropriate for Dp-3-*p*-coumru-5-glc based on its polar characteristics and its $m/z = 919$ (precursor ion). Coupled to LC, the electrospray is generated under atmospheric pressure when a strong electric field is applied to the liquid flowing through the capillary (207). In order for the electric field to be produced a potential difference of 3-6 kV must be applied between the capillary and the counter electrode. There will be charge accumulation at the liquid surface on the end of the capillary and highly charged droplets will form that will contain extremely small amounts of solvent. As the solvent evaporates, the droplets

shrink down and their coulombic forces approach their cohesion forces, thus causing the droplets to burst. These mini “explosions” continually happen and the highly charged ions then desorb (207). The nebulizer gas used in this ionization process is nitrogen (N_2) to help carry the sample into the MS detector. The ESI process is illustrated in Fig. 5.2.

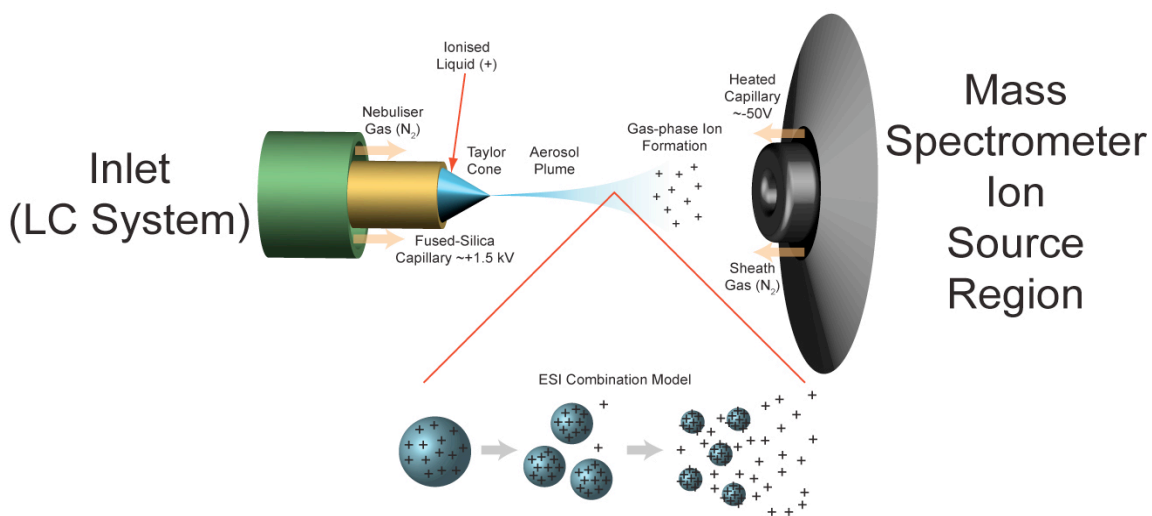


Figure 5.2: Image of electrospray ionization source (208).

A literature review of polyphenol research demonstrates an extensive use of ESI-MS/MS to characterize this large class of plant based compounds (5,8,15,86,143,145,145–149,161,164,168,169,171,174,176,181,191,193,195,209–218). Most often this technique is used because it works well with polar compounds, such as anthocyanins. The type of ions that are produced depends upon the initial charge of the compound (219), meaning a positively charged compound will produce positive ions. Both positive and negative ion modes have been shown to help identify different polyphenols (9,10,143,147,177–180,182–188,217–220). The availability of the instrument also played a key factor in choosing this technique. An ESI-MS/MS was readily available at the USDA with colleagues who were willing to assist. This allowed some first hand knowledge of the

instrument itself to be shared and hands-on experience was obtained. The LC-PDA-ESI-MS/MS conditions for this investigation are outlined in Section 5.4.1.

5.3: Preparation of Standard Plant Material for MS/MS

For comparison purposes, this investigation utilizes three standard plant materials. Samplings of Chinese eggplant (*Solanum melongena*) and Chinese celery (*Apium graveolens* var. *secalinum*) were purchased from local grocery stores in Maryland. The Chinese eggplant was skinned and the skins were retained for testing, while the flesh was discarded. Eggplant is from the Solanaceae family, which includes the genus *Capsicum*. The compound of interest in this investigation is found in the foliage of the purple pepper (*Capsicum annuum* L.) so the use of eggplant skins is a good choice as a standard for comparison, since previous literature has found the same ACN, delphinidin-3-(*p*-coumaroylrutinoside)-5-glucoside, in eggplant skins (8–10,216). The Chinese celery is used to help identify additional polyphenols present in the purple pepper foliage since Chinese celery's polyphenols are well documented (187). The third standard plant material is freshly picked purple pepper foliage from the field, but this standard does not undergo the previously described ACN extraction protocol in Chapter 3. The Chinese eggplant skins and Chinese celery are cut into small pieces then dried at room temperature in a fume hood. The fresh pepper leaves are freeze-dried separately for 24 hours. All the standard plant materials are finely powdered and are then individually passed through 20 mesh sieves prior to extraction. Powdered standard plant materials are stored in airtight containers until analysis.

5.3.1: Preparation of Plant Extracts

The plant extracts are made from the powdered standard plant materials. They are prepared according to Lin *et al.* (177,179–188) by extracting 500 mg of each powdered standard (50 mg for Chinese celery) with 5.00 mL of 60:40 (v/v) methanol-water. This extraction utilizes sonication with a FS30 Ultrasonic sonicator at 40 KHz, 100 W (Fisher Scientific, Pittsburg, PA, USA) for 60 min at room temperature (<35 °C at the end of 60 min) to create a slurry mixture. This slurry is then centrifuged at 2500 rpm for 15 minutes (IEC Clinical Centrifuge, Damon/IEC Division, Needham, MA, USA) to help separate the components. The supernatant is removed and filtered through a 17mm (0.45 µm) PVDF syringe filter (VWR Scientific, Seattle, WA, USA). This filtered supernatant is the plant extract (180). This investigation produces three plant extracts via the Lin *et al.* method: Chinese eggplant skin, Chinese celery and whole freeze-dried purple pepper foliage.

5.3.2: Preparation of Concentrated Purple Pepper ACN Extract

The purple pepper extract is a concentrated ACN that was extracted using the food-grade protocol in Chapter 3 and then underwent the fraction collection protocol from Sections 4.2 – 4.2.3. It is not made from any of the powdered plant materials. This concentrated extract has a higher ACN concentration than the original freeze-dried purple pepper foliage plant extract because it has gone through more purification steps to help remove other polyphenols, as well as steps to concentrate the ACN of interest (Dp-3-*p*-coumru-5-glc). The concentrated purple pepper extract will be compared against the

plant extracts of air-dried Chinese eggplant skins, Chinese celery and freeze-dried whole purple pepper foliage.

5.4: Instrumentation Conditions

When using MS for characterization it is necessary to optimize the instrument conditions in order to obtain useful results from the matrix being analyzed. Some of the conditions are set because of necessity and availability, while others are specific to the sample type. In the instrument's separation method it was vital to maintain the integrity of the ACN complex, especially the flavylum cation, because this structure gives the ACN of interest its intense purple color. If the ACN structure were to be compromised then Dp-3-*p*-coumru-5-glc could not be studied or detected, but instead another delphinidin derivative, which is not the goal of this investigation. Section 5.4.1 outlines the conditions of the LC-PDA-ESI-MS/MS instrument.

5.4.1: LC-PDA-ESI-MS/MS Conditions

The LC-PDA-ESI-MS/MS coupled system used for this step of the characterization is located at the Food Composition and Methods Development Laboratory, Beltsville Human Nutrition Research Center (BHNRC), USDA-BARC in Beltsville, MD, and was under the supervision of Dr. Long-ze Lin and Dr. James Harnly (178–188,190). The conditions presented here are representative of this investigation (190,221), but it is important to note that every system needs to be optimized for the analyte of interest so as to achieve the most accurate results.

The HPLC system was an Agilent 1100 HPLC instrument coupled to a binary pump, an autosampler, a thermostat controlled column compartment and a photodiode array detector (PDA). The analytical column is a Symmetry 100 RP-18 (C18) 150 x 2.1 mm (3.5 μm), with an attached 10 x 2.1 mm (3.5 μm) guard column of the same material. The columns used in this system are both from the Waters Corporation (Milford, MA, USA). The flow rate was held at a constant 0.2 mL/min. The injection volume was 10 μL and the column oven temperature was set at 25 $^{\circ}\text{C}$. This method utilized a gradient system with two major solvents. Solvent A was 0.1% formic acid in water and Solvent B was 0.1% formic acid in acetonitrile. The gradient was from 4 to 20% B (v/v) at 40 min, to 35% B at 60 min, and then to 100% B at 61 min and held constant until 65 min. In order to view real-time displays of the peak intensities, the PDA was set at wavelengths of 530, 520, 350 and 280 nm. The UV spectra were recorded from 200-700 nm (190,221).

The HPLC was connected to a Finnigan LCQ Deca XP Plus ion trap (Thermo Finnigan, San Jose, CA) tandem mass spectrometer (MS/MS) system. The MS/MS was connected to the Agilent 1100 HPLC via an electrospray ionization probe (ESI), which ran in positive and negative ion modes. The acquisition parameters for this experiment were set as follows: mass range from m/z 150 to 2000; ion spray voltage, 4.5 kV; N_2 sheath gas, 80 arbitrary units; N_2 auxiliary gas, 10 arbitrary units; capillary temperature, 250 $^{\circ}\text{C}$; tube lens offset voltage, 30 V; and capillary voltage, 34 V for positive and -7 V for negative mode. Selective ion monitoring (SIM) at m/z 919 was used to confirm the precursor ion and the transitions of m/z 919 \rightarrow 757, m/z 919 \rightarrow 465, and m/z 919 \rightarrow 303 were studied to confirm the product ions. The HPLC and MS/MS were both controlled

via Thermo's Xcalibur software (190,221).

5.5 Characterization Data

By using high-powered magnetic fields to choose specific masses to analyze the MS/MS has the ability to select the m/z for the precursor ion in the first quadrupole and then fractionate the precursor ion in the second quadrupole in order to measure its product ions. Many compounds can have the same $m/z = 919$ for the precursor ion, therefore additional data from the product ions are needed to characterize the ACN of interest. As multiple product ions are produced their patterns are fairly specific and can assist in identifying the molecules that compose the precursor compound (i.e. ACN of interest). Previous research by Ichiyanagi *et al.* (9,10) has identified these specific product ions for Dp-3-*p*-coumru-5-glc to be m/z 757 (loss of glucose), 465 (loss of *p*-coumaric acid and rutoside) and 303 (delphinidin). The MS/MS cannot provide any specific information on how the compound is connected together or determine the attachment sites of the glucosides or acyl moiety. Only NMR analyses can provide this type of data. The NMR investigation for the ACN of interest is discussed at length in Chapter 6.

5.5.1: LC-PDA-ESI-MS/MS Characterization Data

At the Food Composition and Methods Development Laboratory, USDA-BARC, extensive polyphenol and flavonoid identification work for the USDA Flavonoid Database (222), as well as for specific projects, were already completed by Drs. Lin and Harnly (177–188) before this research project began, and were available for this project.

Additionally, the previously prepared plant extracts from the completed projects were also available for use. The extracts were prepared from a wide variety of plant sources. This provided a vast number of options to choose from in order to find plant sources whose profiles are similar to that of purple pepper foliage, but most importantly to assist in characterizing the compounds in the purple pepper foliage.

Referencing earlier investigations of Chinese celery and Chinese eggplant (187,222) determined these two sources to be practical standards to utilize in this investigation in order to determine the ACN of interest, as well as to detect the presence of other polyphenols. These two plant profiles were used to identify most of the compounds in the purple pepper foliage correctly by comparing the retention times, PDA and MS/MS data. It was extremely helpful to have access to the extensive database of previous polyphenol and flavonoid research as well as the superior knowledge and expertise of Dr. Long-ze Lin.

The LC chromatograms analyzed at 350 nm and 520 nm for the plant extracts (Section 5.3.1) of Chinese celery, Chinese eggplant and the freeze-dried purple pepper foliage are shown below in Figures 5.3 and 5.4. The wavelengths used to analyze the plant extracts are consistent with those utilized to create the USDA Flavonoid Database (177–188,222). Eleven peaks were separated in the freeze-dried purple pepper foliage. The Chinese celery and Chinese eggplant standards were essential in determining the identifications of the majority of the compounds in the freeze-dried purple pepper. The freeze-dried pepper foliage analyzed here did not go through the food-grade extraction protocol or the fraction collection protocol (in Chapter 3, Section 4.2.1 – 4.2.3), meaning more peaks are visible in these chromatograms in comparison to the chromatograms for

the concentrated pepper extract. The remaining data that was collected by the LC-PDA-ESI-MS/MS and not presented in this chapter can be found in Appendix B.

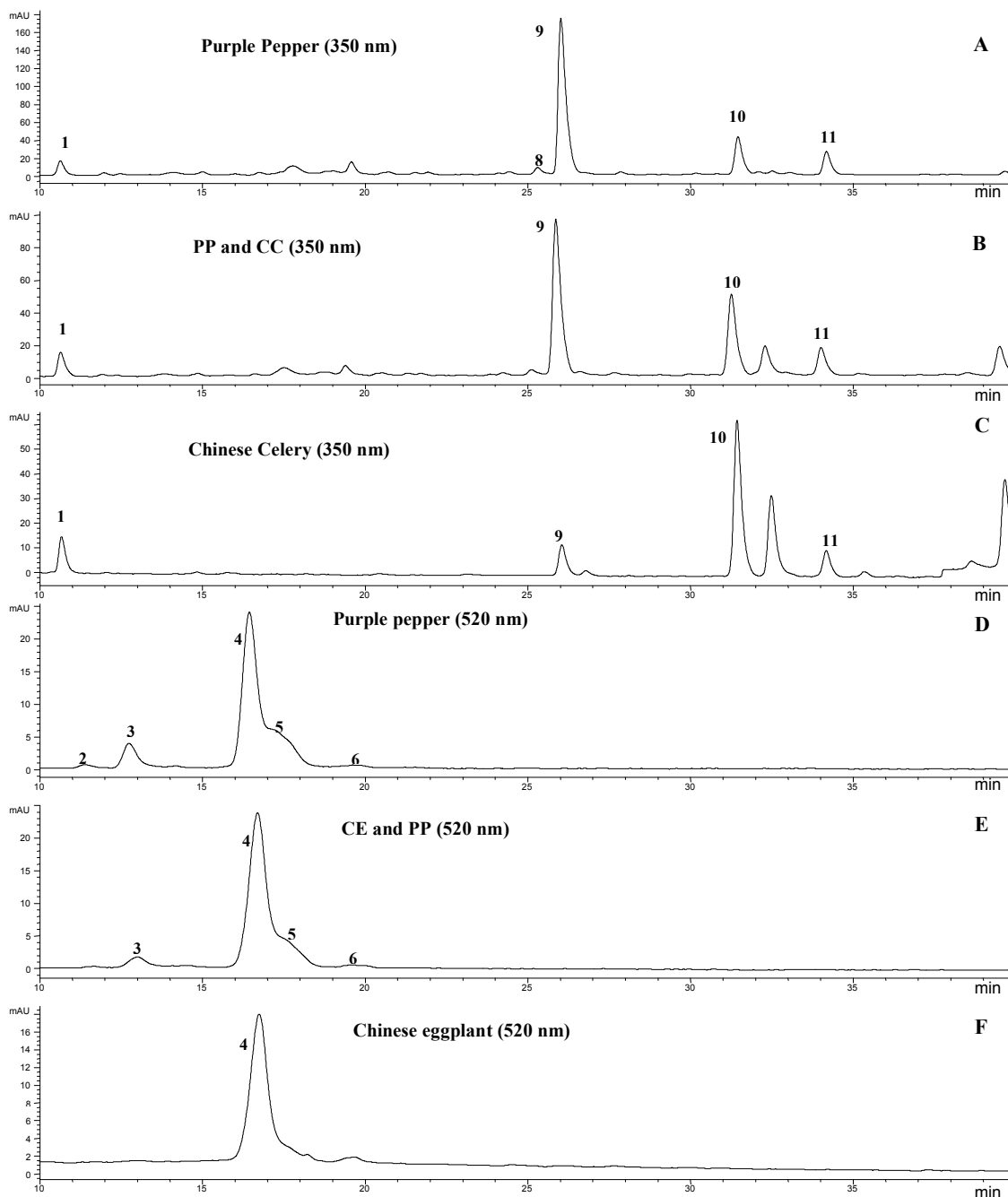


Figure 5.3: Chromatograms from LC-PDA-ESI-MS/MS. Abbreviations, PP = purple pepper (freeze-dried), CC = Chinese celery, CE = Chinese eggplant. (a) PP at 350 nm; (b) PP & CC at 350 nm; (c) CC at 350 nm; (d) PP at 520 nm; (e) CE & PP at 520 nm; (f) CE at 520 nm. Peak identifications are listed in Table 5.1.

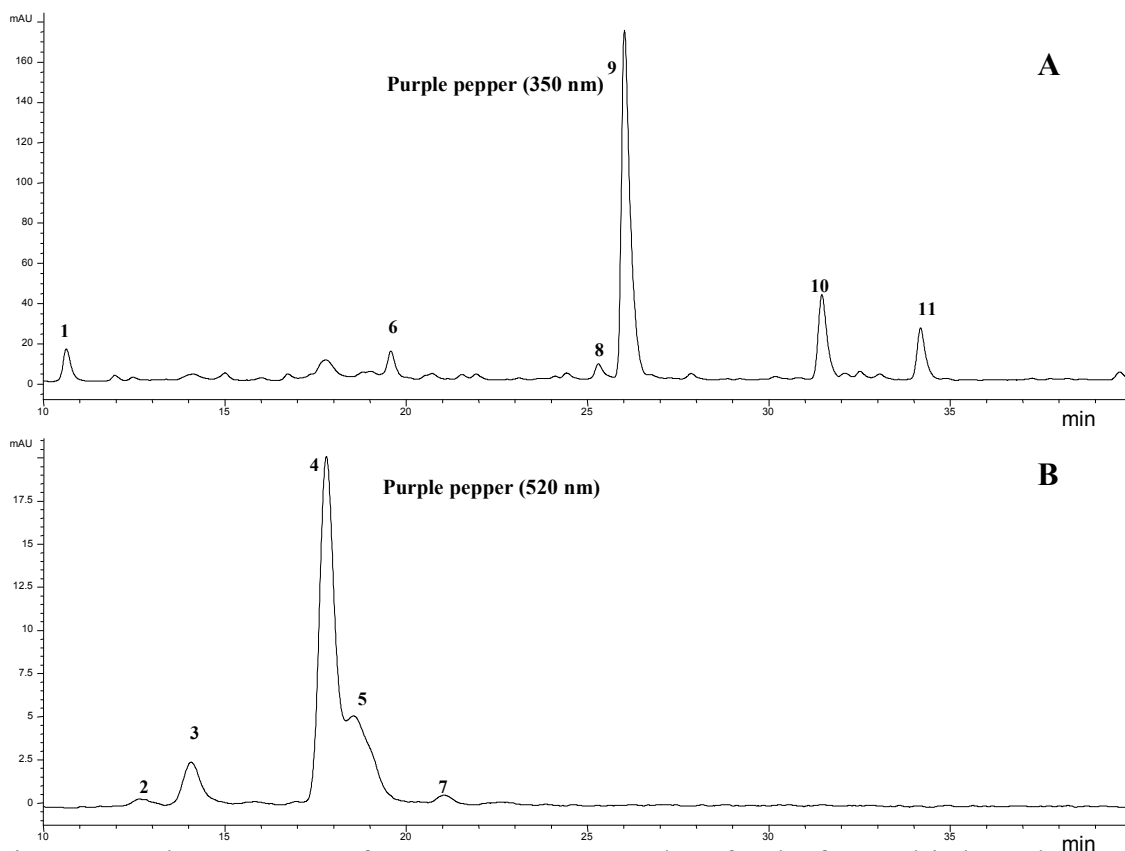


Figure 5.4: Chromatograms from LC-PDA-ESI-MS/MS for the freeze-dried purple pepper at (a) 350 nm and (b) 520 nm. Peak identifications are listed in Table 5.1.

Table 5.1 characterizes the peaks based on the peak numbers and retention times found in Figures 5.3. and 5.4. The UV spectra obtained from the PDA and the MS/MS data acquired for the freeze-dried purple pepper foliage are also listed in Table 5.1. It is imperative to use all of the information for characterization because it is not accurate to simply use retention time, UV spectra or MS/MS data alone. The data was compared to previous works completed at the Food Composition and Methods Development Laboratory, which allowed for the characterization of 7 of the 11 major peaks observed in the purple pepper foliage. The UV spectra are shown in Figure 5.5 a – g for peaks 1, 3-5 and 9-11. Peaks 2 and 6-8 are labeled as unidentified or not detected in Table 5.1 and will not be discussed here.

Table 5.1: Identification of peaks in the freeze-dried purple pepper foliage plant extract.

Peak No.	t_R (min)	$[M+H]^+ / [M-H]^-$ (m/z)	PI/NI aglycone, other ion (m/z)	UV* λ_{max} (nm)	Identification
1	10.6	355/353	---/191,179,173,135	218,238sh, 298sh, 326	chlorogenic acid ^a
2	12.4	nd	nd	292, 316sh, 530	unidentified ^c
3	14.1	935/933	773, 465,303/301	282, 322sh, 530	delphinidin 3- <i>O</i> -caffeoylrutinoside 5- <i>O</i> -glucoside ^b
4	17.4	919/917	757, 465,303/301	296, 310sh, 530	delphinidin 3- <i>O</i> -trans-p-coumaroylrutinoside 5- <i>O</i> -glucoside ^b
5	18.2	919/917	757, 465,303/301	280, 532	delphinidin 3- <i>O</i> -cis-p-coumaroylrutinoside 5- <i>O</i> -glucoside ^b
6	19.6	nd	nd	314	nd
7	20.8	nd	nd	278, 530	unidentified ^c
8	25.3	nd	nd	316	nd
9	26.0	581/579	287/285	254, 266sh, 350	luteolin 7- <i>O</i> -apiosylglucoside ^b
10	31.5	565/563	271/269	268, 338	apigenin 7- <i>O</i> -apiosylglucoside ^b
11	34.2	667/665	287/285	254, 266sh, 348	luteolin 7- <i>O</i> -malonylapiosylglucoside ^b

^a: identified with standard; ^b: identified with the positively identified compounds in Chinese eggplant or Chinese celery; ^c: possible unidentified minor anthocyanin; nd: not determined or identified.

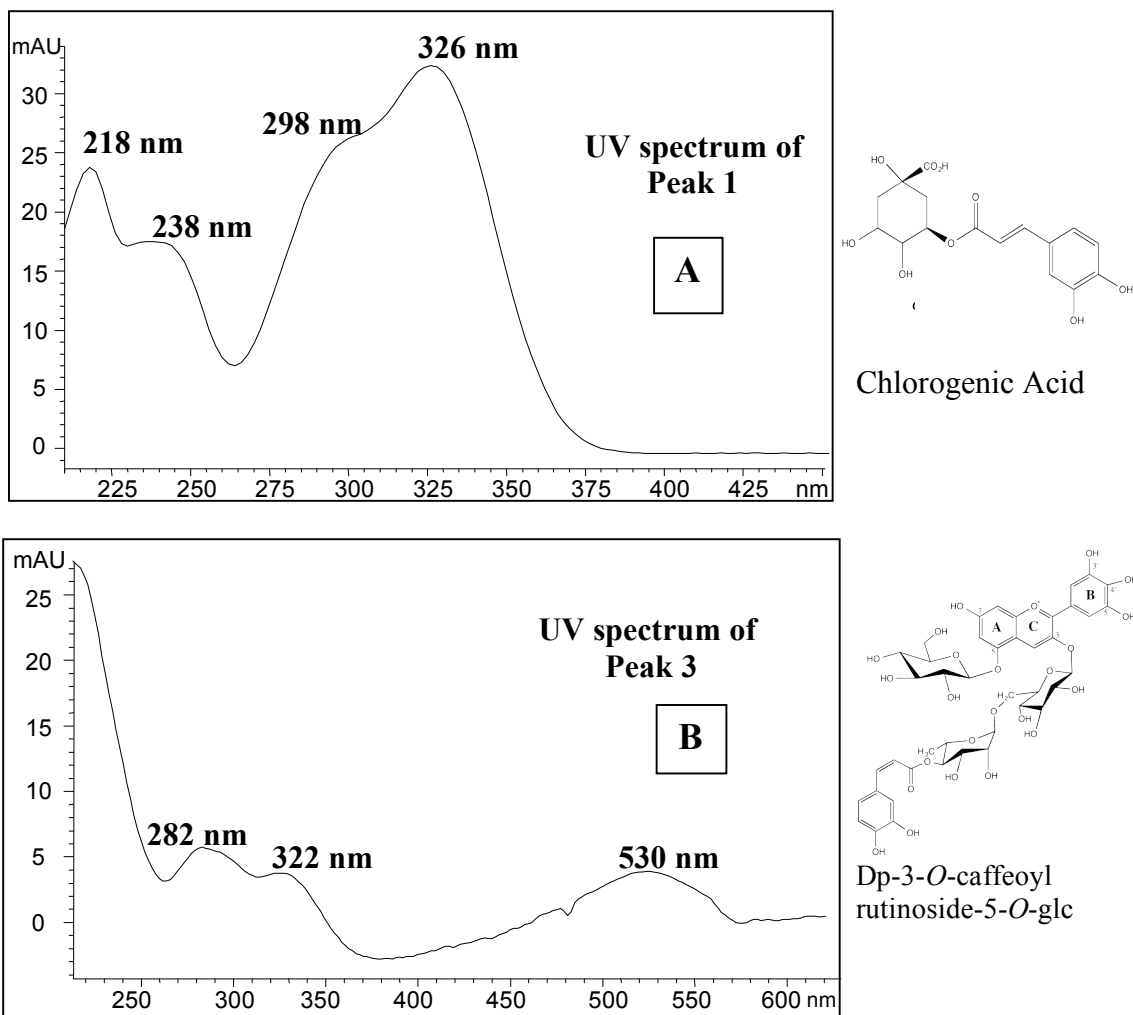
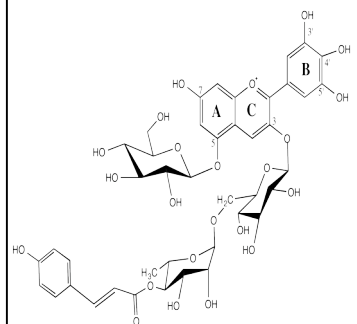
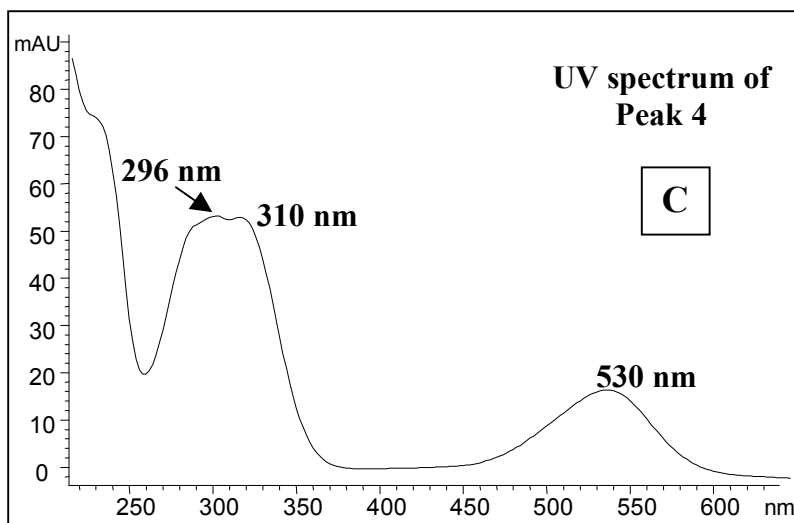
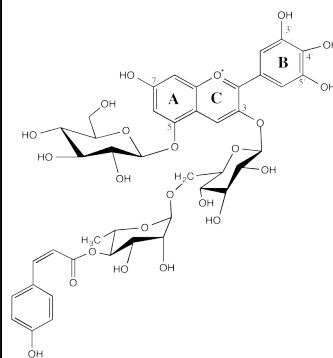
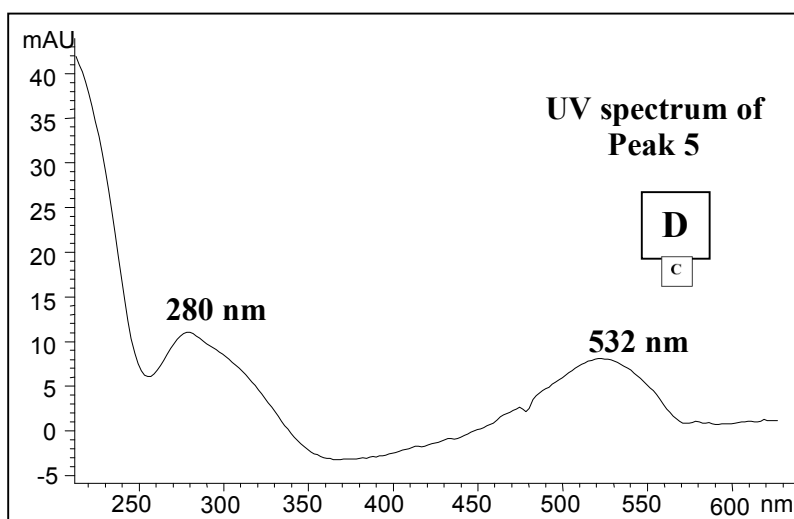


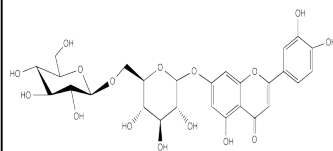
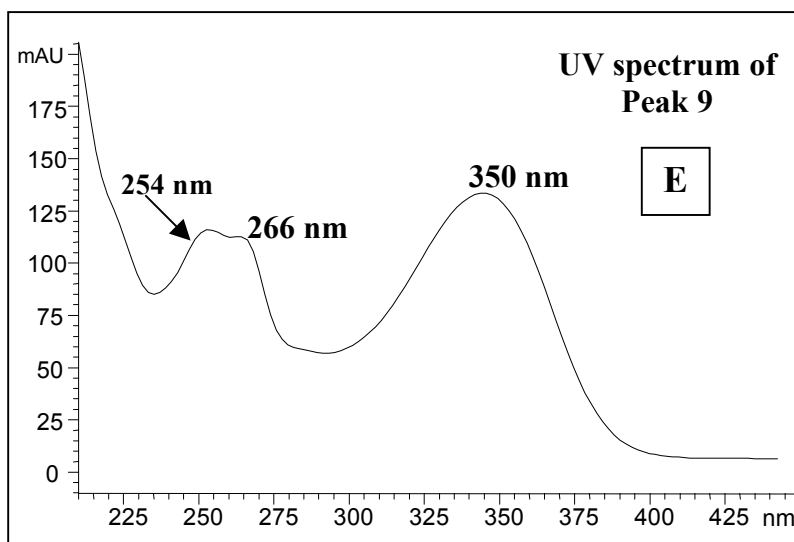
Figure 5.5: The UV spectra of peaks in the freeze-dried purple pepper foliage identified as peaks (a) 1, (b) 3, (c) 4, (d) 5, (e) 9, (f) 10, and (g) 11 in Figures 5.3 and 5.4.



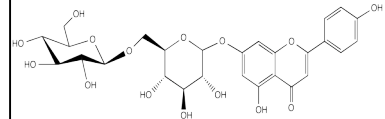
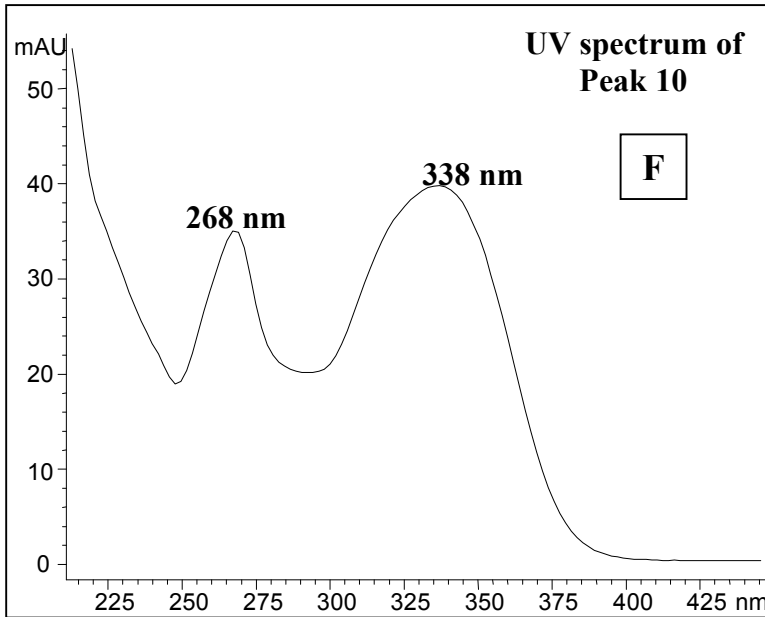
Dp-3-O-trans-*p*-coumrut-5-glc



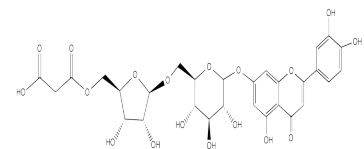
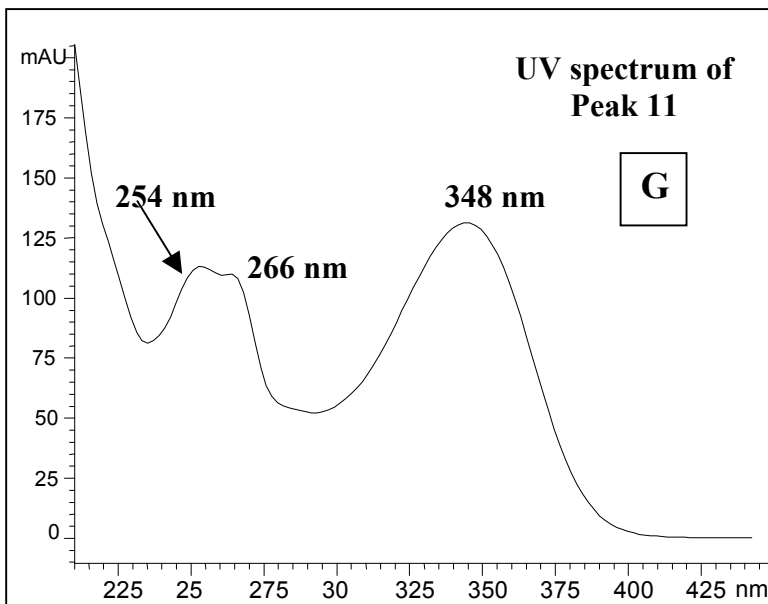
Dp-3-O-cis-*p*-coumrut-5-glc



Luteolin 7-O-apiosylglucoside



Apigenin 7-*O*-apiosylglucoside



Luteolin 7-*O*-malonylapiosyl glucoside

The retention times and PDA data give pertinent information regarding the characterization of the 11 peaks separated in the purple pepper foliage. The MS/MS data gives the researcher the chance to determine the m/z ratio of the ACN of interest's precursor compound, which published literature has demonstrated to be $m/z = 919$ (9,10), as well as the product ions at m/z 757, 465, 303 shown in Figure 5.6. Both the *cis* and *trans* isomers of Dp-3-*p*-coumrut-5-glc have the same precursor and product ions, as seen in Table 5.1.

Once all of the compounds in the freeze-dried pepper plant sample were identified the concentrated pepper ACN extract was injected onto the LC-PDA-ESI-MS/MS for analysis. The MS/MS spectra that were produced demonstrated nearly identical results to those reported by Ichiyanagi *et al.* (9,10) for the major ACN found in eggplant peels. The MS/MS spectrum of the concentrated pepper ACN extract is shown in Figure 5.6. It is clear the precursor ion is at $m/z = 919.14$ and the first product ion at $m/z = 757.10$ (green triangle in Fig. 5.6) demonstrates the loss of glucose, while the second product ion at $m/z = 464.98$ (red circle in Fig. 5.6) demonstrates the loss of both *p*-coumaric acid and rutoside, which leaves the aglycone (i.e. anthocyanidin) delphinidin (purple circle in Fig. 5.6) at $m/z = 303.25$. The aglycone at $m/z = 303.25$ matches very closely with the molecular weight (MW) of delphinidin, which is outlined by the purple box on the far right in Fig. 5.6, and is known to be 303 g/mol since the molecular formula is $C_{15}H_{11}O_7^+$. The MS/MS spectral data shown in Figure 5.6 strongly supports the characterization of the major anthocyanin in the concentrated purple pepper ACN extract to be the anthocyanin Dp-3-*p*-coumrut-5-glc, which corroborates with the research findings of both Lightbourn *et al.* (5) and Sadilova *et al.* (8).

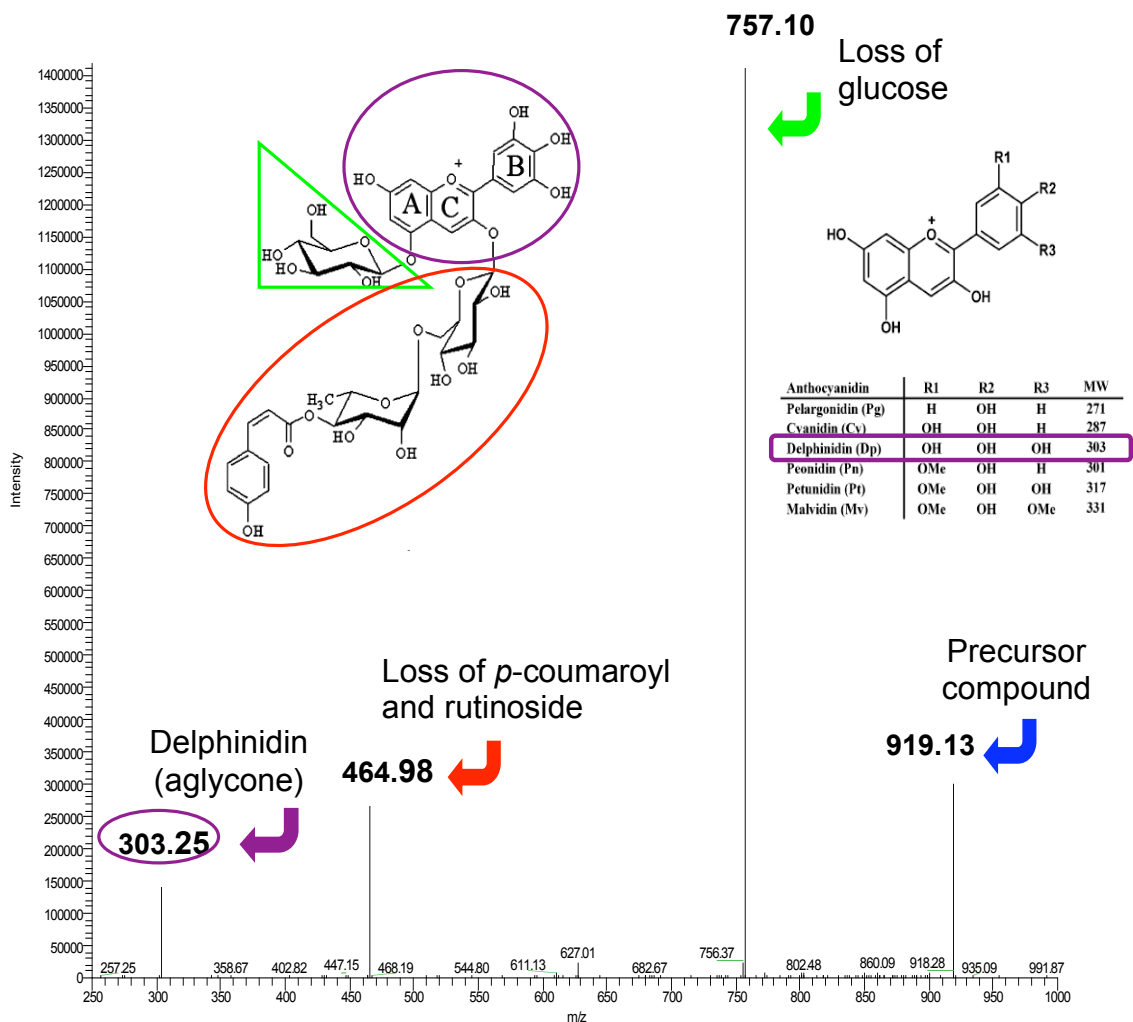


Figure 5.6: MS/MS spectrum of Dp-3-*p*-coumru-5-glc, *m/z* 919 (precursor compound). Loss of the glucose minus water is highlighted in green at *m/z* 757, loss of the *p*-coumaroyl and rutinose minus water is highlighted in red at *m/z* 465 and the remaining aglycone (delphinidin) is highlighted in purple at *m/z* 303. On the far right is a table of the six common anthocyanidins. Note the molecular weight of delphinidin is 303 g/mol.

The compound identified as delphinidin-3-*O*-caffeoylrutinoside-5-*O*-glucoside (Peak 3 from Table 5.1) has a very similar MS profile to the ACN of interest, but its retention time is much earlier in comparison to Dp-3-*p*-coumru-5-glc (Peaks 4 & 5 from Table 5.1) and its UV signature is also different from the ACN of interest. The only major structural difference between these two compounds is caffeic acid is in place of

coumaric acid, while the other compounds remain in the same positions. The comparison of these two compounds is shown below in Figure 5.7 and demonstrates the importance of utilizing retention time, UV data and MS/MS data together in order to identify the compounds present in the purple pepper foliage.

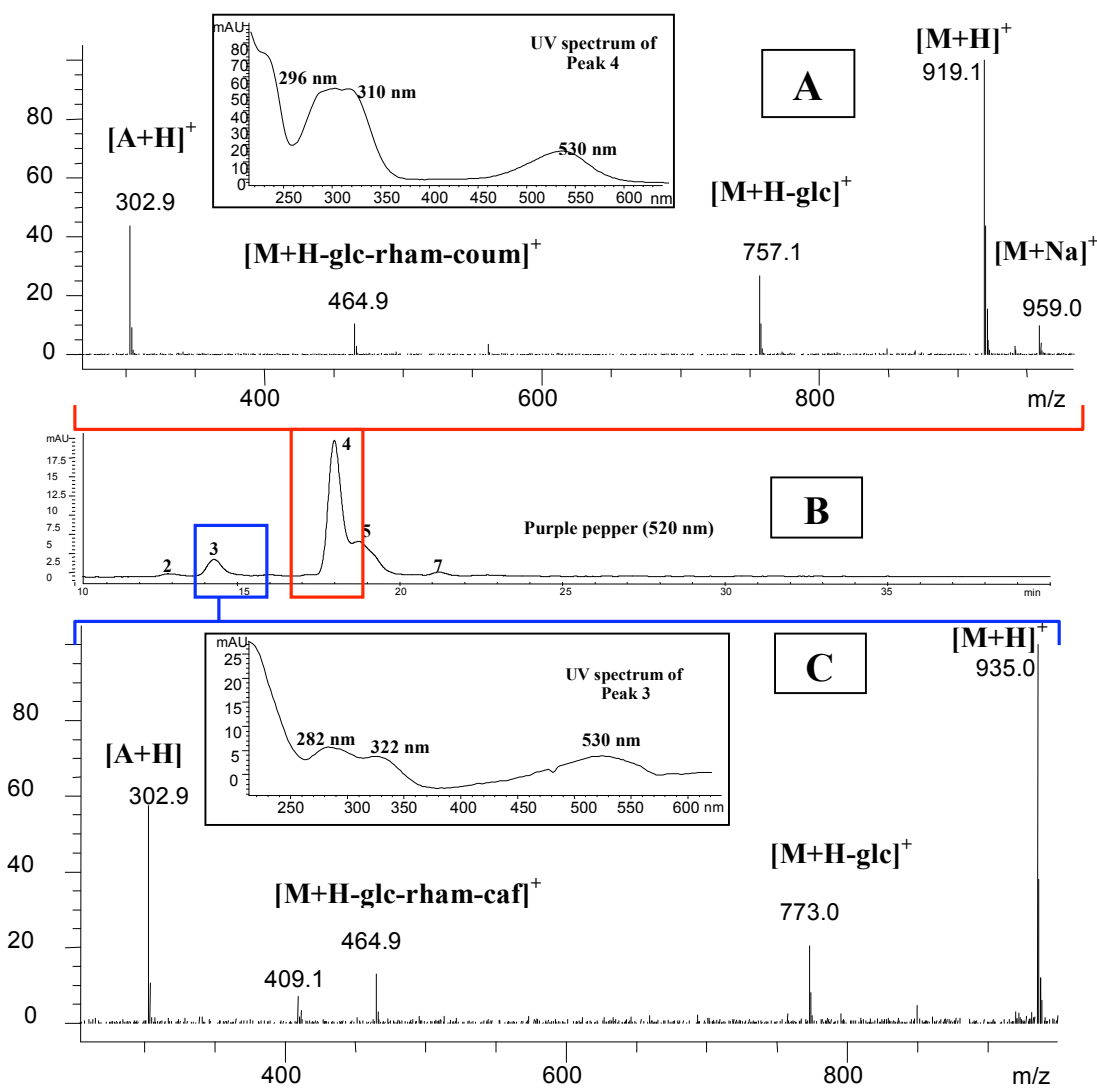


Figure 5.7: MS/MS spectra of (a) Dp-3-p-coumru-5-glc; (c) Dp-3-caffru-5-glc; (b) HPLC chromatogram of purple pepper foliage identifying peaks 3 and 4 in Table 5.1. The UV spectra of each compound is found in the inset.

Using Chinese eggplant skins as one of the standards to identify the ACN of interest, the data shows the compound present in purple pepper foliage is the same compound present in Chinese eggplant. A simple comparison of the HPLC chromatograms demonstrates very similar retention times of 18.85 min for Chinese eggplant and 18.71 min for purple pepper. The MS/MS spectra for the precursor ions in both plants are identical at m/z 919 and the product ions also match at m/z 757 and 303, while m/z 465 was only seen in the pepper foliage, as shown in Figure 5.8, in this investigation. This is most likely because the Chinese eggplant skins standard was not concentrated enough to detect this ion and it is clear the product ion at m/z 465 has a rather weak signal.

Figure 5.8 depicts two types of data to confirm the presence of Dp-3-*p*-coumru-5-glc: HPLC chromatograms (labeled A and B) and full ESI-MS spectra (labeled C and D). In the chromatograms, the m/z range that was chosen for analysis was from 918.00 to 920.00 in order to search for the precursor ion at $m/z = 919$. In the Chinese eggplant the precursor ion peak is at 18.85 min and the purple peppers peak is at 18.71 min, these are circled in blue in Figure 5.8. The second set of data shows the full ESI-MS spectra for these two samples (labeled C and D in Fig. 5.8). The software produces these spectra when the mouse is dragged across the width of the peaks in the chromatograms to show the mass spectral data for the specific retention times identified by the HPLC, in this case 18.85 and 18.71 min, respectively. The Chinese eggplant clearly demonstrates the precursor ion at $m/z = 919.18$, while the purple peppers is almost identical with an $m/z = 919.17$. These values are circled in green in Fig. 5.8. Secondly, the Chinese eggplant has the product ion at $m/z = 757.18$ and the purple peppers displays another nearly identical

match of the same ion at $m/z = 757.14$. The next product ion is not shown in the Chinese eggplant but it easily recognized in the purple peppers at $m/z = 465.96$. Lastly, both samples identify the aglycone delphinidin at $m/z = 303.20$ in Chinese eggplant and another very close match at $m/z = 303.28$ in purple peppers. All of the product ions are circled in red in Fig. 5.8.

The skins of the Chinese eggplant are already known to contain Dp-3-*p*-coumru-5-glc (8-10) and the data in Fig. 5.8 confirms the presence of the same compound in the purple pepper foliage. It is clear this data cannot give conformational information or determine the linkages of the glucosides and acyl moiety to the delphinidin compound. The places where the precursor compound breaks and creates product ions is a very specific pattern that leads to the conclusion that the same anthocyanin is found in both eggplant skins and purple pepper foliage. An NMR investigation will further confirm the attachment sites for the compound extracted and concentrated from the purple pepper foliage.

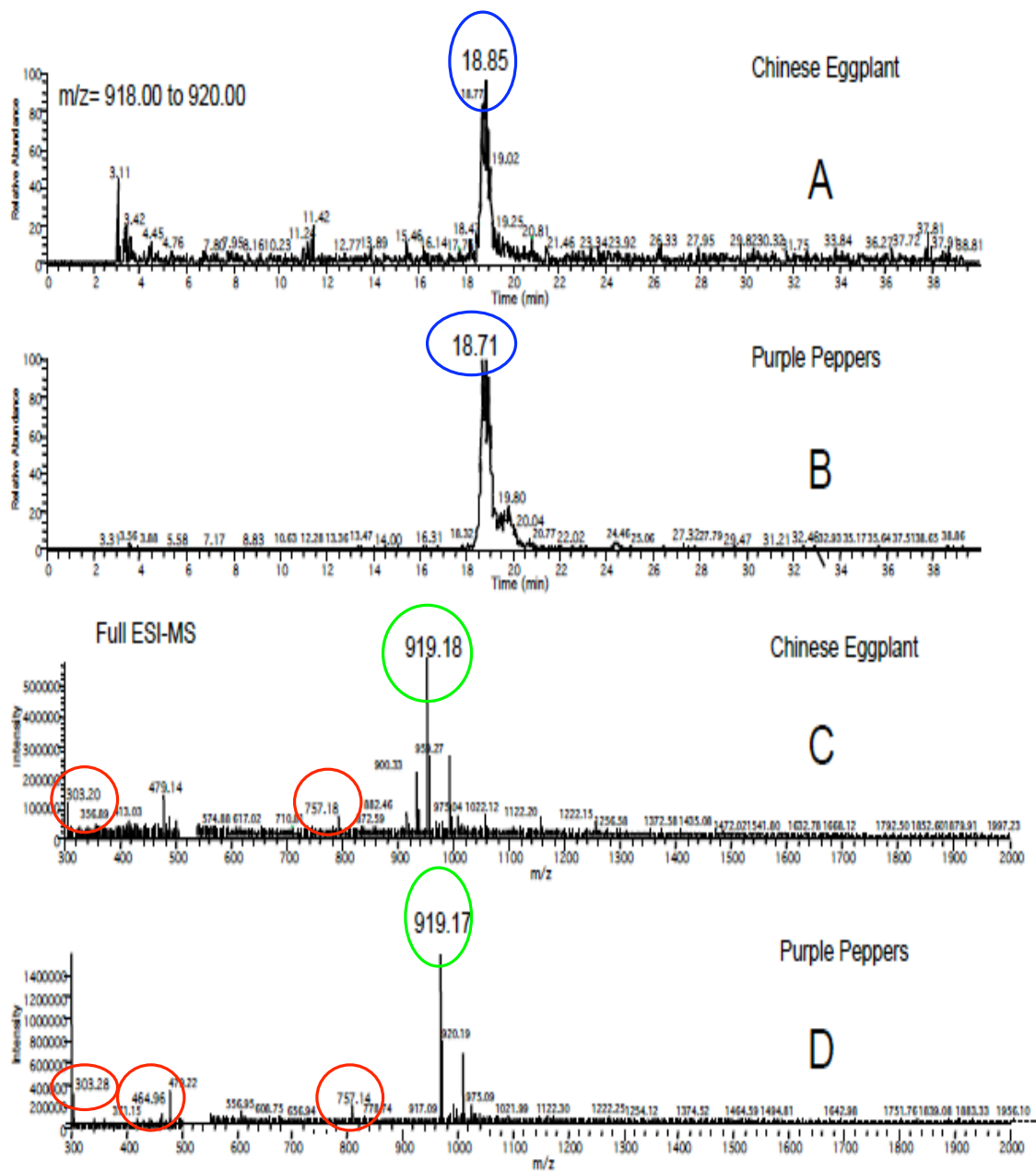


Figure 5.8: HPLC chromatograms for the mass range m/z 918 to 920 of (a) Chinese Eggplant; (b) Purple Peppers. The retention times are circled in blue and nearly identical at 18.85 and 18.71 minutes. The full ion count from the ESI-MS/MS (c) Chinese Eggplant; (d) Purple Peppers. Precursor ion at m/z 919 is circled in green. Product ions at m/z 757, 465 and 303 are circled in red.

The LC-PDA-ESI-MS/MS has the ability to demonstrate some level of purity for the extract since the HPLC is able to separate the compounds fairly well and then the PDA and MS/MS can detect these separated peaks. The original goal of this research was to develop a food-grade extraction method for Dp-3-*p*-coumrut-5-glc from purple pepper foliage so as to create an extract that could be utilized in a human feeding study. Therefore, only GRAS (223) chemicals could be used and resulted in a less pure final product in comparison to other plant extracts that are not restricted to GRAS chemicals that could use stronger solvents such as trifluoroacetic acid (TFA). Keeping this in mind, it was noticed that there was another large peak downfield in the Total Ion Count (TIC) MS spectra around 34 minutes. In order to confirm this peak was not the ACN of interest (m/z 919, 757, 465 & 303), an MS/MS scan was completed and found the precursor ion to be m/z 433, as shown in Figure 5.9 D. This unknown compound was also seen in the PDA scan, meaning it absorbs at 520 nm like Dp-3-*p*-coumrut-5-glc. The MS/MS clearly shows this compound is not the ACN of interest, but it is very likely the compound is another polyphenol. There are many possibilities, but this compound was not further analyzed by NMR since it was determined from the MS/MS data to not be the ACN of interest.

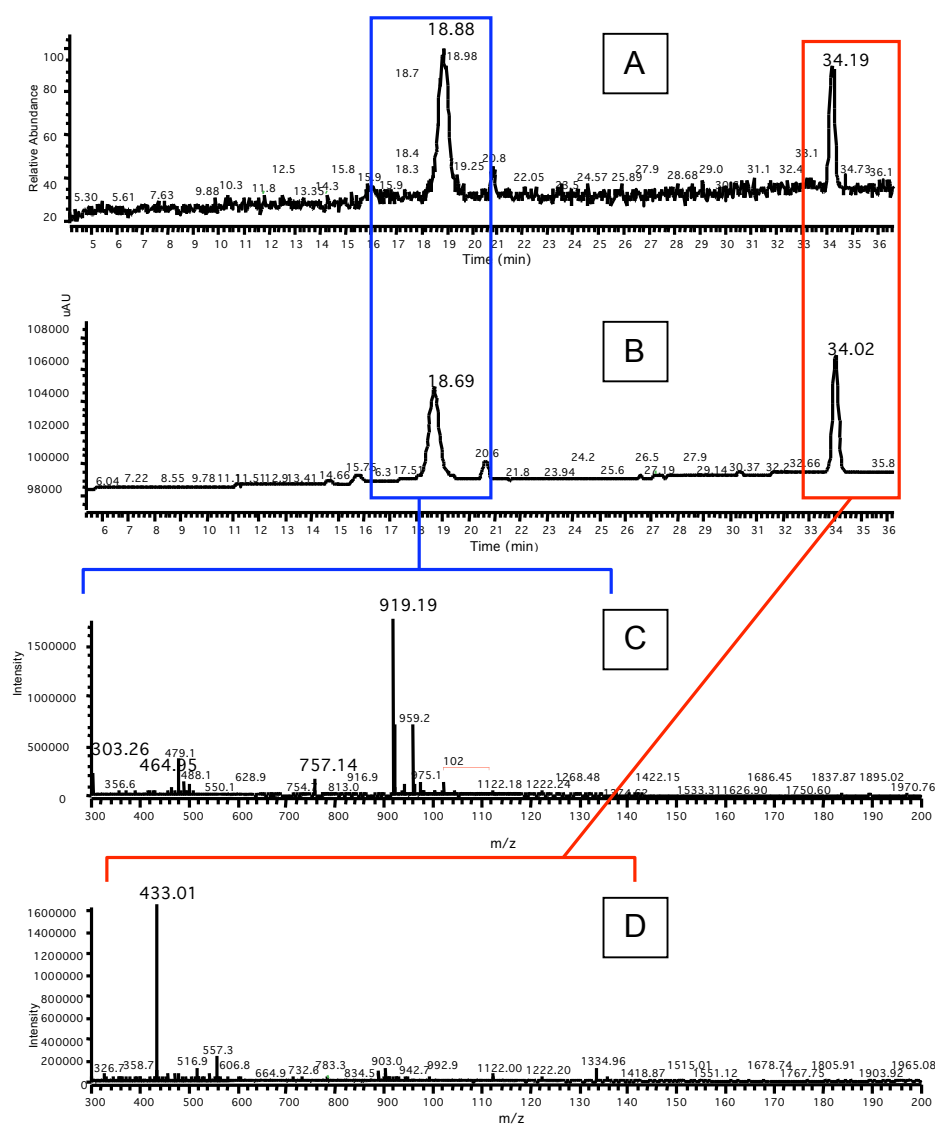


Figure 5.9: (a) Total Ion Count (TIC) MS spectrum of purple pepper foliage; (b) Total PDA scan; (c) MS/MS spectrum from 18.28 – 19.67 minutes highlighted in blue; (d) MS/MS spectrum from 33.90 – 34.43 minutes highlighted in red.

After completion of the MS/MS analysis, the remaining concentrated pepper extract was stored in an airtight glass container and a Teflon lined cap was screwed on top. The storage solution was 1% HCl/MeOH to assist with keeping the pH level low and the container was completely covered in foil and placed in a dark freezer at -20 °C. These precautions help to maintain the integrity of the anthocyanin structure, which is easily

altered by pH, light and temperature, until all of the necessary analyses are complete. The extract was stored in this manner until it could be prepared for NMR analysis.

5.6: Confirmation of the Major Anthocyanin by MS/MS

The characterization data provided by the LC-PDA-ESI-MS/MS clearly demonstrates the precursor ion of Dp-3-*p*-coumrut-5-glc to be present in the purple pepper extract at m/z 919 (Fig. 5.6). The product ions were also confirmed at m/z 757 (loss of glucose minus water), 465 (loss of *p*-coumaroyl and rutinose) and 303 (aglycone, delphinidin). This data correlates well with all of the previous research that identifies Dp-3-*p*-coumrut-5-glc in purple pepper foliage (5,8) and in eggplant peels (9,10,132,133,137). The MS/MS data from this investigation confirms that the major ACN from purple pepper foliage that was extracted in Chapter 3 then collected and concentrated by HPLC in Chapter 4 has the same mass-to-charge ratios as previous data identifying Dp-3-*p*-coumrut-5-glc. The concentrated extract will have its structure elucidated by Nuclear Magnetic Resonance (NMR) in Chapter 6 to confirm that attachment sites of the *p*-coumaric acid and the glucose to the delphinidin aglycone.

Chapter 6: Nuclear Magnetic Resonance

Overview

The use of Nuclear Magnetic Resonance (NMR) as an elucidation technique, Section 6.1, for the concentrated purple pepper ACN extract will be explained in this chapter. A brief explanation of how the dry ACN material was prepared for NMR analysis is given in Section 6.2. Just as all the previous analytical techniques used in this investigation were adjusted to analyze the purple pepper ACN extract, the NMR instrument conditions and sequences were specifically optimized in Section 6.3 in order to produce successful ^1H and ^{13}C analyses. The concentrated purple pepper ACN extract was more dilute than anticipated and had to be re-concentrated in Section 6.4 in order to achieve meaningful ^{13}C data. The elucidation of the anthocyanin structure is demonstrated extensively with spectra and data tables in Section 6.5 for both the ^1H and ^{13}C analyses. The conclusions drawn from the collected ^1H and ^{13}C NMR data regarding the structure of Dp-3-*p*-coumru-5-glc in the purple pepper extract are presented in Section 6.6.

6.1: Elucidation Technique

In order to elucidate the specific anthocyanin of interest and confirm the attachment sites for the glucose and *p*-coumaric acid on the structure of the delphinidin derivative (Dp-3-*p*-coumru-5-glc) it is necessary to perform nuclear magnetic resonance (NMR) analyses. This part of the investigation requires very skilled knowledge of NMR to determine the correct parameters to run in order to obtain the most accurate results.

The researcher is not an NMR expert; therefore the staff at the UMD Analytical NMR Service & Research Center was consulted in order to assist with conducting the appropriate analyses. Dr. Yiu-Fai Lam and Dr. Yinde Wang were extremely helpful and their expertise was essential to the success of this investigation. Frederick Nytko, III was also crucial to the investigation, as his assistance with interpreting the data was unparalleled.

6.2: Preparation of Dry ACN Material for NMR Analysis

The concentrated purple pepper extract that was stored after the completion of the MS/MS analyses (in Section 5.5.1) was dried under N₂ gas in a warm water bath at approximately 40 °C for 2 hours then placed overnight in a desiccator. The purified pepper extract was prepared in trifluoroacetic acid, abbreviated TFA or TFA-*d*₁, from Sigma-Aldrich (HPLC grade, ≥ 99.0%) and deuterated methanol, abbreviated MeOH-*d*₄ or CD₃OD-*d*₄ or MeOD with 0.05% v/v TMS, from Cambridge Isotope Laboratories, Inc at a concentration of 12 mg/ mL. Tetramethylsilane (TMS) is the internal standard for this investigation. Ichiyanagi *et al.* (9) utilized a solvent ratio of 1 part TFA-*d*₁ to 9 parts MeOD in their NMR work to identify the major ACN in eggplant peels, and this ratio was maintained for this investigation. The extract needs to be completely dissolved in solution with no solids remaining.

The sample was analyzed by NMR spectroscopy (500 MHz) using the “zg30” ¹H pulse sequence and “zgdc” ¹³C pulse sequence with ¹H broad-band (BB) decoupling (or composite pulse decoupling, CPD) using the CPD sequence “WALTZ-16” (224) and the

results were compared to those from Ichiyanagi *et al.* (9). Pulse sequences are graphically represented in Appendix C.

6.3: Instrument Conditions

A preliminary investigation utilizing a 400 MHz spectrometer of the deep purple colored, concentrated ACN sample demonstrated that the sample needed a stronger field in order to obtain accurate results. Therefore, a 500 MHz NMR spectrometer equipped with a BBO (Broadband Observe) probe was used to elucidate the sample. This choice of spectrometer and probe are ideal for routine ^1H analysis and best in determining many different nuclei. Dr. Yinde Wang expressed that in his experience he has found colored samples to often have difficulty in conducting traditional ^{13}C analysis, but did not exactly know why this occurred. This difficulty held true for the concentrated ACN sample. To resolve this issue, Dr. Wang suggested utilizing the 500 MHz spectrometer with BBO probe for routine ^1H analysis as well as to observe the ^{13}C nuclei with ^1H decoupling to determine the carbon linkages.

The 500 MHz spectrometer with BBO probe, which is very versatile, is suitable for the ACN sample since it has the capability to detect both ^1H and ^{13}C nuclei. It has two signal detecting coils: the inner coil (e.g. 125 MHz) is tunable and is excellent for observing many different nuclei (^{13}C , ^{15}N , ^{31}P , etc.) and its outer decoupling coil (e.g. 500 MHz) detects ^1H nuclei (225). This is very helpful for analysis of a colored sample since many times traditional ^{13}C analysis is difficult to acquire when the sample is colored, for reasons that are yet to be determined, and the BBO probe provides another avenue to study the ^{13}C nuclei and acquire accurate data.

6.3.1: Instrument Parameters and Sequences

In order to acquire comparable data to that collected by Ichiyanagi *et al.* (9), the instrument parameters were optimized for the concentrated ACN sample. For elucidation, it is essential to collect ^1H and ^{13}C data. For this investigation, the pulse sequence “zg30” was chosen for ^1H and “zgdc” for ^{13}C , which included ^1H broad-band (BB) decoupling (or composite pulse decoupling, CPD) using the CPD sequence “WALTZ-16”. The instrument parameters for “zg30” are in Table 6.1 and “zgdc” in Table 6.2.

Table 6.1: Instrument parameters for the pulse sequence “zg30”. All acronyms are defined in Appendix C.

Instrument Parameters		Channel f1	
TD	49152	NUC1	^1H
NS	64	P1	11.10 μsec
DS	16	PL1	0.00 DB
SWH	8012.820 Hz	SF01	500.1330880 MHz
FIDRES	0.163021 Hz	SI	131072
AQ	3.0671349 sec	SF	500.13300028 MHz
RG	256	WDW	EM
DW	62.400 μsec	SSB	0
DE	6.50 μsec	LB	0.30 Hz
TE	298.2 K	GB	0
TD0	1	PC	1.00

Table 6.2: Instrument parameters for the pulse sequence “zgdc”. All acronyms are defined in Appendix C.

Instrument Parameters		Channel f1			
TD	65536	NUC1	¹³ C	PL1	3.00 DB
NS	3600	P1	12.50 μsec	SF01	125.778299 MHz
DS	16	Channel f2			
SWH	32679.738 Hz	CPDPRG2	Waltz16	WDW	EM
FIDRES	0.498653 Hz	NUC2	¹ H	SSB	0
AQ	1.0027508 sec	PCPD2	60.00 μsec	LB	2.50 Hz
RG	5160.6	PL2	0.00 dB	GB	0
DW	15.300 μsec	PL12	17.80 dB	PC	1.40
DE	6.50 μsec	SF02	500.1325007 MHz		
TE	301.2 K	SI	131072		
TD0	6	SF	125.778299 MHz		

6.4: Reconcentration of ACN sample for NMR analysis

After successfully collecting ¹H data and conducting a few ¹³C analyses, it was advised by NMR staff members to reconcentrate the sample in order to achieve better resolution. Multiple NMR sequences were utilized, but all had difficulty resolving the carbon peaks and Dr. Wang’s experience suggested the sample was not concentrated enough for the NMR to successfully analyze the carbon peaks.

Therefore, the sample was dried a second time under N₂ gas in a warm water bath at approximately 40 °C for 2 hours then placed overnight in a desiccator. This sample looked drier in comparison to the first dried ACN sample when it was removed from the desiccator because it appeared to be more crystalline. The sample was prepared in TFA/MeOD (1:9) and analyzed by NMR spectroscopy (500 MHz).

6.5: Elucidation Data

In order to elucidate the structure of the ACN of interest in this project previous research by Ichiyanagi *et al.* (9) was compared with the data obtained for the purple pepper ACN extract. Briefly, there are two types of coupling that can occur between two different nuclei with a non-zero spin. The first is dipole-dipole coupling (D), which is a direct interaction and the second is an indirect (or scalar) coupling called spin-spin splitting (J) (226). The J coupling values published by Ichiyanagi *et al.* (9) were utilized to help in determining the identification of the components in the proton NMR spectra. Conventional notation to display ^1H NMR is as follows: shorthand notation is ^1H NMR (ppm) value followed by (δ , J in Hertz). The delta symbol “ δ ” represents multiplicity and “s” represents singlet, “d” represents doublet and “t” represents triplet, for example (d, 7.8) is a doublet with a 7.8 Hz J value. This notation will be utilized in this document.

6.5.1: ^1H Analysis Data

As previously mentioned, the 1-D pulse sequence “zg30” was used to analyze the concentrated ACN sample from purple pepper foliage to produce routine proton NMR spectra. The figures in this section will display the collected proton spectra for this sample. The ^1H chemical shift data obtained for this investigation was compared to the published data for analysis of the major ACN found in eggplant peels from Ichiyanagi *et al.* (9). Unfortunately, no spectra were available for comparison purposes despite contacting the authors. Therefore, only the numerical values were used to evaluate the uniformity of the ACN structures analyzed from the two Solanaceae family (i.e. Nightshade) plant sources.

In the full-scale ^1H spectrum, shown in Figure 6.1, there are three large peaks that stand out from the other sample peaks. The first peak at 0 ppm is the internal standard of tetramethylsilane (TMS), which is used universally as an internal standard for NMR analyses. The other two large peaks (5.11 and 3.33 ppm) are the solvents used to prepare the NMR sample, TFA- d_1 /MeOD- d_4 (1:9 ratio). According to the NMR Solvent Data Chart, from Cambridge Isotope Laboratories, Inc. (227), the ^1H chemical shifts in ppm from TMS for MeOD- d_4 are 4.78 ($\delta = 1$) and 3.31 ($\delta = 5$), respectively. In the spectrum, there is some slight shifting from these standard values since this sample has a small amount of TFA as a solvent, as well as a small quantity of HCl used during the extraction method for the concentrated purple pepper ACN sample. Acid will cause signals to shift from one location to another, and it is often tricky to predict these shifts. The presence of acid in the sample is the most logical reasoning for the slight shifts in the NMR peaks.

Full-scale ^1H spectrum

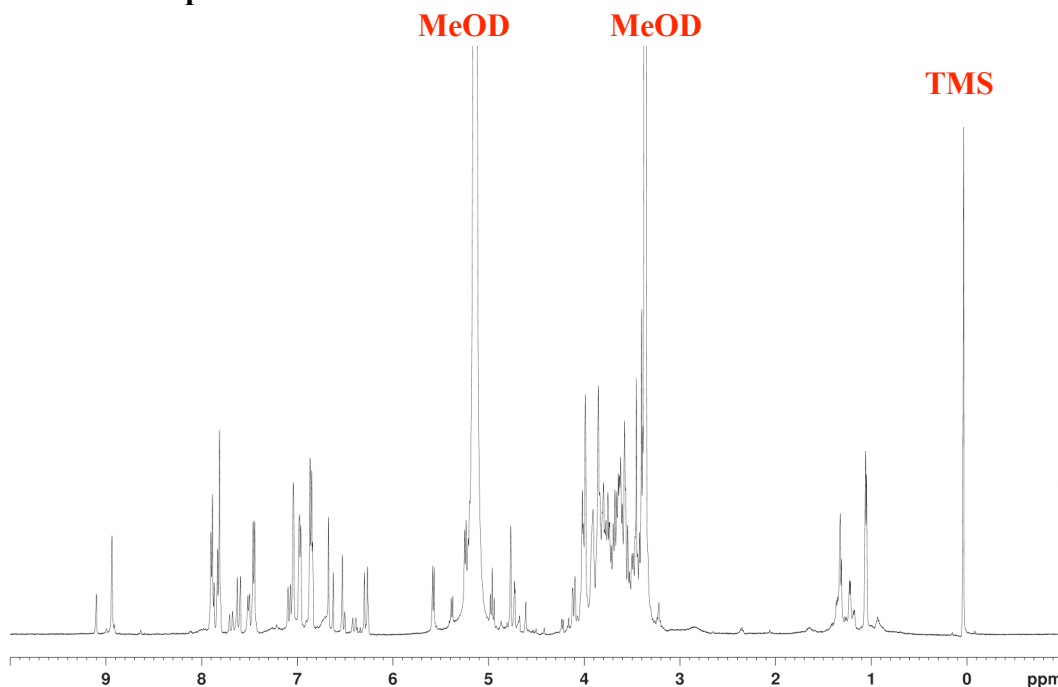


Figure 6. 1: Full scale spectrum of the ^1H analysis utilizing “zg30” pulse sequence. Abbreviations: MeOD = deuterated methanol and TMS = tetramethylsilane.

It is difficult to see the smaller peaks in the full-scale ^1H spectra (Fig. 6.1), therefore zoomed in spectra are presented to help identify the proton signals. Figure 6.2 shows a fully labeled molecule of the *trans* isomer of Dp-3-p-coumru-5-glc and is comparable to the naming presented by Ichiyanagi *et al.* (9). These names correspond with the signal identifications found in the zoomed ^1H spectra shown in Figures 6.3 and 6.4, which demonstrate the specific peaks for the ACN of interest. The rest of the ^1H spectra can be found in Appendix C. The values used to identify the linkages of the anthocyanin found in the purple pepper foliage were from the ^1H spectroscopic data provided by the research of Ichiyanagi *et al.* (9) on eggplant peels. There are some small shifts in the NMR values found in this investigation versus the published literature. The variation is normal from one investigation to another. Unless this experiment was conducted on the exact same instrument and immediately following the research of Ichiyanagi *et al.* (9) it is completely normal to have some slight variations. Also, the presence of small amounts of acid in this investigation can cause the slight shifts.

3-*O*-glycosyl, as shown in Figure 6.2. For example, the proton signal detected at the hydrogen on the 4th carbon of the delphinidin molecule will be identified as “Dp-4” in the spectra and will have purple text color (i.e. Dp-4). There is a slight name difference from Dp-3-*p*-coumru-5-glc because Ichiyanagi *et al.* (9) split the rutinoside molecule into 3-*O*-glycosyl (for the sugar attached at the 3-position on the C-ring of delphinidin) and rhamnosyl (for the sugar attached at the 6-position of the 3-*O*-glycosyl sugar). The positions for the *cis* isomer are named in the same way as the *trans* isomer, but Fig. 6.2 only demonstrates the *trans* isomer. Note that the carbons identified as Dp-4a, Dp-8a and COO in Fig. 6.2 are only utilized in the ¹³C spectra because there are no protons that can be detected at these sites therefore there are no signals in the ¹H spectra corresponding to these positions. Only the carbon positions with detectable protons are identified in the ¹H spectra while all of the carbon positions are detected in the ¹³C spectra in Section 6.5.2.

Based on the HPLC data, the purple pepper extract was anticipated to have a purity > 95%, but the ¹H spectra display some peaks that were not reported by Ichiyanagi *et al.* (9). A few of these peaks (noted by a * in the ¹H spectra) resemble the signals identified as *p*-coumaroyl and are in close proximity to the identified signals. Therefore it would be logical to suggest that another coumarin derivative might be present in the sample. This additional coumarin derivative is a possible degradation product or these peaks could be *cis/trans* isomers with some of the identified signals. There are also some peaks (noted by a # in the ¹H spectra) that are unknown impurities to the extract. These could be additional degradation products that formed when TFA was added to the extract or may be additional polyphenols that were not removed during separation or extraction. These impurities are very obvious in the ¹³C spectra shown in Section 6.5.2.

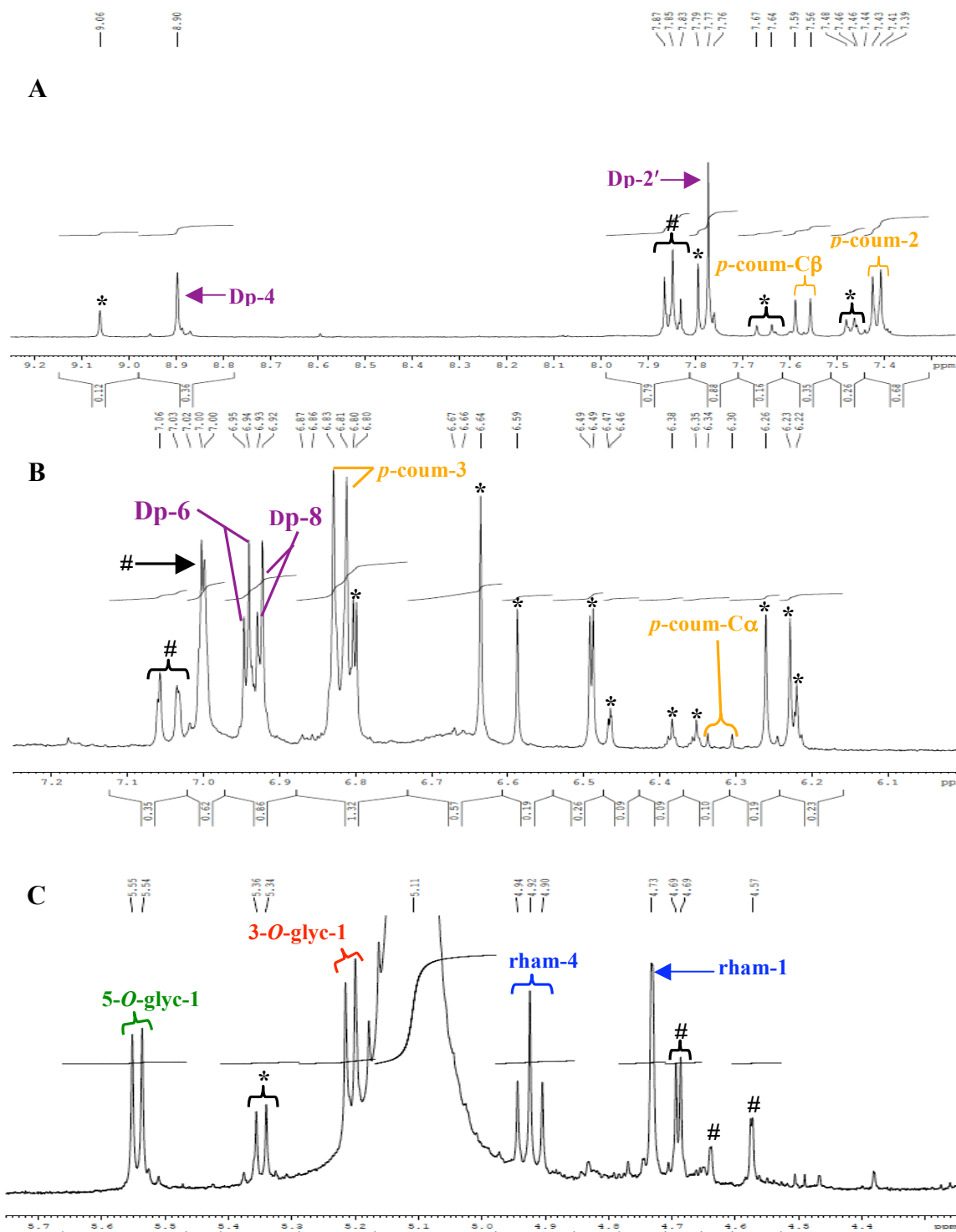


Figure 6.3: (a) Spectrum from 9.25 – 7.25 ppm; (b) spectrum from 7.25 – 6.00; (c) spectrum from 5.75 – 4.25. Abbreviations: Dp = delphinidin, *p*-coum = *p*-coumaroyl, glyc = glycoside, rham = rhamnosyl, * = possible degradation product or *cis/trans* isomer and # = unknown impurity. Text color and molecule identification key is in Figure 6.2. Full list of ^1H shifts can be found in Table 6.3.

The ^1H NMR analysis for the investigation of the anthocyanin found in purple pepper foliage was able to identify all of the same protons for the *trans* isomer presented by Ichiyanagi *et al.* (9) for the anthocyanin found in eggplant peels. Since the spectra from the literature were not available identification relied heavily on the published data, specifically the *J* coupling values. They were especially useful in discerning the *cis* and *trans* isomer peaks. Based on the ^1H data, this investigation demonstrates that the concentrated ACN sample consists mainly of the *trans* isomer of Dp-3-*p*-coumru-5-glc as all of the *trans* signals from Ichiyanagi *et al.* are present in the purple pepper extract (Table 6.4). This correlates with the trend reported by Ichiyanagi *et al.* (9), where in eggplant peels it was found that the *trans* isomer (recovery of 57 mg) was approximately 4.5 times more abundant in comparison to that of the *cis* isomer (recovery 12.5 mg). A typical HPLC chromatogram showing the difference in isomers from the eggplant research was shown in Fig. 4.10 c.

Figure 6.4 demonstrates that most of the concentrated purple pepper ACN sample has the *trans* isomer of Dp-3-*p*-coumru-5-glc. A comparison table of the Ichiyanagi *et al.* (9) ^1H NMR data and the concentrated purple pepper ^1H NMR data is shown in Table 6.4. The only component where a *cis* isomer could be easily identified in the pepper extract was in 3-*O*-glycoside, with a doublet at 5.17 ppm and *J* (in Hertz) of 7.78, which matches well with the published data of 5.18 (d,7.8). There were other *cis* isomer components, but they were singlets and easier to identify. These were found for Dp-2' at 7.77 (s) and Dp-4 at 8.9 (s). There is a possibility other *cis* components are in the sample, but with the peak splitting and shifting that occurred in the spectra it was tough to definitively identify other *cis* isomers. Tentative identification of *cis* isomers for Dp-6

and Dp-8 were found at 6.80 (d, 2.15), but it is very difficult to tell if these are the actual *cis* isomers for these two components, but the *J* values are very comparable to the published literature for Dp-6 at 6.96 (d,2) and Dp-8 (d, 6.94).

The doublet found in the concentrated purple pepper (6.80 ppm) is further upfield in comparison to the doublet found in the eggplant peels (6.96 and 6.94 ppm), leaving some doubt as to the actual identity. The amount of shifting this peak has is larger than the average shifting seen for all the other peaks. Most peaks shifted upfield or downfield at an average of 0.043 ppm, while the possible *cis* isomer peaks for Dp-6 and Dp-8 are shifted downfield 0.16 ppm and 0.14 ppm, respectively. For these reasons, the peaks were labeled as tentative *cis* isomer identifications. A comparison table of Ichiyangi *et al.*(9) ¹H NMR data and the concentrated purple pepper ¹H NMR data is shown in Table 6.3, which lists all of the ¹H NMR shifts observed. The remaining ¹H NMR zoomed in spectra for the individual components not shown in Fig. 6.4 are in Appendix C.

After reviewing the ¹H spectra the sample looks fairly clean as all of the reported signals from Ichiyangi *et al.*(9) were also present in the purple pepper sample, but with some minor impurities signals that were not reported. These impurity peaks could be other polyphenols that were not removed during the extraction process or possibly signals of the *cis* isomer for Dp-3-*p*-coumrut-5-glc. Overall, the ¹H data is very promising and demonstrates a purity level of approximately 90% for Dp-3-*p*-coumrut-5-glc from the foliage of the purple pepper.

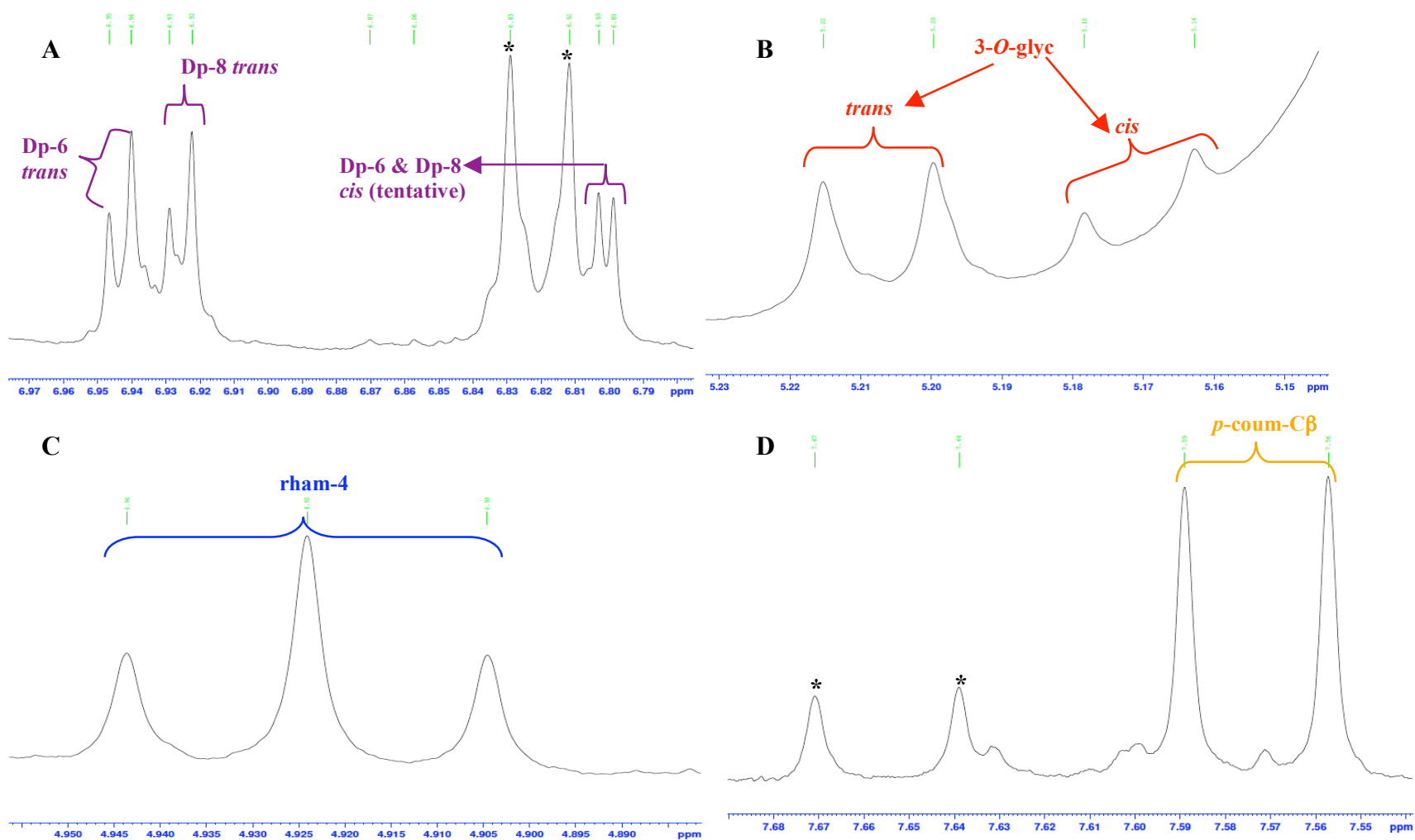


Figure 6.4: Some zoomed in ^1H spectra (a) Dp-6 & Dp-8 (*cis* & *trans*); (b) 3-*O*-glyc (*cis* & *trans*); (c) rham-4 (*trans*); (d) *p*-coum-C β (*trans*). Abbreviations: Dp = delphinidin, glyc = glycoside, rham = rhamnosyl, coum = coumaroyl and * = possible degradation product or *cis/trans* isomer. Full list of ^1H shifts in Table 6.3.

Figure 6.4 displays multiple zoomed in views of the ^1H spectrum to demonstrate the presence of both the *cis* and *trans* isomers in the purple pepper extract. The *trans* isomer signals dominate the purple pepper extract. The *cis* isomer signals are tentative but closely resemble those reported by Ichiyanagi *et al.*(9), as shown in Table 6.3.

Table 6.3: Comparison of proton NMR data. On the left in blue, eggplant peel data from Ichiyanagi *et al.*(9). On the right, purple pepper data from this investigation.^b

Eggplant peel ^1H NMR (δ , J in Hz)			Purple Pepper ^1H NMR (δ , J in Hz)		
Position	<i>cis</i>	<i>trans</i>	Position	<i>cis</i>	<i>trans</i>
delphinidin			delphinidin		
4	8.83 (s)	8.85 (s)	4	8.90 (s)	8.90 (s)
6	6.96 (d, 2)	6.97 (d, 2)	6	6.80 (d, 2.2) ^a	6.95 (d, 1.9)
8	6.94 (d, 2)	6.96 (d, 2)	8	6.80 (d, 2.2) ^a	6.93 (d, 2.1)
2'	7.71 (s)	7.71 (s)	2'	7.77 (s)	7.77 (s)
3-O-glycosyl			3-O-glycosyl		
1	5.18 (d, 7.8)	5.20 (d, 7.7)	1	5.17 (d, 7.8)	5.21 (d, 7.8)
rhamnosyl			rhamnosyl		
1	4.66 (brs)	4.70 (brs)	1	ND	4.73 (brs)
4	4.81 (t, 9.5)	4.90 (t, 9.7)	4	ND	4.92 (t, 9.8)
6	0.86 (d, 6)	1.00 (d, 6)	6	ND	1.02 (d, 6.3)
5-O-glycosyl			5-O-glycosyl		
1	5.56 (d, 8)	5.55 (d, 7.7)	1	ND	5.55 (d, 7.8)
p-coumaroyl			p-coumaroyl		
2	7.58 (d, 8.5)	7.39 (d, 8.5)	2	7.47 (d, 8.5)	7.42 (d, 8.6)
3	6.71 (d, 8.5)	6.80 (d, 8.5)	3	ND	6.82 (d, 8.6)
C α	5.57 (d, 12.6)	6.22 (d, 15.8)	C α	ND	6.32 (d, 15.9)
C β	6.79 (d, 12.6)	7.55 (d, 15.8)	C β	ND	7.58 (d, 15.9)

^b Abbreviations: ND = not detected, s = singlet, d = doublet, t = triplet and ^a = tentative assignment of *cis* isomer.

6.5.2: ^{13}C Analysis Data

The concentrated ACN sample was analyzed by ^{13}C NMR using the pulse sequence “zgdc” and the CPD sequence “WALTZ-16” (Appendix D, Fig. D.2). This combination produced standard ^{13}C NMR spectra and the full-scale is shown in Figure 6.5 with proton composite pulse decoupling (CPD). In this section, the spectra will be presented to demonstrate the correlations between the ^{13}C chemical shifts from this research, analyzing the concentrated ACN found in purple pepper foliage, and the research of Ichiyonagi *et al.*(9) that analyzed the ACN found in eggplant peels. A comparison of the two data sets can be found in Table 6.4.

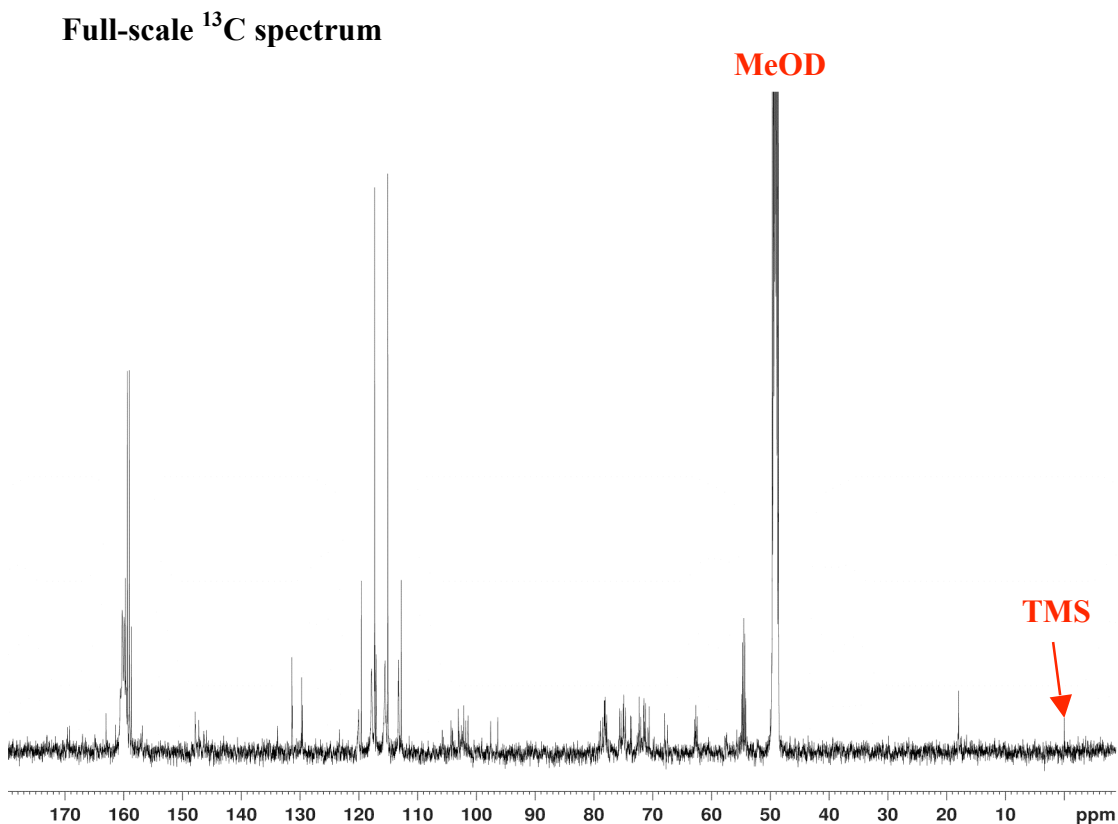


Figure 6.5: Full scale spectrum of ^{13}C analysis utilizing “zgdc” pulse sequence with CPD sequence “WALTZ-16”. Abbreviations: MeOD = deuterated methanol and TMS = tetramethylsilane.

Again, it is difficult to distinguish all of the peaks in the full-scale spectrum in Figure 6.5. Therefore, portions were enlarged to assist in identification as shown in Figures 6.7 – 6.9. The ^1H data demonstrated a very small abundance of the *cis* isomer in the concentrated pepper sample. The sample had to be reconcentrated to obtain adequate ^{13}C NMR data and it is clear the sample is more dilute than anticipated and contains many more impurities. The most reasonable explanation for the presence of increased amount of impurities (compared with the quantity seen in the H-1 NMR spectrum) is that one or more glycosidic linkages were cleaved when the sample was evaporated and resolubilized for a second time in TFA/MeOH (1:9, v/v). This process resulted in degradation of the sample because the environment was very acidic and the compound was not able to maintain its structure, with the sugars most likely being the first molecules to break off from Dp-3-*p*-coumru-5-glc. In the ^{13}C spectra there a lot of extra peaks near the signals that were identified by Ichiyanagi *et al.*(9). They are most likely the sugars that broke off from Dp-3-*p*-coumru-5-glc or coumarin derivatives that were formed during degradation. The spectra suggest impurity carbons are in a similar environment to the identified carbons in the compound, thus the different signals are most likely related due to their close proximity to one another. Many of the peaks were not able to be identified (noted by # in spectra), but they are possibly degradation products due to the effects of TFA on the sample.

This more dilute sample is not optimal because carbon peaks are inherently small. Thus, only the *trans* isomer ^{13}C NMR peaks were identified. According to the published data from Ichiyanagi *et al.*(9), most of the *cis* isomer peaks detected by ^{13}C are very similar (+/- 2 ppm) to those reported for the *trans* isomer (Table 6.4). In future

investigations, increasing the purple pepper foliage sample size to be extracted by at least 10 fold would be needed in order to have a greater abundance of the *cis* isomer in the concentrated sample. The key used to name and identify the carbon signals in Dp-3-*p*-coumru-5-glc in the ^{13}C spectra is shown in Figure 6.6.

trans isomer of delphinidin-3-*p*-coumaroylrutinoside-5-glucoside

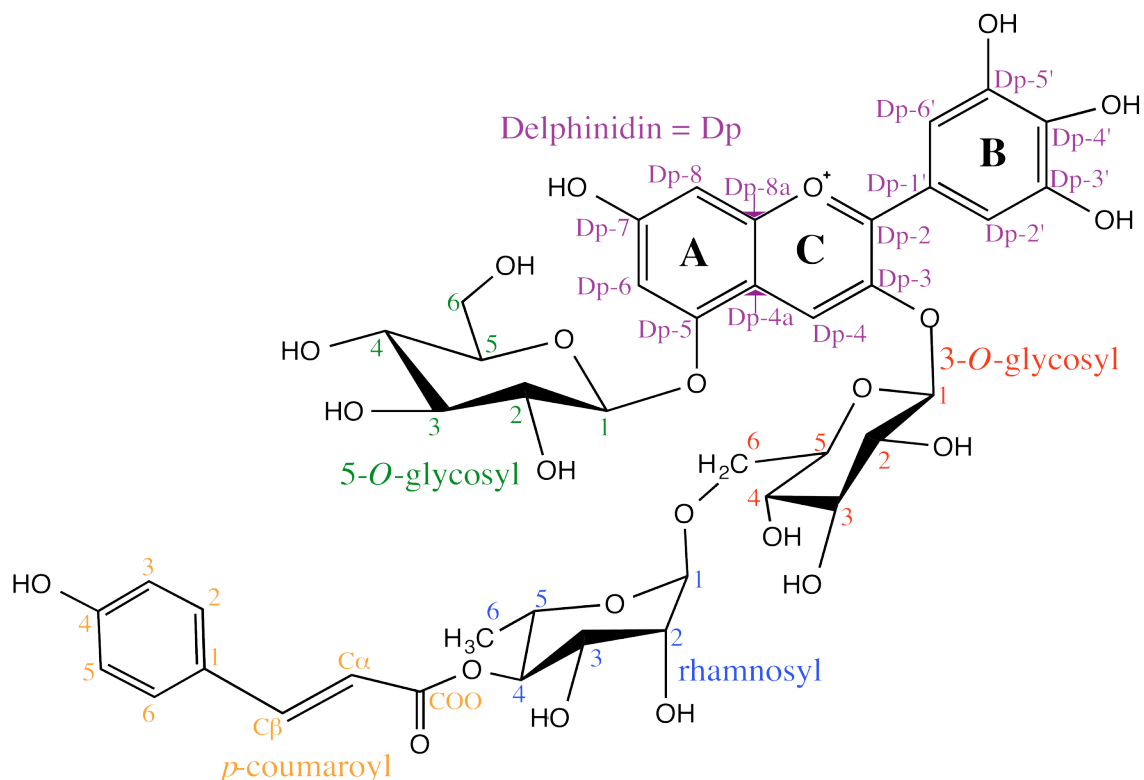


Figure 6.6: Drawing of the *trans* isomer of delphinidin-3-*p*-coumaroylrutinoside-5-glucoside. The molecule is labeled in accordance with the previous NMR data reported by Ichiyanagi *et al.* (9). This drawing will be used as a key to identifying all of the peaks labeled in the ^{13}C spectra. Colors of text correspond to the section of the molecule and are used throughout the zoomed in spectra. Abbreviations: Delphinidin = Dp.

As in the ^1H spectra, the ^{13}C signals are identified by the section of the molecule with an abbreviation (Delphinidin = Dp; 3-*O*-glycosyl = 3-*O*-glyc; 5-*O*-glycosyl = 5-*O*-glyc; rhamnosyl = rham; *p*-coumaroyl = *p*-coum) followed by the carbon position. Again,

the color text will correspond to the molecules section colors shown in Fig. 6.6, i.e. delphinidin is purple. Figures 6.7 – 6.9 show zoomed in ^{13}C spectra where nearly all of the carbons are identified in Dp-3-*p*-coumarut-5-glc.

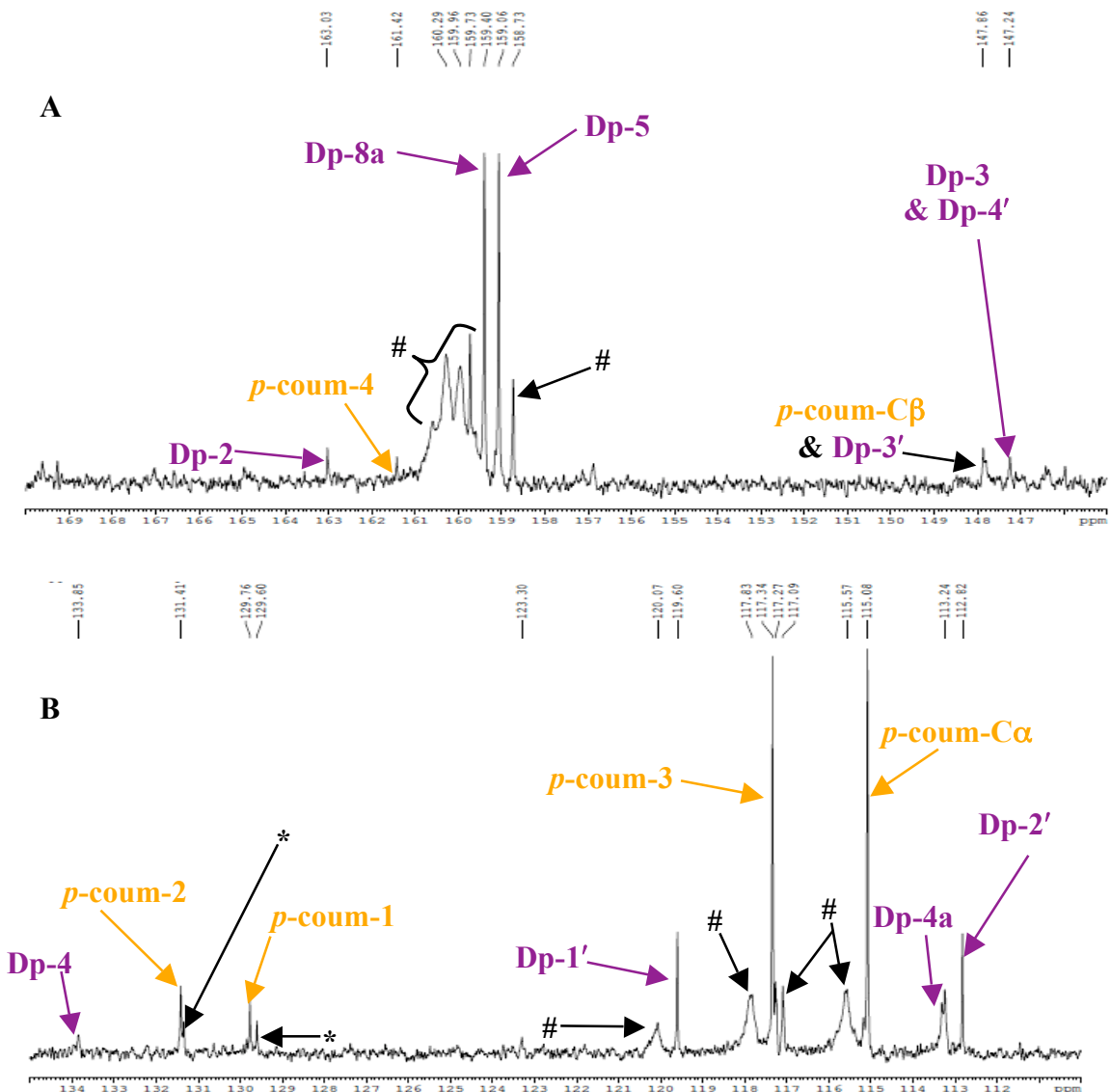


Figure 6.7: (a) ^{13}C spectrum from 170 – 145 ppm; (b) spectrum from 135 – 110 ppm. Abbreviations: Dp = delphinidin, *p*-coum = *p*-coumaroyl, * = possible degradation product or *cis/trans* isomer and # = unknown impurity. Full list of ^{13}C shifts can be found in Table 6.4.

The impurity signals shown in Figures 6.7 – 6.9 are much more obvious in the ^{13}C spectra versus the ^1H spectra. It is clear that the compound was dramatically affected (i.e. degraded) when it was re-concentrated and then solubilized a second time in TFA.

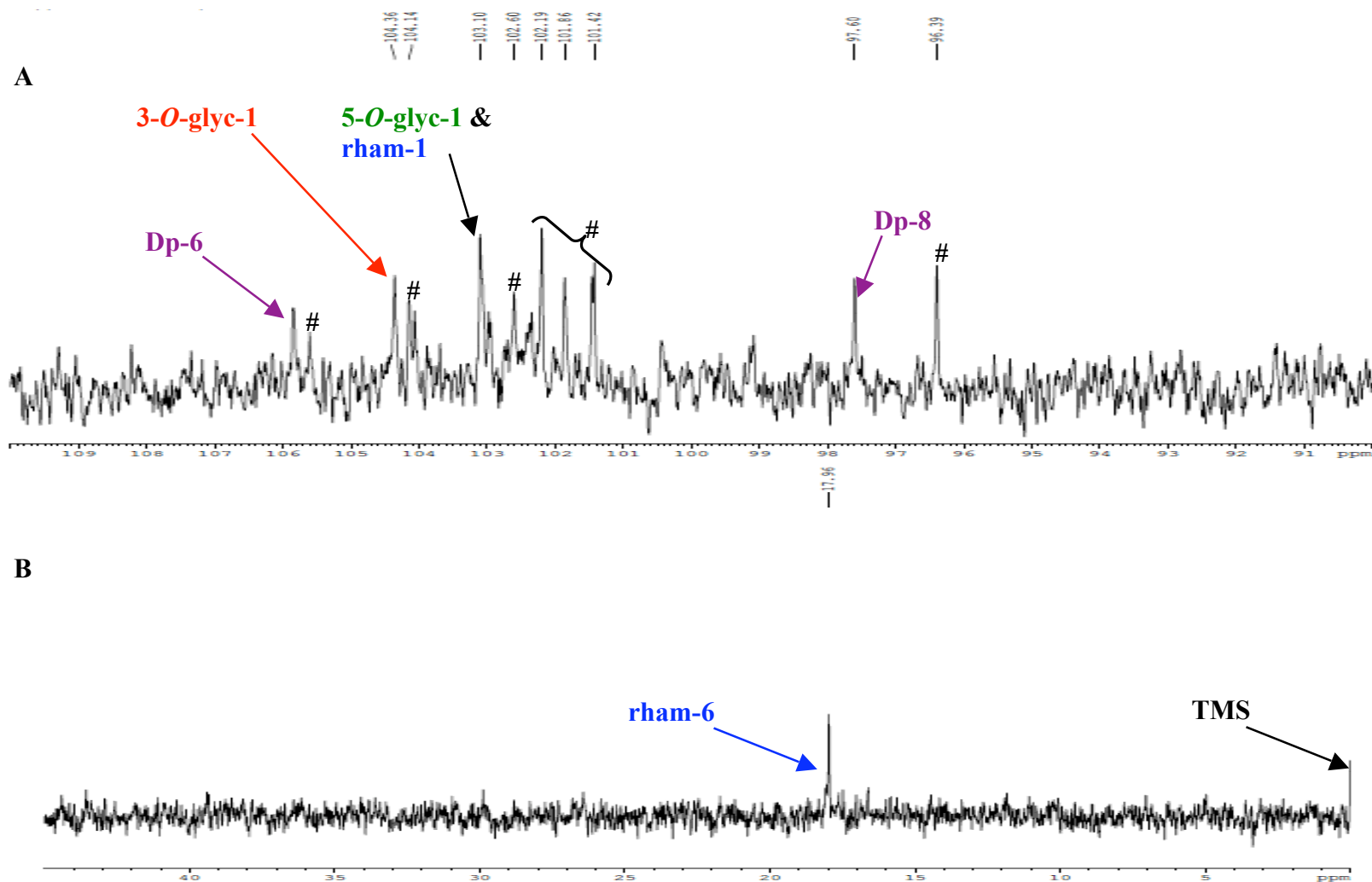


Figure 6.8: (a) ^{13}C spectrum from 110 – 90 ppm; (b) spectrum from 455 – 0 ppm. Abbreviations: Dp = delphinidin, glyc = glycoside, rham = rhamnosyl, # = unknown impurity and TMS = tetramethylsilane. Full list of ^{13}C shifts can be found in Table 6.4.

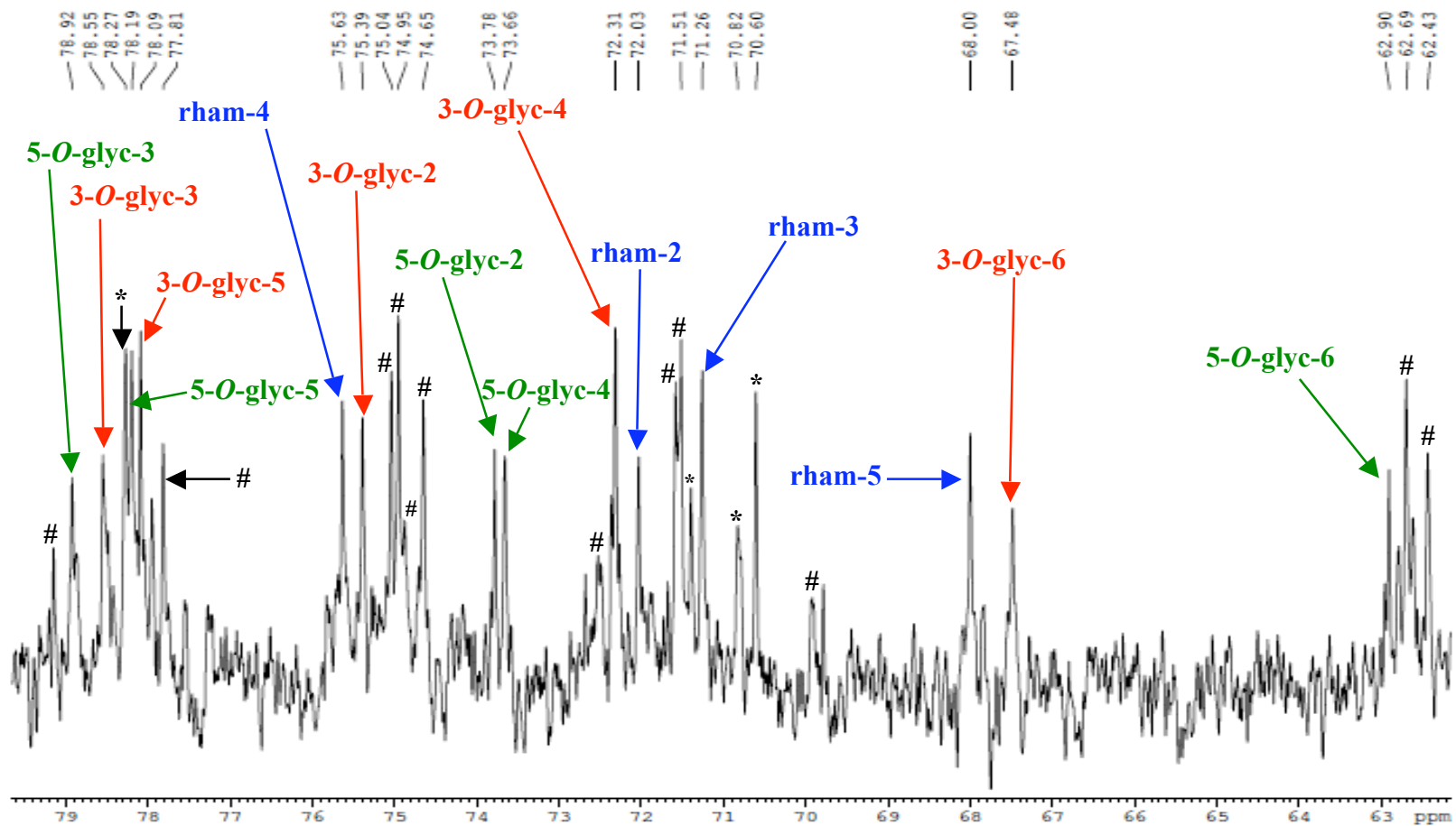


Figure 6.9: ^{13}C spectrum from 80 – 62 ppm. Abbreviations: glyc = glycoside, rham = rhamnosyl, * = possible degradation product or *cis/trans* isomer and # = unknown impurity. Full list of ^{13}C shifts can be found in Table 6.4.

It is obvious from the ^1H NMR data in Table 6.3 that the sample is fairly pure since all the previously reported signals are present in the purple pepper extract, but there are some extra signals that are indicative of degradation. The ^{13}C NMR spectra and data in Table 6.4 demonstrate that the reconcentrated sample most likely degraded causing many additional impurity peaks to be detected along with all the previously reported *trans* isomer peaks and none of the signals for the *cis* isomer were reported. The concentrated purple pepper sample has a high abundance of the *trans* isomer of Dp-3-*p*-coumru-5-glc. Unlike the published ^1H NMR data, the published ^{13}C NMR data does not have accompanying *J* values to assist with identification of the components. The *trans* isomer data from Ichianagi *et al.* (9) was used to determine the appropriate peak assignments for each of the components found in the concentrated purple pepper ^{13}C spectra. The ^{13}C values identified for the concentrated purple pepper sample match very well (± 2 ppm) with the published data for eggplant peels, with the exception of the non-detected peak data for the *cis* isomer components, as well as the two non-detected *trans* isomer peaks for the components of Dp-7 and *p*-coumaroyl-COO from the purple pepper sample (Table 6.4). This close correlation is extremely encouraging and further confirms the presence of the NMR signals for Dp-3-*p*-coumru-5-glc in the foliage of the purple pepper.

Table 6.4: Comparison of ^{13}C NMR data.^a

Eggplant peel ^{13}C NMR Data		
Position	<i>cis</i>	<i>trans</i>
delphinidin		
2	165.0	164.9
3	146.7	146.6
4	134.1	134.1
5	157.5	157.4
6	106.5	106.4
7	170.5	170.5
8	98.3	98.3
4a	113.8	114.1
8a	157.7	157.7
1'	120.7	120.6
2'	113.8	113.8
3'	148.6	148.0
4'	148.8	146.9
3-O-glycosyl		
1	103.7	103.6
2	75.7	75.8
3	79.0	79.0
4	72.1	72.3
5	78.4	78.6
6	67.6	68.1
rhamnosyl		
1	102.6	102.9
2	71.9	71.9
3	71.3	71.3
4	75.9	76.3
5	68.5	68.7
6	18.6	18.7
5-O-glycosyl		
1	102.6	102.9
2	75.3	73.3
3	79.6	79.6
4	73.0	73.0
5	78.8	78.9
6	63.1	63
p-coumaroyl		
1	128.5	128
2	134.8	132.2
3	116.8	117.8
4	161.3	162.2
C α	117.2	116.4
C β	146.7	148.5
COO	168.7	170

Purple Pepper ^{13}C NMR Data	
Position	<i>trans</i>
delphinidin	
2	163.0
3	147.2
4	133.9
5	158.7
6	105.8
7	ND
8	97.6
4a	113.2
8a	159.1
1'	119.6
2'	112.8
3'	147.9
4'	147.2
3-O-glycosyl	
1	104.4
2	75.4
3	78.6
4	72.3
5	78.2
6	67.5
rhamnosyl	
1	103.1
2	72.0
3	71.3
4	75.6
5	68.0
6	17.9
5-O-glycosyl	
1	103.1
2	73.8
3	78.9
4	73.7
5	78.3
6	62.9
p-coumaroyl	
1	129.6
2	131.4
3	117.3
4	161.4
C α	115.1
C β	147.9
COO	ND

^a The eggplant peel data is from Ichyanagi *et al.*(9). Note that there is no column for the *cis* isomer peaks for purple pepper due to lack of abundance in the sample and inability to identify peaks with confidence. Abbreviation: ND = not detected.

6.6: NMR Conclusions

This NMR investigation makes it clear that the linkages of the major ACN found in purple pepper foliage greatly resemble and nearly match the linkages of the major ACN found in eggplant peels. The ^1H NMR data confirms the presence of delphinidin-3-*p*-coumaroylrutinoside-5-glucoside in the purple pepper extract by demonstrating all of the *trans* isomer signals and some of the *cis* isomer signals reported by Ichiyanagi *et al.* (9). There are some minor impurities that are most likely caused by TFA and formed degradation products, which possibly include the presence of an additional coumarin derivative. The comparison of ^1H and ^{13}C NMR spectroscopic data from the purple pepper foliage data collected in this investigation and from the published work on the eggplant peels ACN (9) are found in Tables 6.3 and 6.4. The ^1H data is very encouraging and illustrates that the food-grade extraction was successful at removing the *trans* isomer of the intact ACN of interest and some of the *cis* isomer from the purple pepper foliage. All of the previously reported ^1H signals from Ichiyanagi *et al.* (9) are present in the purple pepper extract with some minor impurities.

The ^{13}C data shows that the extract most likely degraded when it was reconcentrated. Therefore many extra peaks are present in the ^{13}C spectra in addition to the previously reported signals from Ichiyanagi *et al.* (9). All of the ^{13}C signals for the *trans* isomer were present in the purple pepper extract with the exception of the carbons at Dp-7 and *p*-coumaroyl-COO. The extra peaks displayed could have been verified by injecting the sample back onto the HPLC, but due to small sample size this experiment was not performed. Dp-3-*p*-coumrut-5-glc is clearly acid sensitive, needs to be kept away from water and will not survive TFA concentration. Future studies should avoid the

use of TFA in order to minimize the number of degradation products that are likely forming because the glycosidic linkages of the molecule are breaking. If a more concentrated sample is needed for ^{13}C analysis it is best to return to the HPLC and collect additional sample in order to maintain the structure of Dp-3-*p*-coumru-5-glc and reduce the chance of creating degradation products.

Chapter 7: Summary of Results and Conclusion

Overview

The last chapter has a discussion of the entire investigation to remove the intact anthocyanin from the foliage of the purple pepper and analyze it to confirm the presence and structure of delphinidin-3-*p*-coumaroylrutinoside-5-glucoside. It starts with a short review of the creation of the food-grade extraction protocol in Section 7.1.1 and is then followed by the HPLC separation and fraction collection methods in Section 7.1.2. The characterization of the concentrated purple pepper ACN extract by LC-PDA-ESI-MS/MS is summarized in Section 7.1.3. This is followed by a brief reiteration in Section 7.1.4 of the steps followed to elucidate the concentrated ACN extract by NMR analyses. The conclusions drawn from all of the data collected in this study are expressed in Section 7.2. Finally, the future work that could utilize the food-grade extraction protocol, as well as the already prepared and concentrated purple pepper anthocyanin extracts, is described in Section 7.3.

7.1: Summary of Results

In today's society it is important for scientists to support healthy and active lifestyles by providing the public with research based recommendations on what foods to eat, the daily quantities to consume, along with suggested dosages for supplements, and their possible health benefits. Anthocyanins are the water-soluble pigments that mostly color the fruits, vegetables, flowers and other plant tissues in nature (*1*). Their colors range from reds and oranges to purples and blues (*81*). These compounds are naturally

found dissolved in the cell sap inside the vacuole of plant cells (63,81) and are eaten on a daily basis when fruits and vegetables are incorporated into a person's diet. Research has shown that consumption of ACNs is beneficial to a person's health (3,13,24,25,27,49,57,72–78,82,89–134,228) and promote a well balanced diet. They have shown varying levels of bioavailability (11,17–44,46–67,228) in the body and have multiple factors effecting their uptake efficiency, such as: acylation, anthocyanidin structure, and sugar moiety attachment (11). Acylation has been proven to increase the stability of the ACN and, in particular, the stability of the anthocyanin's color (2,6,17–19,39–43,47,49,56–58,60–79).

This research investigation focused on an acylated delphinidin ACN that has been found in high concentrations in the foliage of a purple pepper (*Capsicum annuum* L.). This anthocyanin had been identified by previous researchers (5,8) as delphinidin-3-*p*-coumaroylrutinoside-5-glucoside (Dp-3-*p*-coumrut-5-glc). The three of the four goals of this research investigation were achieved by:

1. Successfully creating an efficient food-grade extraction and isolation method for the major anthocyanin found in purple peppers, as shown in Chapter 3.
2. Effectively applying multiple analytical techniques to confirm the anthocyanin structure of delphinidin-3-*p*-coumaroylrutinoside-5-glucoside in the foliage of purple peppers through the use of HPLC (Chapter 4) to separate and concentrate the extract, MS/MS analysis (Chapter 5) to characterize the ACN, and NMR analyses (Chapter 6) to elucidate the structure of the ACN of interest.

3. Produced a food-grade extract to be utilized in a future human feeding study that could study the bioavailability of the ACN and help to determine which form, acylated or non-acylated, is more bioavailable.

Extensive work on the $^{13}\text{CO}_2$ growth chamber (shown in Appendix D) was completed, but the purple pepper foliage yield was low. Some additional research needs to be completed in order to effectively utilize this environment to produce ^{13}C labeled purple pepper foliage in future studies.

The creation of a food-grade extraction method employing GRAS chemicals in order to maintain the integrity of the major ACN so that it could be used in the feeding study. Due to budgetary constraints, the funding for the feeding study was not renewed, thus prohibiting the feeding study from occurring. The concentrated ACN extract for the feeding study was already produced and ready to be used when the funding was lost. The extract is still available to the scientists at USDA if the finances were to be reinstated.

Multiple analytical techniques were utilized to achieve the goal of this investigation. The separation was completed by HPLC and the ACN of interest was also concentrated using this technique via fraction collection. For characterization of Dp-3-*p*-coumru-5-glc in the purple pepper foliage, both tandem mass spectrometry (LC-PDA-ESI-MS/MS) as well as NMR spectroscopy (^1H and ^{13}C) were utilized to confirm the structure of the ACN of interest. It was necessary for the success of this investigation to utilize all of these techniques, since each one could only provide a portion of the required data in order to achieve the investigation's goals. The data that was obtained from all three analytical techniques clearly demonstrates the success of the food-grade extraction of Dp-3-*p*-coumru-5-glc from the purple pepper foliage.

7.1.1: Food-Grade Extraction Method

The food-grade extraction method utilized 200 proof ethanol (EtOH) and hydrochloric acid (HCl) as 1% HCl/EtOH (v/v). The fresh purple pepper foliage was harvested and the extraction protocol was followed to remove the intact ACN compound. The sample was filtered and dried, rinsed with USP grade acetone until the eluate ran clear, then dried a final time on the rotovap. Once dry, the sample was considered an extract and was resolubilized in 1% HCl/MeOH for further analysis.

7.1.2: HPLC Separation and Fraction Collection

The original extract was first analyzed by HPLC at both 340 nm and 540 nm, as had been done in previous work (5,8). The original extract displayed the most peaks when analyzed at 340 nm (Fig. 4.2 a) for obvious reasons because most polyphenols absorb in this range. The major ACN had the largest % peak area of all peaks identified at 340 nm with 24.701%. The analysis at 540 nm had less peaks in comparison to the analysis at 340 nm and the major ACN peak composed 71.037% of the total peak area (Table 4.1). At both wavelengths, the major ACN peak was the largest peak present with the highest % peak area, % peak height, and absorbance. This demonstrated that the major ACN was in fact present in the purple pepper foliage extract and had a high concentration in comparison to other polyphenols that remained in the extract.

This extract was then utilized to collect fractions of the major ACN peak so that the extract could become more concentrated. A more concentrated sample is easier to characterize by MS and NMR analyses in comparison to a dilute sample. The fractions

were collected over a period of time. The elution time for the major ACN peak to run off the analytical column was approximately 5 minutes. A specific absorbance value of ≥ 2.00 AU was set to determine the collection of the fraction for the major ACN peak. A maximum of 60 fractions were collected for this investigation because at least 2 mg of dry extract were required for NMR analysis. The fractions were stored in a refrigerator at $T = 4\text{ }^{\circ}\text{C}$ until they could be concentrated and tested for purity on the HPLC.

There was a dramatic decrease in the number of peaks identified when compared to the original extract and the % peaks areas of the major ACN also increased when analyzed at 340 and 540 nm in comparison to the original extract (Table 4.5). When the concentrated sample was analyzed at 340 nm the chromatogram confirmed other polyphenols were still present in the sample in very small quantities (Fig. 4.6 and Table 4.3) and it also demonstrated the possible presence of both the *cis* and *trans* isomers. At 340 nm the peaks representing the major ACN (peak numbers 7 & 8 in Table 4.3) had a total % peak area of 94.400%, demonstrating the majority of the sample consists of the *cis* and *trans* isomers of Dp-3-*p*-coumru-5-glc. This data corresponds with the published research of Ichianagi *et al.* (10) that reported the presence of both the *cis* and *trans* isomers in eggplant peels (Fig. 4.9 c). At 540 nm, the single peak of the major ACN had a total % peak area of 98.104% showing that the sample contained almost all of the ACN of interest and < 2% of other polyphenols (Fig. 4.7 and Table 4.4). The concentrated sample was also compared to the Blue Ribbon Iris standard that Asen *et al.* (72,73,77) had produced in the early 1970s. This investigation confirmed by comparison of retention times at 540 nm that the ACN of interest, Dp-3-*p*-coumru-5-glc, present in the purple pepper foliage is the same ACN found in the Blue Ribbon Iris standard (Fig. 4.9 a & b).

7.1.3: Mass Spectrometry Characterization with LC-PDA-ESI-MS/MS

The compounds in the purple pepper foliage were first characterized with a technique that utilized a coupled system known as LC-PDA-ESI-MS/MS. This system was beneficial because not only did it separate the compounds by liquid chromatography (LC) but it also utilized two forms of detection called photodiode array (PDA) and tandem mass spectrometry (MS/MS) to assist in identifying the components. It was important to prepare standard plant material to assist with identification of the concentrated ACN extract. Three plant standards were prepared: Chinese eggplant peels, Chinese celery and bulk purple pepper foliage.

The concentrated ACN extract was injected after the three plant extracts. The system provided HPLC chromatograms, UV, and MS/MS spectra for all of the injections. The data from the plant extracts were very helpful for identification of the compounds found in the ACN extract. Excellent examples of the HPLC chromatograms produced are shown in Figures 5.3 and 5.4, which identify nearly all of the components separated by the HPLC. The UV spectra for the purple pepper foliage were produced to help discern between co-eluting and overlapping peaks from the HPLC chromatograms (Fig. 5.5 a - g). The MS/MS spectra were able to confirm the precursor ion at m/z 919 and the product ions at m/z 757, 465 and 303 for the aglycone (delphinidin) for the concentrated ACN pepper extract as shown in Figure 5.6. All of this data is recorded in Table 5.1, which includes the identification of the compounds found in the freeze-dried pepper plant extract. The data produced in this investigation by the LC-PDA-ESI-MS/MS correlates well with previous research from Lightbourn *et al.* (5) and Sadilova *et al.* (8) that identified the major ACN in purple pepper foliage as Dp-3-*p*-coumru-5-glc as well as the

same ACN being identified by Ichiyanagi *et al.* (9) in eggplant peels. The MS/MS data was a clear match with these previous research investigations, which have shown the presence of Dp-3-*p*-coumrut-5-glc through the use of liquid chromatography, mass spectrometry, and NMR analyses.

7.1.4: NMR Elucidation

The last analytical technique utilized in this investigation was NMR analysis in order to confirm the attachment sites for the glucose and *p*-coumaric acid on the structure of the delphinidin derivative (Dp-3-*p*-coumrut-5-glc). This system was essential for the elucidation of the ACN of interest in order to confirm the presence of delphinidin-3-*p*-coumaroylrutinoside-5-glucoside in the purple pepper foliage. The staff at the University of Maryland's Analytical NMR Service & Research Center was extremely influential in recommending appropriate programs and optimizing instrument conditions to accurately elucidate Dp-3-*p*-coumrut-5-glc.

Previous research on the major ACN found in eggplant peels by Ichiyanagi *et al.* (9) provided MS and NMR values for the *cis* and *trans* isomers of Dp-3-*p*-coumrut-5-glc and was used as a guide in this research investigation. The NMR values obtained here were compared to the previous research of Ichiyanagi *et al.* (9). In order to obtain analogous results it was required for this investigation to produce both ¹H and ¹³C spectra from the concentrated purple pepper extract. It was very important to have a dry sample, free from as much water as possible, to avoid interfering peaks during the NMR analyses.

This NMR investigation utilized a 500 MHz spectrometer equipped with a BBO (Broadband Observe) probe. This setup is very appropriate to acquire routine ¹H analysis

and is best when analyzing other nuclei, such as ^{13}C . The NMR staff has had difficulty in conducting traditional ^{13}C analyses in the past with colored samples, which is why it was suggested to observe the ^{13}C nuclei with ^1H decoupling in order to elucidate the carbon linkages. The pulse sequence of “zg30” (Appendix C) was used to acquire the ^1H data and the instrument parameters are listed in Table 6.1. The pulse sequence “zgdc” (Appendix C) was chosen for ^{13}C and included the ^1H broad-band (BB) decoupling (or composite pulse decoupling, CPD) sequence known as “WALTZ-16” (Appendix C). The instrument parameters for the ^{13}C analysis are listed in Table 6.2. Further explanations of the pulse sequences are found in Appendix C.

The ^1H data collected in this investigation agreed very well with the research published by Ichiyanagi *et al.* (9). The peaks were fairly well resolved (Figs. 6.3 – 6.4 and Appendix C) with some minor impurity peaks. These impurities are most likely degradation products (possibly additional coumarin molecules) that were formed when TFA was added as a solvent. The major ACN in the foliage, Dp-3-*p*coumrut-5-glc, is very acid sensitive and must be kept away from water. It is likely the TFA broke some of the glycosidic bonds in Dp-3-*p*coumrut-5-glc molecule, which would correlate with the impurity signals being close in proximity to the identified signals (Figures 6.3 – 6.4), meaning the protons are most likely in the same environment. These impurities are much more prominent in the ^{13}C data. In comparison to the previously reported values there are slight shifts in the identified ppm values and the multiplicity (δ), while the J values were very comparable to those previously reported for eggplant peels by Ichiyanagi *et al.* (9). The shifting is natural since this investigation was performed on a different instrument using optimized instrument parameters for the concentrated purple pepper extract. Also,

it is well known that acid can causing shifting to occur and TFA was utilized as a solvent along with small amounts of HCl were part of the extraction protocol. These could also be contributing factors to the small shifts and impurity signals observed in the proton data. A comparison of the ^1H data from previous research by Ichiyanagi *et al.* (9) and the data obtained in this investigation can be found in Table 6.3. The obvious difference is the lack of some of the *cis* isomer data for the purple pepper extract. The proton data demonstrated that the purple pepper extract consists mostly of the *trans* isomer (Fig. 6.4) and this correlates with the previous research on eggplant peels (9), which reported that the *trans* isomer (recovery of 57 mg) was approximately 4.5 times more abundant in comparison to the *cis* isomer (recovery 12.5 mg). The difference in the two isomers is demonstrated in the HPLC chromatogram in Figure 4.9 c. In the concentrated pepper extract the only component where a *cis* isomer could be easily identified was in 3-*O*-glycoside, with a doublet at 5.17 ppm and J (in Hertz) of 7.78, which matches well with the published data of 5.18 (d, 7.8). Other *cis* isomer components were easier to identify because they were singlets, such as: Dp-2' at 7.77 (s) and Dp-4 at 8.9 (s). Some tentative identifications of the *cis* isomers for Dp-6 and Dp-8 were at 6.80 (d, 2.15), but the remaining components were left as “not detected (ND)” due to shifting and peak splitting. There was not complete confidence in the identifications of all the *cis* isomer components and hence they are not reported here.

For the ^{13}C analysis, this investigation only reported *trans* isomer data because the proton data demonstrated a great deal of uncertainty for *cis* isomer identifications as well as some impurity signals. Inherently, ^1H peaks are much larger and more easily identifiable in comparison to ^{13}C peaks thus making it even more difficult to detect the

cis isomer components in the carbon spectra for the purple pepper extract. The extract had to be reconcentrated in order to achieve the current carbon spectra shown in Figures 6.7 – 6.9, and the sample was not capable of producing adequate peaks for identification of both the *cis* and *trans* isomers. It was obvious in the ^{13}C spectra that many more impurity peaks were present in addition to those signals corresponding to Dp-3-*p*-coumrut-5-glc. The most likely cause for these additional impurity signals is a degradation of Dp-3-*p*-coumrut-5-glc, where the glycosidic linkages are being broken by the high concentrations of TFA, causing the sugars to fall off the ACN molecule and therefore the NMR is detecting extra signals. These impurities could be prevented in the future by eliminating the use of TFA, preventing water addition to the extract and if a more concentrated sample is needed then additional fractions should be collected from the HPLC and dried *in vacuo* to be utilized for further ^{13}C analyses.

The previous research on eggplant peels (9) reported very comparable ^{13}C values and the difference in values between the *cis* isomer and the *trans* isomer components of Dp-3-*p*-coumrut-5-glc was within +/- 2ppm (shown in Table 6.4). In regards to the *trans* isomer identifications, all of the peaks detected were very comparable (+/- 2 ppm) to those reported by Ichiyanagi *et al.* (9), with the exceptions of the non-detected peaks for Dp-7 and *p*-coumaroyl-COO components seen in Table 6.4. By having to reconcentrate the extract in order to achieve accurate ^{13}C values there is a high probability of additional degradation compounds forming (i.e. impurities) that can be seen in the ^{13}C NMR spectra.

The NMR ^1H and ^{13}C reported for this investigation confirmed the attachment sites for the glucose and *p*-coumaric acid on the delphinidin derivative. The glucose is in

fact connected to the 5-position of the flavylum cation, while the rutinoside and *p*-coumaric acid are attached to the 3-position of the flavylum cation. Nearly all of the positions reported by Ichihyanagi *et al.* were confirmed for the *trans* isomer in this investigation of a concentrated purple pepper extract, thus demonstrating the success of the food-grade extract of Dp-3-*p*-coumrut-5-glc from the foliage of the purple pepper plant.

7.2: Conclusions

A new food-grade extraction method to remove the intact anthocyanin, known as delphinidin-3-*p*-coumaroylrutinoside-5-glucoside (Dp-3-*p*-coumrut-5-glc), was successfully developed for this specific research investigation (Chapter 3). Multiple analytical techniques were employed in order to confirm the effectiveness of this extraction as well as the structure of the anthocyanin present in the purple pepper foliage. These techniques included HPLC (Chapter 4), Mass Spectrometry (Chapter 5), and Nuclear Magnetic Resonance (Chapter 6). Each technique utilized a different type of detection to assist with confirming the presence of the intact ACN of interest, such as: UV-Vis, PDA, MS/MS and NMR detectors. In every instance, the techniques confirmed the presence of Dp-3-*p*-coumrut-5-glc.

All of the data from these analytical techniques confirms the success of the food-grade extraction protocol at removing Dp-3-*p*-coumrut-5-glc from the purple pepper foliage. Despite using GRAS chemicals for the extraction protocol, this study demonstrates the protocol was effective at removing the intact ACN in large enough quantities to have it detected by HPLC, LC-PDA-ESI-MS/MS and NMR. The results of

all the analytical techniques are consistent with the presence of delphinidin-3-*p*-coumaroylrutinoside-5-glucoside in the concentrated purple pepper extract. Both the ^1H and ^{13}C NMR spectra demonstrated that the extract was not as pure as suggested by HPLC and that it was susceptible to degradation, most likely by TFA breaking the glycosidic linkages in the molecule. Despite the presence of these impurities, all of the previously reported values for the *trans* isomer were confirmed, except for two values at Dp-7 and *p*-coumaroyl-COO in the ^{13}C spectra. Overall, the study's goals were achieved and each analytical technique was successful at extracting, separating and characterizing the anthocyanin found in the foliage of the purple pepper.

7.3: Future Work

It would be very interesting in the future to conduct a human feeding study utilizing the food-grade purple pepper extract. This type of study would assist researchers in gaining a greater understanding of the role acylation plays in the bioavailability of an anthocyanin, since the major ACN in purple pepper foliage is acylated. It would be advantageous for future studies to utilize a larger sample size to ensure there is enough extract produced for an effective feeding study. Additional purple peppers could be planted to meet the needs of the human feeding study. Feeding humans a highly concentrated extract of a single anthocyanin, like Dp-3-*p*-coumru-5-glc, from purple pepper foliage would be different from so many of the previous studies because the extract contains such a high concentration of a single ACN. In theory, this would reduce many variables since other polyphenols would not be present and therefore not interfering in the analysis of plasma and urine samples. This should make detection of the ACN

much easier if it remains intact, but if it is metabolized it should be more obvious to the researchers, since the single ACN is the only compound being ingested. Overall, this type of study would be exciting and fascinating to conduct as the potential results could truly help to answer questions regarding anthocyanin bioavailability because of the uniqueness of feeding humans a highly concentrated single anthocyanin extract.

Additionally, a ^{13}C labeled anthocyanin would be even more advantageous to use for the feeding study. This would allow the researchers to easily see if the anthocyanin is absorbed and excreted in its intact form or if it gets metabolized and broken down into other components. Additional research was undertaken with a team of experts at the USDA to optimize growing conditions utilizing $^{13}\text{CO}_2$ in a specialized growth chamber. Unfortunately, the conditions were never fully optimized for purple peppers, but the work was very progressive. With some additional research the conditions could be optimized, the plants could be grown in a ^{13}C labeled environment, and then utilized in the food-grade extraction. Therefore, the foliage used for the extraction would be ^{13}C labeled, thus adding another layer of detection to the human feeding study and provide more useful data to understanding anthocyanin bioavailability. There have been many ^{13}C growth chamber labeling studies that were used as guidance documents for this investigation (45,229–240). The growth chamber information obtained during this research investigation is briefly discussed in Appendix D.

Another possibility for future NMR studies is to grow a large crop of purple peppers, which are harvested solely for extraction purposes. Also, to utilize a different acid from TFA as solvent, which obviously caused the molecule to degrade. In this NMR investigation the *trans* isomer clearly dominated, leading to a lack of ^{13}C NMR data for

the *cis* isomer. The previous work on eggplant peels by Ichiyanagi *et al.* (9) utilized 10 kg of sample and it would be helpful to have a large sample of purple pepper foliage in order to increase the possibility of extracting more of the *cis* isomer of Dp-3-*p*-coumrut-5-glc. This would be a very large undertaking and would require growing the plants out in the field in order to produce enough foliage for harvest. The largest sample size in this investigation was merely 100 g, therefore if a future study could provide at least 1 kg or more this would dramatically increase the potential to detect the *cis* isomer and confirm the ¹³C NMR data for this isomer, as well as detect all of the *cis* isomer peaks in the ¹H NMR analysis.

Lastly, if a feeding study is not the ultimate goal, then future researchers could test other acids for the extraction instead of hydrochloric acid (HCl), such as trifluoroacetic acid (TFA) or experiment with the use of solid phase extraction cartridges. These two small changes could definitely increase the efficiency of the extraction and could remove additional polyphenols that the current extraction protocol was not able to do, thus making the extract more concentrated with pure Dp-3-*p*-coumrut-5-glc. The downside is that these types of changes would not allow the extract to be utilized in a human feeding study because the chemicals do not comply with GRAS regulations from the FDA. These modifications would be helpful for additional characterization and elucidation studies with MS or NMR in order to help confirm previous data for both the *cis* and *trans* isomers of Dp-3-*p*-coumrut-5-glc.

Appendix A: HPLC Data

Table A.1: NMR Fraction Collection Data. These fractions were dried down then prepared for NMR analysis.

Fraction Collection Data for the NMR sample					
Filename	Start (min)	Finish (min)	Total Time (min)	Time of Day	Date
new sample 1-frac #1	32.16	33.75	1.59	1:28:00PM	12/08/09
new sample 1-frac #2	33.17	34.32	1.15	2:50:44PM	12/08/09
new sample 1-frac #3	34.28	35.48	1.20	1:34:56PM	12/11/09
new sample 1-frac #4	26.45	27.05	0.60	3:34:55PM	12/11/09
new sample 1-frac #5	35.30	36.00	0.70	1:44:33PM	12/18/09
new sample 1-frac #6	35.72	36.32	0.60	2:53:43PM	12/18/09
new sample 1-frac #7	35.77	36.33	0.56	4:20:02PM	12/18/09
new sample 1-frac #8	33.23	34.38	1.15	12:52:47PM	01/25/10
new sample 1-frac #9	31.93	32.98	1.05	2:01:39PM	01/25/10
new sample 1-frac #10	31.43	33.05	1.62	3:16:42PM	01/27/10
new sample 1-frac #11	35.28	36.07	0.79	11:06:53AM	01/27/10
new sample 1-frac #12	34.93	35.83	0.90	1:23:02PM	01/27/10
new sample 1-frac #13	34.97	35.88	0.91	2:49:19PM	01/27/10
new sample 1-frac #14	35.00	35.85	0.85	3:53:41PM	01/27/10
new sample 1-frac #15	36.30	37.22	0.92	1:34:36PM	01/29/10
new sample 1-frac #16	36.42	37.27	0.85	2:41:06PM	01/29/10
new sample 1-frac #17	36.05	36.90	0.85	10:37:30AM	02/02/10
new sample 1-frac #18	35.82	36.62	0.80	11:50:01AM	02/02/10
new sample 1-frac #19	35.97	36.67	0.70	1:35:17PM	02/02/10
new sample 1-frac #20	35.78	36.55	0.77	2:39:59PM	02/02/10
new sample 1-frac #21	35.85	36.70	0.85	3:44:09PM	02/02/10
new sample 1-frac #22	35.87	36.65	0.78	4:47:32PM	02/02/10
new sample 1-frac #23	35.97	36.77	0.80	12:58:45PM	02/03/10
new sample 1-frac #24	35.87	36.62	0.75	2:05:38PM	02/03/10
new sample 1-frac #25	36.17	36.93	0.76	3:11:05PM	02/03/10
new sample 1-frac #26	36.08	36.88	0.80	4:15:27PM	02/03/10
new sample 1-frac #27	36.12	36.82	0.70	12:58:40PM	02/12/10
new sample 1-frac #28	35.82	36.55	0.73	2:07:14PM	02/12/10
new sample 1-frac #29	35.82	36.57	0.75	3:21:21PM	02/12/10
new sample 1-frac #30	34.48	35.42	0.94	4:25:36PM	02/12/10
new sample 1-frac #31	34.10	35.10	1.00	1:29:01PM	02/19/10
new sample 1-frac #32	34.27	35.22	0.95	2:33:10PM	02/19/10
new sample 1-frac #33	34.32	35.27	0.95	3:40:01PM	02/19/10
new sample 1-frac #34	34.07	35.02	0.95	4:48:31PM	02/19/10
new sample 1-frac #35	34.30	35.27	0.97	1:49:17PM	02/23/10
new sample 1-frac #36	34.37	35.22	0.85	2:54:18PM	02/23/10

new sample 1-frac #37	34.23	35.18	0.95	3:59:01PM	02/23/10
new sample 1-frac #38	34.42	35.32	0.90	5:05:11PM	02/23/10
new sample 1-frac #39	35.17	35.97	0.80	11:01:45PM	02/24/10
new sample 1-frac #40	34.53	35.48	0.95	1:13:07PM	02/24/10
new sample 1-frac #41	34.50	35.42	0.92	2:21:24PM	02/24/10
new sample 1-frac #42	34.43	35.45	1.02	3:27:22PM	02/24/10
new sample 1-frac #43	34.18	35.18	1.00	4:33:49PM	02/24/10
new sample 1-frac #44	33.78	34.83	1.05	12:29:21PM	03/02/10
new sample 1-frac #45	33.92	34.95	1.03	1:40:39PM	03/02/10
new sample 1-frac #46	33.93	34.88	0.95	2:50:02PM	03/02/10
new sample 1-frac #47	33.57	34.75	1.18	3:55:58PM	03/02/10
new sample 1-frac #48	34.05	35.11	1.06	5:01:56PM	03/02/10
new sample 1-frac #49	34.58	35.50	0.92	3:05:47PM	03/03/10
new sample 1-frac #50	35.55	36.70	1.15	12:44:15PM	03/08/10
new sample 1-frac #51	35.72	36.82	1.10	1:52:57PM	03/08/10
new sample 1-frac #52	35.32	36.40	1.08	2:58:24PM	03/08/10
new sample 1-frac #53	35.05	36.17	1.12	4:05:05PM	03/08/10
new sample 1-frac #54	35.00	36.12	1.12	5:09:01PM	03/08/10
new sample 1-frac #55	33.68	35.12	1.44	1:20:56PM	03/09/10
new sample 1-frac #56	33.52	34.88	1.36	2:37:18PM	03/09/10
new sample 1-frac #57	33.67	34.82	1.15	3:45:53PM	03/09/10
new sample 1-frac #58	32.97	34.02	1.05	5:11:38PM	03/09/10
new sample 1-frac #59	34.27	35.47	1.20	1:55:27PM	03/10/10
new sample 1-frac #60	33.85	35.15	1.30	3:03:30PM	03/10/10
AVERAGE	34.56	35.52	0.96	-	-

Table A.2: Counterpart to Table 4.2. Comparison table for duplicate analysis of concentrated pepper extract at 340 and 540 nm.

Comparison of the Major ACN Peak Values for Concentrated Pepper Extract				
Wavelength (nm)	# of Peaks	Retention Time (min)	% Peak Area	% Peak Height
340	1	34.853	94.24	78.41
540	1	34.811	95.67	92.38

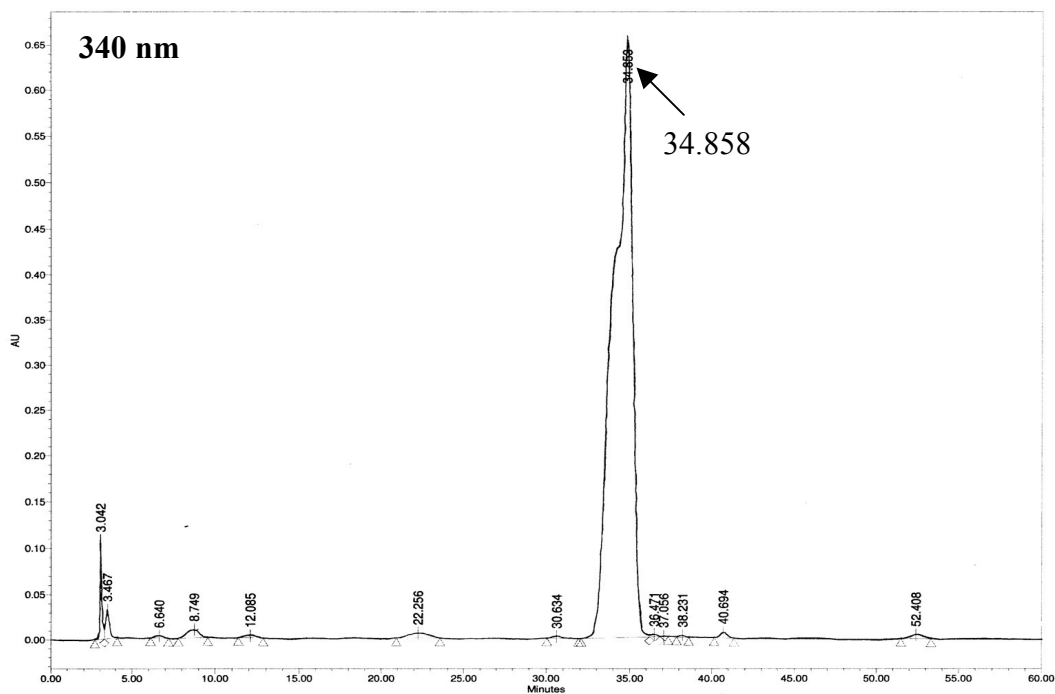


Figure A.1: Counterpart to Figure 4.6. Chromatogram of duplicate analysis of the concentrated purple pepper extract at 340 nm.

Table A.3: Counterpart to Table 4.3. Chromatographic data from the duplicate analysis of the concentrated pepper extract at 340 nm. The major ACN is highlighted in yellow with a % Peak Area of 94.24.

Chromatographic Data from the Concentrated Extract at 340 nm						
Peak #	Retention Time (min)	Area ($\mu\text{V} \cdot \text{s}$)	% Area	Height (μV)	% Height	Width (sec)
1	3.042	823813	1.515	109488	13.171	35
2	3.467	534761	0.983	32199	3.874	50
3	6.640	73194	0.135	2307	0.277	65
4	8.749	468440	0.861	9426	1.134	107
5	12.085	118347	0.218	2492	0.300	87
6	22.256	461537	0.849	5381	0.647	159
7	30.634	88661	0.163	1787	0.215	112
8	34.853	51245618	94.236	651785	78.410	246
9	36.471	68666	0.126	2618	0.315	39
10	37.056	15881	0.029	804	0.097	30
11	38.231	43886	0.081	2155	0.259	45
12	40.694	189674	0.349	6511	0.783	71
13	52.408	247753	0.456	4299	0.517	111
Total	-	54380232	100.000	831251	100.000	-

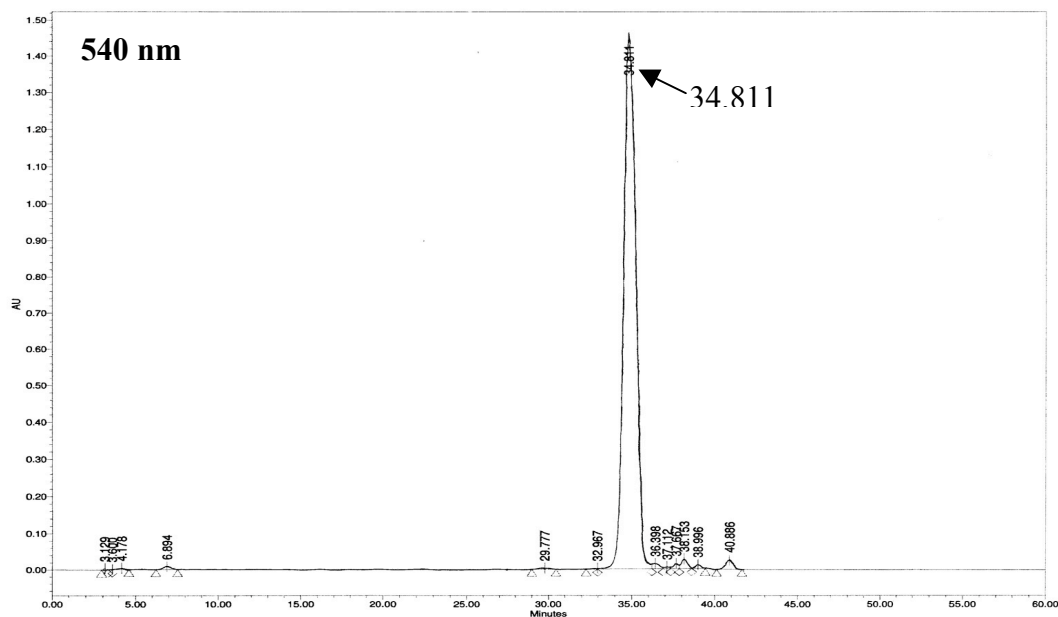


Figure A.2: Counterpart to Figure 4.7. Chromatogram of duplicate analysis of the concentrated purple pepper extract at 540 nm.

Table A.4: Counterpart to Table 4.4. Chromatographic data from the duplicate analysis of the concentrated pepper extract at 540 nm. The major ACN is highlighted in yellow with a % Peak Area of 95.67.

Chromatographic Data from the Concentrated Extract at 540 nm						
Peak #	Retention Time (min)	Area ($\mu V \cdot s$)	% Area	Height (μV)	% Height	Width (sec)
1	3.129	47164	0.062	3740	0.238	23
2	3.600	18370	0.024	1403	0.089	17
3	4.178	119208	0.157	3697	0.236	60
4	6.894	257666	0.339	7571	0.483	79
5	29.777	127264	0.168	2666	0.170	89
6	32.967	47917	0.063	2272	0.145	41
7	34.811	72636206	95.666	1448774	92.379	193
8	36.398	400605	0.528	13818	0.881	41
9	37.112	112905	0.149	5018	0.320	28
10	37.667	307747	0.405	14726	0.939	31
11	38.153	685095	0.902	26625	1.698	46
12	38.996	270581	0.356	11205	0.714	49
13	40.886	895877	1.180	26770	1.707	91
Total	-	75926605	100.000	1568286	100.000	-

Appendix B: Mass Spectrometry Data

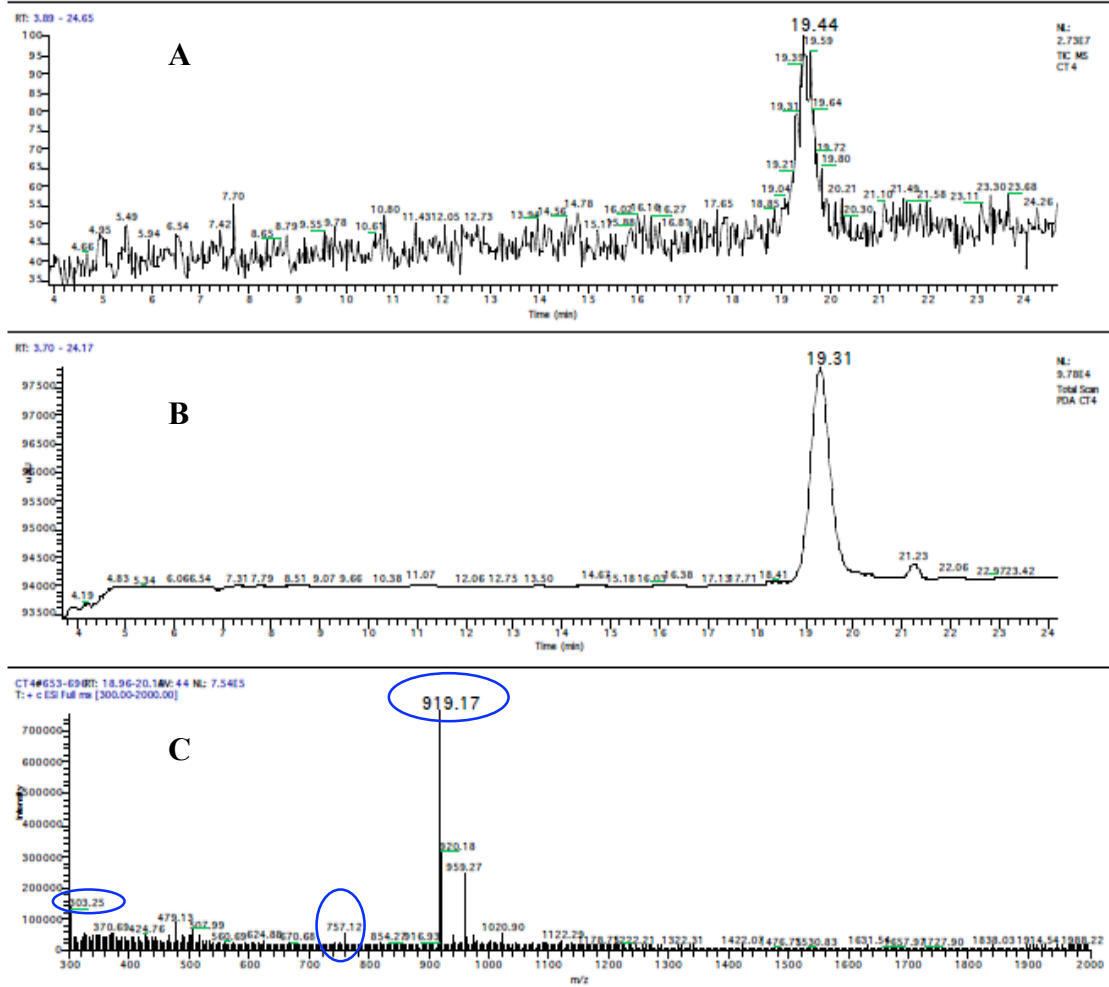


Figure B.1: Spectra from concentrated purple pepper: (a) Total Ion Count MS, (b) UV-PDA, and (c) full ESI MS, circled in blue are the $m/z = 919$ (precursor ion), product ions at $m/z = 757$ and 303 .

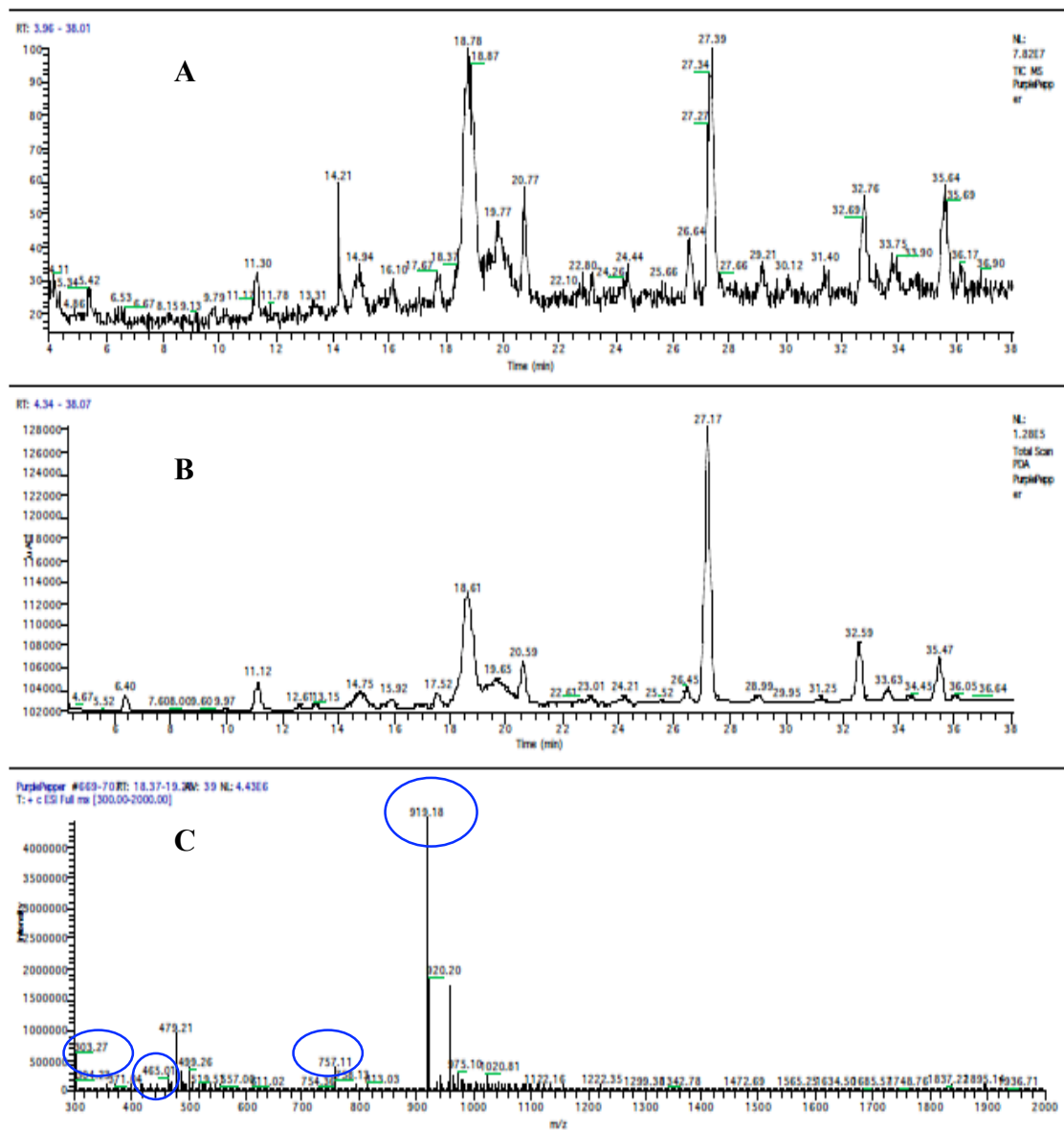


Figure B.2: Spectra of the freeze-dried purple pepper: (a) Total Ion Count MS, (b) PDA, and ESI Full MS, circled in blue are the $m/z = 919$ (precursor ion), product ions at $m/z = 757, 465$ and 303 .

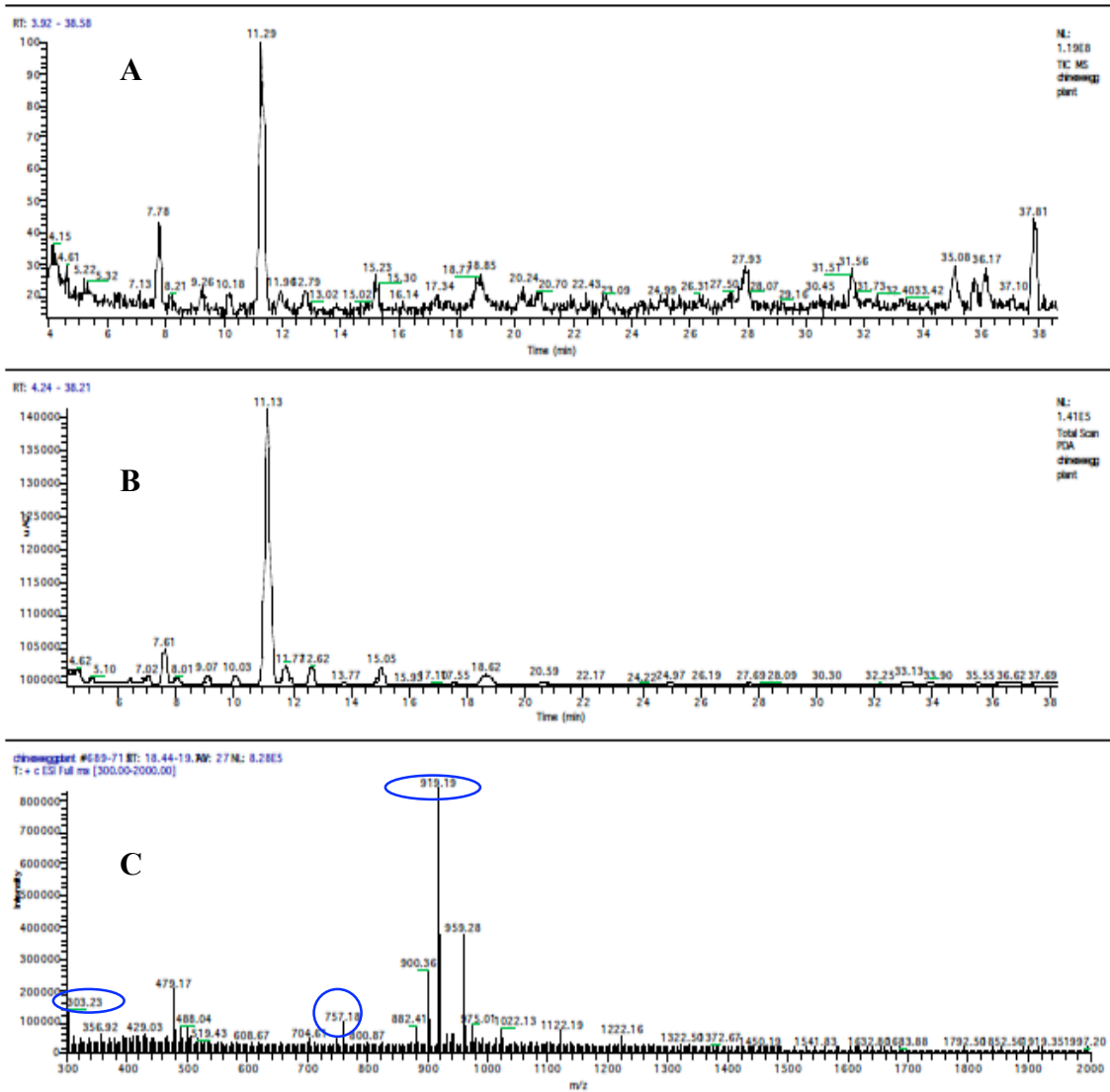


Figure B.3: Spectra of the Chinese eggplant plant extract: (a) Total Ion Count MS, (b) PDA, and ESI Full MS, circled in blue are the $m/z = 919$ (precursor ion), product ions at $m/z = 757$ and 303 .

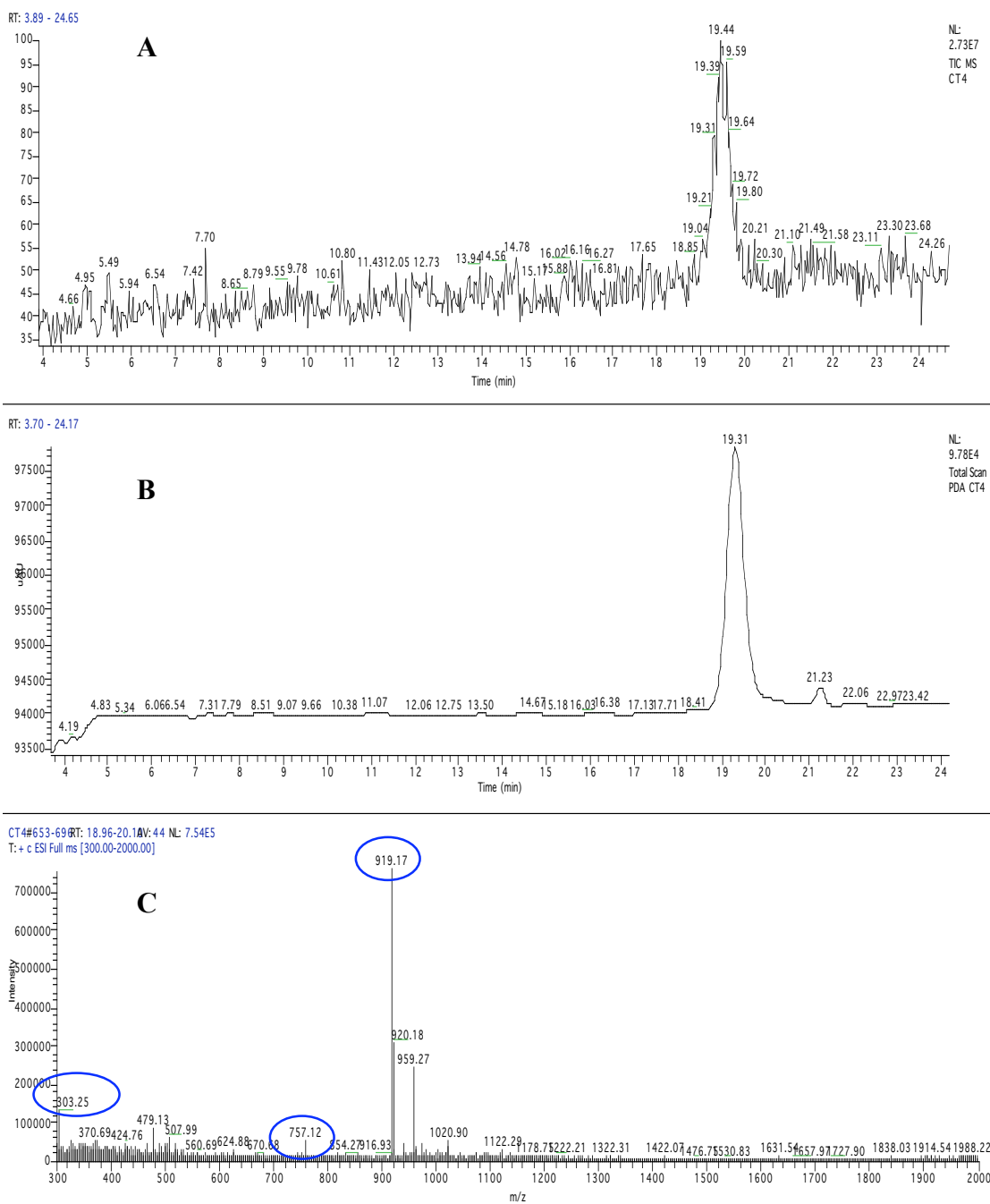


Figure B.4: Spectra from concentrated purple pepper: (a) Total Ion Count MS, (b) UV-PDA, and (c) full ESI MS, circled in blue are the $m/z = 919$ (precursor ion), product ions at $m/z = 757$ and 303 .

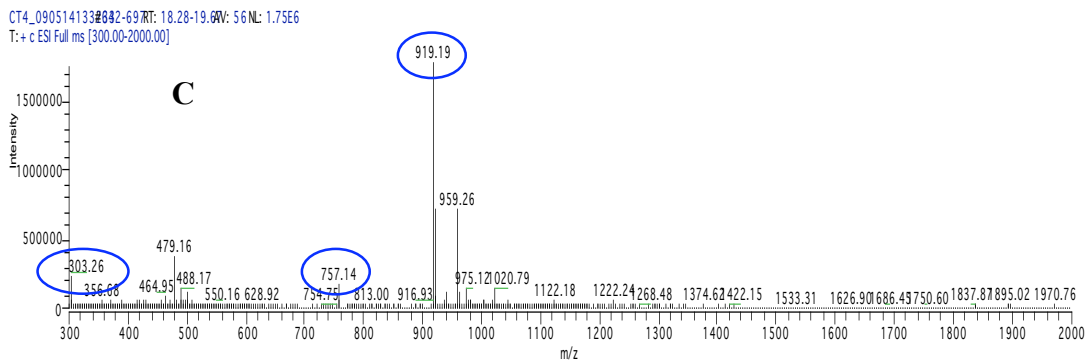
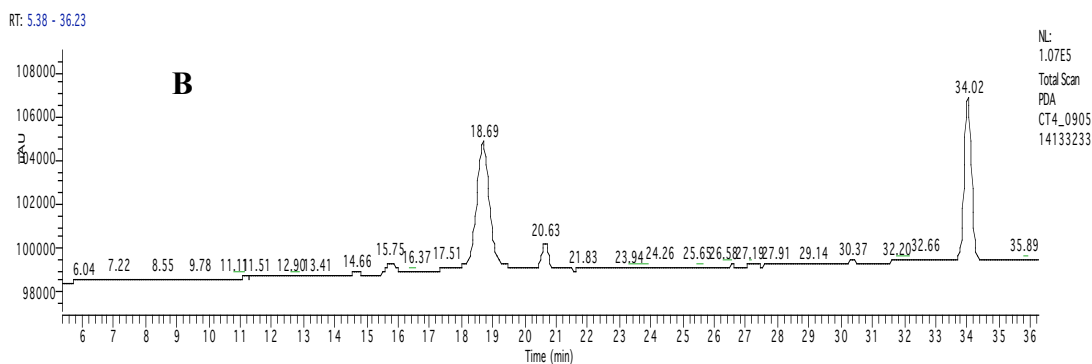
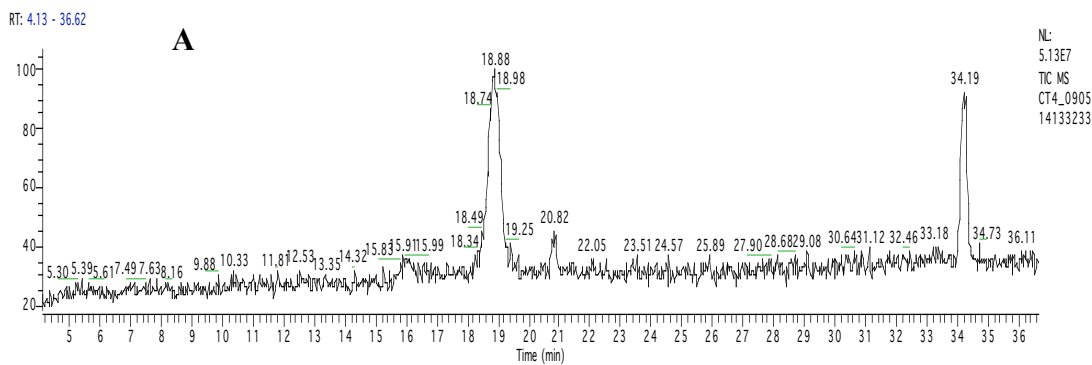


Figure B.5: Spectra from concentrated purple pepper: (a) Total Ion Count MS, (b) UV-PDA, and (c) full ESI MS, circled in blue are the $m/z = 919$ (precursor ion), product ions at $m/z = 757$ and 303 .

Appendix C: NMR

Table C.1: Defined NMR acronyms.

Acronym	Definition (Units, when applicable or specific to this investigation)
INSTRUM	Instrument (spect, for this investigation)
PROBHD	Probe (5 mm BBO2 new, for this investigation)
PULPROG	Pulse Program
TD	Time Domain
SOLVENT	Solvent
NS	Number of Scans
DS	Number of Dummy Scans
SWH	Spectral Width (Hz)
FIDRES	FID Resolution (Hz)
AQ	Acquisition Time (sec)
RG	Receiver Gain
DW	Dwell Time (μ sec)
DE	Pre-scan Delay (μ sec)
TE	Demand Temperature on Temperature Unit (K)
D1	Relaxation Delay (sec)
D11	Delay of disk I/O (sec)
TD0	Loop Counter for Multidimensional Experiments
NUC1	Nucleus for Channel 1
NUC2	Nucleus for Channel 2
P1	90° Transmitter Pulse for Channel 1 (μ sec)
PL1	Power Level Pulse for Channel 1 (dB)
PL2	Power Level Pulse for Channel 2 (dB)
PL12	Pulse Power Level for CPD/BB decoupling (dB)
SF01	Irradiation Frequency for Channel 1 (MHz)
SF02	Irradiation Frequency for Channel 2 (MHz)
SI	Size of Real Spectrum
SF	Spectral Reference Frequency (MHz)
WDW	Window Multiplication Mode (EM, for this investigation)
EM	Exponential Multiplier on FID
SSB	Sinebell Shift
LB	Line Broadening Factor for EM (Hz)
GB	Gaussian Factor
PC	Peak Picking Sensitivity
CPDPRG2	CPD Decoupling Sequence (WALTZ-16, for this investigation)
PCPD2	90° Pulse for Decoupling Sequence

C.1: Pulse Sequences

The ^1H analysis for this investigation utilizes the pulse sequence “zg30”, shown in Figure C.1, because it is a very effective way to achieve a large number of pulses by only flipping the pulse to 30° then returning to the start position on the z-axis of 0° (z_0). Traditionally, the pulse would flip all the way to 90° , but then a longer relaxation time is required so that the pulse may return to z_0 . The potential problem with pulsing to a 90° flip angle is underestimating the required relaxation time. If this occurs, then the pulse would not return to z_0 and therefore pulse early and then past 90° . This would produce subtractive effects, which are very undesirable. By using a 30° flip angle the relaxation time is much shorter and easier to calculate to ensure the pulse returns to z_0 so as to avoid the problem of subtractive effects. The “zg30” pulse sequence is the most common sequence when acquiring ^1H proton data for its speed, efficiency and high number of pulses.

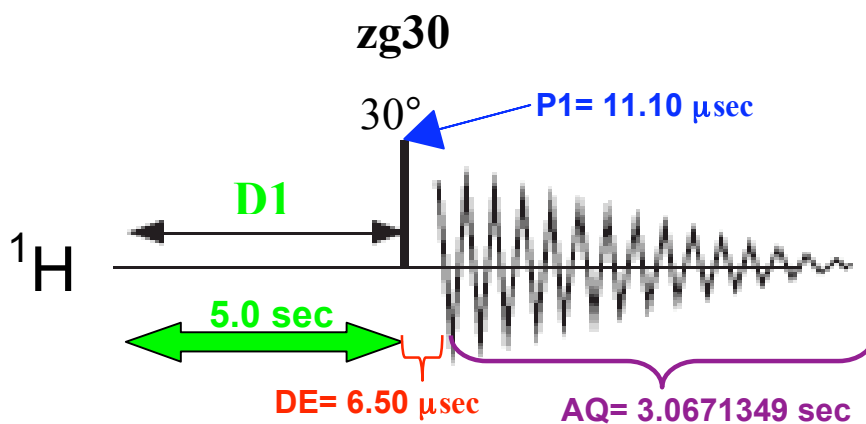


Figure C.1: Graphical representation of pulse sequence “zg30”. D1 = relaxation delay, DE = Pre-scan delay, AQ = Acquisition Time, P1 = pulse length.

In order to obtain accurate ^{13}C data for the ACN of interest the pulse sequence “zgdc”, as shown in Figure C.2, was utilized. In this 1-D sequence, the ^{13}C channel (f1) is observed while the ^1H channel (f2) is the decoupling channel (Table 6.3). The specific composite pulse decoupling (CPD) sequence used is “WALTZ-16” is shown in Figure C.3 and is named for the repetitious dance steps of the waltz where the step count is “1-2-3, 1-2-3...”, similar to the CPD sequence repeatedly flipping from one angle to another over and over. CPD is very helpful to minimize multiplets from forming and clean up the spectra, since ^{13}C peaks are inherently small and sometimes difficult to detect when the peaks are split. In the “WALTZ-16” sequence the decoupler turns off for a split second when the acquisition begins, then turns back on. This allows for the nuclear Overhauser effect (NOE) to still take place.

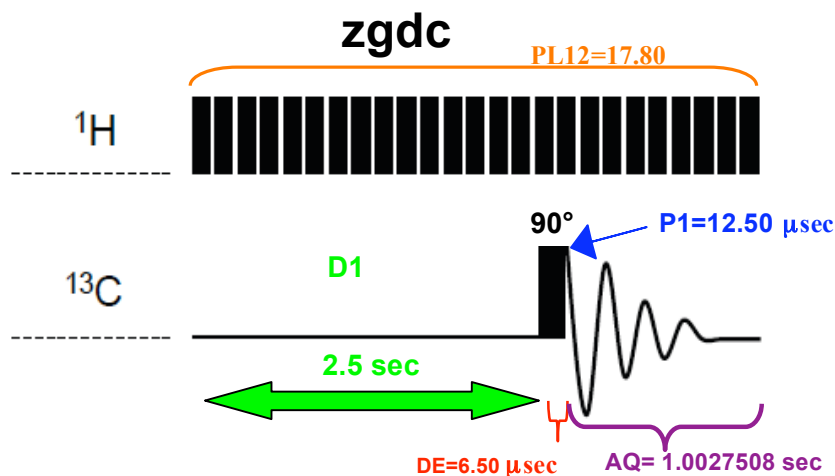


Figure C.2: Graphical representation of pulse sequence “zgdc”; D1 = relaxation delay, DE = Pre-scan delay, AQ = Acquisition Time, P1 = pulse length, PL12 = power level for CPD/BB decoupling.

WALTZ - 16: $\overline{Q\overline{Q}Q\overline{Q}}$, where $Q = 270_x 360_x 180_x 270_x 90_x 180_x 360_x 180_x 270_x$

Figure C.3: Waltz-16, the composite pulse decoupling (CPD) sequence utilized in the ^{13}C measurement with ^1H decoupling for the concentrated ACN sample (241).

NOE is described as the change in intensity of the NMR signal from a nucleus when the spin populations of a nearby nucleus are changed (241). This can occur from an electromagnetic pulse, but this effect does not develop instantaneously and is related to relaxation. For the decoupling of ^1H from ^{13}C , the signal-to-noise enhancement is proportional to the number of ^1H nuclei attached to the ^{13}C nucleus. NOE is also proportional to the density of ^1H nuclei that surround the ^{13}C nucleus. The major benefit of the NOE in broad-band decoupling is that the ^{13}C signal is greatly increased, making the small ^{13}C signals easier to detect and measure (241).

In “WALTZ-16” CPD sequence a 90° flip angle is used so that the pulse is constantly flipping from one angle to the next, i.e. $270^\circ \rightarrow 360^\circ \rightarrow 180^\circ \rightarrow 270^\circ \rightarrow 90^\circ \dots$ etc. This flipping does not allocate enough relaxation time for the pulse to always return back to z_0 , thus no energy is emitted and no signal is detected at these times. This is how the multiplets are reduced because the pulse is constantly being flipped and the full energy cannot be emitted unless the pulse returns to z_0 . The result is a cleaner spectrum with more clearly defined ^{13}C peaks. This CPD sequence is very beneficial for ^{13}C analyses and is the most common decoupling sequence.

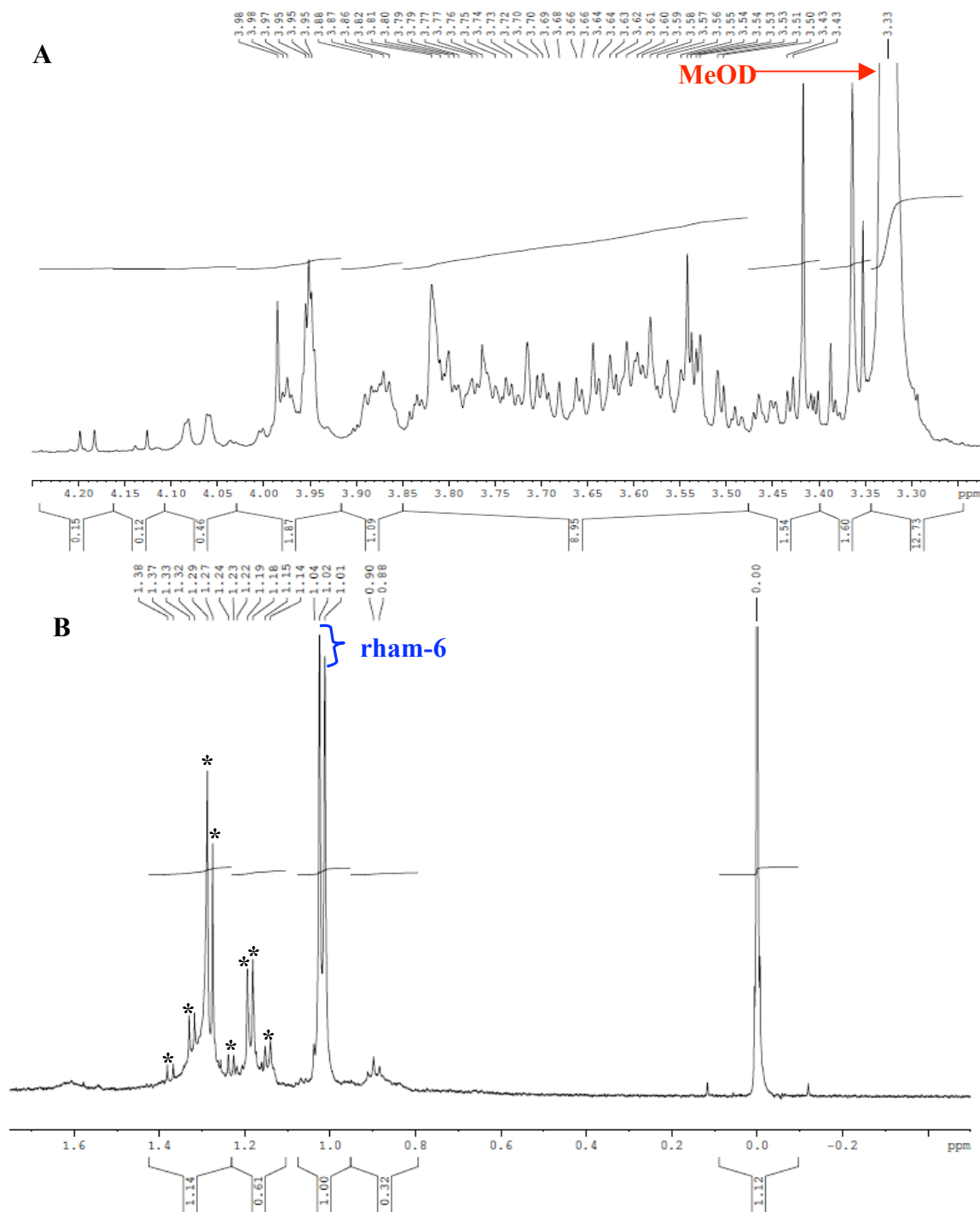


Figure C.4: (a) ^1H spectrum from 4.25 – 3.23; (b) ^1H spectrum from 1.73 – -0.5; Abbreviations: MeOD = deuterated methanol, rham = rhamnosyl and * = possible degradation product or *cis/trans* isomer. Full list of ^1H shifts in Table 6.3.

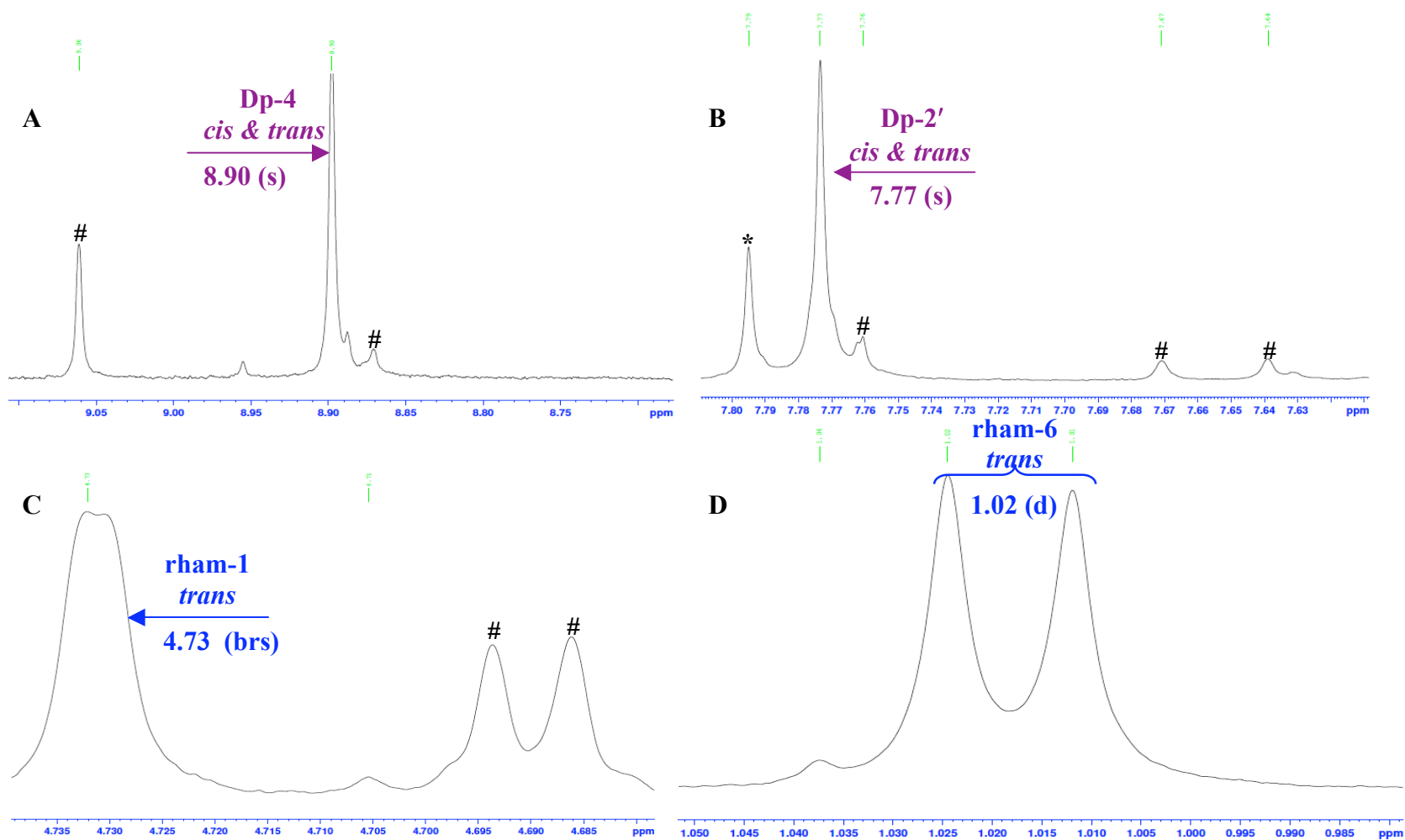


Figure C.5: Some zoomed in ^1H spectra (a) Dp-4 (*cis & trans*); (b) Dp-2' (*cis & trans*); (c) rham-1 (*trans*); (d) rham-6 (*trans*). Abbreviations: Dp = delphinidin, rham = rhamnosyl, * = possible degradation product or *cis/trans* isomer and # = unknown impurity. Full list of ^1H shifts in Table 6.3.

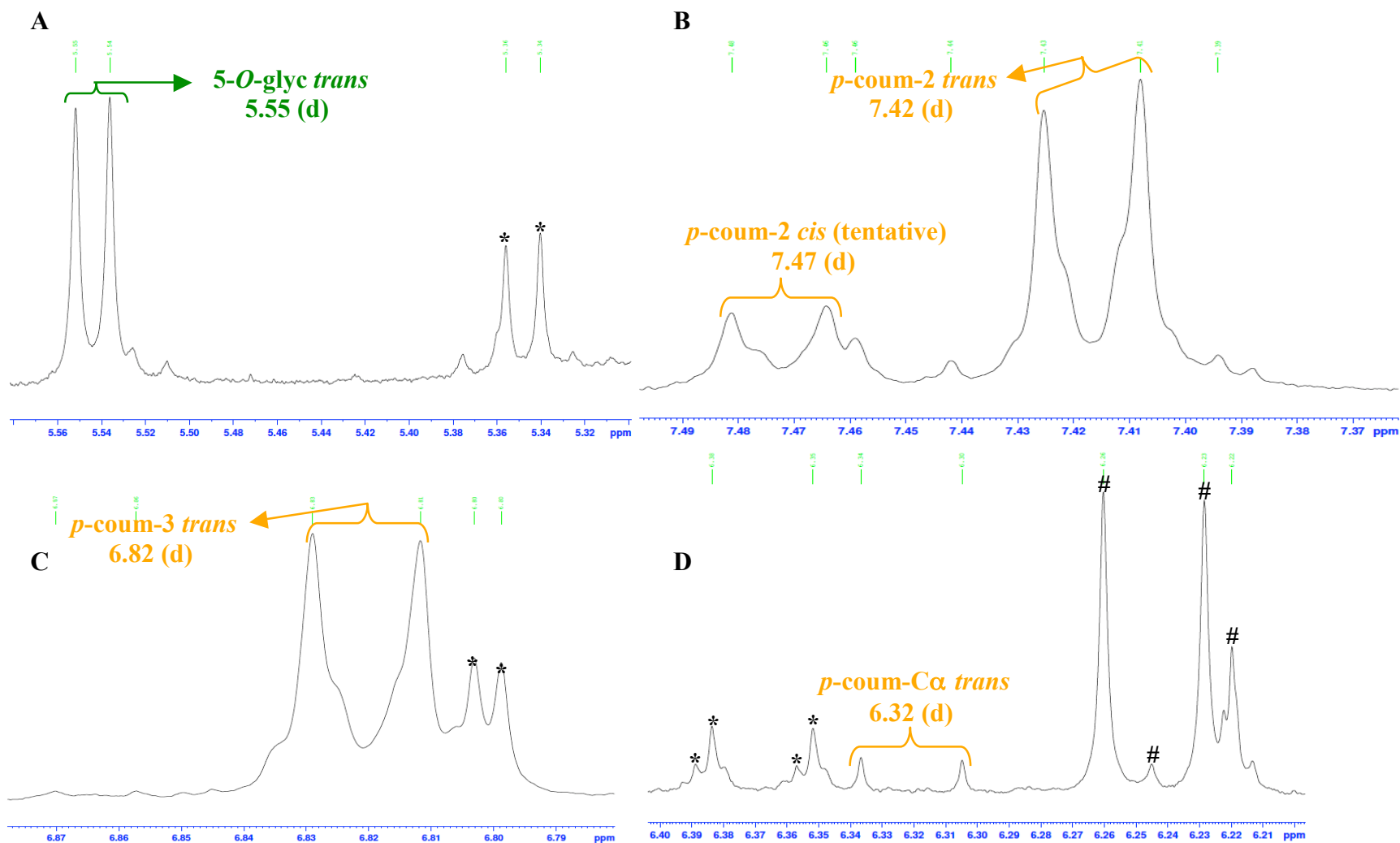


Figure C.6: Some zoomed in ^1H spectra (a) *5-O-glyc (trans)*; (b) *p-coum-2 (cis & trans)*; (c) *p-coum-3 (trans)*; (d) *p-coum-C α (trans)*. Abbreviations: glyc = glycoside, coum = coumaroyl and * = possible degradation product or *cis/trans* isomer and # = unknown impurity. Full list of ^1H shifts in Table 6.3.

Appendix D: CO₂ Plant Chambers

D.1: Background

The most important goal of this research investigation was to produce a food-grade extraction of the major anthocyanin from the foliage of purple pepper plants. With this in mind we thought it would be advantageous to have a ¹³C labeled ACN. By utilizing a ¹³C labeled plant for the food-grade extraction it would make detecting the intact ACN in the urine and plasma very simple once the human subjects had ingested the ACN extract and excreted it. If metabolites formed, then the ¹³C labeled ones would be more obvious to detect. The idea was to provide an added level of detection to help solve the mystery of anthocyanin bioavailability in the human body.

D.2: Study Objectives

This portion of the investigation required the assistance of experts from BHNRC who had previously labeled other plant materials. Dr. Steven Britz (Research Plant Physiologist) and Roman Mirecki (Plant Physiologist) were the main resources and operators of the CO₂ growth chamber when we were trying to optimize the growth conditions for the purple peppers. There were four main objectives for this study:

1. Grow purple pepper foliage in a ¹³CO₂-labeled environment.
2. Harvest the foliage and utilize it for the food-grade ACN extraction protocol.
3. Use analytical techniques (HPLC, MS and NMR) to confirm the presence of the major ACN, Dp-3-*p*-coumru-5-glc, in the extract from the purple pepper foliage.

4. Use the food-grade extract in a human feeding study to evaluate anthocyanin bioavailability.

The main objective was to grow purple pepper plants to a mature state where their leaves could be completely stripped. Then place these stripped plants in a $^{13}\text{C}\text{O}_2$ -labeled box, as seen in Figure D.1, inside of a larger temperature controlled growth chamber. As the new foliage is produced it will be ^{13}C -labeled. Therefore, when the leaves are harvested from these plants and utilized in the food-grade extraction it will make detection of the major ACN (Dp-3-*p*coumru-5-glc) in urine and plasma very easy to detect. Also, any metabolites that may form if the ACN is broken down once it has been ingested and excreted from the body will be easier to detect by conventional technologies.

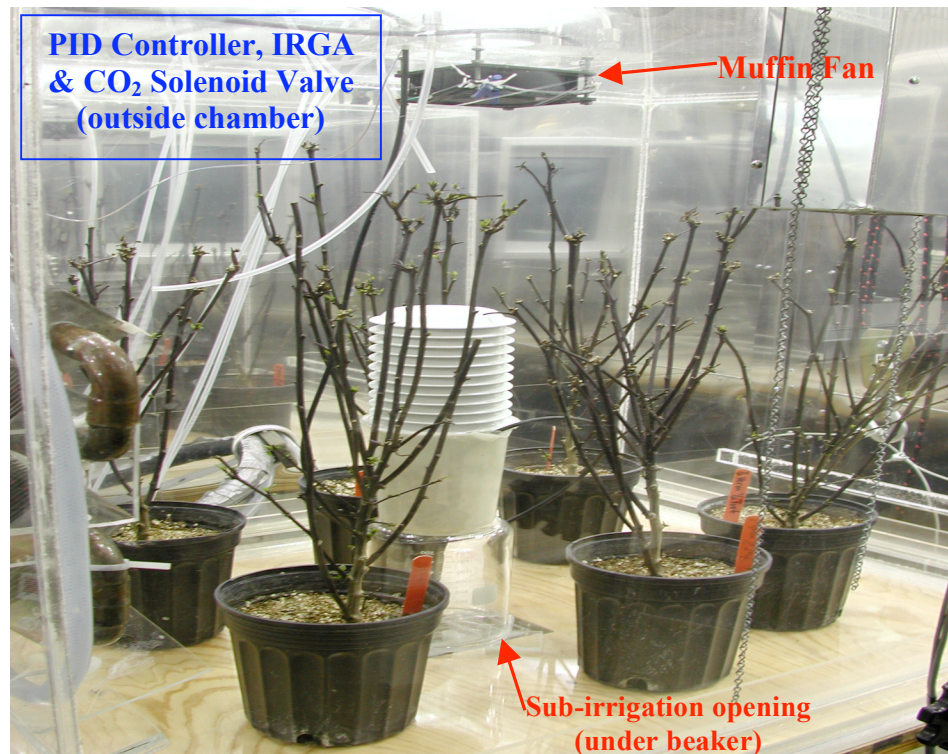


Figure D.1: Mature pepper plants that have been stripped of their leaves and placed in the carbon dioxide (CO_2) Plexiglas chamber inside of a larger growth chamber. See Section D.3 for definitions of PID controller, IRGA, Solenoid Valve and sub-irrigation opening.

D.3: Carbon Dioxide (CO₂) Chamber

Once the plants were > 70 cm in height they were placed inside a separate clear Plexiglas box (Fig. D.1). The acrylic box was placed inside of an environmental growth chamber that was equipped with metal halide lamps. These lamps are best of this setup because they produce more blue light and more UVA radiation. Plexiglas (i.e. acrylic) transmits radiations, which is more conducive for flavonoid (i.e. anthocyanin) production. The Plexiglas box had a separate base that was approximately 6.35 mm thick and an upper enclosure that was approximately 3.18 mm thick. The dimensions and initial readings were as follows:

- Plant height from bottom of pot to top of plant = 72 cm
- Distance from top of acrylic box down to top of plant = 11.5 cm
- Distance from top of acrylic box up to top of growth chamber = 40 cm
- Interior dimensions of acrylic box (L x W x H) = 104 cm x 76.5 cm x 85 cm.
- Light Readings inside the acrylic box: Left = 306 $\mu\text{mol}/\text{m}^2 \cdot \text{s}$; Right = 309 $\mu\text{mol}/\text{m}^2 \cdot \text{s}$
- Light Readings inside the growth chamber (outside acrylic box): Left = 382 $\mu\text{mol}/\text{m}^2 \cdot \text{s}$; Right = 357 $\mu\text{mol}/\text{m}^2 \cdot \text{s}$

The upper enclosure fit into a water-filled trough in the base of the box to form an airtight seal. A muffin fan was mounted in the middle of the upper enclosure to help circulate air. This Plexiglas box was placed inside of a large, walk-in temperature and humidity controlled growth chamber. A coldfinger (Fig. D.4) was also inside the acrylic box in order to help regulate humidity and was regulated by a water bath that was outside of the growth chamber (Fig. D.3). The Plexiglas box had an automated watering system that would pump nutrient solution (239) through a hole in the bottom of the

acrylic box for a specific period of time and then drain back out the same opening. This type of watering is known as sub-irrigation and a beaker was placed over the opening to prevent splashing (Fig. D.1). The nutrient solution filled the trough and would allow the plants to uptake the nutrient from their roots.

Outside of the growth chamber were the regulating controls for the amount of CO₂ that was added to the Plexiglas box. The air within the chamber was sampled using ports on the top of the chamber adjacent to the muffin fan. The air was monitored for CO₂ concentration with an infrared gas analyzer (IRGA). The IRGA was operated in conjunction with a PID controller and a solenoid valve (connected directly to CO₂ tank) to inject the CO₂ through a separate port on top of enclosure on the other side of the muffin fan, where it would then be circulated. A rugged micrologger is attached to the PID controller to store and log data collected from inside the Plexiglas box (see data in Table D.1 & Fig. D.5). The labeling chamber configuration and representative conditions of the acrylic box can be found in Kurilich *et al.* (242). Visual representations of experiment setup are in Figures D.1 – D.4.

The conditions were never fully optimized to grow purple pepper plants successfully in a ¹³CO₂-labeled environment. Also, the funding for the ¹³CO₂-labeling experiment was lost when the funding for the human feeding study was lost. But it's very plausible to optimize the growing conditions for this plant so that the foliage grows well and produces adequate purple leaves that could be harvested for use in the food-grade extraction protocol (Chapter 3) and further concentration, if necessary (Chapter 4). The groundwork has already been started and can be picked up easily if funding were reinstated.

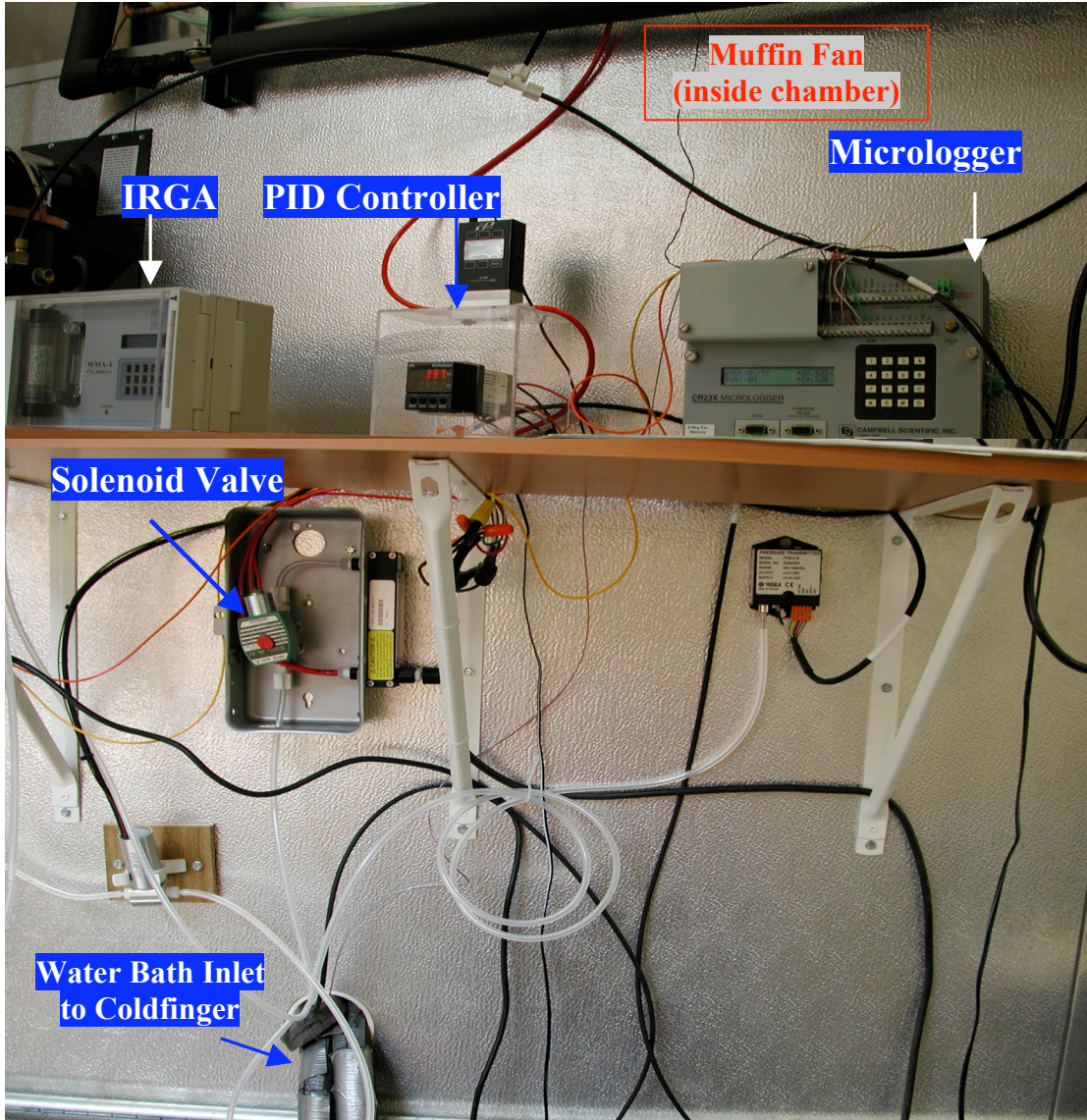


Figure D.2: Photograph outside of the growth chamber, on the back wall of the growth chamber (adjacent to muffin fan, which is inside Plexiglas box, inside growth chamber). The micrologger, PID controller, IRGA and solenoid valve setup (linked directly to CO₂ tank). Water bath setup is shown in Fig. D.3.

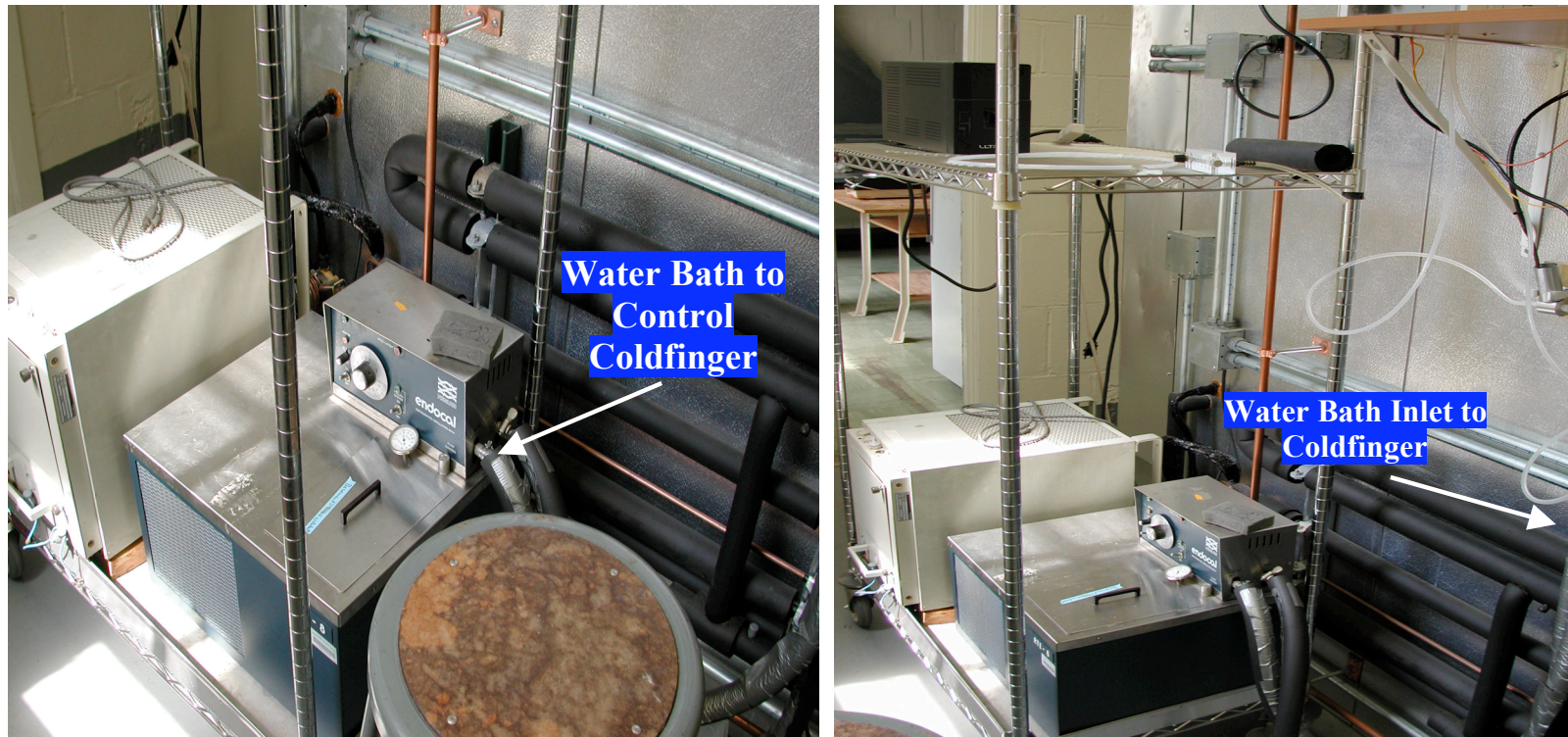


Figure D.3: Outside of the growth chamber, on back wall of the growth chamber. The water bath that controls the coldfinger inside of the Plexiglas box that is inside the growth chamber. This helps to control the humidity inside the Plexiglas box. See a picture of the coldfinger in Fig D.4.



Figure D.4: Picture of inside the Plexiglas box, inside of the growth chamber. The coldfinger, which is controlled by the water bath (outside the growth chamber) is seen along the side of the Plexiglas chamber and helps to maintain the humidity levels inside the Plexiglas chamber.

Table D.1: Collected CO₂ data from Plexiglas chamber during growth optimization experiment for purple peppers.

Data Collection from Plexiglas CO ₂ chamber for Purple Pepper Plants				
DATE & TIME	CO ₂ (mL)	DAY DIFF (time in days)	CO ₂ DIFF (mL)	CO ₂ /DAY (mL/day diff)
1/30/09 14:00	17272	-	-	-
2/2/09 14:30	25924	3.020833333	8652	2864.110345
2/4/09 10:30	33057	1.833333333	7133	3890.727273
2/5/09 13:00	38365	1.104166667	5308	4807.245283
2/6/09 12:30	43499	0.979166667	5134	5243.234043
2/9/09 8:30	61838	2.833333333	18339	6472.588235
2/10/09 13:00	70666	1.1875	8828	7434.105263
2/11/09 11:30	77873	0.9375	7207	7687.466667
2/12/09 17:30	87277	1.25	9404	7523.2
2/13/09 10:00	92752	0.6875	5475	7963.636364
2/13/09 10:00	0	-	-	-
2/15/09 18:00	17573	2.333333333	17573	7531.285714
2/17/09 12:00	30316	1.75	12743	7281.714286
2/18/09 14:00	38177	1.083333333	7861	7256.307692
2/20/09 14:15	53342	2.010416667	15165	7543.212435
2/23/09 9:30	74138	2.802083333	20796	7421.620818
2/24/09 11:00	81745	1.0625	7607	7159.529412
2/24/09 17:45	83745	0.28125	2000	7111.111111
2/25/09 14:30	89479	0.864583333	5734	6632.096386
TOTAL (mL):			164959	-
TOTAL (L):			164.959	-

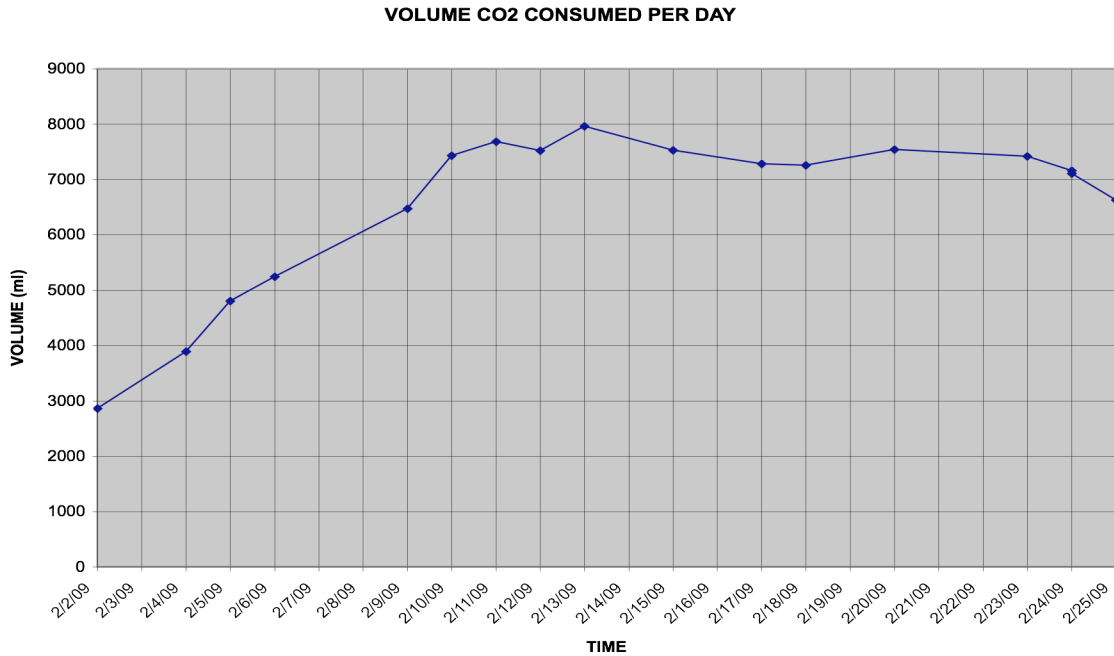


Figure D.5: Graphical representation of the data in Table D.1 depicting the volume of CO₂ consumed (i.e. entered the Plexiglas chamber) each day that data was collected.

D.4: Growing Conditions for Pepper Plants

The first step was to plant purple peppers in soil from seed and grow them in the greenhouse as usual. Then transplant the young purple peppers into various soil types and ratios in order to determine what would be the best mixture to ensure the plants would drain properly. The labeling study will utilize a watering system which fills a container from the bottom and the plants will need to absorb the water from the bottom-up instead of the traditional top-down watering that is usually used in the greenhouse. The first set of plants were transplanted into 4 inch pots and used four soil types, as follows:

- 1) Soil
- 2) 1/3 Vermiculite and 2/3 Perlite
- 3) 1/2 Vermiculite and 1/2 Turface
- 4) 1/3 Vermiculite and 2/3 Turface

These plants were stripped of their leaves when they were transplanted and placed in the greenhouse. After approximately two weeks it was suggested that the pepper plants may need to be in larger pots and it was possible the plants were stripped when they were too young, causing the new leaf production to be very slow.

The second set of transplants, totaled four plants, but utilized only two soil types because these were the best looking plants from the first set. The soil types are as follows:

- 1) 1/2 Vermiculite and 1/2 Turface (one plant in 6" and one plant in 4" pot)
- 2) 100% Vermiculite (one plant in 6" and one plant in 4" pot)

The plants were again stripped of their leaves and placed in the greenhouse for monitoring for one week to determine if the leaves would grow back more quickly in the

6" pots. After a week the plants were placed in a growth chamber. It was found that again the plants were too young to have their leaves stripped and they did not produce new leaves quickly.

A new set of pepper plants were then placed in the following soil types:

- 1) 100% Vermiculite (3 plants in 4" pots)
- 2) 100% Vermiculite (3 plants in 6" pots)
- 3) 1/2 Vermiculite and 1/2 Turface (3 plants in 4" pots)
- 4) 1/2 Vermiculite and 1/2 Turface (3 plants in 6" pots)

These plants were left in the greenhouse to grow larger than the first two sets with the idea that larger, more mature plants could handle having their leaves stripped better than the younger plants. It was thought the leaves would grow back more quickly with larger, more mature purple pepper plants. The plants were left in the green house for approximately 6 weeks to mature. They were then stripped of all their leaves and placed in the Plexiglas chamber and monitored. Unfortunately, they did not prosper in the environment and had to be removed after approximately 4 weeks.

The last set of plants that seemed to grow well were in 16 hours of daylight then 8 hours of night in a temperature and humidity controlled growth chamber in Building 010A at BARC and in the following soil types:

- 1) 100 % Clay (3 plant in 6" pots)
- 2) 100 % Soil (3 plants in 6" pots)

This chamber does not have a Plexiglas setup inside, simply a wire shelf to place the plants on (see Fig. D.6). This is where the growing conditions were experimented with in order to find what was optimal to help the plants re-produce their leaves once they had

been stripped. Multiple sets of plants were placed in this growth chamber using various soil types, pot sizes ranging from 4 – 6”, differing water and fertilizing schedules, as well as varying hours of light and darkness to promote photosynthesis. The settings were never fully optimized before funding was lost for the human feeding study. The last settings that were attempted were as follows:

- 16 hours of daylight and 8 hours of night to grow the plants, then 24 hours of daylight once plants were stripped
- Starting temperature = 23.5 °C
- Humidity = 50%
- Watering and Fertilizing Schedule = 6 days water + 1 day fertilizer

D.5: Conclusions

This project is a very viable and useful study if funding is available. Additional testing would need to be conducted in order to optimize growing conditions for the purple peppers to produce healthy foliage once they have been stripped and placed in the Plexiglas box inside the growth chamber. This is a very plausible project for another graduate student who is interested in $^{13}\text{CO}_2$ labeled phytochemicals, such as anthocyanins. Slightly more research on soil type may also be needed, but it seems that clay was the best type as it is able to draw the nutrient solution most efficient when the watering mechanism is sub-irrigation. Also, 6” pots worked best to product well branched and mature pepper plants that could sustain their leaves being stripped. Once the growing conditions are optimized the food-grade extraction protocol could easily be utilized to produce a food-grade extract that could be used in a future human feeding study.



Figure D.6: Growth chamber in Building 010A that is temperature and humidity controlled. Testing optimal growing conditions for purple peppers.

References

- (1) Brouillard, R.; Harborne, J. B. Flavonoids and Flower Colour. In *The Flavonoids, Advances in Research since 1980*; Chapman and Hall: London, 1988; p. 525.
- (2) Harborne, J. B. *Comparative Biochemistry of the Flavonoids*; Academic Press, Inc.: London, 1967; Vol. 6.
- (3) Wang, H.; Cao, G.; Prior, R. L. Oxygen Radical Absorbing Capacity of Anthocyanins. *Journal of Agricultural and Food Chemistry* **1997**, *45*, 304–309.
- (4) Weber, P. How The Vitamin Industrial Complex Swindled America. *TheWeek.com* **2013**.
- (5) Lightbourn, G. J.; Griesbach, R. J.; Novotny, J. A.; Clevidence, B. A.; Rao, D. D.; Stommel, J. R. Effects of Anthocyanin and Carotenoid Combinations on Foliage and Immature Fruit Color of *Capsicum annuum* L. *Journal of Heredity* **2008**, *99*, 105–111.
- (6) Mazza, G.; Miniati, E. *Anthocyanins in fruits, vegetables, and grains*; CRC Press, 1993.
- (7) Lohachoompol, V.; Srzednicki, G.; Craske, J. The Change of Total Anthocyanins in Blueberries and Their Antioxidant Effect After Drying and Freezing. *J Biomed Biotechnol* **2004**, *2004*, 248–252.
- (8) Sadilova, E.; Stintzing, F. C.; Carle, R. Anthocyanins, colour and antioxidant properties of eggplant (*Solanum melongena* L.) and violet pepper (*Capsicum annuum* L.) peel extracts. *Zeitschrift fur Naturforschung C-Journal of Biosciences* **2006**, *61*, 527–535.
- (9) Ichiyanagi, T.; Kashiwada, Y.; Shida, Y.; Ikeshiro, Y.; Kaneyuki, T.; Konishi, T. Nasunin from Eggplant Consists of Cis–Trans Isomers of Delphinidin 3-[4-(p-Coumaroyl)-l-rhamnosyl (1→6)glucopyranoside]-5-glucopyranoside. *Journal of Agricultural and Food Chemistry* **2005**, *53*, 9472–9477.
- (10) Ichiyanagi, T.; Terahara, N.; Rahman, M. M.; Konishi, T. Gastrointestinal Uptake of Nasunin, Acylated Anthocyanin in Eggplant. *Journal of Agricultural and Food Chemistry* **2006**, *54*, 5306–5312.
- (11) Janet A. Novotny Anthocyanin Bioavailability: Past Progress and Current Challenges. In *Emerging Trends in Dietary Components for Preventing and Combating Disease*; ACS Symposium Series; American Chemical Society, 2012; Vol. 1093, pp. 559–568.
- (12) *The Textbook of Pharmaceutical Medicine*; Griffin, J. P., Ed.; 6th ed.; Wiley-Blackwell: Hoboken, NJ, USA, 2009.
- (13) Noda, Y.; Kneyuki, T.; Igarashi, K.; Mori, A.; Packer, L. Antioxidant activity of nasunin, an anthocyanin in eggplant peels. *Toxicology* **2000**, *148*, 119–123.

- (14) Azuma, K.; Ohyama, A.; Ippoushi, K.; Ichiyanagi, T.; Takeuchi, A.; Saito, T.; Fukuoka, H. Structures and antioxidant activity of anthocyanins in many accessions of eggplant and its related species. *Journal of Agricultural and Food Chemistry* **2008**, *56*, 10154–10159.
- (15) Tanchev, S. S.; Ruskov, P. J.; Timberlake, C. F. The anthocyanins of bulgarian aubergine (*solanum melongena*). *Phytochemistry* **1970**, *9*, 1681–1682.
- (16) Tatsuzawa, F.; Ando, T.; Saito, N.; Kanaya, T.; Kokubun, H.; Tsunashima, Y.; Watanabe, H.; Hashimoto, G.; Hara, R.; Seki, H. Acylated delphinidin 3-rutinoside-5-glucosides in the flowers of *Petunia reitzii*. *Phytochemistry* **2000**, *54*, 913–917.
- (17) Miyazawa, T.; Nakagawa, K.; Kudo, M.; Muraishi, K.; Someya, K. Direct intestinal absorption of red fruit anthocyanins, cyanidin-3-glucoside and cyanidin-3,5-diglucoside, into rats and humans. *Journal of Agricultural and Food Chemistry* **1999**, *47*, 1083–1091.
- (18) Tsuda, T.; Horio, F.; Osawa, T. Absorption and metabolism of cyanidin 3-O-beta-D-glucoside in rats. *FEBS Lett.* **1999**, *449*, 179–182.
- (19) Matsumoto, H.; Inaba, H.; Kishi, M.; Tominaga, S.; Hirayama, M.; Tsuda, T. Orally administered delphinidin 3-rutinoside and cyanidin 3-rutinoside are directly absorbed in rats and humans and appear in the blood as the intact forms. *Journal of Agricultural and Food Chemistry* **2001**, *49*, 1546–1551.
- (20) Nielsen, I. L. F.; Dragsted, L. O.; Ravn-Haren, G.; Freese, R.; Rasmussen, S. E. Absorption and Excretion of Black Currant Anthocyanins in Humans and Watanabe Heritable Hyperlipidemic Rabbits. *Journal of Agricultural and Food Chemistry* **2003**, *51*, 2813–2820.
- (21) Ichiyanagi, T.; Rahman, M. M.; Kashiwada, Y.; Ikeshiro, Y.; Shida, Y.; Hatano, Y.; Matsumoto, H.; Hirayama, M.; Tsuda, T.; Konishi, T. Absorption and metabolism of delphinidin 3-O-β-d-glucopyranoside in rats. *Free Radical Biology and Medicine* **2004**, *36*, 930–937.
- (22) Ichiyanagi, T.; Shida, Y.; Rahman, M. M.; Hatano, Y.; Konishi, T. Extended Glucuronidation Is Another Major Path of Cyanidin 3-O-β-d-Glucopyranoside Metabolism in Rats. *Journal of Agricultural and Food Chemistry* **2005**, *53*, 7312–7319.
- (23) Ichiyanagi, T.; Shida, Y.; Rahman, M. M.; Hatano, Y.; Matsumoto, H.; Hirayama, M.; Konishi, T. Metabolic Pathway of Cyanidin 3-O-β-d-Glucopyranoside in Rats. *Journal of Agricultural and Food Chemistry*. **2005**, *53*, 145–150.
- (24) Wu, X.; Pittman, H. E.; Prior, R. L. Pelargonidin Is Absorbed and Metabolized Differently than Cyanidin after Marionberry Consumption in Pigs. *Journal of Nutrition* **2004**, *134*, 2603–2610.

- (25) Wu, X.; Pittman, H. E.; McKay, S.; Prior, R. L. Aglycones and Sugar Moieties Alter Anthocyanin Absorption and Metabolism after Berry Consumption in Weanling Pigs. *Journal of Nutrition* **2005**, *135*, 2417–2424.
- (26) Walton, M. C.; Lentle, R. G.; Reynolds, G. W.; Kruger, M. C.; McGhie, T. K. Anthocyanin Absorption and Antioxidant Status in Pigs. *Journal of Agricultural and Food Chemistry* **2006**, *54*, 7940–7946.
- (27) Wu, X.; Pittman, H. E.; Prior, R. L. Fate of Anthocyanins and Antioxidant Capacity in Contents of the Gastrointestinal Tract of Weanling Pigs Following Black Raspberry Consumption. *Journal of Agricultural and Food Chemistry* **2006**, *54*, 583–589.
- (28) Marczyklo, T. H.; Cooke, D.; Brown, K.; Steward, W. P.; Gescher, A. J. Pharmacokinetics and metabolism of the putative cancer chemopreventive agent cyanidin-3-glucoside in mice. *Cancer Chemotherapy and Pharmacology* **2009**, *64*, 1261–1268.
- (29) Bò, C. D.; Ciappellano, S.; Klimis-Zacas, D.; Martini, D.; Gardana, C.; Riso, P.; Porrini, M. Anthocyanin Absorption, Metabolism, and Distribution from a Wild Blueberry-Enriched Diet (*Vaccinium angustifolium*) Is Affected by Diet Duration in the Sprague–Dawley Rat. *Journal of Agricultural and Food Chemistry* **2010**, *58*, 2491–2497.
- (30) He, J.; Magnuson, B. A.; Lala, G.; Tian, Q.; Schwartz, S. J.; Giusti, M. M. Intact anthocyanins and metabolites in rat urine and plasma after 3 months of anthocyanin supplementation. *Nutrition and Cancer* **2006**, *54*, 3–12.
- (31) Milbury, P. E.; Kalt, W. Xenobiotic Metabolism and Berry Flavonoid Transport across the Blood–Brain Barrier†. *Journal of Agricultural and Food Chemistry* **2010**, *58*, 3950–3956.
- (32) Felgines, C.; Texier, O.; Besson, C.; Vitaglione, P.; Lamaison, J.-L.; Fogliano, V.; Scalbert, A.; Vanella, L.; Galvano, F. Influence of glucose on cyanidin 3-glucoside absorption in rats. *Molecular Nutrition and Food Research* **2008**, *52*, 959–964.
- (33) Borges, G.; Roowi, S.; Rouanet, J.-M.; Duthie, G. G.; Lean, M. E. J.; Crozier, A. The bioavailability of raspberry anthocyanins and ellagitannins in rats. *Molecular Nutrition and Food Research* **2007**, *51*, 714–725.
- (34) Matsumoto, H.; Ito, K.; Yonekura, K.; Tsuda, T.; Ichiyanagi, T.; Hirayama, M.; Konishi, T. Enhanced Absorption of Anthocyanins after Oral Administration of Phytic Acid in Rats and Humans. *Journal of Agricultural and Food Chemistry* **2007**, *55*, 2489–2496.
- (35) Cao, G.; Prior, R. L. Anthocyanins Are Detected in Human Plasma after Oral Administration of an Elderberry Extract. *Clinical Chemistry* **1999**, *45*, 574–576.

- (36) Talavéra, S.; Felgines, C.; Texier, O.; Besson, C.; Gil-Izquierdo, A.; Lamaison, J.-L.; Rémésy, C. Anthocyanin metabolism in rats and their distribution to digestive area, kidney, and brain. *Journal of Agricultural and Food Chemistry* **2005**, *53*, 3902–3908.
- (37) Felgines, C.; Texier, O.; Garcin, P.; Besson, C.; Lamaison, J.-L.; Scalbert, A. Tissue distribution of anthocyanins in rats fed a blackberry anthocyanin-enriched diet. *Molecular Nutrition and Food Research* **2009**, *53*, 1098–1103.
- (38) Walton, M. C.; Hendriks, W. H.; Broomfield, A. M.; McGhie, T. K. Viscous food matrix influences absorption and excretion but not metabolism of blackcurrant anthocyanins in rats. *Journal of Food Science*. **2009**, *74*, H22–29.
- (39) Lapidot, T.; Harel, S.; Granit, R.; Kanner, J. Bioavailability of Red Wine Anthocyanins As Detected in Human Urine. *Journal of Agricultural and Food Chemistry*. **1998**, *46*, 4297–4302.
- (40) Murkovic, M.; Adam, U.; Pfannhauser, W. Analysis of anthocyan glycosides in human serum. *Fresenius Journal of Analytical Chemistry* **2000**, *366*, 379–381.
- (41) Netzel, M.; Strass, G.; Janssen, M.; Bitsch, I.; Bitsch, R. Bioactive anthocyanins detected in human urine after ingestion of blackcurrant juice. *Journal of Environmental Pathology, Toxicology and Oncology* **2001**, *20*, 89–95.
- (42) Bub, A.; Watzl, B.; Heeb, D.; Rechkemmer, G.; Briviba, K. Malvidin-3-glucoside bioavailability in humans after ingestion of red wine, dealcoholized red wine and red grape juice. *European Journal of Nutrition* **2001**, *40*, 113–120.
- (43) Mülleder, U.; Murkovic, M.; Pfannhauser, W. Urinary excretion of cyanidin glycosides. *Journal of Biochemical and Biophysical Methods* **2002**, *53*, 61–66.
- (44) McGhie, T. K.; Ainge, G. D.; Barnett, L. E.; Cooney, J. M.; Jensen, D. J. Anthocyanin glycosides from berry fruit are absorbed and excreted unmetabolized by both humans and rats. *Journal of Agricultural and Food Chemistry* **2003**, *51*, 4539–4548.
- (45) Felgines, C.; Talavéra, S.; Gonthier, M.-P.; Texier, O.; Scalbert, A.; Lamaison, J.-L.; Rémésy, C. Strawberry anthocyanins are recovered in urine as glucuro- and sulfoconjugates in humans. *Journal of Nutrition*. **2003**, *133*, 1296–1301.
- (46) Felgines, C.; Talavera, S.; Texier, O.; Gil-Izquierdo, A.; Lamaison, J.-L.; Remesy, C. Blackberry anthocyanins are mainly recovered from urine as methylated and glucuronidated conjugates in humans. *Journal of Agricultural and Food Chemistry* **2005**, *53*, 7721–7727.
- (47) Frank, T.; Netzel, M.; Strass, G.; Bitsch, R.; Bitsch, I. Bioavailability of anthocyanidin-3-glucosides following consumption of red wine and red grape juice. *Canadian Journal of Physiology and Pharmacology*. **2003**, *81*, 423–435.

- (48) Kay, C. D.; Mazza, G.; Holub, B. J.; Wang, J. Anthocyanin metabolites in human urine and serum. *British Journal of Nutrition* **2004**, *91*, 933–942.
- (49) Wu, X.; Cao, G.; Prior, R. L. Absorption and metabolism of anthocyanins in elderly women after consumption of elderberry or blueberry. *Journal of Nutrition* **2002**, *132*, 1865–1871.
- (50) Mazza, G.; Kay, C. D.; Cottrell, T.; Holub, B. J. Absorption of anthocyanins from blueberries and serum antioxidant status in human subjects. *Journal of Agricultural and Food Chemistry* **2002**, *50*, 7731–7737.
- (51) Milbury, P. E.; Cao, G.; Prior, R. L.; Blumberg, J. Bioavailability of elderberry anthocyanins. *Mechanisms of Ageing and Development* **2002**, *123*, 997–1006.
- (52) Kurilich, A. C.; Clevidence, B. A.; Britz, S. J.; Simon, P. W.; Novotny, J. A. Plasma and urine responses are lower for acylated vs nonacylated anthocyanins from raw and cooked purple carrots. *Journal of Agricultural and Food Chemistry* **2005**, *53*, 6537–6542.
- (53) Carkeet, C.; Clevidence, B. A.; Novotny, J. A. Anthocyanin excretion by humans increases linearly with increasing strawberry dose. *Journal of Nutrition*. **2008**, *138*, 897–902.
- (54) Charron, C. S.; Kurilich, A. C.; Clevidence, B. A.; Simon, P. W.; Harrison, D. J.; Britz, S. J.; Baer, D. J.; Novotny, J. A. Bioavailability of Anthocyanins from Purple Carrot Juice: Effects of Acylation and Plant Matrix. *Journal of Agricultural and Food Chemistry* **2009**, *57*, 1226–1230.
- (55) Charron, C. S.; Clevidence, B. A.; Britz, S. J.; Novotny, J. A. effect of dose size on bioavailability of acylated and nonacylated anthocyanins from red cabbage (*Brassica oleracea* L. Var. capitata). *Journal of Agricultural and Food Chemistry* **2007**, *55*, 5354–5362.
- (56) Manach, C.; Williamson, G.; Morand, C.; Scalbert, A.; Rémésy, C. Bioavailability and bioefficacy of polyphenols in humans. I. Review of 97 bioavailability studies. *The American Journal of Clinical Nutrition* **2005**, *81*, 230S–242S.
- (57) Bitsch, R.; Netzel, M.; Frank, T.; Strass, G.; Bitsch, I. Bioavailability and Biokinetics of Anthocyanins From Red Grape Juice and Red Wine. *Journal of Biomedicine and Biotechnology* **2004**, *2004*, 293–298.
- (58) Cao, G.; Muccitelli, H. U.; Sánchez-Moreno, C.; Prior, R. L. Anthocyanins are absorbed in glycosylated forms in elderly women: a pharmacokinetic study. *American Journal of Clinical Nutrition* **2001**, *73*, 920–926.

- (59) Murkovic, M.; Mülleder, U.; Adam, U.; Pfannhauser, W. Detection of anthocyanins from elderberry juice in human urine. *Journal of the Science of Food and Agriculture* **2001**, *81*, 934–937.
- (60) Andersen, Ø. M. Anthocyanins. *Encyclopedia of Life Sciences* **2001**.
- (61) Bridle, P.; Timberlake, C. F. Anthocyanins as natural food colours—selected aspects. *Food Chemistry* **1997**, *58*, 103–109.
- (62) Harborne, J. B.; Grayer, R. J. The Anthocyanins. In *The Flavonoids, Advances in Research since 1980*; Harborne, J. B., Ed.; Chapman & Hall: London, 1988; p. 621.
- (63) Timberlake, C. F. Anthocyanins--Occurrence, extraction and chemistry. *Food Chemistry* **1980**, *5*, 69–80.
- (64) Brouillard, R. The in vivo expression of anthocyanin colour in plants. *Phytochemistry* **1983**, *22*, 1311–1323.
- (65) Brouillard, R.; Delaporte, B. Chemistry of anthocyanin pigments. 2. Kinetic and thermodynamic study of proton transfer, hydration, and tautomeric reactions of malvidin 3-glucoside. *Journal of the American Chemical Society* **1977**, *99*, 8461–8468.
- (66) Brouillard, R.; Delaporte, B.; Lazlo, P. Protons and ions involved in fast dynamic phenomena. *Elsevier Amsterdam* **1978**.
- (67) Brouillard, R.; Dubois, J. E. Mechanism of the structural transformations of anthocyanins in acidic media. *Journal of the American Chemical Society* **1977**, *99*, 1359–1364.
- (68) Brouillard, R. Chemical Structures of Anthocyanins. In *Anthocyanins as Food Colors*; Markakis, P., Ed.; Academic Press New York, 1982.
- (69) Robinson, G. M.; Robinson, R. A survey of anthocyanins. II. *Biochemical Journal* **1932**, *26*, 1647–1664.
- (70) Osawa, Y. Copigmentation of Anthocyanins. In *Anthocyanins as Food Colors*; Markakis, P., Ed.; Academic press New York, 1982.
- (71) Brouillard, R. Origin of the Exceptional Colour Stability of the Zebrina Anthocyanin. *Phytochemistry* **1981**, *20*, 143–145.
- (72) Asen, S.; Stewart, R. N.; Norris, K. H. Co-pigmentation of Anthocyanins in Plant Tissues and its Effect on Color. *Phytochemistry* **1972**, *11*, 1139–1144.
- (73) Asen, S.; Jurd, L. The constitution of a crystalline blue cornflower pigment. *Phytochemistry* **1967**, *6*, 577–584.

- (74) Wrolstad, R. E. Anthocyanin Pigments—Bioactivity and Coloring Properties. *Journal of Food Science* **2004**, *69*, C419–C425.
- (75) Sweeny, J. G.; Wilkinson, M. M.; Iacobucci, G. A. Effect of flavonoid sulfonates on the photobleaching of anthocyanins in acid solution. *Journal of Agricultural and Food Chemistry* **1981**, *29*, 563–567.
- (76) Goto, T.; Hoshino, T.; Takase, S. A proposed structure of commelinin, a sky-blue anthocyanin complex obtained from the flower petals of. *Tetrahedron Letters* **1979**, *20*, 2905–2908.
- (77) Asen, S.; Stewart, R. N.; Norris, K. H.; Massie, D. R. A stable blue non-metallic co-pigment complex of delphinin and C-glycosylflavones in Prof. Blaauw Iris. *Phytochemistry* **1970**, *9*, 619–627.
- (78) Mazza, G.; Brouillard, R. Recent developments in the stabilization of anthocyanins in food products. *Food Chemistry* **1987**, *25*, 207–225.
- (79) Suda, I.; Oki, T.; Masuda, M.; Nishiba, Y.; Furuta, S.; Matsugano, K.; Sugita, K.; Terahara, N. Direct Absorption of Acylated Anthocyanin in Purple-Fleshed Sweet Potato into Rats. *Journal of Agricultural and Food Chemistry* **2002**, *50*, 1672–1676.
- (80) Ichianagi, T.; Shida, Y.; Rahman, M. M.; Hatano, Y.; Konishi, T. Bioavailability and Tissue Distribution of Anthocyanins in Bilberry (*Vaccinium myrtillus* L.) Extract in Rats. *Journal of Agricultural and Food Chemistry* **2006**, *54*, 6578–6587.
- (81) Hayashi, K. The Anthocyanins. In *The Chemistry of Flavonoid Compounds*; Geissman, T. A., Ed.; Pergamon Press: New York, 1962.
- (82) Kong, J.-M.; Chia, L.-S.; Goh, N.-K.; Chia, T.-F.; Brouillard, R. Analysis and biological activities of anthocyanins. *Phytochemistry* **2003**, *64*, 923–933.
- (83) Delgado-Vargas, F.; Paredes-López, O. *Natural Colorants for Food and Nutraceutical Uses*; CRC, 2003.
- (84) Strack, D.; Wray, V. The Anthocyanins. In *The Flavonoids: Advances in Research Since 1986*; Harborne, J. B., Ed.; Chapman & Hall: London, 1994; p. 676.
- (85) Timberlake, C. F. Anthocyanins in Fruits and Vegetables. In *Recent Advances in the Biochemistry of Fruit and Vegetables*; Biale, J. B.; Young, R. E.; Friend, J.; Rhodes, M. J. C., Eds.; Academic Press London: New York, 1981.
- (86) Wu, X.; Prior, R. L. Systematic Identification and Characterization of Anthocyanins by HPLC-ESI-MS/MS in Common Foods in the United States: Fruits and Berries. *Journal of Agricultural and Food Chemistry* **2005**, *53*, 2589–2599.

- (87) Clifford, M. N. Anthocyanins - Nature, Occurrence and Dietary Burden. *Journal of the Science of Food and Agriculture* **2000**, *80*, 1063–1072.
- (88) Kähkönen, M. P.; Heinonen, M. Antioxidant activity of anthocyanins and their aglycons. *Journal of Agricultural and Food Chemistry* **2003**, *51*, 628–633.
- (89) Tsuda, T.; Horio, F.; Uchida, K.; Aoki, H.; Osawa, T. Dietary Cyanidin 3-O- β -D-Glucoside-Rich Purple Corn Color Prevents Obesity and Ameliorates Hyperglycemia in Mice. *Journal of Nutrition*. **2003**, *133*, 2125–2130.
- (90) Rossi, A.; Serraino, I.; Dugo, P.; Paola, R. D.; Mondello, L.; Genovese, T.; Morabito, D.; Dugo, G.; Sautebin, L.; Caputi, A. P.; others Protective effects of anthocyanins from blackberry in a rat model of acute lung inflammation. *Free radical research* **2003**, *37*, 891–900.
- (91) Cho, J.; Kang, J. S.; Long, P. H.; Jing, J.; Back, Y.; Chung, K. S. Antioxidant and memory enhancing effects of purple sweet potato anthocyanin and cordyceps mushroom extract. *Archives of pharmacal research* **2003**, *26*, 821–825.
- (92) Galvano, F.; La Fauci, L.; Lazzarino, G.; Fogliano, V.; Ritieni, A.; Ciappellano, S.; Battistini, N. C.; Tavazzi, B.; Galvano, G. Cyanidins: metabolism and biological properties. *The Journal of Nutritional Biochemistry* **2004**, *15*, 2–11.
- (93) Marko, D.; Puppel, N.; Tjaden, Z.; Jakobs, S.; Pahlke, G. The substitution pattern of anthocyanidins affects different cellular signaling cascades regulating cell proliferation. *Molecular nutrition & food research* **2004**, *48*, 318–325.
- (94) Bors, W.; Heller, W.; Michel, C.; Saran, M. Flavonoids as antioxidants: determination of radical-scavenging efficiencies. *Methods in enzymology* **1990**, *186*, 343.
- (95) Kandaswami, C.; Middleton Jr, E. Free radical scavenging and antioxidant activity of plant flavonoids. *Advances in experimental medicine and biology (USA)* **1994**.
- (96) Zheng, W.; Wang, S. Y. Oxygen Radical Absorbing Capacity of Phenolics in Blueberries, Cranberries, Chokeberries, and Lingonberries. *Journal of Agricultural and Food Chemistry* **2003**, *51*, 502–509.
- (97) Cao, G.; Sofic, E.; Prior, R. L. Antioxidant and prooxidant behavior of flavonoids: structure-activity relationships. *Free Radical Biology and Medicine* **1997**, *22*, 749–760.
- (98) Rice-Evans, C. A.; Miller, N. J.; Paganga, G. Structure-antioxidant activity relationships of flavonoids and phenolic acids. *Free radical biology and medicine* **1996**, *20*, 933–956.
- (99) Politzer, M. Experiences in the medical treatment of progressive myopia (author's transl). *Klinische Monatsbl AItter f Ažr Augenheilkunde* **1977**, *171*, 616.

- (100) Timberlake, C. F.; Henry, B. S. Anthocyanins as Natural Food Colorants. *Progress in Clinical and Biological Research* **1988**, *280*, 107.
- (101) Nakaishi, H.; Matsumoto, H.; Tominaga, S.; Hirayama, M. Effects of black currant anthocyanoside intake on dark adaptation and VDT work-induced transient refractive alteration in healthy humans. *Alternative Medicine Review* **2000**, *5*, 553–562.
- (102) Canter, P. H.; Ernst, E. Anthocyanosides of *Vaccinium myrtillus* (Bilberry) for Night Vision—A Systematic Review of Placebo-Controlled Trials* 1. *Survey of ophthalmology* **2004**, *49*, 38–50.
- (103) Casto, B. C.; Kresty, L. A.; Kraly, C. L.; Pearl, D. K.; Knobloch, T. J.; Schut, H. A.; Stoner, G. D.; Mallery, S. R.; Weghorst, C. M. Chemoprevention of oral cancer by black raspberries. *Anticancer research* **2002**, *22*, 4005–4015.
- (104) Harris, G. K.; Gupta, A.; Nines, R. G.; Kresty, L. A.; Habib, S. G.; Frankel, W. L.; LaPerle, K.; Gallaher, D. D.; Schwartz, S. J.; Stoner, G. D. Effects of lyophilized black raspberries on azoxymethane-induced colon cancer and 8-hydroxy-2'-deoxyguanosine levels in the Fischer 344 rat. *Nutrition and cancer* **2001**, *40*, 125–133.
- (105) Huang, C.; Huang, Y.; Li, J.; Hu, W.; Aziz, R.; Tang, M.; Sun, N.; Cassady, J.; Stoner, G. D. Inhibition of benzo (a) pyrene diol-epoxide-induced transactivation of activated protein 1 and nuclear factor kappaB by black raspberry extracts. *Cancer research* **2002**, *62*, 6857.
- (106) Kresty, L. A.; Morse, M. A.; Morgan, C.; Carlton, P. S.; Lu, J.; Gupta, A.; Blackwood, M.; Stoner, G. D. Chemoprevention of esophageal tumorigenesis by dietary administration of lyophilized black raspberries. *Cancer research* **2001**, *61*, 6112.
- (107) Liu, Z.; Schwimer, J.; Liu, D.; Greenway, F. L.; Anthony, C. T.; Woltering, E. A. Black raspberry extract and fractions contain angiogenesis inhibitors. *Journal of Agricultural and Food Chemistry* **2005**, *53*, 3909–3915.
- (108) Breinholt, V. M.; Nielsen, S. E.; Knuthsen, P.; Lauridsen, S. T.; Daneshvar, B.; Sorensen, A. Effects of Commonly Consumed Fruit Juices and Carbohydrates on Redox Status and Anticancer Biomarkers in Female Rats. *Nutrition and cancer* **2003**, *45*, 46–52.
- (109) Olsson, M. E.; Gustavsson, K. E.; Andersson, S.; Nilsson, A.; Duan, R. D. Inhibition of cancer cell proliferation in vitro by fruit and berry extracts and correlations with antioxidant levels. *Journal of Agricultural and Food Chemistry* **2004**, *52*, 7264–7271.
- (110) Malik, M.; Zhao, C.; Schoene, N.; Guisti, M. M.; Moyer, M. P.; Magnuson, B. A. Anthocyanin-rich extract from *Aronia melanocarpa* E. induces a cell cycle block in colon cancer but not normal colonic cells. *Nutrition and Cancer* **2003**, *46*, 186–196.

- (111) Zhao, C.; Giusti, M. M.; Malik, M.; Moyer, M. P.; Magnuson, B. A. Effects of commercial anthocyanin-rich extracts on colonic cancer and nontumorigenic colonic cell growth. *Journal of Agricultural and Food Chemistry* **2004**, *52*, 6122–6128.
- (112) Boniface, R.; Robert, A. M. Effect of anthocyanins on human connective tissue metabolism in the human. *Klin Monbl Augenheilkd* **1996**, *209*, 368–372.
- (113) Scharrer, A.; Ober, M. Anthocyanosides in the treatment of retinopathies. *Klin Monbl Augenheilkd* **1981**, *178*, 386–389.
- (114) Wang, C. J.; Wang, J. M.; Lin, W. L.; Chu, C. Y.; Chou, F. P.; Tseng, T. H. Protective effect of Hibiscus anthocyanins against tert-butyl hydroperoxide-induced hepatic toxicity in rats. *Food and Chemical Toxicology* **2000**, *38*, 411–416.
- (115) Ghiselli, A.; Nardini, M.; Baldi, A.; Scaccini, C. Antioxidant activity of different phenolic fractions separated from an Italian red wine. *Journal of Agricultural and Food Chemistry* **1998**, *46*, 361–367.
- (116) Robert, A. M.; Godeau, G.; Moati, F.; Miskulin, M. Action of anthocyanosides of *Vaccinium myrtillus* on the permeability of the blood brain barrier. *Journal of Medicine* **1977**, *8*, 321.
- (117) Detre, Z.; Jellinek, H.; Miskulin, M.; Robert, A. M. Studies on vascular permeability in hypertension: action of anthocyanosides. *Clinical physiology and biochemistry* **1986**, *4*, 143.
- (118) Akhmadieva, A. K.; Zaichkina, S. I.; Ruzieva, R. K.; Ganassi, E. E. The protective action of a natural preparation of anthocyan (pelargonidin-3, 5-diglucoside). *Radiobiologiya* **33**, 433.
- (119) Minkova, M.; Drenska, D.; Pantev, T.; Ovcharov, R. Antiradiation properties of alpha tocopherol, anthocyanins, and pyracetam administered combined as a pretreatment course. *Acta physiologica et pharmacologica Bulgarica* **1990**, *16*, 31.
- (120) Lazze, M. C.; Pizzala, R.; Savio, M.; Stivala, L. A.; Prosperi, E.; Bianchi, L. Anthocyanins protect against DNA damage induced by tert-butyl-hydroperoxide in rat smooth muscle and hepatoma cells. *Mutation Research/Genetic Toxicology and Environmental Mutagenesis* **2003**, *535*, 103–115.
- (121) Mitcheva, M.; Astroug, H.; Drenska, D.; Popov, A.; Kassarova, M. Biochemical and morphological studies on the effects of anthocyanins and vitamin E on carbon tetrachloride induced liver injury. *Cellular and molecular biology* **1993**, *39*, 443–448.
- (122) Obi, F. O.; Usenu, I. A.; Osayande, J. O. Prevention of carbon tetrachloride-induced hepatotoxicity in the rat by *H. rosasinensis* anthocyanin extract administered in ethanol. *Toxicology* **1998**, *131*, 93–98.

- (123) Karaivanova, M.; Drenska, D.; Ovcharov, R. A modification of the toxic effects of platinum complexes with antocyanins. *Eksperimentalna meditsina i morfologija* **1990**, *29*, 19.
- (124) Knox, Y. M.; Suzutani, T.; Yosida, I.; Azuma, M. Anti-influenza virus activity of crude extract of *Ribes nigrum* L. *Phytotherapy Research* **2003**, *17*, 120–122.
- (125) Zakay-Rones, Z.; Varsano, N.; Zlotnik, M.; Manor, O.; Regev, L.; Schlesinger, M.; Mumcuoglu, M. Inhibition of several strains of influenza virus in vitro and reduction of symptoms by an elderberry extract (*Sambucus nigra* L.) during an outbreak of influenza B Panama. *The Journal of Alternative and Complementary Medicine* **1995**, *1*, 361–369.
- (126) Zakay-Rones, Z.; Thom, E.; Wollan, T.; Wadstein, J. Randomized study of the efficacy and safety of oral elderberry extract in the treatment of influenza A and B virus infections. *The Journal of International Medical Research* **2004**, *32*, 132–140.
- (127) Lietti, A.; Cristoni, A.; Picci, M. Studies on *Vaccinium myrtillus* anthocyanosides. I. Vasoprotective and antiinflammatory activity. *Arzneimittel-Forschung* **1976**, *26*, 829.
- (128) Barak, V.; Halperin, T.; Kalickman, I. The effect of Sambucol, a black elderberry-based, natural product, on the production of human cytokines: I. Inflammatory cytokines. *Europena Cytokine Network* **2001**, *12*, 290–6.
- (129) Meiers, S.; Kemény, M.; Weyand, U.; Gastpar, R.; Von Angerer, E.; Marko, D. The anthocyanidins cyanidin and delphinidin are potent inhibitors of the epidermal growth-factor receptor. *Journal of Agricultural and Food Chemistry* **2001**, *49*, 958–962.
- (130) Sarma, A. D.; Sreelakshmi, Y.; Sharma, R. Antioxidant ability of anthocyanins against ascorbic acid oxidation. *Phytochemistry* **1997**, *45*, 671–674.
- (131) Eddy, B. P.; Mapson, L. W. Some Factors Affecting Anthocyanin Synthesis in Cress Seedlings. *Biochemical Journal* **1951**, *49*, 694–699.
- (132) Kuroda, C.; Wada, M. Coloring matter of eggplant (nasu). In *Proc. Imp. Acad.(Tokyo)*; 1933; Vol. 9, p. 51.
- (133) Kuroda, C.; Wada, M. The colouring matter of eggplant (Nasu). Part II. In *Proc. Imp. Acad.(Japan)*; 1935; Vol. 11, pp. 235–237.
- (134) Noda, Y.; Kaneyuki, T.; Igarashi, K.; Mori, A.; Packer, L. Antioxidant activity of nasunin, an anthocyanin in eggplant. *Research Communication in Molecular Pathology and Pharmacology* **1998**, *102*, 175–187.
- (135) Igarashi, K.; Yoshida, T.; Suzuki, E. Antioxidative activity of nasunin in Chouja-nasu (Little eggplant, *Solanum melongena* L. “Chouja”). *Journal of the Japanese Society for Food Science and Technology (Japan)* **1993**.

- (136) Kayamori, F.; Igarashi, K. Effects of dietary nasunin on the serum cholesterol level in rats. *Bioscience, Biotechnology, and Biochemistry (Japan)* **1994**.
- (137) Kuroda, C.; Wada, M. The Constitution of Natural Colouring Matters, Kuromamin, Shisonin, and Nasunin. *Bull. Chem. Soc. Jpn.* **1936**, *11*, 272–287.
- (138) Matsubara, K.; Kaneyuki, T.; Miyake, T.; Mori, M. Antiangiogenic Activity of Nasunin, an Antioxidant Anthocyanin, in Eggplant Peels. *Journal of Agricultural and Food Chemistry* **2005**, *53*, 6272–6275.
- (139) Asen, S.; Budin, P. S. Cyanidin 3-arabinoside-5-glucoside, an anthocyanin with a new glycosidic pattern, from flowers of. *Phytochemistry* **1966**, *5*, 1257–1261.
- (140) Griesbach, R. J.; Asen, S.; Leonnarat, B. A. *Petunia hybrida* anthocyanins acylated with caffeic acid. *Phytochemistry* **1991**, *30*, 1729–1731.
- (141) BlueRibbonReg.JPG (JPEG Image, 614 × 461 pixels) - Scaled (62%). *American Lillies*.
- (142) Sakamura, S.; Obata, Y. Anthocyanase and anthocyanins in eggplant, *Solanum melongena* L. Part II. Isolation and identification of chlorogenic acid and related compounds from eggplant. *Agric Biol Chem* **1963**, *27*, 121–127.
- (143) Watanabe, S., S. Sakamura, and Y. Obata; Structure of acylated anthocyanins in eggplant and perilla; and the position of acylation. *Agricultural and Biological Chemistry (Tokyo)* **1966**, *30*, 420–422.
- (144) Piovan, A.; Filippini, R.; Favretto, D. Characterization of the anthocyanins of *Catharanthus roseus* (L.) G. Don in vivo and in vitro by electrospray ionization ion trap mass spectrometry. *Rapid Communications in Mass Spectrometry* **1998**, *12*, 361–367.
- (145) Giusti, M. M.; Rodriguez-Saona, L. E.; Griffin, D.; Wrolstad, R. E. Electrospray and Tandem Mass Spectroscopy As Tools for Anthocyanin Characterization. *Journal of Agricultural and Food Chemistry* **1999**, *47*, 4657–4664.
- (146) Wu, X.; Prior, R. L. Identification and Characterization of Anthocyanins by High-Performance Liquid Chromatography–Electrospray Ionization–Tandem Mass Spectrometry in Common Foods in the United States: Vegetables, Nuts, and Grains. *Journal of Agricultural and Food Chemistry* **2005**, *53*, 3101–3113.
- (147) Alcalde-Eon, C.; Saavedra, G.; De Pascual-Teresa, S.; Rivas-Gonzalo, J. C. Identification of anthocyanins of pinta boca (*Solanum stenotomum*) tubers. *Food Chemistry* **2004**, *86*, 441–448.

- (148) Choung, M.-G.; Baek, I.-Y.; Kang, S.-T.; Han, W.-Y.; Shin, D.-C.; Moon, H.-P.; Kang, K.-H. Isolation and Determination of Anthocyanins in Seed Coats of Black Soybean (*Glycine max* (L.) Merr.). *Journal of Agricultural and Food Chemistry* **2001**, *49*, 5848–5851.
- (149) Wu, X.; Gu, L.; Prior, R. L.; McKay, S. Characterization of Anthocyanins and Proanthocyanidins in Some Cultivars of Ribes, Aronia, and Sambucus and Their Antioxidant Capacity. *Journal of Agricultural and Food Chemistry* **2004**, *52*, 7846–7856.
- (150) Takeoka, G. R.; Dao, L. T.; Wong, R. Y.; Harden, L. A.; Edwards, R. H.; Berrios, J. D. . Characterization of black bean (*Phaseolus vulgaris* L.) anthocyanins. *Journal of Agricultural and Food Chemistry* **1997**, *45*, 3395–3400.
- (151) Zhang, Z.; Kou, X.; Fugal, K.; McLaughlin, J. Comparison of HPLC Methods for Determination of Anthocyanins and Anthocyanidins in Bilberry Extracts. *Journal of Agricultural and Food Chemistry* **2004**, *52*, 688–691.
- (152) Garcia-Viguera, C.; Zafrilla, P.; Tomás-Barberán, F. A. The use of acetone as an extraction solvent for anthocyanins from strawberry fruit. *Phytochemical Analysis* **1998**, *9*, 274–277.
- (153) Revilla, E.; Ryan, J.-M.; Martin-Ortega, G. Comparison of Several Procedures Used for the Extraction of Anthocyanins from Red Grapes. *Journal of Agricultural and Food Chemistry* **1998**, *46*, 4592–4597.
- (154) Ichiyanagi, T.; Kashiwada, Y.; Ikeshiro, Y.; Hatano, Y.; Shida, Y.; Horie, M.; Matsugo, S.; Konishi, T. Complete assignment of bilberry (*Vaccinium myrtillus* L.) anthocyanins separated by capillary zone electrophoresis. *Chemical & Pharmaceutical Bulletin* **2004**, *52*, 226–229.
- (155) Ando, T.; Saito, N.; Tatsuzawa, F.; Kakefuda, T.; Yamakage, K.; Ohtani, E.; Koshi-ishi, M.; Matsusake, Y.; Kokubun, H.; Watanabe, H.; Tsukamoto, T.; Ueda, Y.; Hashimoto, G.; Marchesi, E.; Asakura, K.; Hara, R.; Seki, H. Floral anthocyanins in wild taxa of *Petunia* (Solanaceae). *Biochemical Systematics and Ecology* **1999**, *27*, 623–650.
- (156) Slimestad, R.; Solheim, H. Anthocyanins from Black Currants (*Ribes nigrum* L.). *Journal of Agricultural and Food Chemistry* **2002**, *50*, 3228–3231.
- (157) Jing, P.; Giusti, M. M. Effects of Extraction Conditions on Improving the Yield and Quality of an Anthocyanin-Rich Purple Corn (*Zea mays* L.) Color Extract. *Journal of Food Science* **2007**, *72*, C363–C368.
- (158) *Food colours*; Emerton, V., Ed.; John Wiley & Sons, 2008.
- (159) Francis, F. J. Analysis of Anthocyanins. In *Anthocyanins as Food Colors*; Markakis, P., Ed.; Academic Press New York, 1982.

- (160) Kuskoski, E. M.; Vega, J. M.; Rios, J. J.; Fett, R.; Troncoso, A. M.; Asuero, A. G. Characterization of Anthocyanins from the Fruits of Bagaçu (Eugenia umbelliflora Berg). *Journal of Agricultural and Food Chemistry* **2003**, *51*, 5450–5454.
- (161) Cooke, D. N.; Thomasset, S.; Boocock, D. J.; Schwarz, M.; Winterhalter, P.; Steward, W. P.; Gescher, A. J.; Marczylo, T. H. Development of Analyses by High-Performance Liquid Chromatography and Liquid Chromatography/Tandem Mass Spectrometry of Bilberry (*Vaccinium myrtillus*) Anthocyanins in Human Plasma and Urine. *Journal of Agricultural and Food Chemistry* **2006**, *54*, 7009–7013.
- (162) Hong, V.; Wrolstad, R. E. Characterization of anthocyanin-containing colorants and fruit juices by HPLC/photodiode array detection. *Journal of Agricultural and Food Chemistry* **1990**, *38*, 698–708.
- (163) Hong, V.; Wrolstad, R. E. Use of HPLC separation/photodiode array detection for characterization of anthocyanins. *Journal of Agricultural and Food Chemistry* **1990**, *38*, 708–715.
- (164) Chandra, A.; Rana, J.; Li, Y. Separation, Identification, Quantification, and Method Validation of Anthocyanins in Botanical Supplement Raw Materials by HPLC and HPLC- MS. *Journal of Agricultural and Food Chemistry* **2001**, *49*, 3515–3521.
- (165) Ichiyanagi, T.; OIKAWA, K.; TATEYAMA, C.; KONISHI, T. Acid mediated hydrolysis of blueberry anthocyanins. *Chemical & pharmaceutical bulletin* **2001**, *49*, 114–117.
- (166) Wilkinson, M.; Sweeny, J. G.; Iacobucci, G. A. High-pressure liquid chromatography of anthocyanidins. *Journal of Chromatography A* **1977**, *132*, 349–351.
- (167) Tokuşođlu, \Ö; \Ünal, M. K.; Yıldırım, Z. HPLC–UV and GC–MS Characterization of the Flavonol Aglycons Quercetin, Kaempferol, and Myricetin in Tomato Pastes and Other Tomato-Based Products. *Acta Chromatographica* **2003**, *13*, 196–207.
- (168) Wolfender, J. L.; Ndjoko, K.; Hostettmann, K. Liquid chromatography with ultraviolet absorbance-mass spectrometric detection and with nuclear magnetic resonance spectrometry: a powerful combination for the on-line structural investigation of plant metabolites. *Journal of Chromatography A* **2003**, *1000*, 437–455.
- (169) Justesen, U.; Knuthsen, P.; Leth, T. Quantitative analysis of flavonols, flavones, and flavanones in fruits, vegetables and beverages by high-performance liquid chromatography with photo-diode array and mass spectrometric detection. *Journal of Chromatography A* **1998**, *799*, 101–110.
- (170) Nyman, N. A.; Kumpulainen, J. T. Determination of anthocyanidins in berries and red wine by high-performance liquid chromatography. *Journal of Agricultural and Food Chemistry* **2001**, *49*, 4183–4187.

- (171) De Pascual-Teresa, S.; Santos-Buelga, C.; Rivas-Gonzalo, J. C. LC–MS analysis of anthocyanins from purple corn cob. *Journal of the Science of Food and Agriculture* **2002**, *82*, 1003–1006.
- (172) Schauer, N.; Steinhauser, D.; Strelkov, S.; Schomburg, D.; Allison, G.; Moritz, T.; Lundgren, K.; Roessner-Tunali, U.; Forbes, M. G.; Willmitzer, L.; others GC-MS libraries for the rapid identification of metabolites in complex biological samples. *FEBS letters* **2005**, *579*, 1332–1337.
- (173) Braddock, R. J.; Bryan, C. R. Extraction parameters and capillary electrophoresis analysis of limonin glucoside and phlorin in citrus byproducts. *Journal of Agricultural and Food Chemistry* **2001**, *49*, 5982–5988.
- (174) Prior, R. L.; Lazarus, S. A.; Cao, G.; Muccitelli, H.; Hammerstone, J. F. Identification of procyanidins and anthocyanins in blueberries and cranberries (*Vaccinium* spp.) using high-performance liquid chromatography/mass spectrometry. *Journal of Agricultural and Food Chemistry* **2001**, *49*, 1270–1276.
- (175) Exarchou, V.; Godejohann, M.; Van Beek, T. A.; Gerothanassis, I. P.; Vervoort, J. LC-UV-Solid-Phase Extraction-NMR-MS Combined with a Cryogenic Flow Probe and Its Application to the Identification of Compounds Present in Greek Oregano. *Analytical Chemistry* **2003**, *75*, 6288–6294.
- (176) Favretto, D.; Flamini, R. Application of Electrospray Ionization Mass Spectrometry to the Study of Grape Anthocyanins. *American Journal of Enology and Viticulture* **2000**, *51*, 55–64.
- (177) Lin, L.; Harnly, J. LC-MS Profiling and Quantification of Food Phenolic Components Using a Standard Analytical Approach for All Plants. In *Food Science and Technology: New Research*; Greco, L. V.; Bruno, M. N., Eds.; 2008; pp. 1–103.
- (178) Lin, L. Z.; Chen, P.; Harnly, J. M. New phenolic components and chromatographic profiles of green and fermented teas. *Journal of Agricultural and Food Chemistry* **2008**, *56*, 8130–8140.
- (179) Lin, L. Z.; Chen, P.; Ozcan, M.; Harnly, J. M. Chromatographic Profiles and Identification of New Phenolic Components of *Ginkgo biloba* Leaves and Selected Products. *Journal of Agricultural and Food Chemistry* **2008**, *56*, 6671–6679.
- (180) Lin, L. Z.; Harnly, J. M. A screening method for the identification of glycosylated flavonoids and other phenolic compounds using a standard analytical approach for all plant materials. *Journal of Agricultural and Food Chemistry* **2007**, *55*, 1084–1096.
- (181) Lin, L. Z.; Harnly, J. M. Phenolic compounds and chromatographic profiles of pear skins (*Pyrus* spp.). *Journal of Agricultural and Food Chemistry* **2008**, *56*, 9094–9101.

- (182) Lin, L. Z.; Harnly, J. M. Identification of hydroxycinnamoylquinic acids of arnica flowers and burdock roots using a standardized LC-DAD-ESI/MS profiling method. *Journal of Agricultural and Food Chemistry* **2008**, *56*, 10105–10114.
- (183) Lin, L. Z.; Harnly, J. M. Identification of the phenolic components of collard greens, kale, and Chinese broccoli. *Journal of Agricultural and Food Chemistry* **2009**, *57*, 7401–7408.
- (184) Lin, L. Z.; Harnly, J. M. Phenolic component profiles of mustard greens, yu choy, and 15 other Brassica vegetables. *Journal of Agricultural and Food Chemistry* **2010**, *58*, 6850–6857.
- (185) Lin, L. Z.; Harnly, J. M. Identification of the phenolic components of chrysanthemum flower (*Chrysanthemum morifolium* Ramat). *Food chemistry* **2010**, *120*, 319–326.
- (186) Lin, L. Z.; Harnly, J. M.; Pastor-Corrales, M. S.; Luthria, D. L. The polyphenolic profiles of common bean (*Phaseolus vulgaris* L.). *Food Chemistry* **2008**, *107*, 399–410.
- (187) Lin, L. Z.; Lu, S.; Harnly, J. M. Detection and quantification of glycosylated flavonoid malonates in celery, Chinese celery, and celery seed by LC-DAD-ESI/MS. *Journal of Agricultural and Food Chemistry* **2007**, *55*, 1321–1326.
- (188) Lin, L. Z.; Mukhopadhyay, S.; Robbins, R. J.; Harnly, J. M. Identification and quantification of flavonoids of Mexican oregano (*Lippia graveolens*) by LC-DAD-ESI/MS analysis. *Journal of Food Composition and Analysis* **2007**, *20*, 361–369.
- (189) Lin, L.-Z.; Harnly, J. M. Quantitation of Flavanols, Proanthocyanidins, Isoflavones, Flavanones, Dihydrochalcones, Stilbenes, Benzoic Acid Derivatives Using Ultraviolet Absorbance after Identification by Liquid Chromatography–Mass Spectrometry. *Journal of Agricultural and Food Chemistry* **2012**, *60*, 5832–5840.
- (190) Lin, L.-Z.; Sun, J.; Chen, P.; Harnly, J. A. LC-PDA-ESI/MSⁿ Identification of New Anthocyanins in Purple Bordeaux Radish (*Raphanus sativus* L. Variety). *Journal of Agricultural and Food Chemistry*. **2011**, *59*, 6616–6627.
- (191) Giusti, M. M.; Ghanadan, H.; Wrolstad, R. E. Elucidation of the Structure and Conformation of Red Radish (*Raphanus sativus*) Anthocyanins Using One- and Two-Dimensional Nuclear Magnetic Resonance Techniques. *Journal of Agricultural and Food Chemistry* **1998**, *46*, 4858–4863.
- (192) Segura-Carretero, A.; Puertas-Mejía, M. A.; Cortacero-Ramírez, S.; Beltrán, R.; Alonso-Villaverde, C.; Joven, J.; Dinelli, G.; Fernández-Gutiérrez, A. Selective extraction, separation, and identification of anthocyanins from *Hibiscus sabdariffa* L. using solid phase extraction-capillary electrophoresis-mass spectrometry (time-of-flight /ion trap). *Electrophoresis* **2008**, *29*, 2852–2861.

- (193) Timberlake, C. F.; Bridle, P. The anthocyanins of apples and pears: the occurrence of acyl derivatives. *Journal of the Science of Food and Agriculture* **1971**, *22*, 509–513.
- (194) Timberlake, C. F.; Bridle, P. The Anthocyanins. In *The Flavonoids*; Harborne, J. B.; Mabry, T. J.; Mabry, H., Eds.; Chapman & Hall, London, 1975.
- (195) Wu, X.; Beecher, G. R.; Holden, J. M.; Haytowitz, D. B.; Gebhardt, S. E.; Prior, R. L. Concentrations of Anthocyanins in Common Foods in the United States and Estimation of Normal Consumption. *Journal of Agricultural and Food Chemistry* **2006**, *54*, 4069–4075.
- (196) Wu, X.; Prior, R. L. Systematic identification and characterization of anthocyanins by HPLC-ESI-MS/MS in common foods in the United States: fruits and berries. *Journal of Agricultural and Food Chemistry* **2005**, *53*, 2589–2599.
- (197) U.S. Food and Drug Administration; Nutrition, C. for F. S. and A. GRAS Substances (SCOGS) Database - Alphabetical List of SCOGS Substances.
- (198) Markakis, P. Stability of Anthocyanins in Foods. In *Anthocyanins as Food Colors*; Markakis, P., Ed.; Academic Press New York, 1982.
- (199) Wikipedia contributors Azeotrope (data). *Wikipedia, the free encyclopedia* **2012**.
- (200) Skoog, D. A.; Holler, F. J.; Crouch, S. R. Chapter 28: Liquid Chromatography. In *Principles of Instrumental Analysis*; Thomson Brooks/Cole, 2007.
- (201) Separation of chlorophyll a, chlorophyll b, and beta carotene by paper chromatography - Research Papers - Darinaasupina. *StudyMode*.
- (202) Anouar, E. H.; Gierschner, J.; Duroux, J.-L.; Trouillas, P. UV/Visible spectra of natural polyphenols: A time-dependent density functional theory study. *Food Chemistry* **2012**, *131*, 79–89.
- (203) ChromaDex - Reference Standards. *ChromaDex*.
- (204) Giusti, M. M.; Wrolstad, R. E. Characterization and measurement of anthocyanins by UV-visible spectroscopy. In *Handbook of Food Analytical Chemistry, Pigments, Colorants, Flavors, Texture, and Bioactive Food Components*; Wrolstad, R. E.; Acree, T. E.; Decker, E. A.; Penner, M. H.; Reid, D. S.; Schwartz, S. J.; Shoemaker, C. F.; Smith, D.; Sporns, P., Eds.; John Wiley & Sons: Hoboken, NJ, USA; pp. 19–31.
- (205) Sadilova, E.; Stintzing, F. C.; Carle, R. Anthocyanins, colour and antioxidant properties of eggplant (*Solanum melongena* L.) and violet pepper (*Capsicum annum* L.) peel extracts. *Zeitschrift für Naturforschung C-Journal of Biosciences* **2006**, *61*, 527–535.
- (206) Waters 2695 Separation Module, Operator's Guide, 71500269502, Revision B **2001**.

- (207) Barker, J. *Mass Spectrometry: Analytical Chemistry by Open Learning*; Ando, D. J., Ed.; Second.; John Wiley & Sons, 1999.
- (208) University of Dundee, College of Life Sciences Electrospray Ionisation **2010**.
- (209) Goiffon, J. P.; Brun, M.; Bourrier, M. J. High-performance liquid chromatography of red fruit anthocyanins. *Journal of Chromatography A* **1991**, *537*, 101–121.
- (210) Careri, M.; Mangia, A.; Musci, M. Overview of the applications of liquid chromatography-mass spectrometry interfacing systems in food analysis: naturally occurring substances in food. *Journal of Chromatography A* **1998**, *794*, 263–297.
- (211) Dugo, P.; Mondello, L.; Errante, G.; Zappia, G.; Dugo, G. Identification of anthocyanins in berries by narrow-bore high-performance liquid chromatography with electrospray ionization detection. *Journal of Agricultural and Food Chemistry* **2001**, *49*, 3987–3992.
- (212) Kelebek, H.; Canbas, A.; Selli, S. HPLC-DAD-MS Analysis of Anthocyanins in Rose Wine Made From cv. Öküzgözü Grapes, and Effect of Maceration Time on Anthocyanin Content. *Chromatographia* **2007**, *66*, 207–212.
- (213) Loranty, A.; Rembalkowska, E.; Rosa, E. A. ; Bennett, R. N. Identification, quantification and availability of carotenoids and chlorophylls in fruit, herb and medicinal teas. *Journal of Food Composition and Analysis* **2010**, *23*, 432–441.
- (214) Oleszek, W.; Amiot, M. J.; Aubert, S. Y. Identification of some phenolics in pear fruit. *Journal of Agricultural and Food Chemistry* **1994**, *42*, 1261–1265.
- (215) Pawlosky, R. J.; Flanagan, V. P. A Quantitative Stable-Isotope LC- MS Method for the Determination of Folic Acid in Fortified Foods. *Journal of Agricultural and Food Chemistry* **2001**, *49*, 1282–1286.
- (216) Schoch, T. K.; Manners, G. D.; Hasegawa, S. Analysis of Limonoid Glucosides from Citrus by Electrospray Ionization Liquid Chromatography- Mass Spectrometry. *Journal of Agricultural and Food Chemistry* **2001**, *49*, 1102–1108.
- (217) Tian, Q.; Giusti, M. M.; Stoner, G. D.; Schwartz, S. J. Screening for anthocyanins using high-performance liquid chromatography coupled to electrospray ionization tandem mass spectrometry with precursor-ion analysis, product-ion analysis, common-neutral-loss analysis, and selected reaction monitoring. *Journal of Chromatography A* **2005**, *1091*, 72–82.
- (218) Tomás-Barberán, F. A.; Gil, M. I.; Cremin, P.; Waterhouse, A. L.; Hess-Pierce, B.; Kader, A. A. HPLC-DAD-ESIMS analysis of phenolic compounds in nectarines, peaches, and plums. *Journal of Agricultural and Food Chemistry* **2001**, *49*, 4748–4760.

- (219) Smith, J. S.; Thakur, R. A. Chapter 26: Mass Spectrometry. In *Food Analysis*; Nielsen, S. S., Ed.; Springer: New York, 2003.
- (220) Tian, Q.; Giusti, M. M.; Stoner, G. D.; Schwartz, S. J. Characterization of a new anthocyanin in black raspberries (*Rubus occidentalis*) by liquid chromatography electrospray ionization tandem mass spectrometry. *Food Chemistry* **2006**, *94*, 465–468.
- (221) Chen, P.; Harnly, J. M.; Lester, G. E. Flow Injection Mass Spectral Fingerprints Demonstrate Chemical Differences in Rio Red Grapefruit with Respect to Year, Harvest Time, and Conventional versus Organic Farming. *Journal of Agricultural and Food Chemistry* **2010**, *58*, 4545–4553.
- (222) Nutrient Data : USDA Database for the Flavonoid Content of Selected Foods, Release 3.1 (December 2013).
- (223) Nutrition, C. for F. S. and A. GRAS Substances (SCOGS) Database - Alphabetical List of SCOGS Substances.
- (224) Parella, T. TOPSPIN version 2.1 NMR Guide 4.1, Pulse Program Catalog: I. 1D & 2D Experiments.
- (225) Stewart, J. M. *The Use of Carbon-13 Carbonyl Labeled Residues to Develop and Refine Site-specific NMR Secondary Structure Analysis Techniques*; ProQuest, 2009.
- (226) Reich, H. J. 5.3 Spin-Spin Splitting: J-Coupling **2014**.
- (227) NMR Solvents - Stable Isotopes from Cambridge Isotope Laboratories. *NMR Solvent Data Chart*.
- (228) Felgines, C.; Talavera, S.; Gonthier, M. P.; Texier, O.; Scalbert, A.; Lamaison, J. L.; Remesy, C. Strawberry anthocyanins are recovered in urine as glucuro- and sulfoconjugates in humans. *Journal of Nutrition* **2003**, *133*, 1296.
- (229) Baldi, B. G.; Maher, B. R.; Slovin, J. P.; Cohen, J. D. Stable isotope labeling, in vivo, of D- and L-tryptophan pools in *Lemna gibba* and the low incorporation of label into indole-3-acetic acid. *Plant physiology* **1991**, *95*, 1203–1208.
- (230) Britz, S. J. Regulation of photosynthate partitioning into starch in soybean leaves response to natural daylight. *Plant physiology* **1990**, *94*, 350–356.
- (231) Charron, C. S.; Britz, S. J.; Mirecki, R. M.; Harrison, D. J.; Clevidence, B. A.; Novotny, J. A. Isotopic Labeling of Red Cabbage Anthocyanins with Atmospheric $^{13}\text{CO}_2$. *Journal of the American Society for Horticultural Science* **2008**, *133*, 351–359.
- (232) Dawson, T. E.; Mambelli, S.; Plamboeck, A. H.; Templer, P. H.; Tu, K. P. Stable isotopes in plant ecology. *Annual Review of Ecology and Systematics* **2002**, *33*, 507–559.

- (233) Gruhler, A.; Schulze, W. X.; Matthiesen, R.; Mann, M.; Jensen, O. N. Stable isotope labeling of *Arabidopsis thaliana* cells and quantitative proteomics by mass spectrometry. *Molecular & Cellular Proteomics* **2005**, *4*, 1697–1709.
- (234) Grusak, M. A. Intrinsic stable isotope labeling of plants for nutritional investigations in humans. *The Journal of Nutritional Biochemistry* **1997**, *8*, 164–171.
- (235) Janghorbani, M.; Weaver, C. M.; Ting, B. T.; Young, V. R. Labeling of soybeans with the stable isotope ^{70}Zn for use in human metabolic studies. *The Journal of Nutrition* **1983**, *113*, 973.
- (236) Kikuchi, J.; Shinozaki, K.; Hirayama, T. Stable isotope labeling of *Arabidopsis thaliana* for an NMR-based metabolomics approach. *Plant and Cell Physiology* **2004**, *45*, 1099–1104.
- (237) Lieshout, M. van; West, C. E.; Breemen, R. B. van Isotopic tracer techniques for studying the bioavailability and bioefficacy of dietary carotenoids, particularly β -carotene, in humans: a review. *American Journal of Clinical Nutrition* **2003**, *77*, 12–28.
- (238) Novotny, J. A.; Kurilich, A. C.; Britz, S. J.; Clevidence, B. A. Plasma appearance of labeled β -carotene, lutein, and retinol in humans after consumption of isotopically labeled kale. *Journal of Lipid Research* **2005**, *46*, 1896–1903.
- (239) Robinson, J. M. Photosynthetic Carbon Metabolism in Leaves and Isolated Chloroplasts from Spinach Plants Grown under Short and Intermediate Photosynthetic Periods. *Plant Physiology* **1984**, *75*, 397–409.
- (240) Wang, Y.; Xu, X.; Van Lieshout, M.; West, C. E.; Lugtenburg, J.; Verhoeven, M. A.; Creemers, A. F.; Muhilal; Van Breemen, R. B. A liquid chromatography-mass spectrometry method for the quantification of bioavailability and bioconversion of beta-carotene to retinol in humans. *Analytical Chemistry* **2000**, *72*, 4999–5003.
- (241) Urbauer, J. Double Resonance Experiments.
- (242) Kurilich, A. C.; Britz, S. J.; Clevidence, B. A.; Novotny, J. A. Isotopic Labeling and LC-APCI-MS Quantification for Investigating Absorption of Carotenoids and Phylloquinone from Kale (*Brassica oleracea*). *Journal of Agricultural and Food Chemistry* **2003**, *51*, 4877–4883.